



Bettis Atomic Power Laboratory
P.O. Box 79
West Mifflin, PA 15122-0079

Bechtel Bettis, Inc.

B-SE(SPS)IC-008

December 21, 2005

Manager, Pittsburgh Naval Reactors Office
U. S. Department of Energy
Post Office Box 109
West Mifflin, Pennsylvania 15122-0109

Subject: NRPCT Closeout of Prometheus Sensor Development Work for NR Information

Dear Sir:

PURPOSE

This letter submits, for Naval Reactors information, the Naval Reactors Prime Contractor Team (NRPCT) assessment of sensor and instrumentation technology for the Space Nuclear Power Plant (SNPP) Instrumentation and Control (I&C) system as part of the Prometheus Program closeout work.

SUMMARY

Prometheus presents significant technical challenges for development and delivery of sensors and instrumentation. The combination of a 15-20 year operating life, operating temperatures ranging from 200K up to 1200K, and minimal opportunity for recalibration severely constrains the selection of viable sensors for this application. In addition, the interface electronics must withstand high doses of radiation (up to 1 MRad). Therefore the identification and development of sensor technologies was considered a high priority for the instrumentation and control portion of the Prometheus Program.

A comprehensive evaluation of the sensor technologies for measurement of the Prometheus SNPP primary plant parameters has been completed by the NRPCT incorporating input from Oak Ridge National Laboratory (ORNL), results from work at Penn State University, and information from commercial research companies and vendors. Enclosure (1) contains details used in this evaluation regarding the current capabilities of the feasible technologies and the NRPCT SNPP system requirements for each sensor type, including range, accuracy, resolution, stability, lifetime, reliability, and radiation tolerance of the technologies. This enclosure also provides a high level risk assessment for these technologies and their ability to meet the SNPP requirements.

These results indicate that technologies exist that can successfully support a sensor suite for Prometheus, given appropriate development time and resources. These efforts and results are based on the Jupiter Icy Moons Orbiter (JIMO) mission, but are deemed extensible to other space applications such as a lunar surface nuclear power plant.

The following are key conclusions that were reached by the NRPCT assessment:

- It is feasible to develop non-invasive sensors for measurement of relevant plant parameters.
- Ultrasonic and fiber optic technology each have the potential to be used for measurement of several plant parameters, and may reduce the amount of electronics needed.
- Hot leg temperature measurement is the most difficult technical challenge due to the temperature that the sensor must endure and potentially complex reactor piping designs.
- Conventional methods of temperature measurement are prone to long-term drift and will result in large temperature uncertainties. Measurement methods such as Optical Fiber Bragg Gratings can offer a potential solution to this problem.
- Fission counters are the logical choice for nuclear instrumentation. Integration of the fission counters with the shield design can reduce the volume and mass of the counters.

BACKGROUND

Since the initial NRPCT involvement in project Prometheus FY04, a major focus of the NRPCT has been the identification and assessment of sensor technologies for the measurement of the space reactor primary parameters of temperature, flow, flux, and control position. The NRPCT concern has been driven by early recognition that conventional terrestrial sensors would not, in general, meet the demands of the JIMO SNPP. The harsh conditions of space and the reactor, the continuous operation of the plant at power for over a decade, the precision of the measures, the special material and integrity challenges of the plant, and mass limitations, together exceed the capabilities of nearly all standard sensor technologies. Even while a wide variety of space reactor concepts were being developed, the general similarity of the operational conditions for these notional plants allowed the NRPCT to initiate assessments of the sensor research and development necessary to provide a basic suite of I&C sensors for space reactor operation.

Early in FY04 the NRPCT tasked ORNL to review candidate sensor technologies for the primary reactor parameters and to identify those with sufficient promise for further development. Since both liquid metal and gas cooled reactor concepts were being considered at this time, ORNL had to consider both types of coolants in their work. As described in Enclosure (2) ORNL investigated a wide spectrum of candidate technologies for reactor coolant temperature and flow, neutron flux, and control element position, ranked them according to their potential to meet the JIMO SNPP challenges, and defined a sensor development plan for the best technologies. Table 1 summarizes this effort.

In Reference (a) the NRPCT recommended a reactor coolant and energy conversion concept to Naval Reactors which was approved in Reference (b). The selection of a gas coolant for the SNPP resulted in focusing temperature and flow sensor development efforts on methods and technologies appropriate to gaseous fluids, eliminating from consideration those appropriate to liquid metal coolants. And while pressure sensing had not been a part of the original list of reactor plant sensors considered potentially necessary to a space reactor, the choice of a gas coolant and a Brayton power conversion system renewed NRPCT discussions and efforts regarding a pressure sensing capability.

With the ORNL recommendations and the selection of a coolant type and power conversion system, efforts were initiated for the next stage of development. The NRPCT leveraged ORNL expertise in particular sensor technology areas by initiating a set of work efforts to develop conceptual designs and define the materials for Resistance Temperature Detectors (RTD) and Thermocouples (TC) temperature measurement, for fission counter flux detectors, and for an ultrasonic flow system including associated cabling systems. Conceptual designs were completed and reported by ORNL for

these technologies. Additional details and document references on ORNL work can be found in Enclosure (2).

The Pennsylvania State Universities and specific vendors were also engaged in sensor development to leverage key expertise that they possessed. Penn State was tasked to develop and demonstrate ultrasonic temperature sensing using magnetostrictive technology and test the capability of single crystal aluminum nitrate ultrasonic piezoelectric actuators at high temperatures (~1000K). Northrop Grumman (Sykesville, MD) was contracted to develop conceptual designs for nuclear instrumentation and contracts were initiated with Lockheed Martin (Archibald, PA) in the development of an ultrasonic control element position indicator conceptual design and in the development of ultrasonic electronics for a variety of parameter measurements.

TABLE 1: CANDIDATE SENSOR TECHNOLOGIES

Parameter	Technology
Neutron Flux	Fission Chambers/Counters ^{1,2} Boron Coated Ion Chambers ^{1,2} Self-Powered Neutron & Gamma Detectors ¹ Silicon Carbide ¹
Reactor Coolant Temperature	Thermocouples ^{1,2} Resistance Thermometry ^{1,2} Radiation Thermometry/Pyrometry ¹ Ultrasonic Temperature Detectors ^{1,2} Fiber Bragg Grating ³
Reactor Coolant Flow	Ultrasonic Measurement (Time-of-Flight ² , Vortex Shedding ² , Cross Correlation Techniques) ¹ Thermal Mass ¹ Coriolis ¹ Compressor Inferred Flow ¹
Control Mechanism Position – Rotary	Magnetic ¹ Optical Encoder ¹ Resolver ^{1,2} Capacitance ^{1,2} RVDT ¹ Ultrasonic (Magnetostrictive) ³
Control Mechanism Position – Linear	Capacitance ^{1,2} LVDT ^{1,2} Microwave ¹ Magnetic ¹ Eddy Current ¹ Laser Ranging ¹ Potentiometric Techniques ¹ Ultrasonic (Magnetostrictive) ³

¹ORNL identified sensor technology for SNPP.

²ORNL recommended sensor technology for SNPP.

³NRPCT identified sensor technology for SNPP.

DISCUSSION

The NRPCT formed an I&C sensor integrated product team (IPT) to oversee and participate in the sensor development effort. This group engaged industrial and research expertise to supplement its own talent to perform detailed studies of the most feasible sensor technologies. Enclosure (2) summarizes the work conducted at ORNL. Enclosures (3) through (8) report the independent studies and evaluations of sensor technologies completed by the NRPCT. Enclosure (1) provides details regarding the current capabilities of the feasible technologies and the NRPCT SNPP system requirements for each sensor type, including range, accuracy, resolution, stability, lifetime, reliability, and radiation tolerance of the technologies. This enclosure also provides a high level risk assessment for these technologies and their ability to meet the SNPP requirements.

Through these efforts and based upon the latest information regarding of the gas cooled reactor plant design and performance characteristics, the NRPCT has identified the most viable sensor technologies for each of the principle Prometheus SNPP reactor parameters. Based on the key technical challenges and advantages associated with each technology, these have risen above others in their respective groups to represent the most viable technologies for a sensing system that can meet the demands of the SNPP application.

Reactor Coolant Temperature

For the Prometheus SNPP a reactor coolant temperature measurement technology is sought capable of operating continuously near 1200K for over 15 years at gamma radiation levels of 1 Grad and neutron fluences of 1×10^{20} n/cm² (E>1 MeV [nvt]) and with a range from 100K to 1300K with ± 5 K accuracy. The temperature criteria represents the hottest coolant temperature in the reactor plant at full power, while the radiation criteria represented both the Jupiter and reactor environments. Five technologies have been identified by the NRPCT that have the potential to meet these demands including resistance temperature detectors (RTD), thermocouples (TC), ultrasonics (UT), optical pyrometry, and optical fiber bragg gratings (FBG). Table 2 summarizes the key advantages and technical challenges associated with each technology. Based on initial studies by the NRPCT, the fiber bragg grating sensor represents a leading technology choice for primary reactor coolant temperature measurement at high temperatures.

The technical challenges of the reactor coolant outlet temperature measurement (i.e. the hottest temperature in the plant) extend beyond the identification of the right sensor technology to the sensor insertion into a well in the flow stream environment to ensure an accurate and timely measure of the fluid temperature. The reactor coolant piping is to be built of superalloy materials capable of withstanding temperatures to 900K without significant creep or heat loss. The reactor outlet coolant must flow at 1150K through an internally insulated pipe-in-pipe component to the turbine inlet of the Brayton machines. The details of the NRPCT concept of this pipe-in-pipe design can be found in Reference (c).

Several notions have been considered by the NRPCT to fixture the reactor coolant outlet temperature including an attachment to the external surface of the hot leg pipe, a refractory well insertion into the hot leg pipe section, an embedded temperature transducer with a through wall electrical connection, and a cast dry well at the turbine inlet. The attributes of these methods are characterized in Table 3. The cast dry well approach appears superior to the others in its ability of meet the temperature, response time, and noninvasive requirements for the measure, but limited work had been conducted to date to fully evaluate these options.

TABLE 2: Candidate Temperature Sensor Technology Risk Assessment

Technology Choice	Key Advantages	Key Challenges
Optical Fiber Bragg Grating	<ul style="list-style-type: none"> - Potential for many sensors on a single fiber - Demonstrated sensor robustness, accuracy, and low drift at high temperature - Non-amplitude based signal measurement, tolerant to fiber optic transmission line degradation. - Small sensor mass and size 	<ul style="list-style-type: none"> - Radiation tolerance of specialized components, including electro-optical components (diodes, amplifiers, lasers) - Signal processing complexity - Technology largely limited to laboratory applications.
Ultrasonics	<ul style="list-style-type: none"> - Sensing element design with no electrical insulation eliminates thermally induced material composition changes and strains as causes of sensor drift at high temperature. - Small sensor element mass and size. 	<ul style="list-style-type: none"> - Sensing element sensitivity to extraneous small scale phenomena such as changes in element geometry, surface film formation, and exogenous vibrations. - Sensor waveguide susceptible to extraneous reflections (signals) due to bends, pressure points, cracks, that might occur during installation or deployment. - Complex signal processing, fast timing rates required - Technology largely limited to laboratory applications.
Resistance Temperature Detector	<ul style="list-style-type: none"> - Well-known, widely used technology - Simple signal processing 	<ul style="list-style-type: none"> - High temperature drift due to sensing element thermally induced strain, recrystallization, reaction with impurities, and composition changes.
Thermocouples	<ul style="list-style-type: none"> - Well-known, widely used technology - Simple signal processing - Small sensor mass and size 	<ul style="list-style-type: none"> - Sensor drift, accuracy, and fault tolerance affected by many mechanisms including thermal shunting, electric noise, electrical shunting, thermally induced composition changes, reference junction uncertainty, and signal conditioning uncertainty. - Low signal to noise ratio at low temperature - High gain signal processes and complex fault detection algorithms
Optical Pyrometry	<ul style="list-style-type: none"> - First principles measurement technique - Non-contact temperature measurement - Significant industrial experience base - Small sensor mass and size 	<ul style="list-style-type: none"> - Limited to high temperature range with single detector element. - Signal amplitude based method sensitive to emissivity changes of source and degradation of fiber optic transmission line - Radiation tolerance of specialized electro-optical components (diodes, amplifiers, lasers) - Algorithmic complexity (electronics board space) - Fixturing to maintain alignment of multiple optical transmission waveguides elements

TABLE 3: Candidate Reactor Coolant Outlet Temperature Fixturing Assessment

Method	Key Advantages	Key Challenges
External Attachment to Hotleg Pipe	<ul style="list-style-type: none"> - Noninvasive - Simplicity of attachment 	<ul style="list-style-type: none"> - Long time delay. - Significant thermal shunts resulting in bias of measured versus actual coolant temperature
Refractory Well Insertion in Hotleg Pipe	<ul style="list-style-type: none"> - Non-invasive - Fast response - No thermal biases or shunts 	<ul style="list-style-type: none"> - Refractory/Superalloy weld attaching well to exterior pipe - Heat conduction from refractory well material to external superalloy pipe
Embedded Temperature Transducer	<ul style="list-style-type: none"> - Fast response - No thermal bias or shunts 	<ul style="list-style-type: none"> - Invasive. Boundary penetration of transducer electrical connection
Cast Dry Well in Turbine Inlet	<ul style="list-style-type: none"> - Noninvasive - Fast response - No thermal bias or shunts - Simplicity of fabrication 	<ul style="list-style-type: none"> - Well must be located sufficiently upstream of the turbine volute such that flow acceleration effects do not affect measured hot leg temperature

See Enclosures (2), (3), (6), (7), and (8) for further discussions regarding all the SNPP reactor coolant temperature sensing technologies evaluated in the NRPCT work including those presented here.

Pre Decisional – For Planning and Discussion Purposes Only

Reactor Power Neutron Flux

For SNPP a neutron flux reactor power measurement technology was sought that allowed a single detector to measure the full range of reactor operation from initial criticality through full power. The detector technology must be capable of operating near the reactor, fore of the reactor plant radiation shield, or within the shield, to measure reactor flux levels between 10^{-2} and 10^{11} n/cm²-sec ($E > 1$ MeV, [nv]), while subjected to operational temperatures near 1000K or 800K, respectively. Of all the candidate technologies considered, only the fission counter and silicon carbide technologies appeared capable of meeting these criteria. The target accuracy for the neutron detector is 1% of point.

Table 4 presents a risk assessment of these technologies. In the near term, the fission counter technology would be the choice for a space reactor plant. However, if the development of the silicon carbide detector continues to progress satisfactorily, the silicon carbide technology's advantages could make it the ideal sensor for this application.

TABLE 4: Candidate Neutron Flux Detector Technology Risk Assessment

Technology Choice	Key Advantages	Key Challenges
Fission Chamber	<ul style="list-style-type: none"> - Mature technology, widely used in nuclear plant applications - High energy neutron output pulses eases discrimination from gamma induced pulses and allows large separation (up to ~100m) between sensor and electronics. Local preamplification unnecessary. - Capable of full range operation. - Moderate detector bias voltage compared to other ion chamber technologies. - High temperature performance (~800K) 	<ul style="list-style-type: none"> - Handling, shipment, and storage issues associated sensor with highly enriched Uranium coating - Providing startup flux sensitivity and a neutron-moderating environment within a reasonable volume - Complex signal processing may be required to provide pulse counting during startup and current measurement during power operation - Non-traditional materials required for fore-of-shield service at ~1000K. Performance must be demonstrated. - Large size and mass required to achieve necessary sensitivity.
Silicon Carbide	<ul style="list-style-type: none"> - Simple single signal process based on pulse counting. - Easy discrimination of neutron and gamma induced output pulses - Capable of full range operation - Small bias voltage (from 20 to ~200 volts) - Light weight and small size. 	<ul style="list-style-type: none"> - Developmental technology - High temperature performance must be verified for both fore-of-shield and within shield service. - Startup sensitivity and radiation tolerance for 15 year lifetime must be verified.

See Enclosures (2) and (5) for further discussions and references regarding all the SNPP neutron flux sensing technologies considered by the NRPCT including those summarized here.

Reactor Coolant Flow

For the SNPP a reactor coolant flow measurement has been sought to determine the flow through the reactor plant independent of the operation of the flow prime mover(s). Such a measurement provides plant control strategies and options not only for normal full power operations, but also during infrequent or abnormal plant conditions such as reactor or Brayton machine startups or component causalities. A design baseline mass flow rate of approximately 4.5kg/sec through a 800kWt gas cooled SNPP with 2 active Brayton machines at full power leads to volumetric flows at the compressor outlets of 0.12 m³/sec (17m/sec through 9.4cm pipe) and a reactor inlet flow of 0.39 m³/sec . As sensor penetrations through the coolant boundary were considered undesirable, representing a boundary failure risk for the loss of coolant, mission ending event, the flow sensing technology was

required to be noninvasive. In the direct gas cooled Brayton reactor plant concept, the flow through the reactor equals the flow through the active Brayton turbo-alternator-compressor machines. For a single loop plant the flow sensor could be located at either the reactor inlet or at the compressor outlet to measure the coolant flow, the latter being preferable because of the lower operating temperature of the coolant system piping at full power, i.e., ~550K versus 900K. For a multi-Brayton plant design, the same principle applies, though multiple sensors would be necessary at the compressor outlet locations to measure the total reactor coolant flow.

Ultrasonic technology has been the single feasible, non-invasive technology identified for measurement of SNPP reactor coolant gas flow. The particular ultrasonic method showing the most promise within this technology group is the time-of-flight approach using piezoelectric transducers attached to the surface of the piping system directly or through standoffs. The target accuracy for this measurement is +0.25% of point. This approach is assessed for both the reactor inlet and the compressor outlet locations in Table 5.

TABLE 5: Candidate Reactor Coolant Flow Sensor Technology Risk Assessment

Technology Choice	Key Advantages	Key Challenges
Ultrasonic Flow at Reactor Inlet, 900K	<ul style="list-style-type: none"> - Non-invasive flow measurement 	<ul style="list-style-type: none"> - High-temperature piezoelectric transducers do not exist for this service temperature. Development required. - Radiation and aging effects of piezoelectric transducers for long duration service must be verified. - High temperature coupling acoustic wedges and standoffs to coolant piping must be developed.
Ultrasonic Flow, Compressor Outlet, 550K	<ul style="list-style-type: none"> - Non-invasive flow measurement - Widely available piezoelectric materials can be used in transducer. - UT flow systems in wide usage in natural gas industry at this service temperature. - Current materials and design methods may be used to design acoustic couplers and standoffs. 	<ul style="list-style-type: none"> - Radiation and aging effects of piezoelectric transducers for long duration service must be verified.

See Enclosures (2), and (3) for further discussions and references regarding the SNPP flow meter technologies considered by the NRPCT including the ultrasonic flow methods considered here.

Reactor Coolant Pressure

Reactor coolant pressure had only recently been added to the NRPCT list of baseline reactor parameters to be measured by the I&C system. This addition was based on the selection of a gas cooled reactor with Brayton machines as the baseline SNPP with system operational pressures varying from 1 to near 3MPa. In a gas cooled reactor plant, the pressure may be used to independently verify the state of the plant as well as to control and monitor the plant and its components. To date the NRPCT has limited its considerations to non-invasive ultrasonic methods for pressure measurement including measurement of the gas resonances of the closed coolant system that vary as a function of system pressure; measurement of the deflection of a thin-walled bellows subject to actual coolant system pressure, and the measurement of the acoustic impedance variation at the interior pipe wall-gas coolant interface as a result of a pressure change.

Similar to the reactor coolant flow sensor, selecting a location in a cooler section of plant significantly reduces the sensor technology risk. Location of the pressure sensors at the outlet of the Brayton

machine compressors will allow the maximum system pressures to be measured at operating temperatures near 550K, allow the compressor pressure ratio across the Brayton machines to be determined, and permit accurate monitoring of individual machine behaviors in a multi-Brayton plant. While the location of a system pressure sensor at the inlet or outlet to the reactor may be desirable to more accurately monitor reactor pressure, at temperatures above 850K, these locations are a severe challenge to the ultrasonic approach of pressure measurement. The target accuracy for this measurement is approximately 1% of the range.

Two of the viable ultrasonic methods for pressure measurement are assessed in Table 6, with the thin-walled bellows method at the compressor outlet section of the plant representing the most viable approach. The methodology for detecting impedance variation is an amplitude-based technique and is expected to be highly inaccurate for this application, therefore it was not assessed.

TABLE 6: Candidate Reactor Coolant Pressure Sensor Technology Risk Assessment

Technology Choice	Key Advantages	Key Challenges
Ultrasonic Gas Resonance	<ul style="list-style-type: none"> - Non-invasive flow measurement - Ultrasonic transducers and mounting accessories do exist for moderate temperature service less than 550K. UT sensors in wide usage in natural gas industry at this service temperature. 	<ul style="list-style-type: none"> - Ultrasonic transducers and mounting accessories (coupling acoustic wedges and standoffs) for high temperature service above 850K in significant radiation fields do not exist. High risk research and development required. - Radiation and aging effects of piezoelectric transducers for long duration service must be verified. - Accurate, high resolution measurement of closed loop systems of complicated geometries has not be demonstrated at the moderate pressures (1 – 2MPa) of the SNPP.
Ultrasonic Thin-Walled Bellows	<ul style="list-style-type: none"> - Non-invasive flow measurement - Accurate, high resolution measurements demonstrated for low, moderate, and high system pressures. - Ultrasonic transducers and mounting accessories exist for moderate temperature service less than 550K. UT sensors in wide usage in natural gas industry at this service temperature. 	<ul style="list-style-type: none"> - Ultrasonic transducers for high temperature service above 850K in significant radiation fields do not exist. High risk research and development required. - Radiation and aging effects of piezoelectric transducers for long duration service must be verified.
Ultrasonic Acoustic Impedance	<ul style="list-style-type: none"> - Non-invasive flow measurement - Ultrasonic transducers and mounting accessories exist for moderate temperature service less than 550K. UT sensors in wide usage in natural gas industry at this service temperature. 	<ul style="list-style-type: none"> -New concept. Theoretical and experimental research necessary. - Ability to make accurate, high resolution measurements of moderate pressure gas systems must be established.

See Enclosure (3) for a further discussion regarding the SNPP reactor pressure sensing approach considered by the NRPCT.

Control Element Position

The primary method of reactivity control for the SNPP gas-cooled reactor is through control of the neutron leakage from the perimeter of the reactor using either slider or drum reflector control elements mounted adjacent to the outer wall of the reactor pressure vessel. The measurement of the absolute position of these elements is crucial to the safe operation of the plant. Since the NRPCT had yet to select the particular method of control, both linear and rotational position sensing systems have been under review to support the selection of either sliders or drums, respectively. For each control element, a position sensor would be attached to the control element drive mechanism located aft of

the reactor radiation shield subject to ionizing and neutron radiations of 1 Grad and 10^{20} n/cm² and maximum temperatures of 400K. For the slider, the linear sensor must be able to accurately sense 0.5 mm movements over a distance of 45cm; for the drum, rotary movements less than 0.1 degree over an arc of 360 degrees is required. Table 7 evaluates the ultrasonic and electromagnetic position measurement technologies that the NRPCT felt were most viable for Prometheus.

See Enclosures (2), (3) and (4) for further discussions and references regarding the SNPP control element position indication technologies considered by the NRPCT including those summarized here.

TABLE 7: Candidate Control Element Position Sensor Technology Risk Assessment

Position Type	Technology Choice	Key Advantages	Key Challenges
Linear	Ultrasonics	<ul style="list-style-type: none"> - Magnetostrictive ultrasonic position technology commercially available. - Magnetic and insulation materials exist for the magnetostrictive components (magnets, waveguides, coils) that are robust in sensor radiation and thermal environment. - Flexible sensor range of measurement - Relatively moderate sensor mass. 	<ul style="list-style-type: none"> - Performance and lifetime in thermal and radiation environment must be verified. - Significant susceptibility to electromagnetic interference from control element motor. - Large sensor space envelope. Mass of sensor unknown.
	LVDT	<ul style="list-style-type: none"> - Technology widely used in industry - Radiation hardened and high temperature devices are available commercially - Thermal and radiation effects on sensor technology accuracy and resolution well understood. - Demonstrated ability to operate well in electromagnetic environment of motor 	<ul style="list-style-type: none"> - Relatively large sensor space envelope (twice the movement range) and relatively high mass
Rotational	Resolver	<ul style="list-style-type: none"> - Technology widely used in industry - Small size and mass. - Strong vendor base - Thermal and radiation effects on sensor technology accuracy and resolution well understood. - Demonstrated ability to operate well in electromagnetic environment of motor 	
	Ultrasonics	<ul style="list-style-type: none"> - For magnetostrictive approach, magnetic and insulation materials available capable of operation in thermal and radiation environment. 	<ul style="list-style-type: none"> - Rotary ultrasonic position sensor is a new concept. Significant research and development. - Range, accuracy, and resolution unknown. - Concerns with resolution and sensitivity - For piezoelectric approach, transducer materials must be verified for the thermal and radiation environment. - Susceptible to electromagnetic interference from adjacent motor.

CONCLUSIONS

Prometheus presents significant technical challenges for development and delivery of sensor systems for measurement of the primary reactor plant parameters of temperature, flow, pressure, and control element position. The combination of a 15 year operating life without maintenance, the moderate and high temperature operating environments, and the demanding performance requirements, severely constrains the identification of viable sensor technologies for these parameters. In addition, the sensing systems' components including the interface electronics must withstand high doses of

Pre Decisional – For Planning and Discussion Purposes Only

radiation and the reactor coolant sensors must be noninvasive to minimize risk of coolant leakage., Even with these significant challenges, the NRPCT has identified technologies that can be expected to meet the JIMO SNPP requirements. Each of the sensors identified, however, will require significant development.

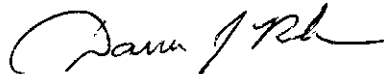
CONCURRENCE

The managers of Bettis Space Plant Systems (D. Hagerty), Space Reactor Engineering (C. Eshelman), Advanced Materials Technology (J. Hack) and KAPL Space Electrical Systems (K. Loomis), Space Power Plant Systems (H. Schwartzman), Space Reactor Engineering (D. McCoy), Space Energy Conversion (J. Ashcroft), and Space Materials (S. Simonson) have reviewed and concur the contents of this letter.

NR ACTION

No Naval Reactors action requested, this letter is for information.

Very truly yours,



Darren J. Robare
Manager, Space I&C Design
Space Engineering

References:

- (a) NRPCT Concept Recommendation, SPP-67110-0005, B-SE-0077 dated March 4, 2005
- (b) NR Approval of Concept Recommendation, I#05-01228 dated April 20, 2005
- (c) Technical Documentation in Support of Project Prometheus Plant Pre-Conceptual Design Report, B-SE(SPS)FMS-008 dated 11/11/05

Enclosures:

- (1) Sensor Performance Matrix
- (2) Summary of ORNL Sensor Development Work
- (3) Ultrasonic Sensor Technology Evaluation
- (4) Position Indication Technology Evaluation
- (5) Neutron Flux Sensor Technology Evaluation
- (6) RTD/Thermocouple Technology Evaluation
- (7) Optical Pyrometry Technology Evaluation
- (8) Fiber Bragg Grating Temperature Sensor Technology Evaluation

Enclosure 1
Sensor Performance Matrix

This page intentionally blank

Overview of Evaluation Matrix

The following performance matrix was initially completed by the sensor technology integrated product teams based on their research and development findings during their evaluation of the various viable sensor technologies for Prometheus. This matrix provides the performance of the current state of technology for each sensor and the target performance for Prometheus for the following criteria:

- Range of Measurement with Single Device
- Accuracy
- Resolution
- Lifetime and Reliability at Temperature
- Reactor Radiation Tolerance of Sensor/Cabling
- Natural Radiation Tolerance of Sensor/Cabling
- Radiation Tolerance of Sensor Electronics
- Ability to Separate Sensor and Electronics

Additional criteria were assessed during the NRPCT evaluation of sensor technologies. These are not included in the performance matrix since these are more system related or programmatic and do not have a current state for comparison or established targets. These criteria were evaluated and discussed for each technology by the NRPCT.

- Cabling Mass
- Cabling Flexibility
- Complexity
- Integration with Reactor Power Plant
- Testability
- Cost Effectiveness
- Manufacturability

Due to the early stages of conceptual designs for the Space Nuclear Power Plant (SNPP), the targets established are preliminary and would likely change as the SNPP design matures, operations become better defined and modeled, and additional information is gained on these sensor technologies through research, development, and testing. This matrix was used as a guide to the NRPCT I&C organization in identifying the key technical challenges associated with each technology to support the formation of a recommended near-term development strategy, which can be found in Enclosure (10).

The assumptions that were taken into consideration were a hot leg temperature of 1150 K, a cold leg temperature of 891 K, lifetime requirements and a production delivery schedule of 15 years, and stability incorporating the use of a calibration technique and/or electronics. Also provided in the matrix is the NRPCT identified current state of technology for each performance metric. Some of this information is well documented and readily available while some is based on engineering judgment and vendor perception. Each parameter was evaluated using an evaluation key which consisted of five levels, from not possible or extremely unlikely to very likely.

Note that this matrix was not and should not be considered a tool for selecting technologies or eliminating technologies, but rather was a tool for identifying and discussing key technical challenges and where to focus efforts and resources. This matrix was utilized as an aid in the NRPCT discussions in identifying the major technology and delivery challenges associated with each technology, from which the recommended near-term development strategy is based. This matrix also includes a preliminary risk assessment identifying the risk perceived with meeting each performance target with the current level of information and knowledge of each technology.

Pre Decisional – For Planning and Discussion Purposes Only

This page intentionally blank

Temperature Performance Matrix

Assumptions: Hot Leg Temperature: 1150K
Cold Leg Temperature: 891K
Lifetime Requirements: 15 years
Production Delivery Schedule: 10 years

Risk of Technology Meeting Target		High Risk			Medium Risk			Low Risk	
Performance Criteria	Development Stage	Ultrasonic - Piezoelectric	Ultrasonic - Magnetostrictive	Thermocouple - Type N	RTD - Wire Element (Pt)	RTD - Ceramic Element (Pt/Al ₂ O ₃)	Optical Pyrometry (Silicon Diodes)	Optical - Fiber Bragg Grating	
Range of Measurement with Single Device	Current State of Technology	UNKNOWN	100-1300 K	3-1573 K	73-1275 K	100-1400 K	<881 to >>1150 K	300-1023 K (Silica) 300K-1530K (Sapphire)	
	Target	200-1150 K	200-1150 K	200-1150 K	200-1150 K	200-1150 K	200-1150 K	200-1150 K (Sapphire)	
Accuracy (Over entire life)	Current State of Technology Initial Accuracy	UNKNOWN	0.20%	0.4% (4.6 K @ 1150 K)	0.16% (1.45 K @ 925 K, Omega)	1%	< 1% (well characterized, isothermal surface)	±0.25% (±2 K) (For 773K, 8.5yrs lifetime, Silica, raw data)	
	Current State of Technology Stability at Temperature	UNKNOWN	0.20%	-0.6% (-9 K) after 27,500 hr (3.12 yrs) @ 1563 K (Type R)	Better than 0.2 K @ 10,000 hr (1.14 yrs) (Omega)	UNKNOWN	No Testing Conducted at Prometheus Requirements, "1-2 degrees over 10 yrs" - unconfirmed vendor	±0.25% (±2 K) (For 1000 K, <10 yrs lifetime, Sapphire, model needs to be verified, raw data)	
Resolution	Current State of Technology	5 K over range after 15 yrs @ 1150 K	5 K over range after 15 yrs @ 1150 K	5 K over range after 15yrs @ 1150 K	5 K over range after 15 yrs @ 1150 K	5 K over range after 15 yrs @ 1150 K	5 K over range after 15 yrs @ 1150 K	5 K over range after 15 yrs @ 1150 K	
	Target	UNKNOWN	2.5 K	<1 K	<1K	<1K	-0.2% (well characterized ,isothermal surface)	±0.25% (±2 K) (For 773 K, 8.5 yrs lifetime) (Silica, raw data) ±1 K (Silica, averaged data)	
Lifetime and Reliability at Temperature	Current State of Technology	1 K over range	1 K over range	1 K over range	1 K over range	1 K over range	1 K over range	1 K over range	
	Target	UNKNOWN	>10 yrs	>27,500 hr (3.12 yrs) @ 1563 K (Type R)	Typically 1 decade or more of operation in power 500K temperatures	UNKNOWN	>10 yrs (not necessarily in continuous use)	8.5 yrs @773 K, ±2 K; 12.75 yrs @ 773 K, ±3 K (Silica) <10 yrs @1000 K, ±2 K; (Sapphire, model needs to be verified)	
Target	15 yrs	15 yrs	15 yrs	15 yrs	15 yrs	15 yrs	15 yrs	15 yrs	

Pre Decisional – For Planning and Discussion Purposes Only

Enclosure 1 to
B-SE(SPS)IC-008
Position Performance Matrix

Assumptions: Hot Leg Temperature: 1150K
Cold Leg Temperature: 891K
Lifetime Requirements: 15 years
Production Delivery Schedule: 10 years

Risk of Technology Meeting Target		High Risk	Medium Risk	Low Risk			
Performance Criteria	Development Stage	Ultrasonic Linear	Ultrasonic Rotary	LVDT	Resolver	Capacitive Linear	Capacitive Rotary
Range of Measurement with Single Device	Current State of Technology	>45 cm	360°	>15 cm	360°	2 cm	300°
	Target	45 cm	360°	45 cm	360°	45 cm	360°
Accuracy (Over entire life)	Current State of Technology (Initial Accuracy)	0.045 mm	.036°	0.75 mm	0.08°	UNKNOWN	UNKNOWN
	Current State of Technology (Stability)	0.09 mm (0.2 %)	0.72° (0.2%)	UNKNOWN	UNKNOWN	UNKNOWN	UNKNOWN
Resolution	Target	0.5 mm	0.1°	0.5 mm	0.1°	0.5 mm	0.1°
	Current State of Technology	2.5 μm	0.001°	<10 μm	0.008° (16 bit resolution)	0.001 μm small range	0.03°
Lifetime and Reliability at Temperature	Target	50 μm	0.01°	50 μm	0.01°	50 μm	0.01°
	Current State of Technology	>10 yrs	>10 yrs	820 K "continuous"	Failure mechanisms similar to motors/transformers	UNKNOWN	UNKNOWN
Reactor Radiation Tolerance of Sensor & Cabling	Target	15 yrs, ~400 K	15 yrs, ~400 K	15 yrs, ~400 K	15 yrs, ~400 K	15 yrs, ~400 K	15 yrs, ~400 K
	Current State of Technology	Radiation data on individual components meets requirements	Radiation data on individual components meets requirements	3x10 ²⁰ n/cm ² ; 10x10 ¹¹ Rad	1x10 ⁹ Rad	UNKNOWN	UNKNOWN
Performance Criteria	Target	3x10 ¹⁷ n/cm ² ; 0.5 GRad TID	3x10 ¹⁷ n/cm ² ; 0.5 GRad TID	3x10 ¹⁷ n/cm ² ; 0.5 GRad TID	3x10 ¹⁷ n/cm ² ; 0.5 GRad TID	3x10 ¹⁷ n/cm ² ; 0.5 GRad TID	3x10 ¹⁷ n/cm ² ; 0.5 GRad TID
	Development Stage	Ultrasonic Linear	Ultrasonic Rotary	LVDT	Resolver	Capacitive Linear	Capacitive Rotary

Pre Decisional – For Planning and Discussion Purposes Only

Natural Radiation Tolerance of Sensor & Cabling	Current State of Technology	Radiation data on individual components meets requirements	Radiation data on individual components meets requirements	Radiation data on individual components meets requirements	Radiation data on individual components meets requirements	Radiation data on individual components meets requirements	Radiation data on individual components meets requirements	Radiation data on motors and transformers similar, therefore similar to LVDT.	UNKNOWN	UNKNOWN
	Target	1GRad TID; 5.7×10^{15} n/cm ² (1 MeV)	1GRad TID; 5.7×10^{15} n/cm ² (1 MeV)	1GRad TID; 5.7×10^{15} n/cm ² (1 MeV)	1GRad TID; 5.7×10^{15} n/cm ² (1 MeV)	1GRad TID; 5.7×10^{15} n/cm ² (1 MeV)	1GRad TID; 5.7×10^{15} n/cm ² (1 MeV)	1GRad TID; 5.7×10^{15} n/cm ² (1 MeV)	UNKNOWN	UNKNOWN
Radiation Tolerance of Signal Processing and Electronics	Current State of Technology	Discrete devices: -0.1 MRad; All components: $>1 \times 10^{12}$ n/cm ² (fast fluence)	Discrete devices: -0.1 MRad; All components: $>1 \times 10^{12}$ n/cm ² (fast fluence)	Discrete devices: -0.1 MRad; All components: $>1 \times 10^{12}$ n/cm ² (fast fluence)	Discrete devices: -0.1 MRad; All components: $>1 \times 10^{12}$ n/cm ² (fast fluence)	Discrete devices: -0.1 MRad; All components: $>1 \times 10^{12}$ n/cm ² (fast fluence)	Discrete devices: -0.1 MRad; All components: $>1 \times 10^{12}$ n/cm ² (fast fluence)	Discrete devices: -0.1 MRad; All components: $>1 \times 10^{12}$ n/cm ² (fast fluence)	Discrete devices: -0.1 MRad; All components: $>1 \times 10^{12}$ n/cm ² (fast fluence)	Discrete devices: -0.1 MRad; All components: $>1 \times 10^{12}$ n/cm ² (fast fluence)
	Target	6×10^{11} n/cm ² ; 1 MRad TID	6×10^{11} n/cm ² ; 1 MRad TID	6×10^{11} n/cm ² ; 1 MRad TID	6×10^{11} n/cm ² ; 1 MRad TID	6×10^{11} n/cm ² ; 1 MRad TID	6×10^{11} n/cm ² ; 1 MRad TID	6×10^{11} n/cm ² ; 1 MRad TID	6×10^{11} n/cm ² ; 1 MRad TID	6×10^{11} n/cm ² ; 1 MRad TID
Separability of Sensor and Electronics	Current State of Technology	60 m	60 m	100 m	>100 m	60 m	60 m	60 m	UNKNOWN	UNKNOWN
	Target	60 m	60 m	60 m	60 m	60 m	60 m	60 m	60 m	60 m

Reactor Power and Volumetric Flow Performance Matrix

Assumptions: Hot Leg Temperature: 1150K

Cold Leg Temperature: 891K

Lifetime Requirements: 15 years

Production Delivery Schedule: 10 years

Risk of Technology Meeting Target

High Risk

Medium Risk

Low Risk

Performance Criteria	Development Stage		Fission Chamber		Full Range Ion Chamber		Silicon Carbide		Proportional Counter		Ultrasonic	
	Current State of Technology	Target	Current State of Technology	Target	Current State of Technology	Target	Current State of Technology	Target	Current State of Technology	Target	Current State of Technology	Target
Accuracy (Over entire life)	Current State of Technology (Initial Accuracy)	1% of point	Current State of Technology	1% of point	as individual proportional and ion chambers	1% of point	Very linear detector output with power demonstrated	1% of point	Demonstrated in reactor plant environments at temperature <400 K	1% of point	1% of point	1% of point
Range of Measurement with Single Device	Current State of Technology	$10^{-2}-10^{-1}$ nv (fore of shield)	Current State of Technology	$10^{-2}-10^{-1}$ nv (fore of shield)	$10^{-2}-10^{-1}$ nv (in shield)	$10^{-2}-10^{-1}$ nv (fore of shield)	$10^{-2}-10^{-1}$ nv (in shield)	$10^{-2}-10^{-1}$ nv (fore of shield)	$10^{-2}-10^{-1}$ nv (in shield)	$10^{-2}-10^{-1}$ nv (fore of shield)	$10^{-2}-10^{-1}$ nv (in shield)	$10^{-2}-10^{-1}$ nv (fore of shield)
	Target	$10^{-2}-10^{-1}$ nv (fore of shield)	Target	$10^{-2}-10^{-1}$ nv (fore of shield)	$10^{-2}-10^{-1}$ nv (in shield)	$10^{-2}-10^{-1}$ nv (fore of shield)	$10^{-2}-10^{-1}$ nv (in shield)	$10^{-2}-10^{-1}$ nv (fore of shield)	$10^{-2}-10^{-1}$ nv (in shield)	$10^{-2}-10^{-1}$ nv (fore of shield)	$10^{-2}-10^{-1}$ nv (in shield)	$10^{-2}-10^{-1}$ nv (fore of shield)
Accuracy (Over entire life)	Current State of Technology (Stability)	1% of point	Current State of Technology (Stability)	1% of point	Demonstrated in reactor plant environments at temperature <400 K	1% of point	Demonstrated in reactor plant environments at temperature <400 K	1% of point	Demonstrated in reactor plant environments at temperature <400 K	1% of point	1% of point	1% of point
	Target	1% of point	Target	1% of point	1% of point	1% of point	1% of point	1% of point	1% of point	1% of point	1% of point	1% of point
Resolution	Current State of Technology	10 cps/nv	Current State of Technology	10 cps/nv	Vendor data suggests 2×10^{13} amps/nv (current mode) = 1 cps/nv (pulse)	10 cps/nv (fore of shield)	10 cps/nv (in shield)	100 cps/nv (fore of shield)	100 cps/nv (in shield)	100 cps/nv (fore of shield)	100 cps/nv (in shield)	100 cps/nv (fore of shield)
	Target	10 cps/nv (fore of shield)	Target	10 cps/nv (fore of shield)	10 cps/nv (in shield)	10 cps/nv (fore of shield)	10 cps/nv (in shield)	100 cps/nv (fore of shield)	100 cps/nv (in shield)	100 cps/nv (fore of shield)	100 cps/nv (in shield)	100 cps/nv (fore of shield)
Lifetime and Reliability at Temperature	Current State of Technology	Demonstrated in reactor plant environments >10 yrs, T < 400 K	Current State of Technology	Demonstrated in reactor plant environments >10 yrs, T < 400 K	Demonstrated in reactor plant environments >10 yrs, T < 400 K	Demonstrated in reactor plant environments >10 yrs, T < 400 K	Demonstrated in reactor plant environments >10 yrs, T < 400 K	Demonstrated in reactor plant environments >10 yrs, T < 400 K	Demonstrated in reactor plant environments >10 yrs, T < 400 K	Demonstrated in reactor plant environments >10 yrs, T < 400 K	Demonstrated in reactor plant environments >10 yrs, T < 400 K	Demonstrated in reactor plant environments >10 yrs, T < 400 K
	Target	Target	Target	Target	Target	Target	Target	Target	Target	Target	Target	Target

Pre Decisional – For Planning and Discussion Purposes Only

REACTOR POWER		REACTOR RADIATION & CABLING		NATURAL RADIATION TOLERANCE OF SENSOR & CABLING		RADIATION TOLERANCE OF ELECTRONICS		SEPARABILITY OF SENSOR AND ELECTRONICS	
Criteria	Development Stage	Current State of Technology	Target	Current State of Technology	Target	Current State of Technology	Target	Current State of Technology	Target
Performance	Fission Chamber	Vendor rating in-core operation at 10^{10} n/cm ² , 10 Grad/year	10^{10} n/cm ² , 10 Grad (FOS) 10^{11} n/cm ² , 1 Grad (IOS) 6×10^{14} n/cm ² , 0.5 Grad (AOS)	High Tolerance to neutron and gamma radiation suggests good general tolerance	1 Grad TID, 5.7×10^{15} n/cm ² (1 MeV)	Discrete devices: -0.1 MRad; ASICS -1.0 MRad; All components: $>1 \times 10^{12}$ n/cm ² (fast fluence)	6×10^{11} n/cm ² , 1 MRad TID	ORNL demonstrated 50 m separation performance	ORNL demonstrated 50 m separation performance
Performance	Full Range Ion Chamber	Demonstrated rating ex-core operation at $\sim 10^{18}$ n/cm ² (Thermal), 5 Grad/year	10^{18} n/cm ² , 10 Grad (FOS) 10^{17} n/cm ² , 1 Grad (IOS) 6×10^{14} n/cm ² , 0.5 Grad (AOS)	High Tolerance to neutron and gamma radiation suggests good general tolerance	1 Grad TID, 5.7×10^{15} n/cm ² (1 MeV)	Discrete devices: -0.1 MRad; ASICS -1.0 MRad; All components: $>1 \times 10^{12}$ n/cm ² (fast fluence)	6×10^{11} n/cm ² , 1 MRad TID	Reactor plant demonstrated > 30 m separation	Reactor plant demonstrated > 30 m separation
Performance	Silicon Carbide	UNKNOWN	10^{18} n/cm ² , 10 Grad (FOS) 10^{17} n/cm ² , 1 Grad (IOS) 6×10^{14} n/cm ² , 0.5 Grad (AOS)	UNKNOWN	1 Grad TID, 5.7×10^{15} n/cm ² (1 MeV)	Discrete devices: -0.1 MRad; ASICS -1.0 MRad; All components: $>1 \times 10^{12}$ n/cm ² (fast fluence)	6×10^{11} n/cm ² , 1 MRad TID	UNKNOWN	UNKNOWN
Performance	Proportional Counter	Demonstrated ex-core operation at $\sim 10^{16}$ n/cm ² (Thermal), 5 Grad/year	10^{16} n/cm ² , 10 Grad (FOS) 10^{17} n/cm ² , 1 Grad (IOS) 6×10^{14} n/cm ² , 0.5 Grad (AOS)	High Tolerance to neutron and gamma radiation suggests good general radiation tolerance	1 Grad TID, 5.7×10^{15} n/cm ² (1 MeV)	Discrete devices: -0.1 MRad; ASICS -1.0 MRad; All components: $>1 \times 10^{12}$ n/cm ² (fast fluence)	6×10^{11} n/cm ² , 1 MRad TID	Reactor plant demonstrated > 30 m separation	Reactor plant demonstrated > 30 m separation
Performance	Ultrasonic	Very Little Known	6×10^{15} n/cm ² , 0.5 Grad	Very Little Known	1 Grad TID, 5.7×10^{15} n/cm ² (1 MeV)	Discrete devices: -0.1 MRad; ASICS -1.0 MRad; All components: $>1 \times 10^{12}$ n/cm ² (fast fluence)	6×10^{11} n/cm ² , 1 MRad TID	154 m	60 m

Pre Decisional - For Planning and Discussion Purposes Only

Enclosure 2

NRPCT Summary of ORNL Sensor Technology
Assessment and Development Work for Prometheus

This page intentionally blank

Table of Contents

1. ORNL Reactor Sensor Technology Development Plan.....	6
1.1. OVERVIEW.....	6
1.2. ORNL RECOMMENDED SENSOR TECHNOLOGIES.....	6
1.2.1 Reactor Power Level – Neutron Flux.....	7
1.2.1.1. Fission Chambers-Counters	7
<p><i>A conventional fission chamber is an ion chamber with an interior surface that has been coated with a fissionable isotope. The principal advantage of this type of detector is the large signal produced by fission reactions as compared to competing types of ionizations. This allows unambiguous measurement of low levels of neutron flux in relatively intense background radiation environments. The limitation to the detection efficiency of these detectors per unit area of fissionable material arises from the limited range of the fission fragments in the deposit. This limits the fissionable material thickness to 2-3 microns.....</i></p>	
1.2.2. Reactor Coolant Temperature	10
<p>THE FOUR TECHNOLOGY CLASSES REVIEWED BY ORNL WERE THERMOCOUPLES, RESISTANCE THERMOMETERS, PYROMETRY (RADIATION THERMOMETERS), AND ULTRASONIC PROBE-BASED THERMOMETRY.....</p>	
1.2.2.1. Thermocouples	10
1.2.2.2. RESISTANCE THERMOMETERS	10
1.2.2.2.1. Classical RTD thermometry	10
1.2.2.2.2. Johnson Noise Thermometry.....	11
1.2.2.2.3. Combining Direct RTD Measurement and Johnson Noise Thermometry.....	11
1.2.2.3. RADIATION THERMOMETERS/PYROMETRY	11
1.2.2.4. ULTRASONIC PROBE-TYPE THERMOMETERS.....	11
1.2.3. Reactor Liquid Coolant Flow.....	12
1.2.3.1. FLOW MEASUREMENT (PENETRATING PIPE BOUNDARY).....	12
1.2.3.1.1. Differential Pressure (Liquid Pipe Boundary)	12
1.2.3.1.2. Orifice	12
1.2.3.1.3. Venturi.....	12
1.2.3.1.4. Elbow.....	12
1.2.3.1.5. Nozzle.....	12
1.2.3.1.6. Pitot Tube.....	12
1.2.3.2. Magnetic-with Internal Electrodes and Insulated Liner (Liquid Flow Only).....	12
1.2.3.3. FLOW MEASUREMENT (NON-PIPE PENETRATING WITH PORTION OF THE METER IN THE FLOW)	13
1.2.3.3.1. Vortex Shedding Flow Sensor (Liquid and Gas Flow)	13
1.2.3.3.2. Turbine (Liquid and Gas Flow)	13
1.2.3.3.3. Target/Drag (Liquid and Gas Flow).....	13
1.2.3.3.4. Positive Displacement (Liquid and Gas Flow).....	13
1.2.3.4. FLOW MEASUREMENT (NON-INVASIVE).....	13
1.2.3.4.1. Liquid-Metal Magnetic Flowmeters (Liquid Only).....	13
1.2.3.4.1.1. Permanent Magnetic (PM) Flowmeter with External Electrodes.....	13
1.2.3.4.2. Magnetic Force/Drag Flowmeters	14
1.2.3.4.3. Non-Contacting Magnetic Induction with External Sensing Coils	14
1.2.3.4.4. Ultrasonic Transit-Time Flow Sensor (Liquid and Gas Flow).....	15
1.2.3.4.5. Coriolis Mass Flowmeter (Liquid and Gas Flow).....	15
1.2.3.4.6. Thermal Mass Flowmeter (Liquid and Gas Flow)	15
1.2.3.4.7. Power Consumption Accountability Of The EM Pump To Infer Work Done On The Fluid....	16
1.2.3.4.8. Measuring The Slip Directly Via Current Signature Analysis.....	16
1.2.3.4.9. Inferring Flow In The EM Pump Based On Magnet Flux Measurements	16
1.2.3.4.10. Inferring Flow From Air Compressor Parameters	16
1.2.3.4.11. Cross-Correlation Techniques (Liquid and Gas Flow).....	16

1.2.4.1. LINEAR MEASUREMENT.....	17
1.2.4.1.1. Capacitance.....	17
1.2.4.1.2. Microwave.....	17
1.2.4.1.3. Magnetic.....	18
1.2.4.1.3.1. Magnetic Microcantilever Switch Array.....	18
1.2.4.1.3.2. Magnetostrictive.....	18
1.2.4.1.4. Laser Ranging.....	18
1.2.4.1.5. LVDT.....	18
1.2.4.1.6. Eddy Current.....	19
1.2.4.1.7. Potentiometric Techniques.....	19
1.2.4.2. ROTARY MEASUREMENT.....	19
1.2.4.2.1. Magnetic.....	19
1.2.4.2.1.1. Hall Sensor.....	19
1.2.4.2.1.2. Magnetoresistive.....	19
1.2.4.2.1.3. Magnetic Microcantilever Switch Array.....	20
1.2.4.2.1.4. Magnetostrictive Rotary Position Sensor.....	20
The same technology of linear magnetostrictive position measurement as described above can be applied to measurement of rotation. The benefits of this technology are high radiation and high temperature tolerance. 20	
1.2.4.2.2. Optical Encoder.....	20
1.2.4.2.3. Resolver.....	20
1.2.4.2.4. RVDT.....	20
1.2.4.2.5. Capacitance.....	20
1.2.4.3. LIMIT SWITCHES.....	21
1.2.4.3.1. Contact Limit Switches.....	21
1.2.4.3.2. Non-Contact Limit Switches.....	21
1.2.4.3.2.1. Induction.....	21
1.2.4.3.2.2. Magnetic.....	21
1.2.4.3.2.3. Capacitance.....	21
1.2.4.3.2.4. Optical.....	21
1.2.5. ORNL Recommended Sensor Technologies and Basis.....	22
1.2.5.1. REACTOR POWER LEVEL (NEUTRON FLUX).....	22
1.2.5.2. REACTOR COOLANT TEMPERATURE.....	23
1.2.5.3. REACTOR GAS COOLANT FLOW.....	25
1.2.5.4. CONTROL ELEMENT POSITION.....	28
1.2.6. References.....	32
2. Fission Chamber Development.....	33
2.1. OVERVIEW.....	33
2.2. KEY POINTS AND CONCLUSIONS.....	33
2.2.1. Basic Principles of Fission Chamber Operation.....	33
2.2.2. Detector Electronics.....	34
2.2.3. Uranium Coatings.....	34
2.2.4. Fore of Shield Design.....	35
2.2.5. In-Shield Design.....	35
2.2.6. Aft of Shield Design.....	35
2.2.7. NRPCT Assessment.....	36
2.2.8. Key Conclusions.....	36
2.2.9. References.....	37
3. Ultrasonic Flow Meter System Conceptual Design.....	38
3.1. OVERVIEW.....	38
3.2. ORNL Recommended Technique.....	38

3.3.	KEY POINTS AND CONCLUSIONS	39
3.3.1.	<i>NRPCT Evaluation</i>	39
	<i>The NRPCT completed an evaluation of ultrasonic flow technology which is presented in Enclosure (3).</i>	
	39	
3.3.2.	<i>NRPCT Comments</i>	39
3.3.2.1.	<i>Transducer Backing Material</i>	39
3.3.2.2.	<i>Signal Processing</i>	39
3.3.2.3.	<i>Mass Considerations</i>	40
3.3.2.4.	<i>Waveguide Considerations</i>	40
3.3.2.5.	<i>Redundancy</i>	40
3.3.2.6.	<i>Torsional Strut Concept</i>	40
3.4.	<i>References</i>	41
4.	Sensor Cable Conceptual Design	42
4.1.	OVERVIEW	42
4.2.	KEY POINTS AND CONCLUSIONS	42
4.2.1.	<i>Electrical Cable</i>	42
4.2.2.	<i>Optical Fiber Technology</i>	43
4.2.3.	<i>Conclusions</i>	44
4.2.4.	<i>Future Work</i>	45
4.2.5.	<i>References</i>	45
5.	Thermocouple Conceptual Design	46
5.1.	OVERVIEW	46
5.2.	KEY POINTS AND CONCLUSIONS	47
5.2.1.	<i>Material Selection</i>	47
5.2.2.	<i>Signal Processing Electronics</i>	47
5.2.3.	<i>Uncertainty Analysis</i>	48
5.2.4.	<i>Manufacture, Assembly, and Testing</i>	48
5.2.5.	<i>Conclusion</i>	48
5.2.6.	<i>References</i>	48
6.	RTD Conceptual Designs	49
6.1.	OVERVIEW	49
6.2.	KEY POINTS AND CONCLUSIONS	50
6.2.1.	<i>Wire Element RTD Conceptual Design</i>	50
6.2.2.	<i>Ceramic Element RTD Conceptual Design</i>	50
6.2.3.	<i>Insulation, Sheath, and Fabrication</i>	50
6.2.4.	<i>Conclusions</i>	50
6.2.5.	<i>References</i>	50

Report Title	JIMO REACTOR SENSOR TECHNOLOGY DEVELOPMENT PLAN
Report Number	ORNL/LTR/NR-JIMO/05-01
Report Date	JANUARY 2005
NRPCT IV	FY04 Task #4

1. ORNL Reactor Sensor Technology Development Plan

1.1. Overview

Early in FY04 the NRPCT tasked ORNL per References (a) and (b) to review candidate sensor technologies for the primary reactor parameters, to identify those with sufficient promise for further development for the Jupiter Icy Moons Orbiter (JIMO) mission, and to recommend a development plan that would lead to a successful production and delivery of the required sensors technologies. The reactor parameters considered in the development plan were neutron flux, control element position, primary coolant flow and temperature. For each reactor parameter the Sensor Technology Development Plan developed by ORNL, Reference (c), contained a survey of the current state-of-the-art to identify candidate measurement technologies given the expected environmental conditions and duration of the JIMO mission, an evaluation of the potential technologies, a description of the selection process rationale underlying the evaluation, and a development plan for future work to prove the suitability of the selected sensor technologies.

1.2. ORNL Recommended Sensor Technologies

The following summarizes the results of the evaluation by Oak Ridge National Laboratory (ORNL) of the measurement technologies required for the Jupiter Icy Moon Orbiter (JIMO) reactor as described in Reference (c). The ORNL report recommends a development plan for each of the specific reactor parameters considered which include neutron flux, temperature, coolant flow, and control element position. In all ORNL assessed approximately 60 different sensor technologies. The most viable technologies investigated by ORNL for Prometheus are shown in Table 1.1.

Based on the mission requirements, strengths, weaknesses, and maturity level of the technologies, ORNL evaluated and recommended the parameter technologies it considered most suitable for the JIMO mission. The top two technologies as ranked by ORNL for each parameter are listed in Table 1.2.

TABLE 1.1: Most Viable Sensor Technologies Investigated by ORNL

Parameter	Technologies	
Neutron Flux	Fission Chambers/Counters Ion Chambers	Self-Powered Neutron & Gamma Detectors Silicon Carbide
Reactor Coolant Temperature	Thermocouples Resistance Thermometers	Radiation Thermometers/Pyrometry Ultrasonic Temperature Detectors
Reactor Coolant Flow	Ultrasonic Measurement (Time-of-Flight, Vortex Shedding, Cross Correlation Techniques)	Coriolis Compressor Inferred Flow Thermal Mass
Control Mechanism Position - Rotary	Magnetic Optical Encoder, Resolver	Capacitance RVDT
Control Mechanism Position - Linear	Capacitance LVDT Microwave Magnetic	Eddy Current Laser Ranging Potentiometric Techniques

TABLE 1.2: ORNL Recommended Sensor Technologies for JIMO

Parameter	Prime Choice	Second Choice
Neutron Flux	Fission Chamber	Helium-3 Detector
Coolant Temperature	Resistance Thermometry	Ultrasonic Thermometry
Coolant Flow	Ultrasonic Time-Of-Flight	Ultrasonic Vortex Shedding
Position Indication-Linear	LVDT	Capacitive
Position Indication-Rotary	Resolver	Capacitive

1.2.1 Reactor Power Level – Neutron Flux

1.2.1.1. Fission Chambers-Counters

A conventional fission chamber is an ion chamber with an interior surface that has been coated with a fissionable isotope. The principal advantage of this type of detector is the large signal produced by fission reactions as compared to competing types of ionizations. This allows unambiguous measurement of low levels of neutron flux in relatively intense background radiation environments. The limitation to the detection efficiency of these detectors per unit area of fissionable material arises from the limited range of the fission fragments in the deposit. This limits the fissionable material thickness to 2-3 microns.

It is preferable that a single detector channel covers the entire range of reactor operations from shutdown, to hot very low power critical experiments, to full power operation. This provides motivation for employing an extended range counting system because of the high-sensitivity requirements. The reactor power measurement system can switch from pulse mode operation to current mode operation once the initial low-power reactor dynamics testing has been performed. The advantage of current mode operation is that lower speed; higher reliability electronics can be used. Using current mode operation requires a one-time switch over of amplification electronics. The extended-range pulse counting circuit appears to be a viable approach but requires that the preamplifier maintains a relatively high bandwidth over the life of the mission. An additional disadvantage of current mode

operation is that the measurement system is more susceptible to current ground loops requiring additional rigor in the implementation of the sensor cabling.

For gas-filled detectors, the fission chamber fill gas is required to stop the fission fragments while generating free electrons and ions in the process, allow field-induced transport of the free carriers, be relatively unresponsive to non-fission induced ionizations, quench field-induced charge multiplication, absorb ultra violet (UV) photons with energies above the work function of the interior surfaces, and endure the mission radiation and temperature without damaging the sensor components. Ion chamber gases fulfill similar purposes. Ion chamber fill gases are required to be more stable than fission chamber fill gases, due to the larger amount of electric field in an ion chamber for amplifying the smaller pulses.

The candidates for gas filled neutron flux detector structural material are carbon composite structure with vitreous carbon insulators and carbide conductors, noble metal lined inconel structure with oxide insulators, and refractory alloy structure with oxide insulators. The candidates for the neutron converter are ^{235}U , ^{10}B , $^3\text{Helium}$, and $^{10}\text{BF}_3$ -Argon. The candidates for the fill gases are Argon-Nitrogen, and Argon-CO, CH_4 , or CF_4 . More analysis on these candidates can be found in the ORNL Sensor Technology Development Plan report table 4-1.

1.2.1.1.1. Micro Fission Chambers

Miniature fission chambers are used in-core in light water reactors for local flux measurement. They respond to a combination of neutrons and gamma rays. They are scaled down versions of conventional fission chambers that are fabricated using micromechanical device techniques. However, because of their small size and consequent low efficiency they are not of interest outside of the core.

1.2.1.1.2 ORNL Ultra High Sensitivity Fission Counter

An ultrahigh sensitivity fast fission counter was developed by ORNL to provide a threshold neutron detector for plasma diagnostics. The device remains at the lab prototype stage of development and has never been commercialized.

1.2.1.1.3. ORNL High-Temperature High-Sensitivity Fission Counter

A high temperature sensitivity fission counter (HTHSFC) was developed by ORNL to provide a ~ 10 cps/nv_{th} neutron detector for source range through power range for the advanced liquid metal breeder reactor program. The HTHSFC was constructed as a set of 19 fission chambers within a single outer shell. The set of fission counters were electrically connected serially with a delay line (inductor) between each counter. Generated current pulses were measured at each end. Only those pulses that occur at delay line timing intervals were recorded. This type of detector has been commercialized in a non-high temperature form by GE Reuter-Stokes Inc. but is not currently available as a catalog item.

1.2.1.2. Ion Chambers

1.2.1.2.1. Boron-10 Coated Ion Chamber

For the JIMO mission, a B-10 based ion chamber could be employed in pulse mode for start-up operation and have a one-time transition to current mode operation for power range monitoring. The challenge is in monitoring the initial hot, low-power critical testing where the current may not yet be high enough for current mode operation but the combined gamma and neutron induced pulse rate

may overwhelm the pulse detection electronics. The advantage is the higher neutron interaction cross section of B-10 relative to U-235, which results in higher detector efficiency when operating in pulse mode for the same area of neutron converter. Boron-10 ion chambers are available from commercial vendors.

1.2.1.2.2. Boron-10 Trifluoride or Helium-3 Ion Chambers

Gaseous neutron converters tend to provide better electronic pulse height resolution. This allows pulse-height-based rejection of most of the competing gamma, proton, and electron produced pulses. Detectors are physically smaller compared to fission chambers for the same efficiency. One advantage is in long-term survival. Since both the He-3 and B-10 reactions produce much smaller gas ionization pulses than a fission chamber, remotely locating the electronics will require more care in the cable shielding and isolation, or higher internal fields to enable gas gain, to reduce cross-talk and noise.

1.2.1.3. Self Powered Neutron Detectors (SPNDs)

The detectors have low enough sensitivity to require in-core application and not be useful as a start-up detector (even in core). Core penetration would increase complexity and decrease reliability. SPNDs are not recommended for use unless all other technology fails. No current available SPNDs would survive core temperatures and would be susceptible to radiation-induced currents and thermal leakages in their cables.

1.2.1.4. Self Powered Gamma Detectors (SPGDs)

The sensitivity of SPGDs are too low to be of interest ex-core or for application as a start-up device. No device currently exists that is capable of performing in the high temperature reactor core environment. SPGDs have very similar problems to the SPNDs.

1.2.1.5. Silicon Carbide

Silicon Carbide based neutron detectors are very new and in the experimental stage. They have very high gamma rejection capabilities due to their thin active depth and the low linear energy transfer of the energetic electrons. SiC based neutron detectors are also capable of very high-speed operation and allow for pulse mode operation through power range. They have the potential to operate at 1075K but damage has been shown to occur between 1075K and 1275K. Operation has only been demonstrated to 625K. Their demonstrated radiation and temperature survival characteristics restrict their long long-term or at power deployment to an aft of shield location.

The main disadvantage in using these devices is their relatively small size and consequent lack of sensitivity. An additional concern is that only a small fraction of the total neutron capture reaction kinetic energy is actually deposited within the detector sensitive volume, and the devices are not operated in an avalanche mode, so the signal pulses are quite small. The pulses tend to have sharp rise and fall times due to the small device capacitance. The cable isolation and grounding quality requirements are more stringent for these detectors and the first stage preamplifiers will need to be located relatively close to the detector.

1.2.2. Reactor Coolant Temperature

The four technology classes reviewed by ORNL were thermocouples, resistance thermometers, pyrometry (radiation thermometers), and ultrasonic probe-based thermometry.

1.2.2.1. Thermocouples

A key concept in thermocouple operation is that thermocouple voltage is developed over regions with temperature gradients and not across the thermoelement junction, which merely serves to provide a common reference electrical potential point. The Seebeck coefficient is known as the change in electric potential in a material with temperature. A thermocouple's voltage is found by integrating its local Seebeck coefficient up one thermoelement leg and back down the other.

Only a few thermocouple materials are available for selection at the high temperatures of a space nuclear reactor. A type C (W5%Re-W26%Re) is attractive due to its ability to work up to 2400K and its high Seebeck coefficient of 14 $\mu\text{V/K}$, which means about 10mV of signal strength at reactor operating temperatures. The type C was used in the SP-100 program due to its ability to tolerate maximum accident conditions (1650K). Type N (nicosil-nisil) is attractive for its ability to work at 1550K and its high Seebeck coefficient of 27 $\mu\text{V/K}$. The Type N was developed in the 1980s to address the known high temperature instabilities of other base-metal thermocouples and consequently had lower drift than other base-metal thermocouples. Another thermocouple considered is Nb1Zr-Mo, which exhibits high stability to radiation-induced drift. This thermocouple has much less information available about the long-term performance and repeatability of this form.

At high temperatures small-diameter mineral-insulated metal-sheathed thermocouples experience both drift and insulation shunting errors. One of the primary drift mechanisms for thermocouples at high temperature is inter-diffusion of the sheath and thermoelement alloy metals. Impurities in the insulators are another source for atoms to alter the thermoelements. Therefore, high as possible purity oxide insulators are recommended. Another principal mechanism for base-metal thermocouple drift is precipitation of the alloy components that supersaturate the host nickel lattice.

Aft-of-shield radiation induced drift is not anticipated to be as significant as the thermally induced drift. An additional, non-typical radiation induced source of thermocouple drift is trapped charge in the insulator oxides. This trapped charge could induce electric potential along the conductors giving rise to an offset.

1.2.2.2. Resistance thermometers

1.2.2.2.1. Classical RTD thermometry

RTDs are among the most common of all temperature sensors and provide accuracy and repeatability over a wide temperature range. Four-wire measurement techniques provide the highest accuracy because variation in lead wire resistance is compensated. But time, temperature, mechanical stress, and neutron capture all alter the transfer function requiring a re-calibration of the Callendar-Van Dusen coefficients. The significant concerns regarding drift and accuracy can be corrected by measuring temperature with an RTD using the traditional method with an added system using a first-principles temperature method to allow periodic calibrations to the curve fitting coefficients.

1.2.2.2. Johnson Noise Thermometry

The Johnson Noise Thermometry is a temperature measurement method based on first-principles physics that derives a temperature value from the random noise generated by an electrical resistance. Space application of Johnson Noise Thermometry applies significant additional constraints to the technology. Among the top constraints are the long-term independent operation and very highly radiation tolerance electronics. The necessity for low-mass, temperature-tolerant electronics, and mechanical ruggedness further restricts the implementation. The Johnson noise thermometry is a solution to drift problem for RTD.

1.2.2.3. Combining Direct RTD Measurement and Johnson Noise Thermometry

The combined temperature measurement approach achieves the speed and accuracy of traditional resistance thermometry while adding the feature of automatic calibration. Overall, the long-term measurement uncertainty at high temperatures is greatly reduced by supplementing the resistance temperature measurement with Johnson noise-based re-calibration. The disadvantage is that the noise signal must be processed and integrated.

1.2.2.3. Radiation Thermometers/Pyrometry

Since the object being measured constantly broadcasts infrared radiation, infrared radiation thermometers measure temperature without contact, which does not interfere with the object's temperature distribution. They can measure distant objects and moving objects at very high temperatures. The radiation thermometers can be very accurate and precise provided that the emittance of the surface is well characterized. A drawback is the measurements depend upon knowledge of the emissivity of the source and requires a stable optical path. The optical path development for fore-of-shield is very developmental and the optical path development for aft-of-shield is just a little less developmental.

1.2.2.4. Ultrasonic Probe-Type Thermometers

Ultrasonic sensors are especially applicable to space-reactor temperature measurement because these operate by measuring the speed-of-sound in a metal wire or rod, which is a known function of temperature. Probe-based ultrasonic temperature measurements have been applied to nuclear reactor core temperature measurements including nuclear thermal rocket propulsion since the late 1960s.

Two primary techniques by which ultrasonic waves are launched into the waveguide include using a piezoelectric actuator and using electromagnetic acoustic transducers (EMATs). A piezoelectric actuator is essentially a piezoelectric speaker element coupled to the transmitting end of the rod. An EMAT is any type of transducer that utilizes the interaction of a static magnetic field and alternating current, including magnetostrictive excitation.

One of the obvious problems with ultrasonic measurements is that of obtaining a high-fidelity return signal and subsequently processing that signal to obtain consistent information. A variety of signal-processing techniques has been developed to accomplish this but a complete overview is beyond the scope of this report. The ultrasonic temperature measurements also have a drift problem over time. The sensors are applicable to very high temperature measurements and can also measure multiple locations with a single sensor.

1.2.3. Reactor Liquid Coolant Flow

1.2.3.1. Flow Measurement (Penetrating Pipe Boundary)

1.2.3.1.1. Differential Pressure (Liquid Pipe Boundary)

The most widely applied method within industry is the differential pressure (DP) flowmeter, which applies Bernoulli's principle by creating a measurable pressure change within a flow system through variation of the flow kinetic energy. The magnitude of the pressure change is related to the flow rate so the velocity of the fluid can be found and thus the flow rate.

1.2.3.1.2. Orifice

The orifice plate is typically a flat, metal plate with a concentric opening. The plate is inserted perpendicular to a flow stream. The volumetric flow rate is directly related to the pressure drop across the orifice and pressure taps that penetrate the pipe wall are used to measure the DP. The orifice hole has to be watched to make sure it does not erode or become plugged as this would significantly alter the DP- flow rate relationship. Accuracy is nominally about +/- 1-2% of full scale and the rangeability is 3-4 and can be extended to 5 in some cases.

1.2.3.1.3. Venturi

A venturi is a flow restriction device designed such that the solid boundary of the restriction better matches the pipe flow profile. Venturis feature longer, smooth-curved restrictions, with a pressure tap located at the position of maximum contraction, or the throat of the device. Fouling and erosion are much less a problem, accuracy is better and rangeability is about the same as an orifice flowmeter. Venturis might be useful for a standard of comparison during an initial calibration of the selected space reactor flowmeter due to its improved accuracy and stability.

1.2.3.1.4. Elbow

Pressure taps are located outside and inside of the elbow which can reproduce DP and thus flow measurements can be made. They are inexpensive but their accuracy is not high, typically about 4% of full scale. They do not work well in gases where the pressure drop is very small.

1.2.3.1.5. Nozzle

Flow nozzles feature a smooth entrance, lengthened in a similar fashion to a venturi, and a sharp exit section, which is characteristic of an orifice plate. The flow rate is related to the square root of the DP as with an orifice. Accuracy can be better than an orifice and its rangeability is similar to an orifice.

1.2.3.1.6. Pitot Tube

The Pitot tube flowmeter infers the fluid velocity by generating a highly localized pressure difference. Multiple taps in a Pitot tube or moving the tube across the pipe diameter is required to obtain an accurate total flow measurement. Accuracy is typically 2-5% of full scale and the rangeability is similar to all DP measurements at about 3-4.

1.2.3.2. Magnetic-with Internal Electrodes and Insulated Liner (Liquid Flow Only)

Magnetic flow sensors are commercially available and were developed for use with relatively poor conducting fluids, such as water-based flow streams. The section of the pipe where the measurement is made must either be non-metallic or must be lined with an electrical insulator or the induced emf will be shorted out. They are well suited to the measurement of bi-directional flow, as only the sign of the

induced emf changes when the direction of flow is reversed. Magnetic flow sensors only work with electrically conductive fluids and for this reason are not useful for measuring gas flow, or the flow of electrically insulating oils.

1.2.3.3. Flow Measurement (Non-pipe penetrating with portion of the meter in the flow)

1.2.3.3.1. Vortex Shedding Flow Sensor (Liquid and Gas Flow)

A bluff body is located within the fluid flow stream inside the pipe, which results in the formation of vortices on the downstream side of the body. This technique can be adapted to measure bi-directional flow provided that the method used to count vortices also distinguishes on which side of the body the vortices are located. The technique does not work for low flow velocities, which restricts the rangeability of the flow sensor, and limits the utility of the sensor during startup, especially in liquid flows. The major concerns with this flow sensor technology are the effects of temperature and radiation on the vortex counting transducers.

1.2.3.3.2. Turbine (Liquid and Gas Flow)

A turbine flowmeter consists of a bladed rotor axially suspended in a pipe section in the direction of flow. The meters can be used for liquids or gases and have accuracies on the order of 0.1 to 0.5% of flow rate with rangeabilities of 10 to 50. A concern is the long-term reliability with moving parts and bearings. Bearing lifetimes can be very problematic, especially with hot gases.

1.2.3.3.3. Target/Drag (Liquid and Gas Flow)

The target/drag flowmeter operates on the principle of inertial driven differential pressure forces balancing viscous drag forces. These meters can be used with liquids or gases, have accuracies of 0.5 to 2% of full scale, and have rangeabilities of 4 to 5. Since there are no moving parts, reliability should be good. The problem is getting the signals outside of the pipe without any penetrations. A wireless communication scheme could work but there are no wireless electronics capable of operating at 1200K available at this time.

1.2.3.3.4. Positive Displacement (Liquid and Gas Flow)

Positive displacement (PD) flowmeters divide the flow into know-volume collection chambers. PD flowmeters are ideal for viscous fluids and batch applications and have been used with gases and liquids. One issue could be the wear and would require recalibration. Secondly, seals and moving parts can be reliability concerns. Measurement accuracy is quite good, 0.5 to 1% of full scale with a rangeability of 10. Designs so far are available for high temperature (up to 600K) and high pressures (10 MPa).

1.2.3.4. Flow Measurement (Non-invasive)

1.2.3.4.1. Liquid-Metal Magnetic Flowmeters (Liquid Only)

1.2.3.4.1.1. Permanent Magnetic (PM) Flowmeter with External Electrodes

For magnetic flow sensing of liquid metals, with electrical conductivity comparable to that of the flow pipe, the use of an insulated liner is not required, and the emf sensing electrode can be located on the outside of the flow pipe. Magnetic flow sensors are well suited to the measurement of bi-directional flow, as only the sign of the induced emf changes when the direction of flow is reversed. A possible concern with the use of permanent magnets is the inability to periodically re-zero the sensor electronics. A major concern with the permanent magnets is the strength of the magnetic field can

undergo changes over long periods of time due to prolonged exposure at elevated temperatures near the maximum rating for the magnet, radiation, shock or other environmental factors; thereby degrading the sensitivity of the flow sensor. These sensors which are based on the use of permanent magnets have been used extensively on liquid metal flow loops. PM flowmeters were used on the SP-100.

1.2.3.4.1.2. Updated Liquid Metal Magnetic Flowmeters with External Electrodes

Magnetic flow sensors based on the use of permanent magnets have been used extensively on liquid metal flow loops in the past but have not had much opportunity for further development in recent years. A major concern with the PM magnetic flow sensor is that the strength of the magnetic field can undergo changes over long periods of time, either due to prolonged exposure at temperatures near the maximum rating for magnets, or due to radiation, shock, or other environmental factors. Another concern is the inability to re-zero the sensor electronics periodically.

Replacing the permanent magnet with an electromagnet could result in significant advantages. An electromagnet can be turned off whenever a re-zeroing of the sensor electronics is required. These modifications could eliminate concerns related to both the long-term drift of the magnetic field strengths and the occurrence of small DC offset voltages in either of the sensor leads to the electronics.

Replacing the magnetic circuit with magnetic field coil would eliminate all of the magnetic materials issues. The development of these advanced modes of operation has benefited the performance of modern magnetic flow sensors but has added complexity to the electronics and expenses.

1.2.3.4.2. Magnetic Force/Drag Flowmeters

In the force flowmeter, the electrical currents induced by the motion of the liquid metal in a transverse magnetic field result in $J \times B$ forces that retard the motion of the fluid. An advantage to this flowmeter is that the target is the liquid metal itself, and the force measurement is performed external to the flow pipe. A possible disadvantage of this approach is that the sensitivity (or calibration) is dependent on the electrical conductivity of the fluid. The dependence on the fluid conductivity can be eliminated by allowing the magnet to move.

1.2.3.4.3. Non-Contacting Magnetic Induction with External Sensing Coils

The major advantage of non-contacting induction flowmeters is that no direct contact with either the coolant pipe or the liquid metal is involved. Both the excitation and the sensing functions are performed using external coils. In one realization of an induction flowmeter, two adjacent AC magnetic field coils are connected in opposing polarity, creating a null field midway in between. In an alternate configuration, a single coil is used to produce an AC magnetic field transverse to the direction of flow.

For high temperature applications, the excitation and sensing coils must be passively cooled and thermally insulated from the flow pipe to avoid problems with the electrical insulation of the coils. Radiation effects on the coil insulation must also be considered. Also, the zero drift of the sensing coils typically increases with temperature, requiring compensation to maintain acceptable accuracy of the measurements

1.2.3.4.4. Ultrasonic Transit-Time Flow Sensor (Liquid and Gas Flow)

Several types of ultrasonic flow sensors have been developed, including time-of-flight, Doppler, and cross-correlation flowmeters. Ultrasonic flow sensing works well for sensing low flow velocities (excellent rangeability), as well as bi-directional flow. The Doppler type flowmeter requires particles in the flow stream. For the Doppler technique to work in a space application, the liquid metal or gas would require seeding of particles, which could cause erosion to piping components and is not recommended. For a clean liquid metal with single phase flow, the relevant technology is the time-of-flight technique. In this method, the propagation time delay of ultrasonic pulses is measured in both the upstream and downstream direction inside the flow pipe.

The ultrasonic time-of-flight flow sensor is an excellent example of a non-intrusive flow technology, as the ultrasonic signals can be coupled through the wall of an existing section of coolant piping. Major issues are the effects of temperature on the ultrasonic transducers and the effects of radiation on the transducers. Significant transducer degradation is tolerable so long as the time delays of the ultrasonic signals can accurately and reliably be measured. Another issue is the coupling of the ultrasonic energy from the transceiver in to the fluid of interest. A third issue is the wetting of the Niobium-1%Ar pipe by the liquid lithium. Ultrasonic flowmeters are the most developed technology for noninvasive gas flowmeters.

New developments (past three years) have overcome the barrier of non-invasive ultrasonic flow measurements because ultrasonic flowmeters are now available for gas systems. The gas cooled reactor conditions are three to six times acoustically better than the current commercial working system.

1.2.3.4.5. Coriolis Mass Flowmeter (Liquid and Gas Flow)

Coriolis flowmeters are also well developed technology for noninvasive flow measurement. These flowmeters measure the mass flow directly and can also measure fluid density directly. The fact that these flowmeters measure the mass flow and density directly makes them the top choice for many applications. These meters are most likely to be affected by external or internal vibrations which are close to the drive frequency or the difference between the coriolis produced frequency and the drive frequency. They are also very sensitive to the zero stability of the measuring system.

The Coriolis flowmeter uses an electromagnetic transducer to vibrationally excite flow tubes at a natural resonance frequency. The Coriolis flow sensor is not completely non-intrusive as specialized shaped configurations of the flow pipe are usually required. The excitation and sensing transducers have limited temperature ranges and will require thermal isolation from the flow pipe. The major issues are the effects of temperature on the transducers, effects of radiation on the transducers, and the possible effects of launch, thaw, vibration, and other stresses on the long-term calibration and accuracy of the flow sensor.

1.2.3.4.6. Thermal Mass Flowmeter (Liquid and Gas Flow)

A thermal mass flowmeter consists of two temperature sensors with an electric heater located in between. Two operating modes are one where a constant current is applied and in a second the downstream probe is held at a fix temperature. For either mode to be a nonintrusive flow sensing technique, the heat must be applied externally to the flow pipe. This approach introduces time delays between the heat input and the temperature probes. It also has the disadvantage that the heat is transferred to the fluid at different rates along the length of the flow pipe, resulting in a non-linear heat

transfer process, and a nonlinear relationship between the mass flow and the temperature measurement.

Thermal mass flowmeters provide the advantage of measuring the mass flow rate directly, instead of an average flow velocity. They also have no moving parts but the method is not well suited for use on high heat capacity coolant loops. Additionally, the time response of this method can be significant, especially if there is substantial pipe wall mass involved.

1.2.3.4.7. Power Consumption Accountability Of The EM Pump To Infer Work Done On The Fluid

The power consumption of a linear induction electromagnetic (EM) pump varies systematically as a function of the flow rate of the liquid metal. Linear induction pumps generally have relatively low efficiency, typically in the 12-18% range, so most of the power is not expended doing the work of moving the fluid, but instead is dissipated by various losses. Basically at a fixed drive voltage, the current drawn by the pump is a function of the fluid flow rate. This probably will not provide a highly accurate measurement of the flow rate, particularly at low flow velocity; it will likely provide a go/no-go indication of fluid flow.

1.2.3.4.8. Measuring The Slip Directly Via Current Signature Analysis

Electromagnetic (EM) pumps are characterized by 1) pressure pulsations in the fluid at multiples of the AC power frequency, and 2) slip between the fluid velocity and the phase velocity of the magnetic field. It is speculated that the current and voltage waveforms will be altered significantly as the slip is varied. The feasibility of this method has not been established.

1.2.3.4.9. Inferring Flow In The EM Pump Based On Magnet Flux Measurements

This method is essentially the same as the Non-contacting Magnetic Induction Flowmeter with External Sensing Coils. The only difference is the sensing coils would be integrated into the design of the EM induction pump, to utilize the AC magnetic field source available there, instead of requiring a separate magnetic field source. A disadvantage is that the optimum frequency used by an induction pump will likely not match the optimum choice of frequency for the flow sensing measurement. This option would only be applicable if an induction-type EM pump such as an ALIP were selected to pump the coolant.

1.2.3.4.10. Inferring Flow From Air Compressor Parameters

The compressor's input power would be measured using voltage sensors and current transformers and then the relationship would be used to calculate the output flow of the compressor from the input power to the compressor. The major issues are the effect of radiation on the voltage sensors and current transformers and the effect of continuous operation on the correlation between the input power to the compressor and its output flow.

1.2.3.4.11. Cross-Correlation Techniques (Liquid and Gas Flow)

The cross-correlation technique for flow measurement has been used for over twenty five years. The technique measures the time-of-flight or transit time of flow disturbances from one location to a separate downstream location in a fluid flow system. This method has been employed successfully with a variety of sensor systems; electrical capacitance or resistance, ultrasonics, radiation, strain gages, and thermal devices. For high temperature application, thermal pulses from a heater and two temperature measuring devices are less than ideal. The electrical capacitance or resistance techniques require probes inside the piping, which introduce pipe penetrations and leak potentials.

Radiation techniques will not work because the turbulent structures do not involve any significant density change so the radiation energy will not be measurably modulated by the structures. For space reactor applications, non-invasive technique could include ultrasonics and strain gages. Some work has been done on high temperature, radiation tolerant strain gages, both ceramic and optically based types. There is a significant amount of research to be done on the strain gage cross correlation technique to account for temperature variation, flight vibration, and shock.

1.2.4. Control Element Position

1.2.4.1. Linear Measurement

1.2.4.1.1. Capacitance

Capacitive displacement measurement is a viable method only for short electrode distances. For a travel of several centimeters or greater, capacitance measurement can be made using a sliding plate configuration but there are various plate configurations possible. The moving plate approach is not commercially available as a position displacement sensor. The sliding capacitor plate concept is highly radiation tolerant, but a means to maintain constant plate spacing would be required, otherwise error would occur.

1.2.4.1.2. Microwave

Linear displacement measurements that use microwave-frequency with either time-domain-reflectometry methods or phase measurement methods are commercially available. These microwave systems use semiconductor microwave devices for signal generation and detection. Therefore, support electronics must be located near the microwave detector to amplify and process signals, which reduces overall radiation tolerance further. Because of the radiation environment, the microwave source and detector would need to be mounted in the mission module. An alternative to the solid-state-approach is to replace the source and detector with vacuum tubes. Klystron, traveling-wave tube, and magnetron technologies are candidates for generation of microwave energy. There are several problems with vacuum tube technologies: 1) vacuum tube filaments have limited lifetimes that are statistically shorter than the mission period; 2) operating voltages are several hundred to several thousand volts; and 3) the tubes and their passive components are significantly more massive than are their solid-state counterparts.

High resolution devices operate at frequencies of 10's of GHz to get the wavelength of the electromagnetic wave and with such high frequency operation may preclude use of vacuum tube devices altogether. Recent developments in commercial microwave displacement sensors measures displacement by launching a continuous microwave signal toward a target of interest and comparing the received signal with the transmitted signal. Radatec, Inc. manufactures a sensor that requires a moving target, which is a disadvantage. Ultimately, the lack of resolution at reasonable wavelengths and degradation of components from high radiation intensity make microwave-based position measurement a difficult technology to employ.

An alternative approach based on high-frequency RF or microwave energy is to create a tuned cavity whose resonance is varied with the insertion of a rod connected to control rod drive. A cylindrical cavity with a linear plunger can be constructed that produces a linear relationship between plunger position and resonant frequency. With this approach electrical contact is not required between the plunger and wall and a simple sliding bearing can be used. No commercial device that uses this approach is available at this time.

1.2.4.1.3. Magnetic

1.2.4.1.3.1. Magnetic Microcantilever Switch Array

The magnetically-actuated microcantilever switch array is made using micro-electro-mechanical systems (MEMS) technology. The measurement technology is not yet commercially available. The components can tolerate high radiation fields without degradation because the materials of construction are silicon and silicon dioxide and its semiconductor properties are not used since the cantilevers operate simply as switches. Degradation will occur from neutron exposure; however, the measurement method is not directly based on field strength and may not be a problem.

1.2.4.1.3.2. Magnetostrictive

Magnetostrictive displacement measurement is actually based on acoustic time-of-flight methods. The time interval between application of the current pulse and the detection of the return torsional wave is a measure of length. There are commercially available MLTs (Magnetostrictive Linear Transducers) that exhibit high resolution (5 microns), excellent linearity (0.02%), wide range (1-120 inches), non-contact measurement, and remote electronics. The three potential vulnerabilities that need to address are the radiation and temperature effects on the magnet, the magnetostrictive wire, and the triggering coil.

1.2.4.1.4. Laser Ranging

Laser range finders may be based on one of several methods including phase measurement, time-of-flight, geometric, structured light, and interferometric. The most easily adaptable and simplest method is based on structured light. Laser range finders are commercially available devices.

All of the laser-based methods share a common need for laser diode emitters and solid-state detectors, which can be a charge-coupled device (CCD) array. Because these solid-state devices are not tolerant of high radiation environments, it becomes necessary to locate all electronics in the mission module including emitters and detectors. The downside of these lasers is the need for as many as 1000 optical fibers to make a precision measurement. Although fabricating CCDs with thousands of elements is common practice, the problem for a high radiation environment becomes one of handling an optical bundle of many fibers.

Optical measurements in high-radiation environments have been made using vacuum-tube-based video cameras because of their very high radiation tolerance. Solid-state cameras based on charge injection devices (CIDs) also offer possibilities. ThermoElectron Corporation is a major supplier of CID based radiation hard imaging devices.

1.2.4.1.5. LVDT

The linear variable differential transformer (LVDT) consists of a ferromagnetic core that passes through a three-winding transformer: a primary and two secondary windings. There are commercially available LVDTs that are radiation and neutron hardened to values greater than the project guidelines and the LVDTs can handle temperature to 930K. The LVDTs accuracy is sensitive to temperature and the measurement range of commercial units must be extended from ~3cm to ~15cm. Other concerns are the cable effects on the measurement with a 25 meter separation and the speed of response of the overall system.

Based on information from SP-100 LVDT testing, a few development items that will need to be addressed:

- An improved bobbin-coil assembly design of the LVDT sensor should permit the length of the LVDT to be extended well beyond the current 5 inch limit.
- A method of terminating the lead wires on the body of the Sensors needs to be developed; lead wire cables of the prototype were difficult to work with and are fragile.
- Use of high frequency excitation to eliminate or reduce temperature dependence effect should be investigated.
- The verification process used in the manufacturing of an LVDT should be eliminated as this could extend the operating temperature range of LVDT.
- A null adjustment (e.g., a movable magnetic slug) for the limit switch needs to be developed.

1.2.4.1.6. Eddy Current

An eddy current displacement sensor consists of a generation/detection coil, target, and necessary electronics. An eddy current sensor can be modeled as a transformer with a coupling coefficient that depends on standoff. Practical eddy current sensors vary in diameter from a few millimeters to a meter and have maximum sensing ranges roughly equal to the radius of the coil. Operating frequencies can be as low as 100 kHz. Temperature drift, a substantial source of uncertainty, can be partially compensated for by independent temperature measurement and the application of a mathematical model. Temperature stability, especially at 780K makes eddy current based position measurement a problematic technology.

1.2.4.1.7. Potentiometric Techniques

Resistor potentiometers are an electrical contact-based technology. The contact, which generates noise, is notoriously unreliable. This particular position measurement technique is clearly not suitable for space reactor applications.

1.2.4.2. Rotary Measurement

1.2.4.2.1. Magnetic

1.2.4.2.1.1. Hall Sensor

A Hall-effect element is a thin sheet of conductive material with output connections perpendicular to the direction of current flow. To measure rotary position, manufactures have devised a vertical Hall sensor that re-routes the magnetic flux lines. Accuracy of 0.35 degrees and resolving power of 0.1 degrees are possible over 360 degrees of rotation. Other advantages are linearity, low power consumption and weight. The limiting factor for space reactor applications is the need for electronic signal conditioning and amplification close to the sensor. The materials of construction of the vertical Hall-effect sensor are silicon, which has limitations at expected service temperature and radiation levels.

1.2.4.2.1.2. Magnetoresistive

Thin-film ferromagnetic materials exhibit a significant change in resistance as a function of direction of magnetization in the film. The resistance of the material is highest when the magnetization is parallel to the electrical current in the film and lowest when it is perpendicular.

Rotary position sensors are commercially available based on the magnetoresistive property. Advantages to this technology are angular range (360 degrees), linearity, resolving power, and weight. The major disadvantage is intolerance to high temperature and radiation.

1.2.4.2.1.3. Magnetic Microcantilever Switch Array

A magnetically-actuated microcantilever switch array can be fabricated to determine rotational position. The resistors and magnet used in this switch array have high radiation tolerance. Deleterious temperature effects can be minimized by using a bridge network.

1.2.4.2.1.4. Magnetostrictive Rotary Position Sensor

The same technology of linear magnetostrictive position measurement as described above can be applied to measurement of rotation. The benefits of this technology are high radiation and high temperature tolerance.

1.2.4.2.2. Optical Encoder

Optical encoders are the most widely used rotary position sensor in industry. They offer precision, long life, low cost, and low power consumption. The drawback of the optical encoder technique is the radiation tolerance of the solid-state optical components. Light-emitting diodes and silicon phototransistors are susceptible to neutron exposure. A 3×10^{12} n/cm² fluence reduces photo current in phototransistors by as much as 90 percent with significant increases in noise. Photo detectors and LED emitters cannot be placed at the encoder because of the aforementioned radiation damage problem. A possible means of overcoming these radiation limitations is to locate the solid-state optical components at the mission module where radiation levels are significantly lower. Although achievable, the optical encoder measurement solution seems like an overly complex approach.

1.2.4.2.3. Resolver

Position measurement by a rotary resolver is based on a rotary transformer that changes output with shaft position. Rotary resolvers are off-the-shelf components from several manufactures. One manufacturer has developed a resolver with up to 360 degree rotational range. This manufacturer has developed and tested resolvers for high gamma radiation environments (1×10^8 rad). Resolvers have a significant temperature coefficient that must be compensated and moving parts that must be lubricated. Resolvers have relatively high excitation voltages, which potentially improves signal-to-noise ratio and eases the burden of designing sensitive electronic circuits.

1.2.4.2.4. RVDT

The rotation variable differential transformer (RVDT) is similar to the rotary resolver in function and conceptually identical to the LVDT. Like the resolver, the RVDT has advantages of commercial availability, radiation and neutron hardening and good signal-to-noise. A unique disadvantage of the RVDT is the limited angle through which it can be rotated, which is ± 30 degrees. Development is required for both the transducer and electronics, which might require a software or firmware solution.

1.2.4.2.5. Capacitance

A capacitance-based rotary position sensor can be developed that will measure ± 90 degrees as required. The concept has been implemented at ORNL but no commercial device is available. With a driving frequency of several tens of kilohertz, response times of less than 1ms should be achievable including averaging, which reduces uncertainty. Moving parts of concern are the same as for resolvers and RVDT- the bearings, which must be lubricated for high temperatures, long mission period, and a few tens of thousands of operational cycles.

1.2.4.3. Limit Switches

Limit switches are binary sensors and may be used to indicate discrete control element position. They can be used for either linear or rotary movement. Limit switches fall into two categories: electro-mechanical micro-switches operated by an external object or proximity sensors operated upon by a non-contact field in their vicinity.

1.2.4.3.1. Contact Limit Switches

Micro-switches are commonly used devices that are found in many terrestrial applications. The standard micro-switch is capable of completing or interrupting current flow without requiring additional electronics. Their simple configuration and material of construction allows them to tolerate harsh environments. The disadvantage is contact welding in a vacuum environment.

1.2.4.3.2. Non-Contact Limit Switches

Non-contact proximity sensors use a variety of sensing schemes: variable inductance or capacitance, ferrous contacts that operate in the presence of a magnetic field, an optical path (by light interruption or reflection), etc. These devices are not subject to contact welding or failure due to mechanical wear out. Their action can be compromised by changes in the actuating field, stray fields and EMI, and aging of the electronics.

1.2.4.3.2.1. Induction

The metal detector principle in which coil inductance changes near a metallic object can be applied in a miniature form where the electronics and an induction coil are housed together to make a compact sensor. The distance at which the sensor gives positive indication is determined by a threshold comparison. The advantages are compactness and characteristic of not being affected by liquids or vapors. The disadvantage for space nuclear applications is the proximal location of electronics, which would not tolerate operating temperatures and radiation environment.

1.2.4.3.2.2. Magnetic

The reed switch is very similar in action to the micro-switch except that it functions as a non-contact measurement. The reed switch can be constructed of materials capable of operating in the space nuclear environment. The temperature limit would be around 830K. Reed switches have been manufactured commercially for more than fifty years. The disadvantage is the strength of the magnetic field determines the distance at which the switch closes, and because the field strength diminishes over time the sensor's trip point will be shifted.

1.2.4.3.2.3. Capacitance

Proximity sensors based on capacitance measurement are available commercially. Their operation is the electrical analog of the induction-based proximity sensor. The electronics must be close to the point of measurement because capacitance values that must be measured are very small. The disadvantage for space nuclear applications is the proximal location of electronics, which cannot tolerate operating temperature and radiation environment.

1.2.4.3.2.4. Optical

Optically-based limit switches require an emitter and detector of light. Two modalities are that of breaking a light beam and receiving a reflection from a mirrored surface. For space nuclear power applications, the electronics package may be located remotely in a lower temperature and radiation environment. Given that the electronics are remote, the remaining disadvantage of optical limit

switches for space nuclear applications is the gradual darkening of optical fibers from gamma exposure. Because of the binary nature of the measurement, darkening may not present a problem.

1.2.5. ORNL Recommended Sensor Technologies and Basis

The following summarizes ORNL selections for each reactor and their technical basis.

1.2.5.1. Reactor Power Level (Neutron Flux)

Fore-of-shield detectors were preferred because of their long-term operation due to their lack of dependence on shield invariance. But an aft-of-shield region provides a milder environment so commercially available fission counters (encased in a moderator layer) can be directly applicable to power-range measurement in this region.

Higher temperature tolerant gas filled detectors were recommended as the only viable detector class for fore-of-shield deployment. Fission chambers, ^{10}B lined ion chambers, and ^3He detectors without hydrogenous or fluorine based quench gasses were potential candidates. Fission chambers were preferred for pulse mode long-cable deployments such as the initial start-up of the JIMO reactor because of their larger pulse sizes. The secondary choice for a fore-of-shield neutron detector was a Helium-3 – argon ion chamber. Table 1.3 shows the ranking for the neutron flux measurement technology for the fore-of-shield region.

Table 1.3. Neutron Flux Technology Ranking for fore-of-shield

Neutron Flux Technology	Ranking
Fission Chambers	1
Helium-3 Detectors	2

Ion chambers were not strong candidates for aft-of-shield deployment due to the large amount of background that would be caused by the Jovian environment. Non-fission based detectors located aft-of-shield can not be used because the radiation environment would significantly contaminate the signals. The choice for an aft-of-shield neutron detector was a commercially available component closely resembling a high-temperature-tolerant, high-sensitivity fission counter encased in a neutron moderator layer. The second choice for an aft-of-shield deployment was to replicate the extremely high temperature fission chamber from the front side of the shield. Table 1.4 shows the ranking for the neutron flux measurement technology for the aft-of-shield region.

Table 1.4. Neutron Flux Technology Ranking for aft-of-shield

Neutron Flux Technology	Ranking
High-Temp, High- Sensitivity Fission Counter (w/ Neutron Moderator Layer)	1
Extremely High Temp Fission Chambers	2

Three different material classes were chosen as candidates for the fore-of-shield fission chamber. The leading candidates for the structural materials were carbon-carbon composite (and/or vitreous carbon) shell materials. Refractory carbides (e.g. ZrC) were a choice as the anode. The cathode choice was an inner uranium carbide layer on the carbon-carbon composite and the electrical insulator choice was vitreous carbon. The second choice for materials was a precious metal alloy as the chamber interior wall/cathode (Ir-Pt alloy) and the anode wire. The choice for the anode to cathode insulator pieces was a single crystal sapphire. The precious metal components were to be thin and backed by an Inconel outer shell to lower chamber costs. The fissile material choice was a uranium oxide (either UO_2 or U_3O_8). The issues for this system were the stability of the fissile material layer at temperature on the precious metal wall and the joining technique for the insulator to metal seal. A third lower preference choice was to fabricate the fission chamber from a refractory alloy. The reason this option was last on the list was because the refractory alloys are very difficult to join, are sensitive to the same oxidative processes that restrict the applicability of the Inconel chambers, are potentially sensitive to nitrogen based radiolytic attack from the fill gas, and may suffer from radiolytically produced oxygen embrittlement.

1.2.5.2. Reactor Coolant Temperature

The four technology classes reviewed by ORNL were thermocouples, resistance thermometers, pyrometry (radiation thermometers), and ultrasonic probe-based thermometry. Tables 1.5 and 1.6 were used by ORNL to provide a recommendation on which technologies were most suitable to pursue for the mission.

ORNL recommended performing a detailed system design to evaluate the degree of difficulty in creating adequately precise high-speed electronics. The overall preferred option to pursue for reactor coolant temperature measurement by ORNL is the resistance thermometry with in-situ recalibration via Johnson noise techniques. The recommended back-up technology was the ultrasonic thermometry specifically for temperature profile mapping during the coolant thaw. ORNL chose ultrasonic thermometry over pyrometry due to the lesser degree of difficulty in developing a probe that was capable of fore-of-shield deployment combined with the possibility to make temperature measurements at multiple points with a single measurement channel. Table 1.7 shows the ranking for the reactor coolant temperature technology.

ORNL concluded that thermocouples were not a choice for the primary coolant temperature measurement because over the course of the mission their measurement channels would likely drift beyond reasonable performance boundaries. Resistance thermometers were also not a choice unless in-situ recalibration circuitry was included with their measurement. Johnson noise based RTD recalibration technology development would likely require significant resources. It was recommended to pursue a more detailed system designed to gain a more accurate evaluation of the how difficult the recalibration electronics development would be. ORNL states that an aft-of-shield radiation thermometry may be useful if the total dose to the optical fibers remains less than 10^4 Gy. Ultrasonic thermometer's biggest issues were seen in the signal processing and ultrasonic drive/receive electronics. ORNL concluded that the transducer elements were adequately radiation tolerant and of low enough drift to perform well aft-of-shield and likely fore-of-shield.

Table 1.5*. Summary of Candidate Temperature Measurement Sensors Strengths and Weaknesses.

Technology	Strengths	Weaknesses	Maturity Level
Thermocouples	<ul style="list-style-type: none"> • Simple electronics • Highly rugged • Well-known • Wide usage base 	<ul style="list-style-type: none"> • Seebeck coefficient drifts with time at temperature and accumulated dose • Electronics challenging to implement in a long-term stable form at the electronics vault dose level • Magnetic susceptibility for several types 	<ul style="list-style-type: none"> • Well-established commercial technology • Radiation tolerant readout electronics developmental
Resistance Thermometry	<ul style="list-style-type: none"> • Wide experience base • Simple electronics • Can be recalibrated in-situ to first principles 	<ul style="list-style-type: none"> • Drifts with time at temperature • Can fail catastrophically for some sensor implementations • Recalibration requires advanced electronics 	<ul style="list-style-type: none"> • Lower temperature tolerant (~1000 K) RTDs widely available • Advanced RTD elements developmental • Recalibration electronics developmental
Pyrometry	<ul style="list-style-type: none"> • Quasi-first principles measurement technique • Applicable to very high temperatures 	<ul style="list-style-type: none"> • Measurement depends upon knowledge of emissivity of source • Requires stable optical path. 	<ul style="list-style-type: none"> • Optical path development for fore-of-shield very developmental • Aft-of-shield optical path somewhat developmental
Ultrasonic Thermometry	<ul style="list-style-type: none"> • Applicable to very high temperatures • Multiple measurement locations with single sensor 	<ul style="list-style-type: none"> • Processing algorithms are complex • Requires high speed electronics • Vulnerable to drift in both transducer and electronics 	<ul style="list-style-type: none"> • Non rad-hard versions commercially available • Radiation hardened system design developmental

Table 1.6*. Overall Conclusions Transducer Evaluation for Reactor Coolant Temperature Measurement

Criteria	Thermocouple	Resistance	Radiation	Ultrasonic
Radiation Tolerance	F	P	P	D
Drift	F	D	D	D
Precision	P	P	P	D
R&D needed	X	3	3	3

Legend:

P=Pass

F=Fail

D=Pass with development

R&D needed - 1=little, 5=lots, X=may not help.

Table 1.7. Reactor Gas Coolant Temperature Technology Ranking

Reactor Coolant Temperature Technologies	Ranking
Resistance Thermometry	1
Ultrasonic Thermometry	2

1.2.5.3. Reactor Gas Coolant Flow

Primary consideration in the selection of flow measurement technologies is to avoid introducing penetrations to the reactor pressure boundary. This left only non-invasive gas flowmeter technologies. These technologies were vortex shedding, clamp-on ultrasonics, coriolis, cross correlation technique, thermal mass flowmeter, and inferred flow from compressor. Table 1.8 and Table 1.9 were used by ORNL to provide a recommendation on which technologies were most suitable to pursue for the mission.

Both the ultrasonics time-of-flight and the vortex shedding technologies were leading candidates because they both were highly developed, had been commercially available for many years, have shown to be reliable in industrial settings, and could have been adapted to high temperature applications. The ultrasonic time-of-flight technology had multiple beams and could have a higher accuracy and rangeability than the vortex shedding meter. Therefore, ORNL's preferred option was the ultrasonic time of flight (TOF) flow sensor. The technology is noninvasive, can withstand sensor degradation, is commercially mature, and has proven high reliability. The backup gas flow measurement technology was the vortex shedding flow meter with clamp-on strain gages. The vortex

shedding method should create relatively large vortices and pressure pulses; larger than the cross correlation technique that relies on inherent flow structures.

Table 1.8*. Comparison of Candidate Gas Flow Technologies

Technology	Strengths	Weaknesses	Maturity Level
Vortex Shedding	Good linearity over 20:1 flow range. Accuracy meets desired value. Flow response is essentially independent of fluid density.	Flow response is sensitive to flow profile. Must be individually calibrated and is sensitive to bluff body profile changes. Vortex detection sensors are not proven at high temperatures and radiation levels.	Commercially available, significant experience in gas flows. Some development required for ultrasonic transducers meeting temperature and radiation; same with strain gage technology although not commercially available with a vortex shedding flowmeter.
Clamp-on Ultrasonics	Very wide rangeability; can measure low flows (to 0.03 m/s, 0.1 ft/s). High accuracy especially with multibeam meters. Completely non-invasive. Potential to measure temperature, density, and mass flow	Affected by flow profile and swirl. Detectors are not proven at high temperatures and radiation levels.	Commercially available, significant experience in liquid flow, much less in gas. Some development required for ultrasonic transducers meeting temperature and radiation.
Coriolis	Measures mass flow and fluid density. Very high accuracy. Good rangeability. Independent of fluid properties and needs very little straight piping upstream.	Requires vibrating piping and is sensitive to equipment-induced pipe vibrations. Uses 5 sensors to make measurement including temperature. Sensitive to elastic modulus changes. Shock sensitive and potential zero shift. Requires special pipe section.	Commercially available. Significant development required for radiation hardening of all 5 sensors and for maintaining calibration.
Cross Correlation Technique	Completely non-invasive. Technique is mature.	Measures flow structure velocity not mean velocity. Structure	Technique used for years, fairly recently commercialized. Some

		velocity to mean velocity relationship varies with Reynolds number. Detectors are not proven at high temperatures and radiation levels.	development for ultrasonic transducers meeting temperature and radiation; same with strain gage technology.
Thermal Mass Flowmeter	Measure mass flow directly	Not suitable for use on high heat capacity coolant loops. Requires a matched pair of highly accurate temperature sensors	Technique has been used for many years.
Inferred Flow from Compressor	Based on Existing System Compressors and use existing current/voltage sensors.	The output flow to power input calibration relationship may be wear related and thus time dependent.	Technique not in common use. Some development needed to determine the expected uncertainty and reproducibility of calibration relationship

Table 1.9*. Strength/Weakness Summary of Candidate Gas Flow Technologies

Flow Technology/Criteria	Vortex Shedding	Clamp-on Ultrasonics	Coriolis	Cross-Correlation	Thermal Mass	Compressor Inferred Flow
Accuracy					W	W
Simplicity			W			S
Maturity				W		W
Degradation Tolerance	S	S	W	S	W	
Launch Survivability			W			
Vibration Sensitivity			W			
Completely Non-invasive	W		W			S
Transducer Location			W			S
Uses Existing System Component						S

In addition, ORNL concluded that the compressor inferred flow technique should not be considered as a candidate for the flow sensor. This method would not result in highly accurate flow measurements (less than 5-10%), and there were concerns about compressor changes (wear) that could affect the power to flow relationship that would result in calibration shift. ORNL did state that the coriolis flowmeter had a significant advantage because it measured the mass flow which is directly related to the heat transfer ability of the gas coolant. Still the coriolis flowmeter was ranked the lowest option because of the number of sensors involved and material effects due to temperature and radiation. The technique was very intrusive on the flow pipe and required a special designed pipe. The thermal mass flowmeter was attractive in that it measured flow directly and it functioned in a very non-intrusive way because it used a clamp-on technique. ORNL concluded that this method was not suited for use on high heat capacity coolant loops where the temperature differences are inevitably small. The cross

correlation technique was attractive because it was non-invasive and could function as a clamp-on flowmeter. This technique does not measure the velocity directly, but instead measures the velocity of turbulent structures. Also, because the cross section correlation technique depends on the presence of turbulent flow structures, it cannot provide measurements during thaw and start-up when the flow velocity is low. Table 1.10 shows the ranking for the reactor gas coolant flow technology.

Table 1.10. Reactor Gas Coolant Flow Technology Ranking

Reactor Gas Coolant Flow Technologies	Ranking
Ultrasonic Time-Of-Flight	1
Vortex Shedding	2
Cross-Correlation	3
Thermal Mass	4
Coriolis	5
Compressor Inferred Flow	Not Considered

ORNL also performed an evaluation on measuring flow when a liquid coolant was used instead of a gas coolant. This evaluation strongly recommended two methods; the magnetic conduction flow sensor and the ultrasonic time-of-flight sensor. The magnetic conduction flow sensor minimizes contact with the flow pipe, which is desirable because of the high temperature of the contained liquid metal. During the down-select the reactor coolant was determined to be a gas instead of a liquid.

1.2.5.4. Control Element Position

The eight technology classes reviewed by ORNL for linear position were capacitance, microwave, magnetic microcantilever switch array, magnetostrictive, laser rangefinder, LVDT, eddy current, and potentiometric. The eight technology classes for rotary position were the hall effect sensor, magnetoresistive, magnetic microcantilever switch array, magnetostrictive, optical encoder, resolver, RVDT, and capacitance. Table 1.11 was used by ORNL to provide a recommendation on which technologies were most suitable to pursue for the mission.

ORNL concluded from their assessment that no single technology displayed characteristics and performance metrics that make it clearly superior to the other technologies. The primary recommendation for position measurement was LVDT for linear and resolver for rotary. These top technologies are mature with commercially available models but the models do not meet mission requirements. Table 1.12 shows the ranking of the linear position measurement technologies.

ORNL backup recommendation for both types of position measurement is capacitive position sensing. The selection of the capacitive position sensing as a backup is due to the overall robustness to temperature and radiation. However, their use as a position measurement instrument is not as commercially developed as the LVDT and resolver. Table 1.13 shows the ranking of the resolver position measurement technologies.

Table 1.11*. Comparisons of candidate technologies strengths, weaknesses, and maturity level.

Technology	Strengths	Weaknesses	Maturity Level
Linear Position			
Capacitance	Sensor immune to radiation effects. Can be made of materials to withstand full operating temperature. Reasonable accuracy and resolution is feasible. Should be a reliable technology. Transducer is relatively simple. Electronics can be remote.	Good engineering and materials selection is necessary to obtain a high capacitance ratio. Prevention of charge buildup must be incorporated.	Linear capacitors are made for high power RF systems. However, they are not commercially available for linear displacement. A development effort will be required to bring this technology to deployment level.
Microwave — time domain reflectometry or phase measurement	Non-contact method	Wavelength needs to be very short to attain fine resolving power. Electronics has to be near the Gunn diodes; therefore may not very radiation tolerant. Vacuum tube solutions do not work at sufficiently high frequencies and have lifetime issues.	Commercially available but not to the requirements of space reactor applications. Development of millimeter wave measurement requires significant effort.
Microwave — resonant cavity	Linear response to position. Measurement is based on a frequency measurement, which can be made very accurately.	Complex circuitry required to sweep frequencies of a few Gigahertz.	Not commercially available. Development required.
Magnetic Microcantilever Switch Array	Highly linear response. Positive discrete response as magnet is moved along array. Electronics can be remote. High signal levels for good signal-to-noise. Good immunity to radiation. High temperature operation should be possible.	Fine engineering needed to make microcantilevers robust to launch vibration. Compensation needed since magnet is subject to field strength reduction with exposure to radiation.	Technology is not available commercially. Development required.
Magnetostrictive	Potentially tolerant to high radiation environments. Electronics can be remote. High resolution possible. Basically, an ultrasonic measurement.	Magnet subject to field strength reduction with prolonged exposure to radiation. So long as field reduction does not affect timing, it may not be a disadvantage.	Commercially available but not to the requirements of space reactor applications. Further development needed.

Technology	Strengths	Weaknesses	Maturity Level
Laser Rangefinder	Non-contact. High resolution possible.	For commercial devices, optical transducers are mounted very close to the point of measurement. For high temperature and radiation environment, sensitive transducers must be connected through fiber optic bundle. Fibers are gamma sensitive.	Commercially available but not to the requirements of space reactor applications. Fiber connected system is not commercially available. Development required.
LVDT	Tolerant to high radiation and temperature environments expected in space nuclear applications.	Accuracy is sensitive to temperature and must be compensated. Measurement range of commercial devices must be extended.	Commercially available and one of the most mature linear position measurement technologies. However, some development still required.
Eddy Current	Reliable and repeatable method. Non-contact measurement. Components are simple and very radiation tolerant.	Practical eddy current systems require a large coil and target. The diameter of the target is sufficiently large (25 cm or larger) as to make a system of 12 instruments difficult to engineer.	Systems are commercially available. Development required to effect size reduction.
Potentiometric	Simple electronics. Simple concept.	Sliding electrical contact is notoriously noisy and subject to dead spots from corrosion, deposition, and material migration.	One of the most commercially mature technologies. Potentiometers and rheostats have been around since the turn of the 19 th century.
Rotary Position			
Hall Effect Sensor	Small package. Excellent accuracy and resolving power. Full rotational range of 360 degrees.	Readout electronics must be near the transduction device because of small signal levels involved. Thus, will be subject to temperature and radiation in excess of its ability to withstand.	Commercially available off-the-shelf technology. Cannot be made robust to the space nuclear environmental conditions.
Magneto-resistive	Small package and excellent resolving power. Full rotational range of 360 degrees.	Readout electronics must be near the transduction device because of small signal levels involved. Thus, will be subject to temperature and radiation in excess of its ability to withstand.	Commercially available off-the-shelf technology. Cannot be made robust to the space nuclear environmental conditions.

Technology	Strengths	Weaknesses	Maturity Level
Magnetic Microcantilever Switch Array	Linear response. Positive discrete response created as magnet is rotated. Accuracy and resolving power fixed by design of cantilevers. Electronics can be remote. High signal levels for good signal-to-noise. Good immunity to radiation. High temperature operation should be possible. Full 360 degree rotational range possible. Very low drift.	Fine engineering needed to make microcantilevers robust to launch vibration. Compensation needed since magnet is subject to field strength reduction with exposure to radiation.	Technology is not available commercially. Development required.
Magnetostrictive	Tolerant to high radiation environments. Electronics can be remote. High resolution possible. Basically an ultrasonic measurement.	Magnet subject to field strength reduction with prolonged exposure to radiation.	Not commercially available but similar to the linear counterpart. Further development needed.
Optical Encoder	Can be made to meet wide range of measurement accuracies. Full 360 degree rotation. Excellent accuracy specifications.	Optical sensors are always placed next to encoder wheel. Sensors are not temperature and radiation tolerant. Optical fibers or waveguides can be used to permit placement of sensors remotely; however, many fibers would be required.	One of the most popular angular measurement technologies. Mature and commercially available technology. However, development of a multi fiber cable would be required to adapt the optical encoder for space nuclear applications.
Resolver	Full 360 degrees of rotation available. Good accuracy. High excitation voltages result in good signal-to-noise ratio.	Significant temperature coefficient must be compensated.	Radiation and temperature tolerant resolver commercially available from Empire Magnetics. Some development required for full adaptation to space nuclear environment.
RVDT	Good linearity and accuracy. Low temperature coefficient. Fast response. Components are potentially tolerant to high radiation and temperature environments.	Rotation angle of only ± 30 degrees. Manufacturer only rates this component to 150°C, with engineering can be made higher.	Commercially available and one of the most mature linear position measurement technologies. Development is required to realize wider rotation range and temperature tolerance.

Technology	Strengths	Weaknesses	Maturity Level
Capacitance	Rotation to 180 degrees available and possibly more if needed. Materials can be used to make fully radiation and temperature tolerant. Reasonable accuracy and resolution is achievable. Should be a reliable technology. Transducer is relatively simple. Electronics can be remote.	Good engineering and materials selection is necessary to obtain a high capacitance ratio. Prevention of charge buildup must be incorporated.	This style of radio tuner capacitor has been available since the 1930's. No commercially available device has been applied to rotation measurement. A development effort is required to bring this technology to deployment level.

Table 1.12. Ranking of linear position measurement technologies

Linear position measurement technology	Ranking
LVDT	1
Capacitive	2
Magnetostrictive	3
Microwave Resonant Cavity	4
Laser Rangefinder	5
Magnetic Microcantilever Switch Array	6

Table 1.13. Ranking of rotary position measurement technologies

Rotary position measurement technology	Ranking
Resolver (Empire Magnetics)	1
Capacitive	2
RVDT (Schaevitz and Trans-Tek)	3
Magnetostrictive	4
Magnetic Microcantilever Switch Array	5
Optical Encoder	6

In conclusion ORNL chose the following primary options for each specific reactor parameters: Fission Chambers for Neutron Flux, Resistance Thermometry for Temperature, Ultrasonic Time-Of-Flight for Flow, LVDT for Linear Position, and Resolver for Rotary Position. More details on each of the sensing techniques can be found in Reference (c).

1.2.6. References

- (a) SPP letter, SPP-67510-0002, Request for NR 08: Technical and Funding Approval of LANL, ORNL, Y-12 Laboratory Support for Space Nuclear Power Systems Development and Request for SNR Action to Transfer FY2004 Funds, for NR and SNR Action, dated July 7, 2004
- (b) NR letter NR:RE:STBell I#04-02412, Space Nuclear – Jupiter Icy Moons Orbiter Reactor – DOE Laboratory Work scopes – Approval with Comment, dated July 14, 2004
- (c) ORNL Report: "JIMO Reactor Sensor Technology Development Plan", Document ORNL/LRT/NR-JIMO/05-01 dated January 2005

Report Title	FISSION CHAMBER DEVELOPMENT
Report Number	ORNL/LTR/NR-PROM1/05-17
Report Date	JULY 2005
NRPCT IV	ORNL-SPP-05-0028

2. Fission Chamber Development

2.1. Overview

In Reference (a) ORNL reported the results of their investigations into fission and boron detectors, silicon carbide (SiC) detectors, and self-powered detectors. As a mature technology with the demonstrated ability to meet the full operational range requirement for the predicted flux levels forward and within the shield, ORNL recommended the pursuit of fission chamber technology at all the various locations, identifying that only the first two locations provided sufficient flux for full range operation. None the less, the severity of the temperature environments in these two locations suggested the need for a non-standard detector whose materials and design would allow it to endure this state for more than a decade.

The NRPCT pursued ORNL recommendation for fission chamber technology and in References (b) through (d) engaged ORNL to develop conceptual designs of fission chambers for monitoring the flux of a nuclear reactor for space applications, as part of NASA's Prometheus project. ORNL developed and reported this effort in Reference (e). The following is a summary of this report (separated by section) followed by an assessment by the Naval Reactors Prime Contractor Team (NRPCT) of the final state of the fission chamber development work for the Prometheus SNPP.

Fission chamber designs were conceived for each of three locations in relation to the reactor shield. The maximum operating temperature requirements for the fore-of-shield (FOS), inside-of-shield (IOS), and aft-of-shield (AOS) locations are 1200 K, 800 K, and 600 K respectively. The fission chambers should monitor reactor power level via measurements of neutron flux from startup through full power, over 9 to 10 orders of magnitude.

The NRPCT completed an evaluation of nuclear instrumentation technology which is presented in Enclosure (5).

2.2. Key Points and Conclusions

2.2.1. Basic Principles of Fission Chamber Operation

A fission chamber is an ion chamber that uses a fissionable isotope (typically ^{235}U -based) to line the detection volume and convert neutron radiation into a measurable ion charge. The chamber's efficiency in detecting neutrons is limited by the thickness of the fissile layer, the thinness and neutron reactivity of the wall material, the fission cross section, and the available surface area. Approximately 0.2% of the estimated 2 grams of uranium applied to the chamber will undergo fission over the duration of the mission.

The high temperature requirements combined with the demands of the fill gas greatly affect the appropriate design choices for the devices, especially for the FOS location. The fill gas

must remain pure over the lifetime of the device, so out-gassing of chamber components must be considered. Negative-ion-forming gases cannot operate at high rates because individual pulses superimpose on each other. Argon is commonly used in fission chambers because it has a high electron-drift velocity, it is inert and relatively inexpensive, and its ion-stopping power is sufficiently large. A polyatomic gas is often added to the noble gas to tailor the gas properties. Nitrogen is the additive of choice because it is relatively inert and does not lead to the deposition of conducting debris inside the chamber. However, carbon and many metals will react with nitrogen at 1200 K, thus limiting the number of candidate structural materials. In addition, the spacing between the electrodes depends on the range of fission fragments in the fill gas. The range in argon at 1 atm pressure is estimated at 1.5 mm, which also dictates the applied voltage to be set from 450 to 500 V.

The report supplies a calculation of how well the FOS detector might perform at reactor startup. The minimum operating flux is specified to be 1 nv, equating to 9.25×10^7 neutrons/s assumed to be available for detection. As an estimate, if the reactor is started with k_{eff} of 0.975, the required source strength is 2.31×10^6 neutrons/s. Radioactive sources of this size are readily available, if necessary. If approximately 100 s is considered a reasonable time to wait, then step changes of k_{eff} by 0.005 or greater can be detected with a 95% confidence level for values of k_{eff} greater than 0.975.

2.2.2. Detector Electronics

The fission chamber usually collects charge from a neutron event within tens of nanoseconds, so very high detection rates are possible. Due to the wide dynamic range of potential rates, several signal processing techniques are employed together to cover the entire range. For the low (startup) rates of the source range, neutrons are counted by individual pulses in *pulse mode*. A discriminator can be set to trigger on the larger neutron-induced fission pulses and ignore the smaller gamma-induced pulses. Pulse pile-up limits the maximum count rate as reactor power increases through the intermediate range, at which point *Campbelling mode*, or mean-square voltage mode, can be employed. In *Campbelling mode*, the pulse stream is AC-coupled, and the remaining signal is proportional to the square root of the variance. One advantage of this mode is that the difference in signal amplitude between neutrons and gammas is enhanced by the square of their ratio. At higher rates in the intermediate and power ranges, the need to discriminate neutrons and gammas is diminished, and a simple *current mode* can be employed so that the voltage across an output resistor is proportional to the event rate in the detector. An alternative *extended-range counting mode* is also considered, because it allows a larger counting range without switching and can tailor the sensitivity to the current operating level. The report includes the descriptions of implementation methods for these various modes.

2.2.3. Uranium Coatings

Uranium oxide is the initial choice for fissile coating material over uranium metal, uranium carbide, and uranium nitride. In Ar-10%N₂ fill gas, uranium oxide is predicted to be stable and without nitride-production at 1273 K. However, the effects of thermal cycling of oxide films on the candidate materials should be evaluated. The current coating method of choice is electrodeposition, a plating process, although other methods are available in case of adhesion problems. The metal surface must be clean and smooth for proper adhesion. Also, long-term compatibility between the base metal and the coating must be determined experimentally.

2.2.4. Fore of Shield Design

The FOS device is envisioned to be a two-gap, three-electrode instrument constructed from concentric cylinders of oxide dispersion-strengthened nickel, with an exterior diameter of 5 cm and a length of 30 cm. Single crystal sapphire (Al_2O_3) is the clear choice for insulating material due to its high-temperature stability. The chamber is expected to use approximately 2 grams of ^{235}U spread over an estimated area of 1300 cm^2 . The optimum fill gas is Ar-10% N_2 , simultaneously supplying both sufficient stopping power and high electron and ion mobility. Noble gas mixtures could be studied as alternative fill gases. The designed thermal neutron sensitivity is 1 count per second per unit incident flux (cps/nv_{th}). The FOS detector is intended to function up to 1200 K, without significant performance degradation due to radiation and temperature effects throughout the mission.

The best candidate material is a dispersion-strengthened nickel-alloy with up to 4% ZrO_2 or Y_2O_3 . This material will not react with the nitrogen gas and has good reported mechanical properties. Literature indicates adequate creep strength to permit wall thickness of 1 mm or less to contain the fill gas at 1200K. Aside from platinum alloys, all other commercially available materials either do not have adequate strength or are not compatible with nitrogen gas. Coating a base material (carbon, for example) to prevent nitrogen reactions presents an unacceptable risk of system failure. The nickel material requires no coating and, if used in 3-mm walls, will result in a sensitivity of about 1 cps/nv. However, the material is sufficiently strong that a thinner wall can be used for increased sensitivity. For the benefits of lighter weight and higher sensitivity, carbon infiltrated by silicon carbide and coated with platinum or rhenium could be evaluated as an alternative structural material.

For most candidate materials, the sensitivity of the FOS chamber will increase with decreasing temperature. This is a consequence of the faster increase of the uranium cross section with decreasing neutron energy compared to the wall material's capture cross section. The higher sensitivity at low temperatures should aid the detection of low flux levels at reactor startup.

2.2.5. In-Shield Design

The IOS device can utilize the same FOS design if it is located in the forward area of the shield, because the thermal neutron flux should be similar to FOS levels. Since the maximum temperature specification is relaxed to 800 K, the structural material may change from dispersion-strengthened nickel to an Inconel alloy. ORNL previously designed another potential device, called the High Temperature Moderate Sensitivity Fission Chamber (HTMSFC), with four times the sensitivity of the FOS design. A 7-tube version of the HTMSFC that would be appropriate for the IOS device requires 4.5 grams of ^{235}U , is 67 cm in length and 6.7 cm in diameter. The neutron flux levels will vary dramatically with position within the shield, so the higher-sensitivity chamber may be considered. Centronic, Ltd. In the UK sells the FC538 fission chamber with 0.5 to 1.8 cps/nv sensitivity at a maximum temperature of 773K in a package 4.75 cm diameter by 55.1 cm long. ORNL recommends the FOS design using the alternative Inconel material, plus testing the Centronic chamber at 800K as a possible cost-effective solution.

2.2.6. Aft of Shield Design

Commercially available fission chambers with similar dimensions to the custom units should be satisfactory to meet the temperature requirement of 600K for the AOS position. The AOS device has no chance to observe startup of the reactor, since the flux levels should be at least

4 to 5 orders of magnitude lower than FOS. A 1-cps/nv chamber in the AOS position may only operate above a reactor power level of 1 to 10 percent. ORNL recommends the purchase and evaluation of appropriate commercial devices for the AOS location.

2.2.7. NRPCT Assessment

The FOS detector design developed by ORNL was strongly driven by the high temperature requirement of 1200 K, that itself was based on the possibility of a refractory metal pressure vessel operating at near the maximum reactor outlet temperature of 1150 K. As development work on the Prometheus reactor plant concept has continued, superalloy materials have supplanted the refractory metals for the vessel and piping system. These would have a maximum operating temperature limit near 900 K. On this basis the NRPCT was evaluating a relaxation of the 1200-K temperature requirement for the FOS fission chamber to 1000K or lower, depending on the outcome of thermal analyses. For the IOS detector design, the temperature requirement of 800K was driven by the notional lithium hydride shield concept. The lithium hydride shield has the highest shield operating temperature (600-800 K) of all the concepts being considered by the NRPCT which include Be-B₄C, H₂O, and other organic and hydrogenous systems. Until the final selection of a shielding concept and material the temperature requirement for the IOS would probably remain 800 K. In general, NRPCT recognizes that a lower environmental temperature for all the detector locations can significantly ease the detector design requirements that could allow the use of other structural materials with more desirable properties and/or better commercial availability. One considered alternative is Inconel, which was recommended for the IOS conception of the fission chamber.

Enclosure (5) of this closeout report details the NRPCT work and evaluations regarding the Prometheus SNPP nuclear detector. In the enclosure, the notional arrangement concepts of the nuclear detectors forward of the shield and within the radiation shield are presented for a gas cooled reactor with slider reflector reactivity control. The fore-of-shield detectors are located in the fixed external beryllium reflector near the forward face of the reactor shield with four detectors positioned in separate quadrants about the ring. The in-shield detectors are located within a few centimeters of the front face of the shield embedded in a layer of beryllium. Several possible detector configurations are postulated for this location. In the concepts for both regions, the beryllium acts to thermalize the leakage neutrons for neutron detector operation. These arrangements would have been used by the NRPCT working with the shielding and neutron detector designers to achieve an optimum detector size and sensitivity for the SNPP.

2.2.8. Key Conclusions

The following are key conclusions and recommended future work determined by the NRPCT regarding the ORNL conceptual designs of the fission chambers for the various locations.

- The high temperature of the operational environments for the FOS and IOS detectors is drives significant development risk into the detector designs. Strong efforts should be made to reduce the temperature requirements at both locations.
- The ORNL detector designs of Reference (e) were developed at a time when environmental temperatures near the reactor were near 1200 K and there was limited information existed regarding the reactor plant arrangements and the shielding and structural materials for the gas cooled Brayton SNPP. The environmental temperatures have been reduced and the plant arrangements and materials at the closeout of the

NRPCT work are better understood. Future detector design efforts should avail themselves of this information.

- The NRPCT anticipates that a fission chamber located either FOS or IOS should be capable of full flux range monitoring. The AOS detector could be developed as a partial-range alternative, to be considered for implementation in tandem with a reactor-startup detector, in case a workable full-range detector cannot be developed.
- ORNL recommended the evaluation of commercial fission chambers as potential cost-effective solutions for the in-shield and aft-of-shield locations. NRPCT agrees with this consideration, being mindful of the need to limit the size and weight of the detectors in these locations. .

2.2.9. References

- (a) ORNL Report: "JIMO Reactor Sensor Technology Development Plan", Document ORNL/LRT/NR-JIMO/05-01 dated January 2005
- (b) SPP-67610-0002, Request for NR 08K Technical and Funding Approval of Oak Ridge National Laboratory (ORNL) Support for Space Nuclear Power Systems Instrumentation and Controls Development, for Action, dated February 3, 2005
- (c) NR letter NR:IC:SJKurth K#05-00718, Space Nuclear Power Plant – Instrumentation and Control Equipment – Workscopes for Sensor Development and Systems Development by Oak Ridge National Laboratory; Approval of, dated February 22, 2005
- (d) Information To Vendor (Space Power Plant Program), ORNL-SPP-05-0028, Sensor Technology Development – Reactor Neutron Flux, dated March 1, 2005
- (e) ORNL Report: "Fission Chamber Development", Document ORNL/LRT/NR-PROM1/05-17, dated July 2005

Report Title	ULTRASONIC FLOW METER SYSTEM CONCEPTUAL DESIGN
Report Number	ORNL/LTR/NR-PROM1/05-19
Report Date	AUGUST 2005
NRPCT IV	ORNL-SPP-05-0031

3. Ultrasonic Flow Meter System Conceptual Design

3.1. Overview

This paper contains the comments and assessments of the NRPCT on the report written by ORNL, "Ultrasonic Flow Meter System Conceptual Design" ORNL/LTR/NR-PROM1/05-19. The task of ORNL was to define a conceptual design for an ultrasonic reactor coolant flow measurement system that would provide an accurate, fast-response flow measurement for 15 to 20 years. The report covered the transducer and measurement methods, including the electronics and signal processing. It also included a conceptual design including a description and analysis of the components and the overall flow measurement system.

3.2. ORNL Recommended Technique

In the initial phase of NRPCT sensor development two forms of reactor coolant were under consideration by the SNPP, liquid metal (Li, Na, NaK) and gas (He-Xe), contained inside a refractory metal reactor coolant system. For both coolant systems, a flow technology was sought that would allow accurate measurement of flow independent of the pump, circulator, or machine inducing it. Moreover, as sensor penetrations were considered to represent potential leak paths for the coolant, this technology was to be noninvasive. In Reference (a) ORNL identified ultrasonic flow technology as the only viable candidate for a gas cooled reactor. In References (b) through (d), ORNL was engaged work was engaged in the development of a conceptual design for such a sensor to measure the coolant flow at the reactor inlet at 1100K service temperature. ORNL performed this work and reported their results in Reference (e).

The primary ultrasonic flow measurement technique chosen by ORNL was the crossed-path transit time method. This measurement system concept addresses the high temperature environment, the signal-to-noise ratio, the flow profile effects, and creates some measurement redundancy. In the crossed-path transit time method, shear waves are generated by an ultrasonic transceiver and transmitted into a shear waveguide that is welded to the pipe wall. The shear waves then go through a mode conversion at the pipe wall/gas interface and are converted into longitudinal waves. The longitudinal waves traverse the gas within the pipe, are then converted back to shear waves and travel through a second waveguide to a second transceiver. Two transceiver pairs are used to create a crossed-path measurement path. The velocities from each path are averaged to produce a result that is less sensitive to flow profile effects. The recommended setup for the ultrasonic flow measurement can be seen Figure 3.1.

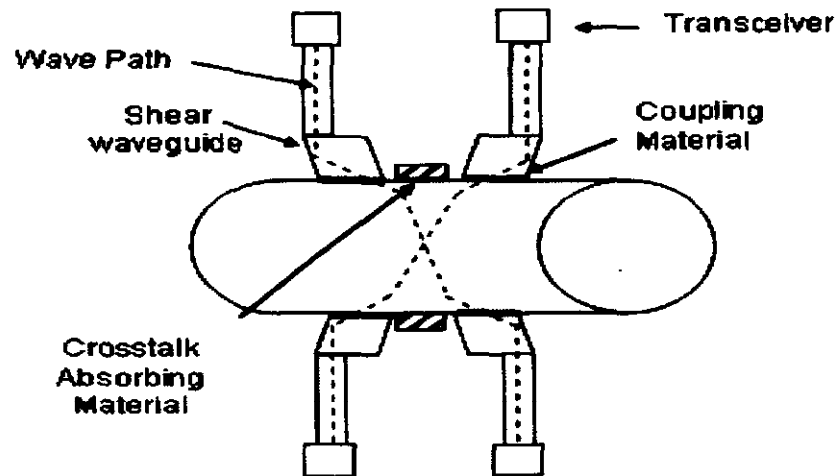


FIGURE 3.1 ORNL Recommended Flow Measurement Layout

3.3. Key Points and Conclusions

3.3.1. NRPCT Evaluation

The NRPCT completed an evaluation of ultrasonic flow technology which is presented in Enclosure (3).

3.3.2. NRPCT Comments

3.3.2.1. Transducer Backing Material

The backing material is used to absorb or dispose of the ultrasonic energy traveling in the wrong direction in the transducer housing from the piezoelectric element. Since the energy needs to be absorbed by the backing material then the material should have similar acoustic impedance to the piezoelectric element. If the material does not match the acoustic impedance of the element then the ultrasonic energy would be reflected by the backing material and would then bounce around inside the transducer housing and some would escape through the wear plate into the pipe. This could cause delayed return signals producing incorrect measurements. ORNL has identified that the backing material of the piezoelectric transducer should not match the acoustical impedance of the element. The NRPCT and Penn State have concluded independently that the material should match the acoustical impedance of the piezo-element. Additional research and testing would need to be conducted to determine the appropriate guidelines for backing material.

3.3.2.2. Signal Processing

For the concept recommended, ORNL identified that one of the disadvantages of the time-of-flight method is the additional electronics that will be needed to switch between transmit and receive modes of the transducer. The NRPCT does not share this concern and considers that

switching should not be a significant issue or major weakness. It is common to use an ultrasonic setup with a single transducer for both transmit and receive modes. The transducer voltage is constantly read and displayed whether the voltage is coming from the pulser electronics to excite the crystal and transmit a signal, or if the voltage is coming from the received, reflected mechanical signal causing a voltage to be generated across the piezoelectric material. The NRPCT sees this as simply a difference of operation when compared to the operation of one transducer used as both a transmitter and receiver to having two transducers in a pitch-catch mode. Multiple techniques would need to be investigated and evaluated factoring in complexity, response time, and processing implications to determine the most effective signal processing technique for Prometheus.

3.3.2.3. Mass Considerations

For the crossed-path transit method chosen as the primary technique by ORNL it is implemented with four transducers for redundancy and to mitigate any measurement errors due to "cross flow" or other flow profile irregularities. If a normal flow profile is assumed a flow sensor using time-of-flight measurement can be implemented with only one set of transducers. As a general objective, the NRPCT worked to limit the sensor and cabling mass as much as possible in the sensor assessment. The implications of mass may need to be assessed as a discriminator in the choice of sensor design. The four transducer design compared to the two transducer design, would result in additional mass associated with the transducers, standoffs, cabling and potentially with the electronics. This would need to be factored into a design recommendation, recognizing that the four-transducer would be a better option because of the redundancy, ability to mitigate any measurement errors, and if flow profiles became a concern.

3.3.2.4. Waveguide Considerations

The recommended waveguide length from ORNL was 10 cm assuming a high temperature (>700K) transducer was available. ORNL also presented other scenarios in Table 3 of their report, which listed waveguides of 20 cm or even 40 cm. The NRPCT has identified that trade studies would need to be conducted to fully assess the operating temperature of the transducer versus the length of the waveguide. Furthermore, this assessment would need to incorporate reactor plant integration concerns, vibration susceptibility, and fatigue susceptibility.

3.3.2.5. Redundancy

The ORNL recommended ultrasonic flow measurement technique of the crossed-path transit time method represents a concept with built-in redundancy concept. The level of redundancy would need to be fully assessed and trade studies would be required to fully assess various techniques and system configurations and their implications on mass and complexity.

3.3.2.6. Torsional Strut Concept

ORNL included in their report information regarding the Lynnworth's torsional strut concept, which is another ultrasonic method for obtaining flow via a separate, independent mechanism. Furthermore, this strut could be hollowed out and used as a through well for co-located temperature indication. The NRPCT recognizes potential advantages with this technique and would recommend further investigation and testing of this technique for future Prometheus efforts.

3.4. References

- (a) ORNL Report: "JIMO Reactor Sensor Technology Development Plan", Document ORNL/LRT/NR-JIMO/05-01 dated January 2005
- (b) SPP-67610-0002, Request for NR 08K Technical and Funding Approval of Oak Ridge National Laboratory (ORNL) Support for Space Nuclear Power Systems Instrumentation and Controls Development, for Action, dated February 3, 2005
- (c) NR letter NR:IC:SJKurth K#05-00718, Space Nuclear Power Plant – Instrumentation and Control Equipment – Workscopes for Sensor Development and Systems Development by Oak Ridge National Laboratory; Approval of, dated February 22, 2005
- (d) Information To Vendor (Space Power Plant Program), ORNL-SPP-05-0031A, Sensor Technology Development – Ultrasonic Reactor Coolant Flow Measurement, dated March 17, 2005
- (e) ORNL Report: "Ultrasonic Flow Meter System Conceptual Design", Document ORNL/LRT/NR-PROM1/05-19, dated August 2005

Report Title	SENSOR CABLE CONCEPTUAL DESIGN
Report Number	ORNL/LTR/NR-PROM1/05-20
Report Date	AUGUST 2005
NRPCT IV	ORNL-SPP-05-0030

4. Sensor Cable Conceptual Design

4.1. Overview

The NRPCT requested sensor cabling conceptual designs to be development by ORNL per References (a) through (c). ORNL examined the electrical cabling and related connection technologies for the JIMO space based nuclear reactor application. Cable material behavior in extreme temperature and radiation environments was studied and used to select optimum cable types for the various spacecraft temperature regions as shown below in Figure 4.1. ORNL reported their results in Reference (d).

FIGURE 4.1: Electrical Cable Temperature Regions



4.2. Key Points and Conclusions

4.2.1. Electrical Cable

Electrical cable vendors suggested by Reference (d) include Gore (region 5 only), Harbour (region 5 only), Meggitt, Thermocoax, IST Sensing Systems, and Omega. Cables by Omega were the highest temperature capability of all vendor cables (1273K) but they were not coaxial cables. IST is a leading NI cable candidate and lists both Pt and alumina as materials for NI cable construction. Section 7.1.5 identifies the I&C system sensor and actuator cables. Table 4.1 below shows the types of cables identified in Reference (d) for each sensor and actuator in each region.

TABLE 4.1: Types of Electrical Cable

SPACECRAFT REGION	SENSOR OR ACTUATOR	ELECTRICAL CABLE TYPE PER REFERENCE (a)
Region 1 – Reactor	NI Detectors Safety Rod Actuators	1. Standard Mineral Insulated (MI) Cable
Region 2 – Inside Shield	NI Detectors	1. NI: Pt wire/ Al_2O_3 Dielectric 2. Others: Standard MI Cable
Region 3 - Behind Shield	Reflector Stepper Motors Reflector Position Sensors	1. NI: Pt wire/ Al_2O_3 Dielectric 2. Others: Standard MI Cable
Region 4 – Birdcage, i.e., Power Conversion Region	Temperature Sensors Pressure Sensors Valve Actuators In addition, Region 4 to Region 5 is a transition point for some cable types.	1. JNT: Cu wire/MgO Dielectric 2. NI: Pt wire/ Al_2O_3 Dielectric 3. Thermocouples, RTDs, and LVDTs: Inconel wire/MgO Dielectric 4. Others: Standard MI Cable
Region 5- Boom, i.e., Signal and Power Transmission and Radiator Region	No sensors or actuators are located in Region 5. However, all sensor and actuator cables must pass through the boom to reach the electronics vault.	1. Inside Boom: PEEK or Kapton dielectric polymer insulated cables 2. External to Boom Near HRS: MI cable

4.2.2. Optical Fiber Technology

Reference (d) also examined various fiber optic technologies including those used in more than fifteen missions flown by NASA. Photonic crystal (PC) optical fiber waveguides is a relatively new technology potentially suitable for some applications of the JIMO reactor. The current state-of-the-art for PC optical fiber waveguides including the associated electro-optical interface devices (optical sources, modulators and detectors) were examined. In addition, three fiber architectures were examined. Pyrometry measures platinum surface temperature from 1273 K to 1724 K. Interferometry & optical time domain reflectometry (TDR) measures reflector position. Data links carry sensor data over fiber optic cable.

Optical Fiber Transmitters

Most semiconductor optical fiber transmitters have good radiation tolerance due to materials used (GaAs & InGaAs). Super luminescent diodes have the coupling advantages of laser diodes without the sharp threshold but need to be tested and qualified for radiation tolerance. Vertical cavity surface emitting lasers (VCSELs) at 840 nm are becoming the laser source of choice due to low threshold current, low divergence, integration / packaging, high yield array configurations, and high modulation rate (>2.5 Gbps). Experiments at CERN showed that VCSELs are more sensitive to neutron radiation but are satisfactory at fluences $<10^{15}$ n/cm².

Optical Fiber Modulators and Detectors

There are two excellent candidates for radiation tolerant modulators but these need to be qualified in accordance with Reference (e):

- Multi-quantum well (MQW) InGaAs/InP Asymmetric Fabry-Perot modulator (AFPM) devices
- Micro mirror digital light processing (DLP) devices

There are three candidates for radiation tolerant detectors but these also need to be qualified in accordance with Reference (e):

- Si based detectors (phototransistors, photodiodes & avalanche photodiodes) showed significant degradation with <250 kGy exposure from a ⁶⁰Co gamma source
- InGaAs photo detectors are far more radiation tolerant than Si based detectors
- Metal semiconductor metal (MSM) on silicon-on-insulator (SOI) detectors are used from UV to near IR and show promise as rad-hard devices

Optical Fiber Qualification Testing

NASA has performed a substantial amount of qualification testing of fiber optic cables and components for space-based applications. Optical fibers considered or used by NASA include WL Gore and Brand Rex types of Kevlar, Teflon, Gore Tex, PFA, FEP Teflon, Hytrel, Acrylate Buffers, and Polyimide Buffers. NASA is currently using many of the same devices for optical sources and detectors that are being used in the nuclear science community including: double heterojunction hardened LEDs, injection laser diodes, VCSELs, and InGaAs photo detectors. NASA is also considering InP, SiGe, and SiO technologies for radiation hardened electronic components and are developing FPGAs for signal processing. No NASA work in the area of MEMs or quantum well modulators has been found.

4.2.3. Conclusions

Most of the electrical I&C cables in the vicinity of the sensors will require metal sheath mineral insulated (MI) cables which are permanently attached to the associated sensors. Standard polymer insulated cables may be used inside the boom for connection to the electronics located in the vault at the aft section of the spacecraft.

Silica fiber is susceptible to radiation but sapphire fibers are not. However, Sapphire is not suitable for long-distance communication but is uniquely suitable for harsh environments. Most fiber technology currently flown by NASA can be used in space reactors but needs to be qualified in accordance with Reference (e).

PC optical fiber waveguides and their associated electronic interfaces will require a significant amount of design and qualification testing to verify consistent and reliable long-term performance in harsh JIMO space environments.

4.2.4. Future Work

Several future work activities have been established as follows:

- IST is a leading NI cable candidate and lists both Pt and alumina as materials for NI cable construction.
- Electrical cable testing is needed to verify required cable performance and stability over time under extreme temperature and radiation conditions.
- Sensor cable shielding effectiveness should be investigated due to the high power magnetic fields radiated from the Brayton turbine alternators and their associated power cabling. These magnetic fields are a potential noise source for sensor signals.
- Since connectors are not nearly as robust as the cables they are used with, further development of connector technology with the suggested cable companies should be pursued to establish connectors with improved harsh environment performance.
- The largest area of concern for optical fiber cables and their the associated electro-optical interface devices (optical sources, modulators and detectors) is the lack of testing at high temperature and high radiation levels expected near the reactor aft of the shield.

4.2.5. References

- (a) SPP-67610-0002, Request for NR 08K Technical and Funding Approval of Oak Ridge National Laboratory (ORNL) Support for Space Nuclear Power Systems Instrumentation and Controls Development, for Action, dated February 3, 2005
- (b) NR letter NR:IC:SJKurth K#05-00718, Space Nuclear Power Plant – Instrumentation and Control Equipment – Workscopes for Sensor Development and Systems Development by Oak Ridge National Laboratory; Approval of, dated February 22, 2005
- (c) Information To Vendor (Space Power Plant Program), ORNL-SPP-05-0030, Sensor Technology Development – Cables, dated March 1, 2005
- (d) ORNL Report ORNL / LTR / NR-PROM1 / 05-20, Sensor Cable Conceptual Design, dated August 2005
- (e) MIL-STD-1773, Hardware for Space-Based Reactor Application (NASA Developed)

Report Title	THERMOCOUPLE CONCEPTUAL DESIGN FOR SPACE NUCLEAR POWER SYSTEMS
Report Number	ORNL/LTR/NR-PROM1/05-05
Report Date	OCTOBER 2005
NRPCT IV	ORNL-SPP-05-0034

5. Thermocouple Conceptual Design

5.1. Overview

The NRPCT pursued the development of a conceptual design of a thermocouple system for Prometheus. A request to develop this system was issued to NR per Reference (a) and approved per Reference (b). In Reference (c) the NRPCT requested further evaluation by ORNL of the capabilities of thermocouple systems and the development of a conceptual system capable of measuring coolant and component temperatures of the spacecraft nuclear power plant. In Reference (d) ORNL developed a first principles based approach to the development of a TC design for a space reactor application discussing the many considerations affecting the choice and implementation of this technology. Design topics including the selection of the TC type, the formation of the sensing system including the sensor, cabling, and electronics, an assessment of system accuracy, and an assessment of the faults modes and their identification for these systems. The NRPCT in Enclosure (6) separately addressed the TC sensor technology for the space nuclear reactor with perhaps a broader consideration of non-traditional materials in the TC implementation.

The task of ORNL was to define a conceptual design for a thermocouple (TC) based reactor coolant temperature measurement system that would provide an accurate, fast-response, low-drift temperature measurement for 15 to 20 years. The report covered the principals of TC design including material selection, amplifier and signal processing issues, architecture, uncertainty analysis, radiation effects, manufacturing, and testing.

The final sensor design recommended by ORNL was a metal sheathed, mineral insulated Type N TC (Ni-14Cr-1.5Si vs. Ni-4.5Si-0.1Mg) with a bilayer sheath made of materials chosen for compatibility with the thermoelements and piping material (no specific materials were recommended). Several common mineral insulators were reviewed but none was specifically recommended. The recommended fill gas was helium but no cold-end sealing method was reviewed or recommended. Architecturally, ORNL recommended an ungrounded junction connected to a signal processing system consisting of a low pass (1-4 Hz) filter, a successive-approximation-register A/D converter, RTD/software based cold junction compensation, and several layers of comparison between TC output and other plant parameters for drift/failure identification.

5.2. Key Points and Conclusions

5.2.1. Material Selection

Both ORNL and the NRPCT recognize the critical importance of minimizing sources of TC drift and failure through careful choice of materials. The ORNL report provides a comprehensive listing of these failure modes along with a rough ranking of their importance. Some of these drift and failure mechanisms are discussed in some detail in the report.

ORNL began their analysis with several principal thermoelement combinations and downselected to their final combination based on the justifications summarized in the table below. Although the materials issues raised by ORNL for the rejected thermoelement types are valid, the NRPCT believes additional work is required prior to rejecting some types based on a lack of information. The NRPCT also feels that other results from previous high temperature TC development efforts (such as those of Pratt and Whitney CANEL, Westinghouse Astronuclear, Westinghouse Hanford, and Atomics International) should be further explored and understood.

Table 5.1 provides a summary of TC types that were rejected by ORNL and the reason.

TABLE 5.1: ORNL Rejected TC Types

TC Type	Reason for rejection
Pt-Rh system (Types B, R, S, and Pt-40Rh vs. Pt-20Rh)	Pt evaporation and transmutation of Rh to Pd. Non letter-designated TCs have little supporting information.
Platinel II (Pd-31Pt-14Au vs. Au-35Pd)	Little high radiation experience.
W-Re system (Type C and W-25Re vs. W-3Re)	Type C – Low output EMF below 600K. Non letter-designated TCs have little supporting information.
Ni-Cr system (Type K and N)	Type K is inferior to Type N. Type N was selected.
Ir-40Rh/Ir	Non letter-designated TCs have little supporting information.
Nb-1Zr/Mo	Non letter-designated TCs have little supporting information.

5.2.2. Signal Processing Electronics

In the sections covering system electronics, ORNL described the major signal processing concerns and addressed each of them separately. Although the detailed coverage of some issues is adequate, the NRPCT feels that additional work in this area is required, including a thorough diagram of the overall proposed signal processing system, to fully assess the conceptual design. Additional work is deemed necessary in the area of EMI and common-mode voltage is also desired. Common-mode voltage is a concern but EMI is not the exclusive source for common-mode voltage.

5.2.3. Uncertainty Analysis

Given the preliminary nature of the thermocouple design and the reactor itself, an uncertainty analysis of the thermocouple output must invoke many assumptions. The ORNL report outlines many of the contributors to uncertainty and makes an estimate of their magnitude. This portion of the report lays a good foundation for a later, more complete analysis to be carried out on the final design.

5.2.4. Manufacture, Assembly, and Testing

Analysis of previous high temperature TC development projects by the NRPCT indicates that the drift and lifetime performance of the TC is strongly dependant on the purity of the materials and the cleanliness of the initial components and assembly environment. The ORNL report describes the major processes used to make one kind of TC (the swaged and drawn design). If a compatible set of materials are used, material purity and cleanliness are important factors in obtaining drift-free operation and long life and would required significant effort.

The NRPCT agrees with ORNL that long term furnace testing is essential to characterizing the drift performance of the TC before it is placed in service. Contrary to ORNL, the NRPCT has not seen enough evidence to suggest that the low gamma intensities and neutron fluences in the high-temperature aft-of-shield environment will lead to sensor drift that is different from the temperature effect alone.

5.2.5. Conclusion

This report discusses the most critical issues in high temperature TC design. In its entirety, it represents a strong starting point in the process of selecting a final instrument layout. Given that many of the plant and mission parameters are undefined, it is recognized that it is difficult to present a complete conceptual design at this time and much work is required to complete a design for a SNPP thermocouple system.

5.2.6. References

- (a) SPP-67610-0002, Request for NR 08K Technical and Funding Approval of Oak Ridge National Laboratory (ORNL) Support for Space Nuclear Power Systems Instrumentation and Controls Development, for Action, dated February 3, 2005
- (b) NR letter NR:IC:SJKurth K#05-00718, Space Nuclear Power Plant – Instrumentation and Control Equipment – Workscopes for Sensor Development and Systems Development by Oak Ridge National Laboratory; Approval of, dated February 22, 2005
- (c) Information To Vendor (Space Power Plant Program), ORNL-SPP-05-0034, Sensor Technology Development – Thermocouples, dated March 1, 2005
- (d) ORNL Report: "Thermocouple Conceptual Design for Space Nuclear Power Systems", Letter Number: ORNL/LTR/NR-PROM1/05-05, October 2005

Report Title	RESISTANCE TEMPERATURE DETECTOR CONCEPTUAL DESIGN
Report Number	ORNL/LTR/NR-PROM1/05-11
Report Date	JUNE 2005
NRPCT IV	ORNL-SPP-05-0029

6. RTD Conceptual Designs

6.1. Overview

The NRPCT pursued the development of a conceptual design of a resistance temperature detector (RTD) system for Prometheus. A request to develop this system was issued to NR per Reference (a) and approved per Reference (b). In Reference (c) NRPCT requested that ORNL develop a resistance temperature detector conceptual design including the sensor design method and material selection approach. The ORNL work is reported in Reference (d). It describes the critical material and sensor parameters and their impact on RTD performance and longevity. Conceptual designs are developed for both a wire wound RTD and a ceramic RTD meeting the Prometheus temperature and radiation requirements. The NRPCT in Enclosure (6) separately addresses the challenges of an RTD sensor for the space nuclear reactor, particularly those associated with materials, sensor design, and sensor mounting. Generally it was considered that the RTD wire wound technology should be able to provide a sensor that covered full range of operation with minimal long term drift.

The task of ORNL was to define a conceptual design for a resistance temperature detector (RTD) based reactor coolant temperature measurement system that would provide an accurate, fast-response, low-drift temperature measurement for 15 to 20 years. The report covered the principals of RTD design including material selection, wire element RTD design, and ceramic element RTD design. Two sensor designs were requested by the NRPCT and developed by ORNL. The first was for a wire element design and the second employed a ceramic element. The recommended wire-element design was a 100 Ω element composed of 127 μ m Mo-41Re wire coiled into a 4-hole alumina insulation preform. A 4-wire design was recommended with alumina insulated lead wires. The sheath was a Ni-superalloy with a 50 μ m thick layer of Mo-41Re on its inner surface for element compatibility. The specified fill gas was He and the cold end of the sheath was to be sealed with a double glass-to-metal seal.

The ceramic design was identical to the wire design except in the area of the sensing element. ORNL recommended a Pt/alumina cermet with Pt alloy electrodes and a titanium or Zirconium adhesion layer. The sensor lead wires were to be brazed to the electrodes with a Pt-based braze. The wires would also be held in place by a sapphire "holder" that was thermal expansion matched to the cermet.

Furthermore, in Reference (e), ORNL suggests a temperature measurement and calibration technique referred to as Johnson Noise Thermometry (JNT) for the high temperature space reactor RTD. This technique would measure the thermally induced electron noise, i.e., voltage, in the RTD element to determine the actual element temperature, that would allow correction of the Wheatstone bridge determined temperature through compensation of element resistance value for material changes caused by extended operation at high temperatures. In the Reference (d) report ORNL continued to identify the need to consider a JNT technique for periodic recalibration of an

RTD sensor to compensate for thermally induced drift mechanisms. The JNT technique is highly developmental method of measuring temperature with few, if any instances of its actual application in a real power plant setting, particularly one in which the sensor system architecture requires a large distance between the sensor and the electronics. The NRPCT initiated efforts with ORNL for developing a conceptual design of a JNT system in References (f), (g), and (h). However, this effort before any progress was made due to the cancellation of the Prometheus Program.

The NRPCT completed an evaluation of RTD technology which is presented in Enclosure (6).

The following discusses some of the key points of this report.

6.2. Key Points and Conclusions

6.2.1. Wire Element RTD Conceptual Design

In outlining the wire element RTD design, ORNL described several wire support mechanisms and materials. The decision to use Mo-41Re as a resistance element seems to have been made based on ductility, high temperature resistance, and compatibility with alumina. Response time, electrical resistance drift, thermal strains, element failure mechanisms, and self heating were also discussed. Overall, the NRPCT feels that the ORNL analysis represents a good analysis of RTD design issues.

6.2.2. Ceramic Element RTD Conceptual Design

Ceramic elements were discussed in the report along with ORNL recommendation. Very little research is available on this kind of element and ORNL provided an overview of the key issues. At this time, the NRPCT believes that the lack of operating data on this element type results in the need for extensive development and testing to fully assess its viability as a Prometheus temperature sensor.

6.2.3. Insulation, Sheath, and Fabrication

ORNL included an analysis of sheaths, insulators, and cold end seals that were applicable to both element designs. Sheath materials were evaluated on the basis of lateral strength, thermal mass, manufacturability, and coolant pipe and insulation compatibility. Mineral insulation was evaluated based on chemical compatibility, electrical resistance, and material specific issues. The proposed glass seal was based on the SP-100 design. In all choices, the NRPCT sees this work as a good starting point for a detailed evaluation.

6.2.4. Conclusions

This report discusses a number of the key issues that are important in RTD design. The design chosen for the wire element RTD appears to be a strong candidate, but additional research, development and testing should be conducted to fully assess this design and others, including a ceramic element RTD, as a viable temperature measurement device for SNPP.

6.2.5. References

- (a) SPP-67610-0002, Request for NR 08K Technical and Funding Approval of Oak Ridge National Laboratory (ORNL) Support for Space Nuclear Power Systems Instrumentation and Controls Development, for Action, dated February 3, 2005 Approval for conceptual design

- (b) NR letter NR:IC:SJKurth K#05-00718, Space Nuclear Power Plant – Instrumentation and Control Equipment – Workscopes for Sensor Development and Systems Development by Oak Ridge National Laboratory; Approval of, dated February 22, 2005
- (c) Information To Vendor (Space Power Plant Program), ORNL-SPP-05-0034, Sensor Technology Development – Thermocouples, dated March 1, 2005
- (d) ORNL Report: “Resistance Temperature Detector Conceptual Design for Space Nuclear Power Systems”, Letter Number: ORNL/LTR/NR-PROM1/05-11, June 2005
- (e) ORNL Report: “JIMO Reactor Sensor Technology Development Plan”, Document ORNL/LRT/NR-JIMO/05-01 dated January 2005
- (f) SPP-67610-0004, Request for NR 08K Technical and Funding Approval of Oak Ridge National Laboratory (ORNL) Support for Johnson Noise Thermometry Development, for NR Action, dated June 14, 2005
- (g) NR letter NR:IC:SJKurth K#05-03024, Space Nuclear Power Plant – Instrumentation and Control Equipment – Sensor Development – Course of Action to Further Investigate Johnson Noise Thermometry: Approval of with Comment
- (h) Information To Vendor (Space Power Plant Program), ORNL-SPP-05-0032, Sensor Technology Development – Johnson Noise Thermometry, dated July 5, 2005

This page intentionally blank

Enclosure 3

Ultrasonic Sensor Technology Evaluation

Ray Blasi, *Bettis-Advanced Material System Integration*

Jake Evans, *Bettis-Advanced Material System Integration*

Christine Fedoris, *Bettis-Space I&C Design*

Ryan Kristensen, *KAPL-Space Electrical Systems*

Harvey Mikesell, *Bettis-Space I&C Design*

Andrew Ruminski, *Bettis-Advanced Material System Integration*

Eric Simon, *Bettis-Space I&C Design*

This page intentionally blank

Table of Contents

THIS PAGE INTENTIONALLY BLANK	4
PRELUDE	5
EXTENSIBILITY TO OTHER SPACE MISSIONS	5
1. EXECUTIVE SUMMARY	6
2. OPERATIONAL REQUIREMENTS	9
2.1. OPERATIONAL ENVIRONMENT.....	9
2.2. MISSION DURATION.....	10
2.3. MEASUREMENT REQUIREMENTS.....	10
2.4. NONINVASIVENESS	11
3. ULTRASONIC SENSOR TECHNOLOGY OVERVIEW	13
3.1. TEMPERATURE.....	14
3.2. FLOW	18
3.3. PRESSURE	19
3.4. POSITION	20
4. COMMON ISSUES	22
4.1. MEASUREMENT SENSITIVITY AND CALIBRATION	22
4.2. CABLING.....	23
4.3. INTERFACE CARDS.....	25
4.4. SOFTWARE.....	26
5. ULTRASONIC TRANSDUCERS	27
5.1. PIEZOELECTRIC.....	27
5.2. MAGNETOSTRICTIVE.....	32
6. TEMPERATURE MEASUREMENT ISSUES	39
6.1. MAGNETOSTRICTIVE.....	39
6.2. PIEZOELECTRIC – DUAL TRANSDUCER	43
7. FLOW MEASUREMENT ISSUES	46
7.1. TRANSDUCER ELEMENT (PIEZOELECTRIC).....	46
8. PRESSURE MEASUREMENT ISSUES	47
8.1. TRANSDUCER ELEMENT (PIEZOELECTRIC).....	47
8.2. TECHNIQUE DEVELOPMENT.....	48
9. POSITION MEASUREMENT ISSUES	49
9.1. COMMON ISSUES FOR LINEAR AND ROTARY POSITION MEASUREMENT	49
9.2. LINEAR POSITION MEASUREMENT ISSUES	51
9.3. ROTARY POSITION MEASUREMENT ISSUES.....	52
10. REFERENCES	53

This page intentionally blank

Prelude

The evaluation contained herein considers the use of ultrasonic temperature, flow, pressure, and position sensor technologies to measure the principle parameters of a space nuclear power plant (SNPP) for the Prometheus Project Jupiter Icy Moon Orbiter (JIMO) mission. These technologies are evaluated with respect to their predicted ability to continuously measure the reactor operational parameters reliably and accurately during a 15 year mission to explore the icy moons of Jupiter. The SNPP concept forming the basis of this study is the Direct Gas Cooled Brayton Reactor Plant in which the inlet and outlet reactor coolant temperatures, the coolant flow and pressure, and the positions of the reactivity control sliders or drums are the reactor plant parameters of principle interest.

During the JIMO mission the sensing systems will be exposed to a wide range of temperatures and radiations due to the planetary and interplanetary environments through which the spacecraft will travel, and the local radiation and thermal environments created by the reactor plant. The sensor systems are distributed over the entire length of the spacecraft from the sensing elements located in the reactor plant region at its forward end to the electronics housed in a shielded vault 60 meters away at its rear. A long boom connects the two regions and houses the cables interconnecting the sensing elements with their instrumentation. The sensing systems will be exposed to local environments in these regions that differ significantly with the reactor plant system temperatures and radiations comparatively high, and the boom and vault regions at room temperature with reactor-induced radiations diminishing as the distance from the reactor increases.

For this study it is assumed that all of the sensing elements will be located aft of the reactor shield in the vicinity of the shield and power conversion equipment where the environmental temperatures will be controlled by a thermal management system and radiation levels are maintained sufficiently low for proper sensor performance over the life of the mission.

This evaluation has been performed with the most recent space reactor plant design information available. However, not all design information was available when performing the evaluation. For example, the reactor plant coolant piping material was not known and, as a result, materials compatibility issues between the sensor housings and the coolant piping were not performed but were estimated.

Extensibility to Other Space Missions

Refocusing the Prometheus project to a mission other than JIMO will have broad-reaching implications for the mission as a whole. The extent to which the reactor systems are affected will depend on what particular mission is chosen. Regardless of mission choice, ultrasonics could still play a key role in the measurement of the primary reactor plant parameters. A new mission may relax or tighten certain requirements or even introduce new ones. This discussion focuses on how requirements of the ultrasonic systems may be affected by refocusing the forthcoming mission to a lunar-based system.

Radiation

In a lunar surface-based application, the environmental radiation conditions would be much less severe than those around the planet Jupiter, though solar flares would still be an issue. This reduction in radiation levels will have minimal impact on the ultrasonic sensing elements themselves or their connected cabling, which will still be required to endure the reactor plant radiation. However, it should result in significant benefits to the plant through the reduction or elimination of protective shielding mass for otherwise radiation sensitive components, such as electronics, and by allowing the

use of electronics with substantially reduced rad-hardening requirements than those required for the JIMO mission .

1. Executive Summary

The following tables summarize the classification of issues contained in this document. Classifications were designated as low, medium, or high. The tables are broken down according to each particular section in the report, and they order the issues from high to low within each section.

Section 4: Common Issues

Issue	Risk
Measurement sensitivity and calibration	Moderate
EMI: Radiated Susceptibility	Moderate
EMI: Radiated Emission	Low
EMI: Conducted Susceptibility	Low
EMI: Conducted Emission	Low
EMI: Electrostatic Discharge	Low
Cabling	Low
Interface Cards	Low
Software	Low

Section 5.1: Piezoelectric Transducers

Issue	Risk
Housing Attachment of transducer & standoff to piping	High
Piezoelectric Element Temperature/Radiation Compatibility	High
Piezoelectric Element Material Degradation (Temp/Radiation effects)	High
Absorbent Backing Temperature/Radiation Compatibility	High
Housing Temperature/Radiation Compatibility	Moderate
Housing Material Degradation (Temp/Radiation effects)	Moderate
Housing Attachment of transducer to standoff	Moderate
Wear Plate Temperature/Radiation Compatibility	Moderate
Wear Plate Material Degradation (Temp/Radiation effects)	Moderate
Pulse Transmission/Receiving Noise	Moderate
Pulse Transmission/Receiving Signal Drift/Calibration requirements	Moderate
Piezoelectric Element Construction Material (crystal, ceramic, etc.)	Low
Housing Construction/Materials	Low
Housing Cabling Connector(s)	Low
Absorbent Backing Construction/Material	Low
Absorbent Backing Material Degradation (Temp/Radiation effects)	Low
Wear Plate Construction/Material	Low
Pulse Transmission/Receiving Dampening	Low
Pulse Transmission/Receiving Time Response	Low
Pulse Transmission/Receiving Interference/Crosstalk Susceptibility	Low
Number of Cables	Low

Section 5.2: Magnetostrictive Transducers

Issue	Risk
Bias Magnet Field Degradation (Temp/Radiation effects)	High
Pulse Transmission-Receiving Signal Drift/Calibration requirements	High
Housing Attachment of transducer to waveguide (positive capture)	Moderate
Bias Magnet Degaussing	Moderate
Pulse Coil Temperature/Radiation Compatibility	Moderate
Housing Construction/Materials	Moderate
Housing Temperature/Radiation Compatibility	Low
Housing Attachment of transducer to plant	Low
Cabling Connector(s)	Low
Bias Magnet Field Strength Required	Low
Bias Magnet Construction/Material	Low
Bias Magnet Power requirements (electromagnet only)	Low
Pulse Coil Conductor Material	Low
Pulse Coil Field Strength	Low
Pulse Transmission-Receiving Noise	Low
Pulse Transmission-Receiving Dampening	Low
Pulse Transmission-Receiving Intermediate Waveguide Attachments	Low
Pulse Transmission-Receiving Time Response	Low
Pulse Transmission-Receiving Interference/Crosstalk Susceptibility	Low
Number of Cables	Low

Section 6: Temperature Measurement

Issue	Risk
Magnetostrictive – General	
Attachment of waveguide to spacecraft	Moderate
Joining of magnetostrictive wire to waveguide	Moderate
Length of waveguide	Low
Composition of waveguide	Low
Stray Signal Dampening	Low
Transducer	Low
Magnetostrictive – Notched Waveguide	
Depth of notch	Moderate
Shape of notch	Low
Spacing of notches for multiple measurements	Moderate
Attachment of the sensor to the component	Low
Materials compatibility of sensor and component	Low
Magnetostrictive – Guided Wave In Plate	
Attachment of plate to component	High
Dimensions of plate and acoustic horn	Low
Attachment of waveguide to the acoustic horn	Low
Materials compatibility of sensor and component	Low
Piezoelectric – Dual Transducers	
Fatigue life of the piezoelectric crystal	High
Attachment of transducers and standoffs to piping	Moderate
Transducer - Standoff requirements	Low
Operation frequency	Low
Temperature compatibility of transducers	Low
Housing construction	Low

Section 7: Flow Measurement

Issue	Risk
Fatigue life of the piezoelectric crystal (at temperature)	High
Attachment of transducers and standoffs to piping	Moderate
Transducer Standoff requirements	Low
Operation frequency	Low
Temperature compatibility of transducers	Low
Housing construction	Low

Section 8: Pressure Measurement

Issue	Risk
Fatigue life of the piezoelectric crystal (at temperature)	High
Amplitude change sensitivity to gas pressure	High
Low pressure measurement limit	High
Attachment/coupling of standoff & transducer to piping	Moderate
Transducer Standoff requirements	Low
Operation frequency	Low
Temperature compatibility of transducers	Low
Housing construction	Low
Materials compatibility of transducers and interface	Low

Section 9: Position Measurement

Issue	Risk
General Issues	
Magnet - Radiation/temperature sensitivity	High
Pulse Coil - Temperature sensitivity of coil	Moderate
Waveguide – Composition	Moderate
Transducer – Temperature compatibility	Moderate
Magnet - Field strength	Low
Pulse Coil – Field strength required / turns per inch and current / Frequency	Low
Pulse Coil - Conductor/Insulator Material	Low
Pulse Coil - Attachment of coil to waveguide	Low
Waveguide – Degaussing	Low
Transducer – Frequency, Amplitude, Pulse Width	Low
Linear	
Attachment of waveguide to structure	Moderate
Magnet - Physical shape/size of marker	Low
Magnet - Attachment of marker to device	Low
Magnet - How to guide travel of marker along waveguide/pulse coil	Low
Rotary	
Attachment of waveguide to structure	Moderate
Physical shape/size of marker	Low
Attachment of marker to device	Low
How to guide travel of marker along waveguide/pulse coil	Low

2. Operational Requirements

The operation requirements for the SNPP Instrumentation and Control (I&C) sensing systems detailed herein has been developed from a compilation of SNPP reference and design documents that are fully described in the Project Prometheus NRPCT Final Report Reference (20).

2.1. Operational environment

Ultrasonic sensors for the JIMO mission will be required to survive various stressors, which include temperature, radiation, and mechanical shock. The JIMO spacecraft will experience a broad spectrum of external environments ranging from terrestrial conditions on earth near 300K, 1 atmosphere, and no radiation, to the 100K vacuum and Van Allen belt radiations of Earth orbit, to the 4K temperatures and cosmic and solar radiations of its interplanetary journey, to the 4K temperatures and harsh electron-proton radiation fields of Jupiter and its moons. Reactor plant operation generates its own local thermal and radiation environment that combine with these external effects to create the temperature and radiation environment seen by the sensing system components distributed over the entire spacecraft. The sensor systems will be subjected to combined radiation from reactor, cosmic, and galactic sources. This includes a combined neutron (fast and thermal), energetic proton, energetic heavy ion, energetic electron, reactor gamma ray, and cosmic ray doses. Their temperature environment, on the other hand, will be controlled by a thermal management system that maintains the sensor system components within their design range.

In addition to the thermal and radiation stressors, the sensors must endure mechanical shocks originating from the loading of the launch vehicle, launch, explosive ordnances employed to jettison the boosters, and transit to Jupiter. Mechanical shock during transportation and loading onto the launch vehicle should remain below 6 g_{rms} . The mechanical stress experienced during the launch will depend on the launch vehicle, which has not been determined at this time. It has been estimated that an acoustic energy band between sub-hertz through 10,000 Hz will be experienced during the launch with a peak sound pressure level of approximately 140 dB between 100 and 250 Hz. A gravity loading of at least 1.5 g with a peak between 4-6 g will be exerted by the launch vehicle acceleration. The activation of explosive ordnances to jettison vehicle components will produce a 500-1000 g, short duration (less than 5 ms), transient shock. The majority of the ordnance energy, however, should be absorbed into the spacecraft structure before reaching the sensors in the SNPP. Forces experienced during the remaining phases of the mission (i.e. earth orbit escape, transit to Jupiter, and maneuvering around the moons of Jupiter) will be much smaller than those of launch.

2.1.1. Sensor Environment

In the SNPP the sensors for reactor coolant temperature, flow, pressure, and control element position will all be located in a thermally controlled environment with an ambient temperature ranging from 250K to 400K. Prior to reactor startup all sensors will be maintained at a temperature of 250K or greater. At full power, those sensors in close proximity to the hotter portions of the coolant system may see their local temperature rise further toward 400K, and those in direct contact with a reactor coolant system, pressure vessel, shielding surface or pipe may be exposed to significantly higher temperatures yet.

Temperature sensors in direct contact with the reactor coolant system may be required to contact and measure temperatures between 450K and 1300K depending upon their location in the coolant system. The baseline reactor inlet and outlet temperatures are 890K and 1150 K at full reactor power during the spacecraft transit to Jupiter. Other sensors, such as flow and pressure, should be located in the cooler sections of the coolant system consistent with their function, e.g. at the inlet or outlet of the Brayton compressor, where temperatures of 400 to 500K are anticipated. Moreover, standoffs may be included in some of these sensor designs to reduce the maximum temperature even further.

Lowering the temperature would increase the number of available transducer materials and also mitigate a number of other problems associated with operating ultrasonic systems above 800 K.

At full power operation, the sensor elements radiation levels located in the region directly behind the shield will be subject to a neutron flux level of 1×10^{15} n/cm²/sec (1 MeV) and a gamma exposure rate of 10 MRads/year. It is expected that all regions of the spacecraft, including the sensors, will receive at most a radiation dose of 100 MRad(Si) from space originated sources. The majority of the space radiation will come from the radiation belts surrounding Ganymede and Europa. Additional radiation, including gamma rays and neutrons, will originate from the reactor. The predicted neutron 1-MeV equivalent Si-fluence for 12 years of full reactor power from a gas cooled Brayton system is 6.0×10^{15} n/cm² at the rear of the shield. A similar value for the gamma ray Si-damage dose was calculated to be 5.0×10^8 Rad. Currently, the distance of the sensors from the back wall of the shield is uncertain. However, there will be no sensors situated fore of the shield. Thus, the above predictions are conservative.

Maximum expected mechanical shock and vibration occur during launch. Sensors should be able to survive the maximum absolute launch values. Expected launch vibration is approximately 5.5 g. Thus, the sensors should be able to withstand a minimum of 10 g for 10 ms at a frequency of 2 kHz without failing or de-calibrating. Sensor system sound pressure levels at launch time could exceed 135 dB, and the systems should be able to withstand this level by 15 dB.

2.1.2. Aft Electronics Environment

Signal processing electronics will be placed in a location remote from the reactor plant within a shielded vault up to 60 m from the measurement surface. The thick walled (25.4mm) aluminum vault reduces the external radiation dose levels of 1Grad TID and 5.7×10^{15} n/cm² (1 MeV) equivalent (charged particle) from the Jupiter environment to an interior level between 300KRad and 1000KRad TID where the rad-hardened electronics, designed for these levels, reside. The radiation contribution from the reactor plant at the vault location by design is 25KRad TID and 5×10^{10} n/cm² (1 MeV). The electronics vault will be equipped with electrical heat sources to maintain temperatures in the 200-400 K range at all times even when the spacecraft is in low-earth orbit before reactor start-up. The electronics in the vault should be designed to survive the same mechanical shock and vibration requirements as the sensors detailed in Section 2.1.1.

2.2. Mission Duration

The anticipated Prometheus Project JIMO mission duration is approximately 15 years with 12 years at full reactor power. Sensors must successfully operate without maintenance and preferable without externally applied calibration over this time period. This requirement suggests that the drift of the device with high temperature operation must remain strictly bounded such that the device meets its accuracy requirement throughout its service life.

2.3. Measurement Requirements

The baseline design requirements established for a SNPP temperature, flow, pressure, and linear reactivity control elements' (slider reflectors) continuous position sensing systems in Reference (20) are listed in Table 2.3-1. The sensor range represents the actual span of the measured parameter that the sensor can endure without failure. The full power value represents the best estimate of the measured parameter's value at full reactor power. The accuracy of the parameter is the maximum uncertainty in its absolute value over the entire operational range of sensor. The resolution of the parameter is the minimum change of the physical parameter that must be sensible by the sensor.

Table 2.3-1: Pre-Conceptual Baseline Parameter Requirements

Measurement Type	Temperature	Flow	Pressure	Slider Position
Sensor Range	100-1300 K	0-7 kg/sec	0-2.5 MPa	0-45 cm
Full Power Value	1150K	4.53 kg/sec	2.0 MPa	Various
Accuracy	± 5.0K	± 0.1 kg/sec	± 45kPa	± 0.5mm
Resolution	± 1.0K	± 0.02 kg/sec	± 9kPa	± 0.05mm
Response Time	10 sec.	1 sec.	1 sec.	1 sec.

The baseline temperature requirements represent the particular requirements for the SNPP reactor coolant outlet temperature sensor which will see the severest service during plant operation. The reactor outlet piping passes from the reactor vessel, through a radiation shield, to the power conversion equipment. The reactor coolant hot leg piping is to be insulated over this entire length. The notional location for the temperature sensor is just aft of the shield to minimize sensor and cabling radiation levels. Ideally the reactor coolant outlet temperature sensor would be immersed in the coolant flow stream to measure its temperature most accurately and with the smallest delay. Realistically the sensor will be housed in a well inserted into the outlet piping or attached to the piping external surface. The expected gamma dose and neutron fluence radiation levels at this location are of the order of 2×10^8 TID rads(Si) and 3.6×10^{15} n/cm², respectively.

The baseline reactor coolant flow requirements represent the particular requirements for the SNPP flow as measured at the outlet of the Brayton machine compressor based for the single coolant loop system. This location reduces the temperature stress on the flow sensing element, thereby reducing the research and development risk for the technology. The operational temperature of the sensor should be approximately 540K. The gamma dose and neutron fluence levels are of the order of 2×10^8 TID rads(Si) and 6×10^{14} n/cm², respectively.

The baseline reactor coolant pressure requirements represent the SNPP pressure as measured at the outlet of the Brayton machine compressor for the single coolant loop system. It measures the highest pressure in the plant. As with the flow sensor, its location reduces the temperature stress on the pressure sensing element, thereby reducing the technology risk. The gamma dose and neutron fluence levels are of the order of 2×10^8 TID rads(Si) and 6×10^{14} n/cm², respectively.

The baseline reactor reactivity control element position sensor considered in this study is the linear form of the sensor that would be associated with a slider reflector. The position detector will be attached to the control element drive motor in a region immediately aft of the reactor radiation shield. The operational temperature of the detector should normally range from approximately 250K to 400K. The expected gamma dose and neutron fluence radiation levels are of the order of 2×10^8 TID rads(Si) and 3.6×10^{15} nvt, respectively.

2.4. Noninvasiveness

The material being considered for the reactor coolant piping system is based on superalloys. For a superalloy reactor coolant piping system, penetrations and welding are considered acceptable, based on the comparative maturity of welding technology for this class of materials. For these systems, sensor wells and penetrations through the piping wall to allow direct sensing of the gas coolant, are allowed and, in some cases, are considered necessary. The superalloy metal maximum temperature is limited to approximately 900K, substantially less than the nominal reactor coolant outlet temperatures at full power operation. A pipe-in-pipe concept is being contemplated for the hot leg piping, formed of an interior refractory metal pipe or sleeve, an intermediate layer of insulation, and

the outer superalloy pipe. With this system, the external pipe would be insulated from the hot coolant gases such that the surface temperature would never exceed 900K. To measure reactor outlet coolant temperature under this circumstance, a well penetration into the coolant stream is desirable to achieve an accurate measure of the coolant hot leg temperature within a reasonable time frame. The development of a leakproof well compatible with both the superalloy exterior pipe and a refractory metal interface to the hot coolant is a significant technology challenge. The other sensors, including other temperature measurements, should be located in cooler regions of the piping system that do not exceed 900K and as a result, more traditional methods for insertion of a well or penetration should be possible.

3. Ultrasonic Sensor Technology Overview

Ultrasonic technology is a viable tool for many non-invasive industrial sensing applications. Commercially available, high accuracy ultrasonic sensors have been developed on the basis of sound wave propagation principles, and recent advancements in transducer technology, signal processing, and data analysis software. Such sensors have been demonstrated to be capable of reliable performance in hostile environments, such as high temperature ovens, vacuums, cryogenic systems, and the high radiation fields of an operating nuclear core.

Ultrasonic sensors are designed on the basis of sound wave propagation in a particular material of interest. The material of interest can be either the material whose physical parameters are to be measured (e.g., flow of a gas or liquid in a pipe stream), or it can be a secondary material immersed in the environment from which data is sought (e.g., a metal plate or rod whose temperature represents the environment in which it is located or in contact with; be that a gas, a liquid, or a solid). Most industrial ultrasonic sensors operate in the 1 to 10 mm wavelength range, the 0.1 to 20 MHz frequency range, and the 1 to 10 mm/ μ s range. In these systems, the sound waves propagate in the material of interest as longitudinal waves or shear waves whose velocities are inversely proportional to the density of the material and directly proportional to the bulk elastic modulus and the shear elastic modulus, respectively. Sound velocity measurements in the form of pulse echo and through transmission are typically used to obtain temperature, flow, pressure, and position data (see Figure 3-1).

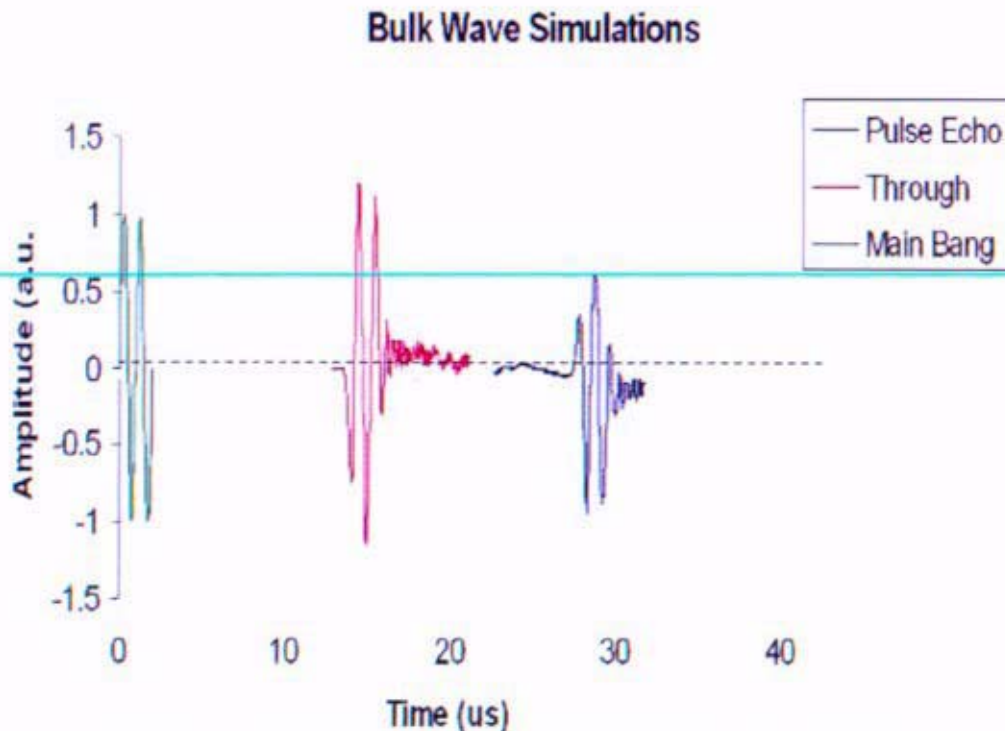


Figure 3-1: Ultrasonic Time-of-Flight Bulk Wave Simulations

In the pulse echo technique, the same transducer is used to send and receive the sound signal. In the through transmission technique, separate transducers are used to send and receive the sound signal.

In general, three types of transducers are used to launch ultrasonic waves into a material; magnetostrictive, piezoelectric and electro-magnetic acoustic. Magnetostrictive and piezoelectric transducers are considered to be rugged and reliable and have been shown to be useful for applications in hostile environments. Electro-magnetic acoustic transducers (EMAT) will not be considered for space reactor applications because of the low signal strength generated by these transducers and the extensive development needed to make these transducers usable in hostile environments. Magnetostrictive and piezoelectric transducers operate as follows:

Magnetostrictive: Interaction of an alternating current and bias magnetic field induce a strain in a magnetostrictive material, which creates an elastic waveform that propagates through the material. The return (or reflected) waveform creates a change in the magnetic polarization properties of the magnetostrictive material at the instantaneous point of deformation, which induces a current in the pulse coil which serves as the source of detection. Remendur or Premendur magnetostrictive materials are typically used in this technique due to their excellent magnetic properties and general availability.

Piezoelectric: A voltage is applied across a piezo-crystal which causes an elastic strain in the crystal and launches a waveform into the material to which the crystal is coupled. When waveform reflections return to the crystal, the waveforms distort the crystal, and a measurable voltage is developed across the crystal due to the loss of symmetry.

The transducers are typically controlled with pulse generator/receivers and data is collected, processed, and stored with either an oscilloscope or a computer with data acquisition capabilities.

3.1. Temperature

Three ultrasonic measurement techniques were considered for development for space reactor temperature sensing. These techniques include a notched waveguide technique, a guided wave in plate technique, and a dual transducer technique. In all three techniques, temperature of a system or system component is inferred primarily from a measured change of the speed of sound in either the sensing element or the component itself with a very small contribution to the measurement arising from a detected change in length of the sensing element or component as a function of temperature. These three techniques are described below.

3.1.1. Notched Waveguide Technique

The primary components of this system are a notched waveguide that serves as the sensing element, a transducer, an interface card, and data processing software as shown in Figure 3.1.1-1. A transducer creates ultrasound waveforms in the waveguide, which consists of a thin metallic wire (~ 60 mils diameter) that contains a notch machined into the distal end. The waveforms propagate through the waveguide, reflect off both the notch and the end of the waveguide, and are detected by the transducer. Round trip time-of-flight measurements of the waveforms are used to determine the temperature of the sensor element by relating the time-of-flight differences to a change in sound velocity in the waveguide material. The sound velocity is a function of temperature in conjunction with a very small contribution to the measurement arising from a change in length of the waveguide material as a function of temperature. In this application, the sensor element of the waveguide must be in intimate contact with the component whose temperature is to be sensed or must be fully immersed in the environment to be monitored (e.g., gas, liquid, or solid).

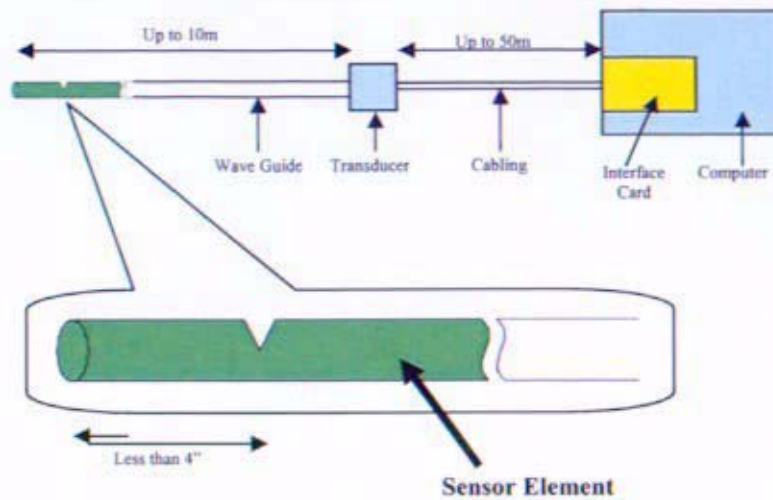


Figure 3.1.1-1: Notched Waveguide Temperature Sensing Concept

Two types of transducers are practical for this technique; magnetostrictive and piezoelectric. In the case where a magnetostrictive transducer is used, a magnetostrictive material must be used to couple the transducer to the waveguide of interest. Typically, Remendur or Premendur wire is used and must be seamlessly joined to the waveguide to minimize waveform reflection and loss of signal. In the case where a piezoelectric transducer is used, a transducer-to-waveguide ferromagnetic coupler is not needed, but an acoustic horn must be used to couple the transducer to the waveguide.

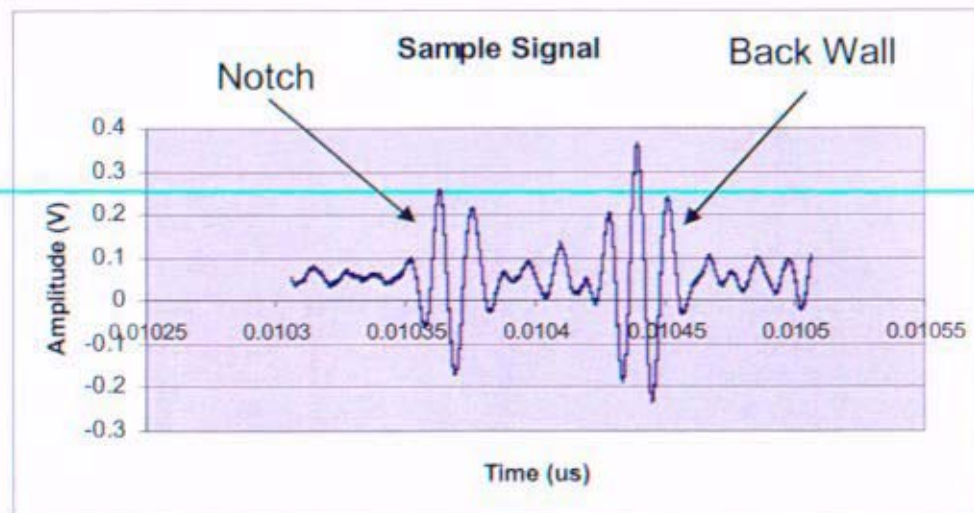


Figure 3.1.1-2: Sample waveguide data

A plot of sample data is shown in Figure 3.1.1-2. Testing at Bettis has shown that the notch can be placed within a few inches of the distal end of a refractory metal waveguide, such as Molybdenum, Tantalum, or Tungsten, and multiple notches can be used to obtain up to four temperature measurements from four different environments with one single waveguide. However, there may be challenges associated with transferring this capability from a lab to a production application. Testing

has also shown that stainless steel waveguides can be as long as 10 m, and the cable connecting the interface card to a magnetostrictive transducer can be as long as 65 m.

The transducers are typically controlled with pulse generator/receivers, and data is collected, processed, and stored with either an oscilloscope or a computer with data acquisition capabilities.

3.1.2. Guided Wave in Plate Technique

The primary components of this system are a rectangular plate that serves as the sensing element, a waveguide, a transducer, an interface card, and data processing software as shown in Figure 3.1.2-1. A transducer creates ultrasound waveforms in the waveguide, which consists of a thin metallic wire (~ 60 mils diameter) that is coupled to a rectangular plate via an integral acoustic horn. The waveforms propagate through the waveguide to the acoustic horn, where the waveform is split into several guided waveforms that travel at different speeds through the rectangular plate. Waveform reflections from the point of entry to the acoustic horn and the end of the plate are detected by the transducer. Time-of-flight measurements of the reflected waveforms are used to determine the temperature of the plate by relating the time-of-flight differences to a change in sound velocity in the waveguide material. The sound velocity is a function of temperature in conjunction with a very small contribution to the measurement arising from a change in length of the waveguide material as a function of temperature. In this application, the sensor element of the waveguide must be in intimate contact with the component whose temperature is to be sensed or must be fully immersed in the environment to be monitored (e.g., gas, liquid, or solid).

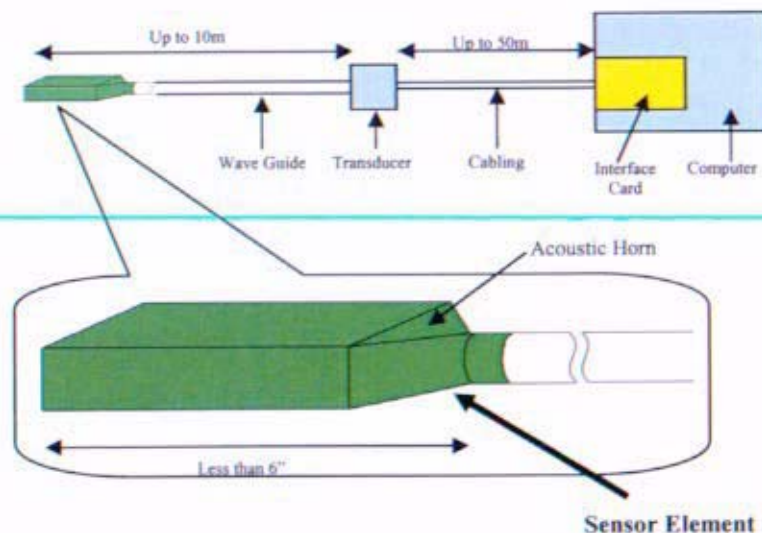


Figure 3.1.2-1: Guided Wave in Plate Temperature Sensing Concept

Two types of transducers are practical for this technique; magnetostrictive and piezoelectric. In the case where a magnetostrictive transducer is employed, a magnetostrictive material must be used to couple the transducer to the waveguide of interest. As with the notched waveguide technique described above, Remendur or Premendur wire is typically used as the ferromagnetic coupler and must be seamlessly joined to the waveguide to minimize waveform reflection and loss of signal. In the case where a piezoelectric transducer is used, a transducer-to-waveguide ferromagnetic coupler is not needed, but, an acoustic horn must be used to couple the transducer to the waveguide.

Testing at Bettis has demonstrated that a rectangular plate with dimensions of 10 cm X 2 cm X 0.6 cm produces a sufficient number of resolved guided waves of varying time-of-flights created at the joint of the waveguide to the acoustic horn and the end of the plate to accurately determine the temperature of the plate. Shorter plate lengths cause overlap of the guided wave reflections and confound the measurement. Testing has also shown that stainless steel waveguides can be as long as 10 m, and the cable connecting the interface card to a magnetostrictive transducer can be as long as 65 m.

The transducers are typically controlled with pulse generator/receivers, and data is collected, processed, and stored with either an oscilloscope or a computer with data acquisition capabilities.

3.1.3. Dual Transducer Technique

The primary components of this system are two transducers, an interface card, and data processing software as shown in Figure 3.1.3-1. In this system, the two transducers are anchored to the item of interest. One transducer creates ultrasound waveforms in the item of interest, and the other transducer detects the waveforms in a pitch-catch arrangement. Time-of-flight measurements of the waveforms are used to determine the temperature of the item by relating the time-of-flight differences to a change in sound velocity in the component of interest. The sound velocity is a function of temperature in conjunction with a very small contribution to the measurement arising from a change in length of the component as a function of temperature.

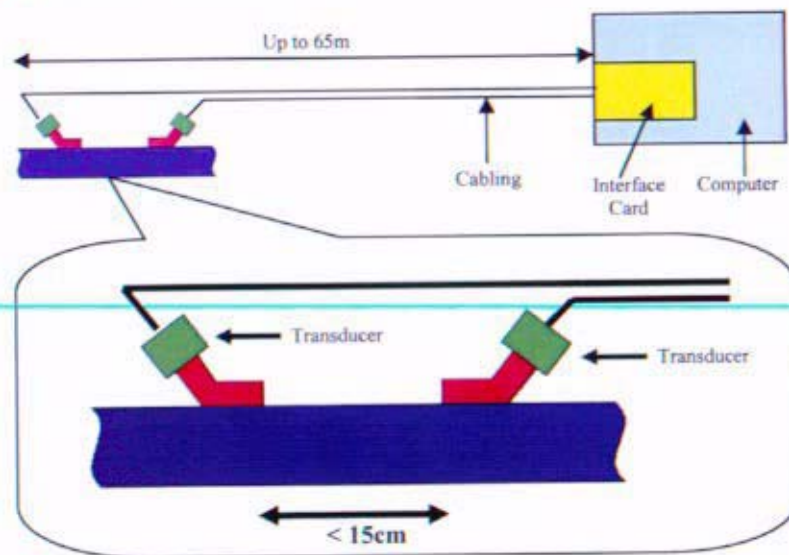


Figure 3.1.3-1: Dual Transducer Temperature Sensing Concept

Piezoelectric transducers must be used for this technique. The transducers must be anchored to the item of interest to prevent movement and must be acoustically coupled to the item of interest to effectively launch and detect waveforms.

The transducers are typically controlled with pulse generator/receivers and data is collected, processed, and stored with either an oscilloscope or a computer with data acquisition capabilities.

3.2. Flow

One ultrasonic measurement technique was considered for development for space reactor gas flow sensing. This technique is based on measuring two waveform travel times; one in the direction of the gas flow and one in the opposite direction. This technique is described below.

3.2.1. Gas Flow Measurement

The primary components of this system are a pipe containing flowing pressurized gas, two transducers, transducer interface acoustic wedges, an interface card, and data processing software. Figure 3.2.1-1 and 3.2.1-2 show typical configurations of this system. In a typical application of this technique, two piezoelectric transducers are mounted on the pipe with acoustic wedges. The wedges are used to create shear waves in the pipe, which convert to longitudinal waves upon entering the gas in the pipe. An ultrasonic waveform is first transmitted from transducer A to transducer B, in the direction of the gas flow, and the travel time is measured. Then, an ultrasonic waveform is transmitted from transducer B to transducer A, in the opposite direction of the gas flow, and the travel time is measured. In the first case, the measured velocity is equal to the velocity of the waveform in the gas plus the velocity of the gas. In the second case, the measured velocity is equal to the velocity of the waveform in the gas minus the velocity of the gas. Since the velocity of the waveform in the gas in both cases is equal, the velocity of the gas is equal to the difference of the two measurements divided by two.

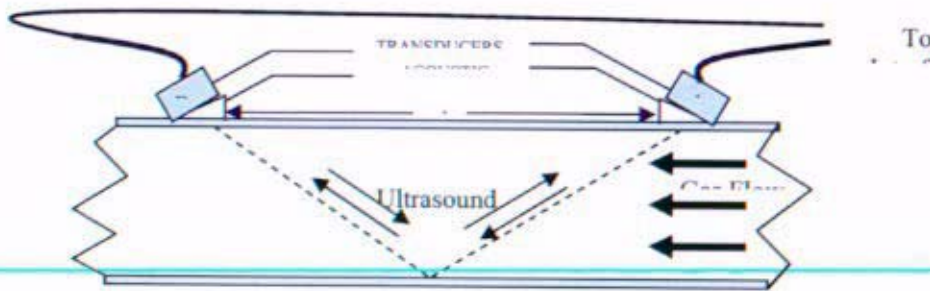


Figure 3.2.1-1: Gas Flow Sensing

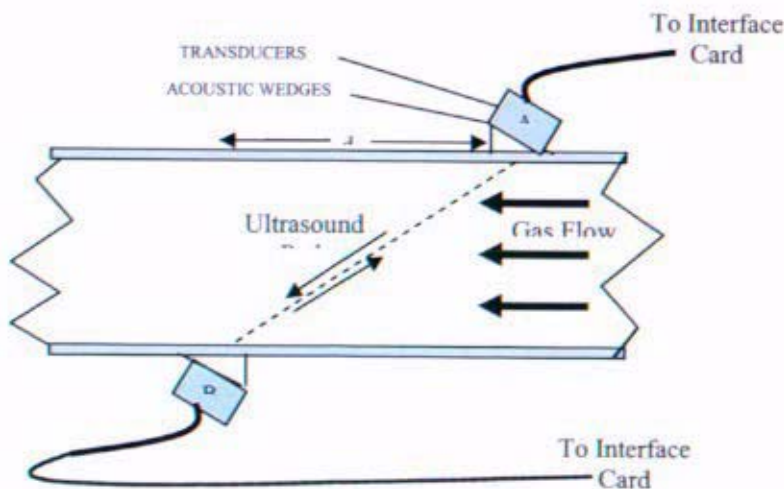


Figure 3.2.1-2: Gas Flow Sensing

In using piezoelectric transducers with this technique, the transducers must be anchored to and acoustically coupled to the pipe. Typically, acoustic wedges are used to accomplish this coupling.

The transducers are typically controlled with pulse generator/receivers, and data is collected, processed, and stored with either an oscilloscope or a computer with data acquisition capabilities.

3.3. Pressure

One ultrasonic measurement technique was considered for development for space reactor pressure sensing. This technique is based on the measurement of the amplitude of the reflected waveform from the inside surface of a pipe wall, which is inversely proportional to the pressure of the gas in the pipe. This technique is described below.

3.3.1. Amplitude Attenuation Technique

The primary components of this system are a pipe containing pressurized gas, a transducer, a transducer standoff reference block, a reference reflection mark in the reference block, an interface card, and data processing software. Figure 3.3.1-1 shows a schematic of this system.

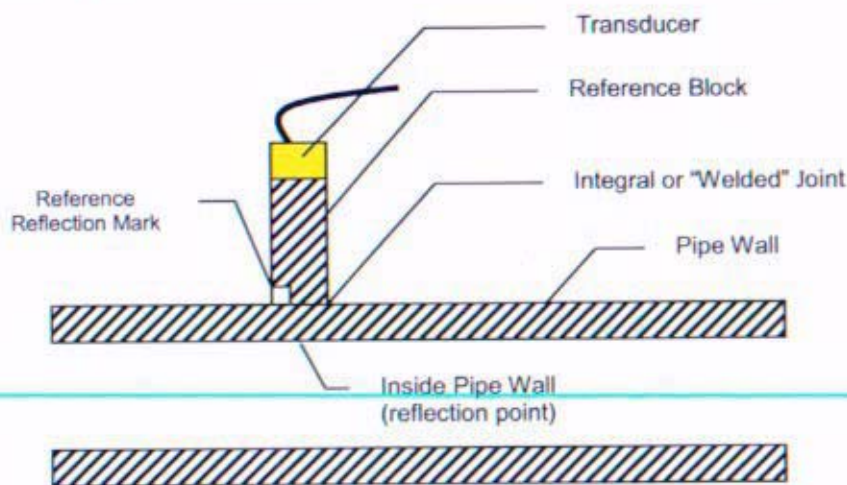


Figure 3.3.1-1: Pressure Sensing Concept

In this technique, a piezoelectric transducer creates ultrasound waveforms which propagate through the reference block, through the integral joint, through the pipe wall, and couple into the gas in the pipe. Waveform reflections will be received from the pipe wall inside surface and the reference mark in the reference block. The acoustic impedance of the gas will increase with gas pressure, bringing its impedance value closer to that of the pipe. As a result, more ultrasound energy will be coupled into the gas as the gas pressure increases, and correspondingly, the reflected signal amplitude will decrease. Therefore, monitoring of the amplitude of the reflected signal from the pipe wall inside surface can be used to monitor the pressure in the pipe. Note that amplitude based measurements are subject to significant errors and this would need to be seriously considered for production use.

The amplitude of the reflected pipe wall signal will also vary with changes in the ultrasonic coupling between the transducer and the reference block, and with changes in the reference block and pipe wall materials during the space reactor mission. Therefore, a reference marker is added to the

reference block, and the amplitude of the reflection from this marker can be used to compensate for these changes.

A piezoelectric transducer would typically be used for this technique, but a magnetostrictive transducer with a waveguide horn can also be used. The transducer (or horn) must be anchored to and acoustically coupled to the reference block.

The transducers are typically controlled with pulse generator/receivers, and data is collected, processed, and stored with either an oscilloscope or a computer with data acquisition capabilities.

3.4. Position

One ultrasonic measurement technique was considered for development for space reactor position sensing. This technique uses magnetostrictive principles to measure both linear and rotary positions. These linear and rotary techniques are described below.

3.4.1. Magnetostrictive Linear Position Technique

Figure 3.4.1-1 represents the basic concept of the linear ultrasonic position indicator (PI) sensor. It is composed of a ferromagnetic waveguide wrapped with two or three sets of coils: a set of coils for DC bias excitation (bias coils), a set of coils for AC pulse excitation (drive coils), and optional coils (compensating coils) to adjust the measurement to temperature gradients in the waveguide. An ultrasonic transducer is attached to one end of the waveguide. The transducer can be either magnetostrictive, which couples directly with the waveguide, or piezoelectric, which uses an acoustic horn to attach to the waveguide. A permanent magnet is attached to the control drive mechanism (CDM) and moves with the CDM relative to the waveguide.

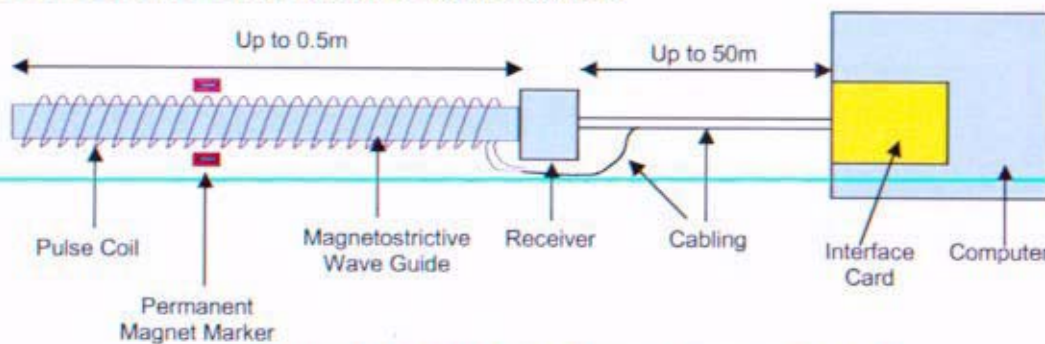


Figure 3.4.1-1: Linear Position Sensing Concept

With no magnetic fields present, the dipoles in the waveguide are randomly aligned. In the proximity of the magnet, the dipoles tend to line up in N to S orientation along the magnetic field lines of the magnet. Note that due to the mechanical structure of the material the line up is close to but not exactly N to S. With no current through the coils, the dipoles outside the influence of the magnet remain randomly aligned. When the drive winding is energized, the dipoles outside of the magnet region also line up in N to S arrangement. Again, the line up is not exactly N to S due to the material structure. This causes the rod to lengthen and thin (i.e. stretch out). When the drive winding current is removed, the dipoles outside of the magnet region "snap" back to their random order. This causes the entire rod to compress (shorten and thicken). The rate and extent of the compression is significantly greater in the region outside the influence of the magnet, since the fields from the magnet tend to keep the dipoles in their original N to S alignment. Although some compression does occur within the magnet's region, the difference is great enough to produce a strain in the waveguide in the region, resulting in a compressional (longitudinal) ultrasonic sound wave that travels along the

waveguide's length. This sound wave is picked up by the transducer. By measuring the time differential between application of the drive pulse and reception of the ultrasonic wave, the position of the magnet, and thus the CDM, can be inferred.

After the drive winding current is removed, the dipoles go back towards their original random starting state. The exception is that the dipoles do not go all the way back and retain some level of magnetism that is closer in line with the N to S arrangement that existed when the current was applied. Repeated application of drive current pulses will only work towards further retention of dipoles in the aligned N to S arrangement along the rod length. The rod will become more magnetized. Subsequent drive winding current removal will result in a reduced compressive reaction, thereby reducing the generated ultrasonic sound wave. To offset this effect, a DC bias current is applied to the bias coils immediately after the completion of the drive winding pulse. The effect of the current is to offset the residual magnetism so that the dipoles can return to a known starting state. Effectively the bias winding is a degaussing coil. The bias winding current is applied for more than 99% of the time.

3.4.2. Magnetostrictive Rotary Position Technique

The primary components of this system are identical to those in the magnetostrictive linear position technique. The rotary sensor has the same principal of operation, except that the ferromagnetic waveguide takes the form of a circle (Figure 3.4.2-1). Due to this configuration, the ultrasonic pulse travels both directions on the waveguide to the transducer. Benefits to accuracy and calibration can result from the additional information of the second pulse.

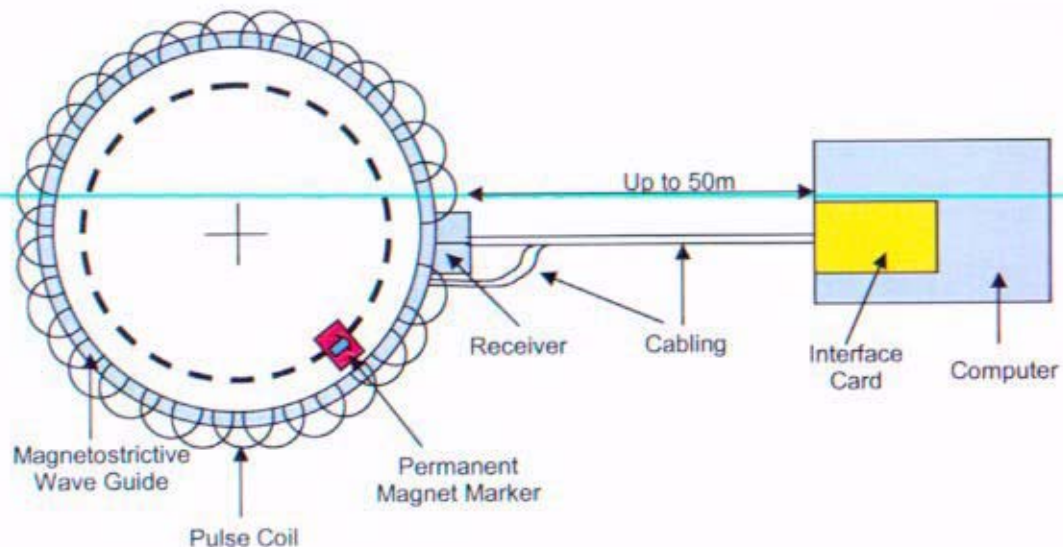


Figure 3.4.2-1: Rotary Position Sensing Concept

4. Common Issues

4.1. Measurement Sensitivity and Calibration

The sensors are required to measure various system parameters within a specified range and accuracy. Therefore, instrument sensitivity will be impacted by phenomena that vary among measurement types and strategies. Each measurement type must be scrutinized on a case-by-case basis to determine the achievability of the sensitivity requirements. Examples of these requirements are outlined in Table 2.3-1.

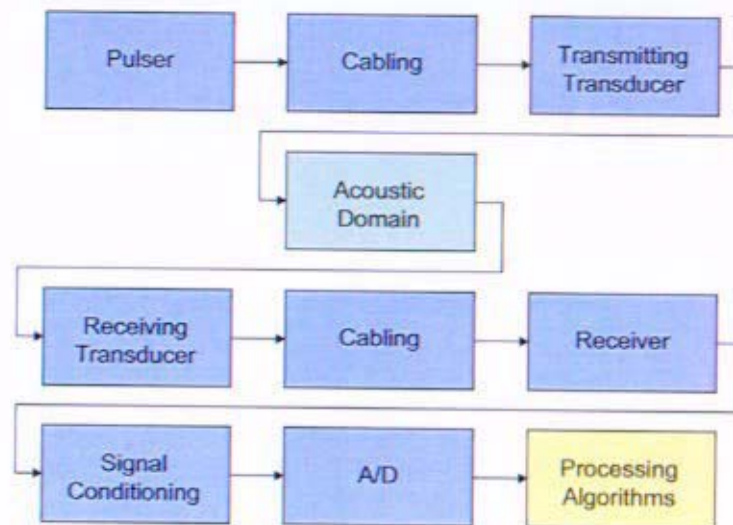


Figure 4.1-1: Complete signal path

The complete path that each signal will follow is depicted in Figure 4.1-1. The signal will take the form of electrical (blue), mechanical (green), and digital (yellow) quantities throughout its duration. Some general factors affecting sensitivity in the electrical and digital regions are:

1. Signal noise
2. Signal attenuation
3. Electromagnetic interference
4. A/D resolution
5. Processing precision

Although these factors are an important part of the sensitivity analysis, they are well-known phenomena and are not seen as jugular issues.

The broadest impact of measurement sensitivity resides in the acoustic domain. Here, the sensitivity of each measurement is based on the system's ability to detect a change in the ultrasonic energy resulting from the change in the parameter of interest. These changes in the ultrasonic energy may also be affected by other parameters. For example, acoustic impedance of a gaseous material changes with pressure as well as temperature, thus in order to derive pressure from acoustic impedance, temperature must also be known within a certain accuracy. The system's ability to isolate the parameter of interest from other effects will directly impact sensitivity to that parameter.

Sensor drift over the life of the mission is another attribute that affects instrument accuracy and needs to be investigated on a case-by-case basis. Some type of calibration will be required in order to compensate for drift. The ability to calibrate each instrument effectively must be explored thoroughly.

The piezoelectric methods cause the greatest sensitivity concerns since they involve interaction of the ultrasonic waves with the gas. Due to the enormous impedance mismatch between the pipe wall and the gas, very little ultrasonic energy will couple into the gas and then back into the pipe wall. Once the ultrasonic energy is in the gas, attenuation becomes a concern, especially at higher frequencies and low pressures. For these reasons, achieving adequate measurement sensitivity and calibration techniques carries moderate risk.

4.2. Cabling

The bulk of the cabling will be 50-ohm coaxial or triaxial cable and will run from the instrument vault (aft of spacecraft) to each remote transducer location near the sensing element. Each sensor system will need one or two cables to carry the excitation signals from the vault electronics to the transducers and to carry the response signals from the transducers back to the vault. Electrical signal frequencies in the cables will be below 5 MHz. The cabling must be able to withstand extreme temperature swings and gradients, the radiation environment of space, and flexing during spacecraft deployment.

4.2.1. Bending ability

During launch, the spacecraft will be folded into a payload fairing. Upon reaching orbit the spacecraft will be deployed to its full length for the remainder of the mission. Thus the cabling running the length of the spacecraft ~~must be able to fold, with some bending radius restriction, up to 180 degrees on~~ itself. This effect may be exacerbated by vibration and thermal shock during the pre-launch, launch, and deployment phases of the mission. The cabling must be resilient enough to maintain signal integrity under these circumstances.

4.2.2. Length

The cable run to each sensor will be approximately 65 m. Coaxial cables were tested at Bettis in a laboratory setting without the presence of electromagnetic interference for magnetostrictive ultrasonic signal integrity with lengths up to 200 ft (>60 m) with no apparent loss in signal amplitude or resolution. Figures 4.2.2-1 and 4.2.2-2 show the results of these tests for the cables uncoiled and coiled, respectively. The only discernible difference between the three configurations is a slight delay for longer cables due to the extra distance the excitation and response pulses must travel between the interface card and transducer. This delay can be easily accounted for and filtered out with processing techniques.

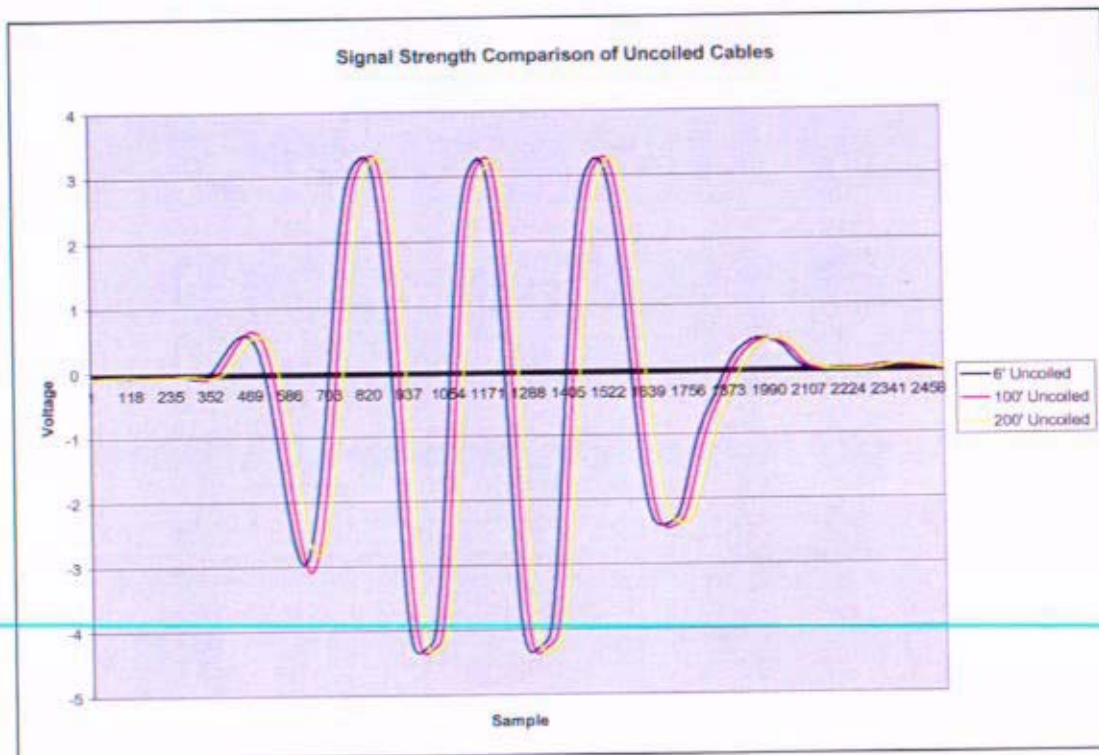


Figure 4.2.2-1: Comparison of three uncoiled coaxial cables of 6', 100', and 200'

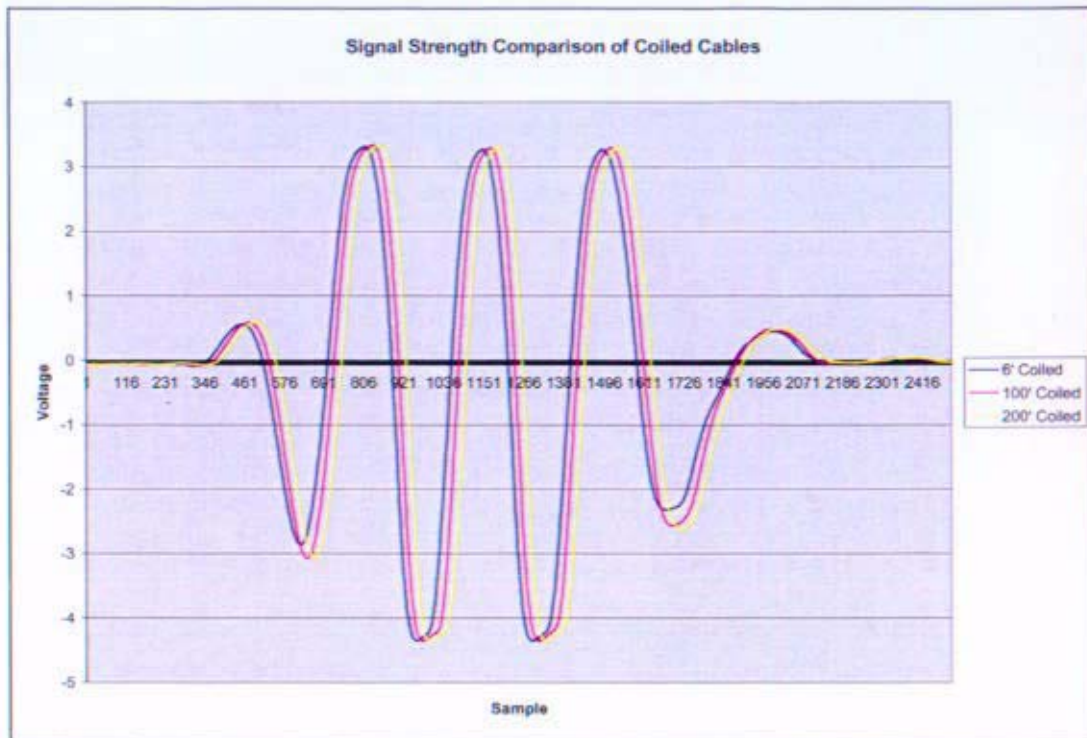


Figure 4.2.2-2: Comparison of three coiled coaxial cables of 6', 100', and 200'

4.2.3. Attachment to spacecraft

The cabling must be secured to the spacecraft in such a way as to minimize cable strain during spacecraft deployment. To avoid EMI, it is necessary to attach the signal cables as great a distance as possible from the power supply lines or any other potential noise sources.

4.2.4. Attachment to sensor housing

The transducers will be housed in some type of protective container and the cables running from the vault will interface with the transducers through standard space-grade coaxial or triaxial connectors (BNC, SMA, and Microdot). Hermetic connections may be required. The connections through the housing to the transducer must maintain an impedance match to minimize (electrical) reflections at the connection interfaces.

4.3. Interface Cards

Ultrasonic sensors would require an interface card configured as part of the reactor instrumentation and control system. The interface cards will house all functionality necessary to perform the ultrasonic measurements, including timing, pulsing and receiving, analog-to-digital conversion, signal conditioning, data buffering and queuing. Development of the interface cards with sufficient rad-hardness is judged to hold moderate risk.

4.3.1. Availability

As no commercial printed circuit board cards include all the functionality required for the Prometheus mission ultrasonic measurements, customized space-grade cards must be made. Several potential vendors have been identified.

4.3.2. Compatibility with computer

The reactor control computer and peripheral cards are anticipated to have either Compact PCI (cPCI) or PXI bus architectures. The interface cards will be designed to the specifications of the chosen architecture.

4.3.3. Connectors

The interface cards will connect to the reactor control computer through the cPCI or PXI bus in the instrument vault. They will connect to the ultrasonic sensors through space-grade coaxial or triaxial connectors. Since the instrument vault will be in a hermetically sealed container, additional connections may be necessary to pass the cabling through the hermetic barrier. To minimize signal attenuation, low-loss connectors and impedance matching should be maintained throughout.

4.4. Software

Custom software must be written to control, acquire, and process data from the ultrasonic sensors. It is envisioned that software would be resident on the ultrasonic interface card.

4.4.1. Complexity

The overall complexity of the ultrasonic system software will be moderate. The hardware drivers, data handling, and control code will be fairly straight forward. Processing algorithms that convert the raw ultrasonic signals into engineering data will pose a greater challenge. Well-developed techniques, such as cross correlation or wavelet transforms, will likely be employed.

5. Ultrasonic Transducers

5.1. Piezoelectric

Piezoelectric transducers will be considered for the pressure, flow, and temperature measurements. A candidate piezoelectric transducer concept is shown in Figure 5.1-1. The Lithium Niobate piezoelectric element is bordered on one side by carbon/carbon absorbent backing, which doubles as the positive excitation terminal. Gold foil is attached to the other side as both an ultrasonic couplant and the ground excitation terminal. The nylon insulation electrically isolates the carbon/carbon backing from the stainless steel housing in this example, but nylon will not be suitable for the space environment and a different material will have to be used. A standard BNC (Bayonet Neill-Concelmann) connection is used to transfer signals to and from the transducer.

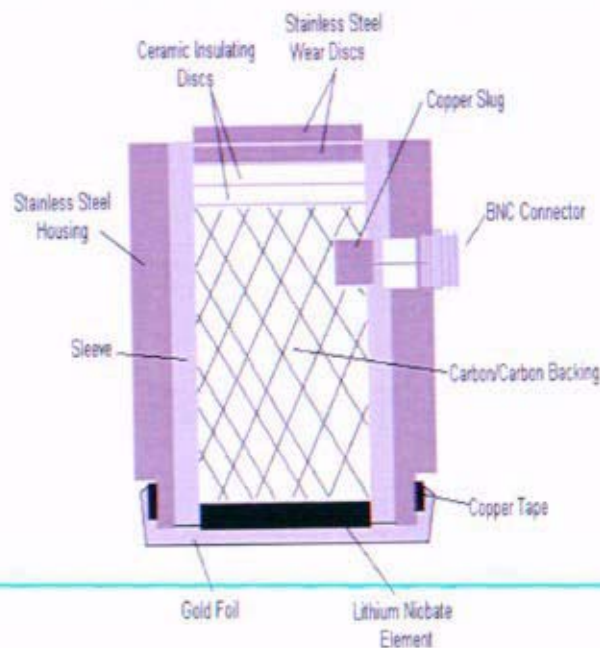


Figure 5.1-1: Piezoelectric transducer concept drawing

To expand on ultrasonic signal generation as briefly mentioned in Section 3, a waveform is generated when a voltage is applied across the piezoelectric crystal. When a voltage is applied across the piezo-crystal the crystal elastically deforms and launches a waveform into the wear plate or gold foil. The waveform then travels through the standoff, pipe, and gas then back again until it reaches the piezoelectric crystal. When the reflected waveform returns to the crystal, the waveform then deforms the crystal and a measurable voltage is developed across the crystal due to the loss of symmetry.

5.1.1. Housing

In general, the main design concern of the transducer housing is material compatibility with the mission environment and other interfacing materials. Since much testing and analysis is needed to assess the impact of materials in the transducer housing design, this area is assumed to have moderate risk.

5.1.1.1. Construction/Materials

The transducer housing must provide protective containment for transducer components. Materials with stability at high temperatures, such as nickel-based superalloys (i.e. Inconel-600) and stainless steels (i.e. type 310) will be considered. The various options available make material choice a low-risk issue.

5.1.1.2. Temperature/Radiation Compatibility

The material must endure a maximum temperature of 1150K and a total neutron fluence of 3×10^{14} n/cm² and 100 MRad gamma radiation. The materials that a commercial off-the-shelf (COTS) sensor is made of currently will fail under the high temperatures and radiation conditions of the mission. The temperature and radiation compatibility of the housing is a moderate risk issue and requires engineering. The Pennsylvania State University is in the process of developing ultra-high-temperature transducers that will be able to withstand the high temperature environment.

5.1.1.3. Material Degradation (Temp/Radiation effects)

At temperatures up to 1150 K both stainless steel Type 310 and Inconel-600 will not melt and will not corrode in a vacuum. The creep rates of both materials increase with high temperatures, and the mechanical strength of both materials will be significantly reduced at 1150 K. Advanced testing will have to occur to determine if the materials can mechanically withstand the defined temperatures of the mission. Both creep and mechanical strength are not serious issues but can be of concern and must be investigated thoroughly.

For both stainless steel and Inconel-600 the neutron radiation these materials will see will most likely be too small to cause any material degradation. If these alloys are proven inadequate, there are other stainless steels and Inconel alloys that may have the strength and creep resistance that are needed at high temperatures.

5.1.1.4. Attachment of transducer to standoff

The standoff can be either a block shape for the pressure sensor or a wedge shape for the temperature and flow sensors. A near perfect contact between the transducer and standoff is desired. A soft metal such as gold or platinum will be used as a couplant to attach the transducer to the standoff. The couplant is used to allow transfer of the ultrasonic energy into the standoff from the piezoelectric element. In order to minimize the losses associated with this interface, the acoustic impedance of the material will be investigated to ensure a proper impedance match. The couplant material must also be compatible with the standoff material at the elevated operating temperatures. Engineering must be performed in order to identify the best possible candidate, so this carries moderate risk.

5.1.1.5. Attachment of transducer & standoff to piping

A near perfect contact between the transducer and standoff to the pipe is desired to maximize ultrasonic energy transfer into the pipe wall. An interface metal or soft metal such as gold or platinum will be used as a couplant to attach the standoff or wedge to the pipe. Regardless of how well the standoff is attached, reflections will still occur at the interface. The materials involved must be acoustically impedance matched in order to minimize energy loss due to the reflections. Since the standoff-piping interface is fairly close to the gas in the pipe (pipe wall thickness – conceptually designed at 0.25 cm), the pulse duration and frequency must be designed to avoid interference from the standoff-piping interface reflections. Finally, the couplant will be in direct contact with the pipe at a temperature up to 1150 K, so care must be taken to ensure material compatibility. In addition to the couplant a clamp-on technique can also be used in attaching the standoffs to the pipe. In summary,

attaching the transducer and standoff to the piping is a high risk issue and must be carefully investigated.

5.1.1.6. Cabling Connector(s)

The housing of the transducer must provide for connection of one coaxial cable for control of the piezoelectric element. The connection must be mechanically rugged to withstand launch and should comply with applicable MIL or NASA standards. Commercial transducers use standard BNC, SMA, or Microdot connections. Risks associated with cabling are assessed to be low.

5.1.2. Piezoelectric Element

The piezoelectric element in the transducer is the material that converts electrical signals to physical signals and the reverse. Due to the location of the transducers, the piezoelectric element must endure temperatures up to 800 K, a total neutron fluence of 3×10^{14} n/cm² and 100 MRad gamma radiation. Several materials are under consideration, but none have been used before for this type of application.

5.1.2.1. Construction Material (crystal, ceramic, etc.)

High-Curie point piezoelectric materials under consideration include Aluminum Nitride, Lithium Niobate, Bismuth Titanate, Tourmaline, Langasite, Lead Metaniobate, and Lead Zirconate Titanate. Both single and poly-crystalline types will be considered. The thickness of the material is inversely proportional to the operating frequency of the element. Due to the many options available, selection of piezoelectric material is low risk.

5.1.2.2. Temperature/Radiation Compatibility

The piezoelectric material must be able to withstand a defined maximum temperature of 1150 K. The use of standoffs can reduce this to 800 K or less. Table 5.1.2.2-1 gives the Curie temperature and operating temperature of the piezoelectric elements that are being looked at for the piezoelectric transducers.

Table 5.1.2.2-1: Piezoelectric Element Temperature Compatibility (MP = Melting Point)

Material	Curie Temp (K)	Max Operating Temp (K)
LiNbO ₃ (Lithium Niobate)	1423	673
Lithium Niobate w/Na	1423	1073
AlN (Aluminum Nitride)	MP > 2473	873-1173
Pz46 (BiTiO ₁₂ , Bismuth Titanate)	923	823
La ₃ Ga ₅ SiO ₁₄ (Langasite)	MP = 1743	1273
CP-103 (Tourmaline)	none	923
K-12 Kezite (Bismuth Titanate)	1093	755

The most compatible with the high temperature is Langasite, Aluminum Nitride, and Lithium Niobate with Sodium. With the use of a standoff, all the above materials can withstand the mission temperature requirement of 800K. The material of choice must be able to withstand a total neutron fluence of up to 3×10^{14} n/cm² and 100 MRad gamma radiation. For example, Tourmaline is quoted to withstand 10^9 Rad gamma radiation and a total neutron fluence of 1×10^{18} n/cm². The temperature and radiation compatibility of the piezoelectric element is a high risk issue because most of the

piezoelectric material radiation compatibility is unknown and a variety of materials need to be investigated.

5.1.2.3. Material Degradation (Temp/Radiation effects)

With normal use the electrical activity of common polycrystalline piezoelectric material degrades as a half-life function. Normal drift rates are on the order 1% over a period of 15 to 20 years following the first 100 days after polarization. However, temperature and radiation affect the properties of piezoelectric materials. If the temperature were to exceed the Curie temperature of the material, this would cause loss of polarization and severely degrade transducer performance. Elevated temperatures can cause phase transformations or chemical decomposition in piezoelectric materials. Neutron and energetic particle irradiation are likely to damage the crystal lattice of the piezoelectric elements and thus degrade the piezoelectric properties of the crystal. Both radiation and elevated temperatures have the potential to severely damage or destroy the piezoelectric response of the transducer element. The use of Aluminum Nitride is predicted to mitigate some of these risks because it has no Curie temperature. Significant testing must be performed in this area before a piezoelectric transducer could be utilized in this environment for a 15-20 year mission. High risk is assigned to degradation of the piezoelectric element due to radiation and elevated temperatures.

5.1.3. Absorbent backing

5.1.3.1. Construction/Material

The backing will be a dense, highly attenuative material whose function is to absorb energy radiating from the back side of the piezoelectric element. This is done to control the vibration experienced by the transducer itself, and can also be used to control signal amplitude. Choosing a material with an acoustic impedance similar to that of the active element will cause more sound energy to be absorbed into the material. One material of choice is Alumina (Al_2O_3), which has an acoustic impedance of $25.5 \times 10^5 \text{ g/cm}^2\text{-sec}$, similar to the piezoelectric element. Overall, the general material choice carries low risk.

5.1.3.2. Temperature/Radiation Compatibility

The transducers will be located on a standoff behind the shield so the material of the absorbent backing must be able to withstand the predicted conditions experienced in this location. The housing construction may only be able to absorb some of the heat from the pipes and space environment. Since the transducers will be located on a standoff away from the surface of the pipes, the transducers can experience a temperature of 800K, and a total neutron fluence of $3 \times 10^{14} \text{ n/cm}^2$, and 100 MRad gamma radiation. The temperature and radiation compatibility of the absorbent backing is a high risk issue and requires engineering.

5.1.3.3. Material Degradation (Temp/Radiation effects)

Alumina (Al_2O_3) is thermally stable and should not be greatly affected by temperature or radiation. This material should degrade very little due to the high temperatures and radiation and is considered to be low in risk.

5.1.4. Wear Plate

5.1.4.1. Construction/Material

The wear plate provides protection between the piezoelectric element and the test specimen. It can also function as an acoustic transformer by using the principle of superposition if the plate is designed to have a thickness of 1/4 of the operating wavelength. Materials under consideration are stainless steel Type 310 and Inconel-600. Choice of wear plate materials carries low risk.

Pre Decisional – For Planning and Discussion Purposes Only

5.1.4.2. Temperature/Radiation Compatibility

The transducers will be located behind the shield so the material of the wear plate must be able to withstand the predicated conditions experienced from this location. Since the transducers will be located on a standoff away from the surface of the pipes, the transducers can experience a temperature of 800 K, and a total neutron fluence of 3×10^{14} n/cm², and 100 MRad gamma radiation. The temperature and radiation compatibility of the wear plate carries moderate risk and requires engineering.

5.1.4.3. Material Degradation (Temp/Radiation effects)

At temperatures up to 800 K both stainless steel Type 310 and Inconel-600 will not melt and will not corrode in a vacuum or in air. The creep rates of both materials increase with high temperatures, and the mechanical strength of both materials will be significantly reduced at 800 K. Advanced testing will be needed to determine if the materials can mechanically withstand the defined temperatures of the mission. Both creep and mechanical strength are not jugular issues, but this issue carries moderate risk due to testing required.

For both stainless steel and Inconel-600 the neutron radiation these materials will see will most likely be too small to cause any material degradation. If these alloys are proven inadequate, there are other stainless steels and Inconel alloys that may have the strength and creep resistance that are needed at high temperatures.

5.1.5. Pulse Transmission-Receiving

The frequencies, amplitudes, and pulse widths of the different piezoelectric measurement concepts may vary depending on the optimal arrangement for each. Piezoelectrics can be constructed to resonate at all ultrasonic frequencies of interest (50 kHz – 5 MHz), so this should not be a significant issue. Tradeoffs will be made based on transducer size, signal integrity, and measurement sensitivity.

5.1.5.1. Noise

The piezoelectric transducers produce a relatively small signal compared to magnetostrictive transducers. Noise in the piezoelectric instrumentation will have a direct impact on measurement sensitivity. A thorough sensitivity analysis must be done for each piezoelectric transducer to quantify the effects of noise. Signal amplification and filtering can be done to overcome any significant noise issues. Signal noise carries moderate risk due to its impact on measurement sensitivity and our current lack of understanding on its impact.

5.1.5.2. Dampening

After signal transmission, the transducer will continue to vibrate for a short time until it dissipates all of its energy. If the reflected signal returns before the vibration is completely dampened it can confound the detection of the signal of interest. The dampening takes a relatively short amount of time so this usually only creates a problem when expecting very rapid reflections. Delay lines are used to counteract any problems of this nature, and are on the order of several millimeters in thickness. Long standoffs will be required for use with a piezoelectric transducer (as will be explained in a later sections). Therefore, the transducer should have ample time to cease vibrating, and dampening is not an issue.

5.1.5.3. Time Response

The time response requirements of sensors using piezoelectric transducers are not demanding. The specifications at this time are within the capabilities of the transducer and are thus low risk.

5.1.5.4. Signal Drift/Calibration requirements

Since the speed of sound in a material varies with several material properties, timing measurements may be affected by conditions at various stages of the mission. Transmission characteristics may also change due to radiation or time at temperature as well. Various methods are under development to determine the speed of sound in the material and apply corrections to the measurements. The risk associated with drift is moderate.

5.1.5.5. Interference/Crosstalk Susceptibility

It is possible that many transducers will be used for the various sensors. Crosstalk between the different transducers becomes a concern whenever multiple signals of similar frequencies are in close proximity. Careful filtering or even sequencing the measurements from each transducer may help to avoid this, which makes this a low-risk issue.

5.1.6. Interface

5.1.6.1. Number of Cables

Piezoelectric transducers require one coaxial cable per transducer. Very low risk is expected for cabling requirements.

5.1.6.2. Multi-functionality

Piezoelectrics are being considered for gas flow, temperature, and pressure. It is possible that measurement of multiple parameters could be made with the same transducer or transducer sets. For example, flow and the dual-transducer temperature measurement possess the same basic configuration. It may be possible that both temperature and flow can be extracted from a single set of transducers.

5.2. Magnetostrictive

The primary components of a magnetostrictive transducer are the housing, permanent magnet, and pulse coil. The transducer must also interface to a control cable and to the magnetostrictive waveguide into which the acoustic pulse is launched. Figure 5.2-1 shows a schematic of the transducer. As briefly mentioned in Section 3, a magnetic field is generated by an alternating current in the coil. The field interacts with the magnetostrictive waveguide by aligning its magnetic dipoles in the direction of the field. This produces a mechanical strain that propagates as an elastic wave through the waveguide. For signal reception, the reflected acoustic pulse creates minute mechanical disturbances as it travels the waveguide. These deformations cause an instantaneous change in the polarization of the material, which causes a change in the magnetic field inside the coil. The varying magnetic flux induces an electric current in the coil which is detected by the receiver electronics.

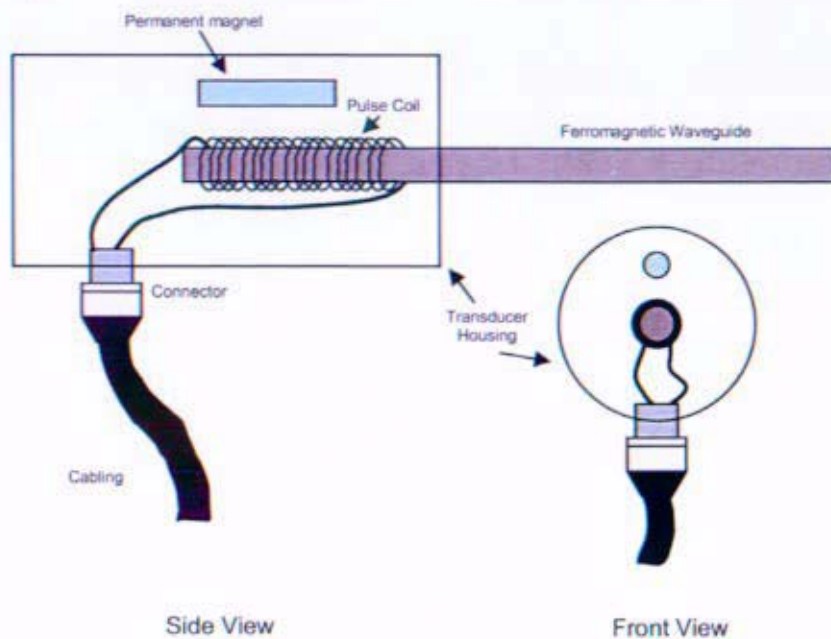


Figure 5.2-1: Schematic of a Magnetostrictive Transducer

5.2.1. Applications

The potential sensor applications using magnetostrictive transducers are position indication (linear and rotary) and two of the three temperature measurement options (notched waveguide and guided wave in plate).

5.2.2. Housing

5.2.2.1. Construction/Materials

The transducer housing shall be manufactured to support the functional components of the transducer while providing protection from the harsh environments experienced during the life of a space reactor. Inconel 600 and stainless steels are likely candidates for this application. Some development will be needed to ensure that environmental compatibility is better than what is commercially available.

5.2.2.2. Temperature/Radiation Compatibility

The housing material must endure predicted conditions experienced by a transducer located behind the shield on a standoff. These include a maximum temperature of 800 K, a total neutron fluence of 3×10^{14} n/cm², and 100 MRad gamma radiation. Identifying materials that can withstand these conditions will not be difficult and the risk associated with doing so is low.

5.2.2.3. Attachment of transducer to plant

The attachment of a magnetostrictive transducer to the spacecraft does not present the same concerns as with a piezoelectric transducer. It does not require attention to acoustic coupling since signal generation is through magnetic interactions with the waveguide, and not through physical contact of the face of the transducer with the medium. A rugged connection of the transducer housing to the craft can be made, preferably in the lowest temperature/radiation environment possible, with the only requirement being proper location and orientation allowing for attachment to the waveguide. Welding, brazing, or clamping methods can be used to affix a magnetostrictive transducer to the spacecraft. A magnetostrictive transducer has more flexibility as to where it is located because the

length of the waveguide can be relatively long. The overall risk related to attachment of a magnetostrictive transducer is low.

5.2.2.4. Attachment of transducer to waveguide (positive capture)

A magnetostrictive transducer requires that the wire waveguide be inserted into its housing and inside the coil windings. It must be in a fixed position not allowing for movement or realignment that could cause signal attenuation or inconsistencies in signal timing measurements. The attachment itself must also not impede signal transmission in the waveguide. This has been accomplished commercially for sensors of this type, but any adhesives or epoxies currently used may not be compatible with the high mission temperatures. Using the waveguide to carry the ultrasonic signals to the location of measurement, the transducer, and thus the waveguide attachment, can be placed at a distance from the high temperatures. This will possibly relax the temperature requirement of the adhesive. Also, other alternatives for waveguide attachment are being investigated. For these reasons, risk involved with waveguide attachment is foreseen to be moderate.

5.2.2.5. Cabling Connector(s)

The housing of the transducer must provide for connection of one coaxial cable for control of the pulse coil, and possibly one more cable if an electromagnet is used. The connection must be mechanically rugged to withstand launch and should comply with applicable MIL or NASA standards. Commercial transducers use standard BNC, SMA, or Microdot connections. Risks associated with cabling are low.

5.2.3. Bias Magnet (Permanent or Electromagnet)

5.2.3.1. Field Strength Required

The strength of a magnetic field drops off roughly exponentially with distance and is calculated differently for each magnet geometry (ring, bar, disc, etc.). An electromagnet might prove to be most desirable because of the ability to manage the field strength by means of the power supplied to it. Typically, magnets designed to withstand higher temperatures have lower field strengths, but not so low as to be a risk.

5.2.3.2. Field Degradation (Temp/Radiation effects)

The permanent magnet will be of a high-Curie temperature material that will not lose magnetization over the life of the mission. SmCo and FeCo magnets have Curie temperatures in the 1000K-1200K range, but extended exposure to high temperatures still below the Curie temperature can cause loss of field strength. Thermal stabilization below the maximum rated temperature of the magnet reduces these losses. The effect of time itself on magnetic flux is minimal at <1% for the Rare Earth permanent magnets, and <3% for Alnico types.

The radiation sensitivity of a permanent magnet is of less concern than the temperature sensitivity depending on the material. All magnets lose field strength at high temperature, but they all do not have the same response to radiation. Previous tests to total fluences greater than expected during the Prometheus Project showed that there is no significant effect on the field strength of Sm₂Co₁₇ due to irradiation. NdFeB magnets, however, are known to be more susceptible to demagnetization by irradiation. It is also desirable that any magnet not be subject to direct heavy-particle irradiation.

The major risk with magnets is the potential for total loss of field strength if it is exposed to temperatures above its Curie temperature. Small losses of field strength may not be a concern since typical measurements using magnetostrictive systems are not amplitude based. Again, the use of an electromagnet may prove ideal because of the ability to combat any field degradation by increasing

the supplied power. However, cabling mass to operate the electromagnetic will add to the total mass inventory of the system. Though magnets with required Curie temperatures do exist, overall risk associated with magnet degradation is high because temperatures could approach operational limits.

5.2.3.3. Construction/Material

The bias magnet of commercial transducers is a simple rod or thin cylinder that is mounted in the transducer housing in close proximity to the pulse coil. Several candidate materials include grades of SmCo, Alnico, and NdFeB with respective Curie temperatures of 1100 K, 1115 K, and 600 K. The recommended operating temperature for magnets is typically 200-300 K below the Curie temperature. The performance of the different materials in a high temperature/high radiation environment will have the highest priority in material selection.

5.2.3.4. Degaussing

When the magnetostrictive waveguide is in the field of the permanent magnet for extended periods of time the dipoles of the waveguide become arranged in a way that interferes with the transducer's ability to generate acoustic signals in the waveguide. This results in attenuation of the signals in the measurement system.

Possible methods of counteracting this effect include:

- Using an electromagnet in place of the permanent magnet to limit the amount of time the magnetic field is applied to the waveguide (e.g., no magnetic field will be applied during the off duty cycle of the transducer).
- Slowly sweeping around the hysteresis loop via an alternating current through the pulse coil to relieve the residual magnetic stresses in the waveguide.
- Applying a DC bias to the coil to realign the magnetic dipoles. This method is used in magnetostrictive position indicators already in use in the NR Program.

Risks with this issue are moderate because these techniques are developmental for use with a transducer.

5.2.3.5. Power requirements (electromagnet only)

The two purposes for using an electromagnet in place of a permanent magnet are to combat the effects of temperature and radiation on magnetic field loss, and for potential degaussing methods. This would introduce another control cable but is not foreseen to be complicated or have any major power requirements.

5.2.4. Pulse Coil

5.2.4.1. Conductor Material

It is preferable that the coil be composed of a material with as low a thermal coefficient of resistance as possible with the ability to withstand high temperature. The properties of some conductors are listed in Table 5.2.4.1-1. Copper and silver are very similar with respect to these properties, with copper being able to endure slightly higher temperatures.

Table 5.2.4.1-1: Conductor Properties

Material	Resistivity (Ω m) ($\times 10^{-8}$)	Temp. Coef. of Resistance per K ($\times 10^{-3}$)	Temp. Coef. of Expansion per K ($\times 10^{-5}$ mm/mm)	Melting Point K
Copper	1.61	3.9	1.8	1356
Silver	1.59	3.8	2.0	1235
Aluminum	2.8	3.9	2.5	930
Nickel	6.84	5.8	1.7	1726

5.2.4.2. Temperature/Radiation Compatibility

With increasing temperature, the electrical resistance of the coil will increase causing a decrease in current. The field strength of the coil is dependent on current, so this will cause a decrease in the field strength of the coil. Once again, since typical measurements using magnetostrictive systems are not amplitude based, this may not present a major problem as long as the signal is not severely attenuated down to an undetectable amplitude.

Increasing the temperature of the coil also causes thermal expansion. If the insulation or housing surrounding the coil does not have a coefficient of thermal expansion compatible with the coil, or if the coil assembly does not have enough clearance to expand, damage can occur to the coil or insulation. This can be mitigated by choosing materials with similar coefficients of thermal expansion (See Table 5.2.4.2-1).

Table 5.2.4.2-1: Housing Properties (from J. L. Everhart, Engineering Properties of Nickel and Nickel Alloys, pp.60 and 132, Plenum Press, New York-London, 1971.)

Material	Temp. Coef. of Expansion per K ($\times 10^{-6}$ mm/mm)	Melting Range K
Inconel 600	16.4	1644-1700
S.S. 310	17.5	1616-1727

Due to the wide range of temperatures the transducer is expected to experience, environmental compatibility of the pulse coil is a moderate risk.

5.2.4.3. Field Strength

The magnetic field generated by the pulse coil is strongest inside the coil itself and acts on the inserted portion of the waveguide (see Figure 5.2-1) to create an acoustic pulse. The strength of the field (B) created inside the coil is determined by the equation $B = \mu_0 n I$ where (n) is the number density of turns per unit length in the coil, (I) is the current, and (μ_0) is the permeability constant. The current and number of turns can be varied to meet field strength needs, making the risk low for this issue.

5.2.5. Pulse Transmission-Receiving

5.2.5.1. Noise

The signals in a magnetostrictive ultrasonic system are typically less susceptible to noise contamination than in a piezoelectric system. This is because higher amplitude signals can be generated by magnetostrictive transducers, making it a low-risk issue.

5.2.5.2. Dampening

A magnetostrictive waveguide is required for all applications of magnetostrictive transducers, and for some applications it is necessary to couple that to another waveguide material. This connection introduces a reflection point for the acoustic signal and creates a ringing pattern (reflections of reflections) between this point and the transducer end of the waveguide. This will dampen out with time, but if this reflective ringing lasts too long, it can interfere with the signal of interest when it returns to the transducer. In a laboratory setting an absorbent material, such as clay, can be applied to the waveguide and increase the rate at which the ringing is dampened. This is not a suitable solution for the conditions experienced by a sensor on a space reactor. A new material or method of dampening will need to be developed but is a low-risk issue.

5.2.5.3. Intermediate Waveguide Attachments

The waveguide will be supported by its connection to the transducer and at its attachment, if any, at its sensing location. Depending on its length, position, and other connections provided by each application, secondary attachments may be needed to provide adequate support to withstand the shock and vibration of launch without becoming detached, broken, or misaligned. Any clamps, connectors, etc. must not interfere with the transmitted signal by acoustically coupling the waveguide to another material creating large signal losses, or by creating a reflection point in the waveguide. Knife edge attachments or sleeves composed of materials with acoustic impedances very different than that of the waveguide are potential candidates. Since this can affect all magnetostrictive applications, testing will be required to determine the method that introduces the least amount of signal attenuation. The risk associated with utilizing intermediate waveguide attachments is low.

5.2.5.4. Time Response

The time response requirements of sensors using magnetostrictive transducers are not demanding. The specifications at this time (10 milliseconds) are within the capabilities of the transducer.

5.2.5.5. Signal Drift/Calibration requirements

The speed of sound in a material varies with temperature. The range of temperatures experienced by the reactor at different stages of the mission is relatively large, so this will have an effect on the timing measurements of signals traveling through a waveguide of varying temperature. Since many magnetostrictive sensor technologies are based on the ability to accurately measure the differences in the time-of-flight measurements of ultrasonic signals, this effect must not confound sensor measurements. A reference reflection from a known position in the waveguide could be used to determine the speed of sound in the material and apply a correction to the measurement of interest. This could also help to correct for changes in transmission characteristics due to radiation or time at temperature as well. This and other possible solutions will need to be investigated. This is a high-risk issue because the large range of temperatures may require a complex solution.

5.2.5.6. Interference/Crosstalk Susceptibility

Interference concerns arise from the signal cables being in close proximity with the 2250 Hz power cables along the boom and from electromagnetic fields from the Brayton alternator. Magnetically

shielded housing may be required such that external magnetic influences do not interfere with the magnetically dependent signal transmission and receiving capabilities of the transducer.

It is possible that there will be several magnetostrictive transducers in use for position and/or temperature sensors. Crosstalk between the different transducers and their cabling becomes a concern whenever multiple signals of similar types are in close proximity. Careful filtering or even sequencing the measurements from each transducer may help to avoid this, making this a low-risk issue.

5.2.6. Interface

5.2.6.1. Number of Cables

A magnetostrictive transducer can transmit and receive signals with the use of one coaxial cable. The use of an electromagnet for the bias magnet would require one additional cable.

5.2.6.2. Multi-functionality

Temperature and position measurement are two applications for use with a magnetostrictive transducer. The sensor technologies utilizing magnetostrictive transducers do not provide the same option of performing two different types of measurements with the same exact transducer or set of transducers as offered by piezoelectrics. The notched waveguide temperature sensor, however, does have the capability of measuring the temperature at multiple locations with the use of just one magnetostrictive transducer and waveguide. Also, the sensors using magnetostrictive transducers primarily use time-of-flight measurement which is common among many ultrasonic technologies.

A high-temperature piezoelectric transducer will most likely need to be developed because of the lack of non-invasive sensor options for gas flow and pressure, but that should not influence the choice of temperature sensing technology if a magnetostrictive method does in-fact prove to be the best. Other position measurement technologies are being assessed in a different evaluation, but the development of a high-temperature magnetostrictive transducer could be useful for two sensor technologies just as with a piezoelectric transducer.

6. Temperature Measurement Issues

Three ultrasonic measurement techniques are being considered for development for space reactor temperature sensing. These techniques include a notched waveguide technique, a guided wave in plate technique and a dual transducer technique. In all three techniques, temperature of a system or system component is inferred from a measured change in the speed of sound in either the sensing element or the component itself. A general technology overview of these three techniques is provided in Section 3. Development issues associated with each of these three techniques are presented in this section.

6.1. Magnetostrictive

6.1.1. Waveguide

6.1.1.1. Length of waveguide

Ultrasonic signal strength in a magnetostrictive sensor system is expected to decrease as the waveguide length increases. Testing has shown that a 10 m long, 1.5 mm diameter stainless steel wire waveguide attached to a 40 cm long magnetostrictive wire lead-in provides sufficient waveform signal strength to accurately measure length changes in a specimen attached to the waveguide. Testing with 50 m waveguide lengths has not been performed. As a result, for all practical purposes at this stage of development, it must be assumed that the waveguide length of the sensor system for the space reactor application will be restricted to less than or equal to 10 m requiring the transducer to be placed outside the electronics vault nearer to the source of heat to be measured. In practice, waveguide lengths < 1 meter can be used provided the transducer is rugged enough to withstand the heat of the surrounding environment. 10 m lengths should be a sufficiently long enough waveguide length to assure the transducers are kept at a reasonable temperature. The use of waveguide lengths ranging from 1 – 10 m contains no risks.

6.1.1.2. Composition of waveguide

The two main physical characteristics of a waveguide that enable ultrasonic sensing are the speed of sound in the waveguide and the resistance of the waveguide composition to oxidation at high temperatures. Sound velocities in the range of 0.2 to 0.6 cm/ μ s in a waveguide are needed to obtain accurate sensing measurements. Stainless steels, refractory metals and nickel based super alloys all have sound velocities in this range and these materials can all be manufactured into a suitable wire for ultrasonic sensing applications. However, only the stainless steels and nickel super alloys are oxidation resistant at high temperatures whereas refractory metals oxidize quite readily at high temperatures. If oxidation films form on a waveguide, the propagating waveforms can couple to the film and will, in most cases, travel faster in the film than the metal leading to an inaccurate temperature measurement. In the refractory metal cases, the waveguide must be kept in an inert atmosphere or a high vacuum to prevent oxidation at elevated temperatures. Also, joining a ferromagnetic lead-in wire to the waveguide will require strict materials compatibility to accomplish a seamless bond (discussed below) and to prevent terrestrial galvanic corrosion and subsequent failure of the system. Risks associated with using refractory metal waveguides are considered to be moderate with respect to joining to a magnetostrictive lead-in wire. The risk associated with joining ferromagnetic lead-in wires to nickel super alloy waveguides is judged to be low.

6.1.1.3. Attachment of waveguide to spacecraft (loss of signal concerns)

The waveguide must be attached to the spacecraft in such a fashion as to assure the waveguide can withstand the physical rigors of spacecraft launching and vibrations from on-board operating

machinery. A long wire-like waveguide (~ 10 m) will require several attachment points to meet this requirement. Each attachment point is a source for acoustically coupling the ultrasound out of the waveguide and into the spacecraft structure resulting in a severe loss of signal strength at each attachment point. Acoustic coupling at the attachment points can be reduced by minimizing the surface area of the attachment point and the force of the attachment. Therefore, knife edge attachment points with low forces are needed to attach long waveguides to the spacecraft structure. Even so, the number of the attachment points need to be minimized and it must be understood that signal losses will occur, no matter how sharp the knife edge and how delicate the applied force. Therefore, the waveguide should be designed to the minimum length possible. The risk associated with attaching a waveguide to the spacecraft is judged to be moderate and will decrease with decreasing waveguide length.

6.1.1.4. *Joining of magnetostrictive wire to waveguide*

A magnetostrictive system requires the bonding of a magnetostrictive wire, in which the transducer creates the ultrasound waveform, to a longer, more practical, waveguide. The bonding of the ferromagnetic wire to the waveguide must be as near to seamless as possible. If not, the bond seam will reflect ultrasound resulting in loss of signal strength and, depending on the length of the waveguide, the creation of interfering reflecting waveforms that confound or entirely mask the desired waveforms. In addition, material incompatibilities that may cause terrestrial galvanic corrosion need to be addressed. Soldering has been shown to be an effective method to join magnetostrictive Remendur wire to a stainless steel waveguide for short term (1 yr) application with acceptable signal loss due to bond corrosion. However, signal loss at this joint was significant but tolerable for the application. Explosion bonding will provide a more near to seamless bond with less signal loss, but, material incompatibilities must be addressed for long-term applications such as a 15 - 20 year space mission. The risk associated with joining ferromagnetic lead-in wires to waveguides is judged to be moderate.

6.1.1.5. *Stray Signal Dampening*

As mentioned in the previous section, the bond between the magnetostrictive wire and the waveguide must be made as seamless as possible because this bond will cause the waveforms to be reflected and, as a result, the desired signal to be attenuated. In addition, the reflected signal will return to the transducer, get detected, reflect off the proximal end of the ferromagnetic wire and propagate back to the bond. This process will continue until the signal sufficiently attenuates to a non-detectable point. If the waveguide is sufficiently short, this stray signal will interfere with or completely mask the desired signal. Therefore, this stray signal needs to be dampened.

Typically, a clay-like material can be placed on the magnetostrictive wire or waveguide into which the unwanted signals will couple and attenuate rapidly to a point where they no longer interfere with the desired signal. The incorporation of this material needs to be engineered into the design of the sensor system. This material must be positively contained and must be kept below a specified temperature. The risk associated with engineering a clay dampener (or other dampening material) into a system is judged to be low.

6.1.2. *Transducer*

A detailed discussion of magnetostrictive transducers is provided in Section 5.2. In addition to the information provided in Section 5.2, it should be noted that magnetostrictive transducers used for temperature sensing typically operate in the 100 – 125 kHz frequency range. The frequency of such transducers is determined by the number of windings of the pulse coil in the transducer. Fabrication of custom magnetostrictive transducers needs to address the number of windings to assure the correct frequency is obtained. Bettis has successfully manufactured several custom transducers for

use in the Advanced Test Reactor in Idaho. Alternatively, a piezoelectric transducer with an acoustic horn may be used. Therefore, the risk associated with identifying and/or manufacturing custom transducers is considered to be low.

6.1.3. Sensor Element – Notched Waveguide

6.1.3.1. Depth of notch

As described in Section 3.1.1, a notch in a waveguide will provide a point of reflection for a propagated waveform. In addition, each point of reflection, regardless of the origin, consumes a finite amount of the total energy of the waveform. Therefore, each successive reflection decreases the signal strength and, as a result, measurement techniques that are based on more than one reflection are limited by the total number of reflections that can be detected. In the case of reflections from a notch in a waveguide, it has been shown that the depth of the notch is proportional to the total waveform energy lost during the reflection. Correspondingly, if the notch is too deep, subsequent reflections will be too weak to detect which will degrade the multiple measurement technique. If one single point measurement is to be performed, it should be determined experimentally how deep a notch should be to produce equal height signals - one from the notch and one from the end of waveguide. If a notched waveguide is to be used to determine temperatures from multiple areas, which require multiple notches, a notch depth study needs to be conducted to maximize the number of temperature zones that can be monitored with one waveguide. In this later case, it is expected that only three of four areas can be monitored simultaneously with one waveguide. Risks associated with single point notched waveguide systems are considered to be very low. The risk associated with multiple point notched waveguide systems measuring up to three environments is considered to be low to moderate. (It should also be understood that discs and clamps can be used in lieu of notches to produce the same effect.)

6.1.3.2. Shape of notch

The shape of the notch also affects the signal strength of the reflected waveform but with less severity than the depth of the notch. Notches can be of any practical shape that is convenient for machining. These shapes include v-shaped, as shown in Figure 3.1.1-1, square bottom and round bottom, to name a few. In all cases, the long axis of the notch should be perpendicular to the propagation axis of the waveform to provide maximum reflection. Unfortunately, notches reduce the physical strength of the waveguide. Therefore, notch shapes should be investigated to determine which shape provides the least amount of stress to the waveguide with the highest reflection capability. There are no risks associated with engineering the shape of a notch to produce maximal signal strength.

6.1.3.3. Spacing of notches for multiple measurements

As mentioned above, multiple notches along the length of a waveguide can be used to determine the temperature of more than one area with one waveguide. Since the temperature measurement is based on time-of-flight differences between two reflections, the notches must be sufficiently spaced apart so that the reflected waveforms arrive at the detector at different times and are completely resolved. Notch spacing studies performed at the Pennsylvania State University have shown that notched pairs need to be spaced approximately 2 to 4 in apart to provide accurate temperature measurements when using stainless steel and refractory metal waveguides. In addition, when multiple areas are being monitored with the same waveguide, the notched pairs must be sufficiently spaced apart as well. However, there may be challenges associated with transferring this capability from a lab to a production application..

6.1.3.4. Attachment of the sensor to the component

Temperature measurements are based on measuring the change in sound velocity in a waveguide as a function of the temperature of the waveguide. Therefore, the sensor must be in intimate contact with the component or environment of interest to affect thermal transport from the component or environment to the waveguide. However, intimate contact of the waveguide to a component provides a source for acoustic losses, especially if the sensing portion of the waveguide is clamped to a component with one or more clamps. The best method to attach a sensing element to a component to affect maximum thermal transport in the sensing area is by sandwiching the waveguide between the component and a suitable piece of metal or insulator with minimum compressive forces. It is imperative that the compressive forces are sufficiently large enough to firmly hold the waveguide in place while small enough to prevent strong acoustic coupling causing signal strength loss. The amount of compressive forces that can be applied to the waveguide without producing a detrimental loss of acoustic signal needs to be investigated.

Thermal transport properties of the waveguide determine the speed at which measurements can be made. If rapid temperature measurements are required, a waveguide with high thermal transport properties, such as a refractory metal, should be used. The risk associated with engineering the attachment of the sensor element to the component of interest is considered to be low.

6.1.3.5. Materials compatibility of sensor and component

Materials compatibility of the waveguide with the component of interest is of high concern during the terrestrial lifetime of the sensor system. During this time, and in the presence of moisture or another electrolytic conducting medium, dissimilar metals in contact with each other will corrode due to galvanic coupling. This corrosion can degrade or confound the measurement, deteriorate the sensor to failure or, in the worst case, cause a component of the reactor system to fail. If possible, the waveguide should be made of the same material as that of the component to prevent galvanic coupling terrestrial residence before launch into space. Since the sensing element can have the same material composition as the component being measured, no risk is associated with this issue.

6.1.4. Sensor Element – Guided Wave in Plate

6.1.4.1. Dimensions of plate and acoustic horn

As described in Section 3.1.2, temperature measurements can be made by measuring time of flights of reflected guided waves in a rectangular plate sensing element. In this method, the waveforms in the waveguide must be efficiently coupled into the rectangular plate. This is accomplished by machining an acoustic horn onto the end of the plate as shown in Figure 3.1.2-1. The size and shape of the acoustic horn are determined by the dimension of the rectangular plate. Computer programs are available (at the Pennsylvania State University) to calculate the most efficient size and shape of an acoustic horn given a particular set of rectangular plate parameters. These programs can be applied to all rectangular plate sizes.

The size of the rectangular plate must also be considered. In practice, the width and thickness of the plate do not grossly affect the measurement provided they are greater than half the wavelength of sound used in the measurement. However, the length of the plate in which the guided waveforms travel must be of sufficient size to assure the reflected guided waves are well separated and do not interfere with each other. Testing has shown that rectangular plates that are 4 inches long or longer suffice for these measurements and that the longer the plate, the better the separation of the reflected waveforms. Plate widths as narrow as 12.5 mm have been shown to be effective in making temperature measurements. Plate thicknesses as small as 1.6 mm can also be used. Determination of plate and acoustic horn dimensions present no risk.

6.1.4.2. Attachment of waveguide to the acoustic horn

The waveguide must be firmly attached to the sensing plate via the acoustic horn as shown in Figure 3.1.2-1. Because the temperature measurements are made with the recorded time-of-flights of the waveforms reflected off the waveguide-to-acoustic horn joint and the waveforms reflected off the end of the rectangular plate, the waveguide-to-acoustic horn joint must promote a suitably strong reflection signal as well as being a robust bond. Testing has shown that this joint can be accomplished by welding the waveguide while inserted into a flat bottom hole machined in the apex of the acoustic horn. *Welding of a waveguide to an acoustic horn presents no risk if the horn and the waveguide are manufactured from the same material.*

6.1.4.3. Attachment of plate to component

Temperature measurements are based on measuring the change in sound velocity in a rectangular plate as a function of the temperature of the plate. Therefore, the plate must be in contact with the component or environment of interest to affect thermal transport from the component or environment to the plate. However, intimate contact of the plate to a component provides a source for acoustic losses, especially if the plate is clamped to a component with one or more clamps. The best method to attach a plate to a component to affect maximum thermal transport is by sandwiching the plate between the component and a suitable piece of metal or insulator with minimum compressive forces. It is imperative that the compressive forces are sufficiently large enough to firmly hold the plate in place while small enough to prevent strong acoustic coupling causing signal strength loss. The compressive forces that can be applied to the plate without producing a detrimental loss of acoustic signal need to be investigated. The risk associated with attaching a rectangular plate to a cylindrical component such as a length of coolant piping is considered to be high because geometries of the two components preclude good thermal contact and it is not known if a form-fitted plate can be used instead of standard rectangular plate.

Thermal transport properties of the plate determine the speed at which measurements can be made. Efforts should be made to use a plate with a smallest mass possible. If rapid temperature measurements are required, a plate with high thermal transport properties, such as a refractory metal, should be used. The risk associated with designing a plate with high thermal transport with the lowest mass are considered to be small. However, the length of plate and the geometry of the plate (as described above) increase the risk to a high level.

6.1.4.4. Materials compatibility of sensor and component

Materials compatibility of the plate with the component of interest is of high concern. During the times when the sensor system is located on earth, dissimilar metals in contact with each other and a suitable electrolytic medium, such as moisture, will corrode due to galvanic coupling. This corrosion can degrade or confound the measurement, deteriorate the sensor to failure or, in the worst case, cause a component of the reactor system to fail. *If possible, the plate should be made of the same material as that of the component to prevent galvanic coupling.* Since the sensing element can have the same material composition as the component being measured, no risk is associated with this issue.

6.2. Piezoelectric – Dual Transducer

6.2.1. Transducers

A detailed discussion of piezoelectric transducers and their use in a space reactor application is provided in Section 5.1. In addition to the information provided in Section 5.1, the following system attributes apply.

6.2.2. Standoff requirements

Section 3.2 describes an application where two piezoelectric transducers are attached to a section of piping with wedge-like standoffs. These standoffs facilitate the launching of the waveforms into the piping which then couple to the flowing gas in the pipe. The standoffs must be acoustically coupled to both the transducer and the piping and all materials must be compatible to prevent galvanic coupling while in the earth's atmosphere to prevent corrosion and to minimize acoustic impedance mismatching. The shapes of the standoffs will determine the angle at which the waveforms are launched into the flowing gas stream and the spacing of the standoffs will be governed by the angle of launching. If the piezoelectric transducers must be kept below a specified temperature, the thickness of the standoff can be increased to affect cooling. The risk associated with designing a suitable standoff is considered to be low.

6.2.2.1. Attachment of transducers and standoffs to piping

A soft metal such as platinum can be used to attach the transducer to the standoff, and, if necessary, the standoff to the pipe. Platinum has a melting point of 2000 K and can withstand the high temperature of the mission. In addition an integral or "welded" joint can be used to attach the standoff to the pipe. The integral or "welded" joint is used so that there will not be any reflection or change in acoustic coupling between the standoff and the pipe wall. A near-perfect contact between the transducer and standoff, and standoff and pipe is desired to limit the reflection of the ultrasonic signals. The attachment of the standoff and transducer to the pipe needs to be investigated thoroughly. This is a major issue because an integral joint or other technique will have to be used reduce reflections or change the acoustic couplings. The risks associated with engineering the attachment of a transducer to a standoff and a standoff to reactor coolant piping are together considered to be moderate.

6.2.2.2. Operation frequency

Piezoelectric transducers used for flow sensing typically operate at frequencies in the 1 – 5 MHz range which will improve the signal quality of the measurement as compared to a magnetostrictive technique. Therefore, no risk is associated with the use of high frequency piezoelectric transducers.

6.2.2.3. Temperature compatibility of transducers

Table 5.1.2.2-1 is a list of COTS piezoelectric elements whose operating temperatures range from 673 K to 1273 K with the majority of the listing showing operating temperatures above 800 K which is the target design temperature for the sensor system. Therefore, piezoelectric materials already exist that are temperature compatible with the defined space reactor application. Because several different elements are commercially available that are suitable for use in a space application, the risk associated with choosing a piezoelectric transducer for the space mission is low.

6.2.2.4. Fatigue life of the piezoelectric crystal

Table 5.1.2.2-1 is a list of the COTS piezoelectric elements that are under consideration for a space application. Since the housing of the transducer will only reduce the amount of heat that the piezoelectric material will experience, the material must still withstand a significantly high temperature. As the maximum operating temperatures of the piezoelectric materials are approached, the materials will start to fatigue. Materials such as Aluminum Nitride, Langasite and Lithium Niobate with sodium have operating temperatures near 1300 K. Above these temperatures the materials will no longer be a piezoelectric material, might become chemically unstable, and could change crystal structure. The fatigue life of the piezo crystal is a moderately high risk issue and needs to be investigated thoroughly. Near-term testing is required to verify the maximum limits of the piezo crystal.

6.2.2.5. *Housing construction*

The transducer housing must be manufactured to withstand the harsh space environment. The housing is used as a protective containment for the piezoelectric element, electrical leads, absorbent backing, and wear plate. Materials such as nickel-based super alloys such as Inconel 600 will be considered because they are stable at high temperatures. Stainless steels may also be considered as a material choice. Defining a suitable housing construction material is considered to be low in risk.

7. Flow Measurement Issues

One ultrasonic measurement technique was considered for development for space reactor gas flow sensing. This technique is based on measuring two waveform travel times; one in the direction of the gas flow and one in the opposite direction.

7.1. Transducer element (piezoelectric)

A detailed discussion of piezoelectric transducers and their use in a space reactor application is provided in Section 5.1. In addition, to the information provided in Section 5.1, the following system attributes apply.

7.1.1. Standoff requirements

Section 3.2 describes an application where two piezoelectric transducers are attached to a section of piping with wedge-like standoffs. These standoffs facilitate the launching of the waveforms into the piping which then couple to the flowing gas in the pipe. The standoffs must be acoustically coupled to both the transducer and the piping and all materials must be compatible to prevent galvanic coupling to prevent corrosion and to minimize acoustic impedance mismatching. The shapes of the standoffs will determine the angle at which the waveforms are launched into the flowing gas stream and the spacing of the standoffs will be governed by the angle of launching. If the piezoelectric transducers must be kept below a specified temperature, the thickness of the standoff can be increased to affect cooling. The risk associated with designing a suitable standoff is considered to be low.

7.1.2. Attachment of transducers and standoffs to piping

A soft metal such as platinum can be used to attach the transducer to the standoff, and the standoff to the pipe. Platinum has a melting point of 2000 K and withstand the high temperature of the project. In addition an integral or "welded" joint can be used to attach the standoff to the pipe. The integral or "welded" joint is used so that there will not be any reflection or change in acoustic coupling between the standoff and the pipe wall. A near-perfect contact between the transducer and standoff, and standoff and pipe is desired to limit the reflection of the ultrasonic signals. The attachment of the standoff and transducer to the pipe needs to be investigated thoroughly. This is a major issue because an integral joint or other technique will have to be used reduce reflections or change the acoustic couplings. The risks associated with engineering the attachment of a transducer to a standoff and a standoff to reactor coolant piping are together considered to be moderate.

7.1.3. Operation frequency

Piezoelectric transducers used for flow sensing typically operate at frequencies in the 1 – 5 MHz range which will improve the signal quality of the measurement as compared to a magnetostrictive technique. Therefore, no risk is associated with the choice of frequency in using piezoelectric transducers.

7.1.4. Temperature compatibility of transducers

Table 5.1.2.2-1 is a list of COTS piezoelectric elements whose operating temperatures range from 673 K to 1273 K with the majority of the listing showing operating temperatures above 800 K which is the target design temperature for the sensor system. Therefore, piezoelectric materials already exist that are temperature compatible with the defined space reactor application. Because several different elements are commercially available that are suitable for use in a space application, the risk associated with using a piezoelectric transducer for the space mission is low.

7.1.5. Fatigue life of the piezoelectric crystal (at temperature)

Table 5.1.2.2-1 is a list of the COTS piezoelectric elements that are under consideration for a space application. Since the housing of the transducer will only reduce the amount of heat that the piezoelectric material will experience, the material must still withstand a significantly high temperature. As the maximum operating temperatures of the piezoelectric materials are approached, the materials will start to fatigue. Materials such as Aluminum Nitride, Langasite and Lithium Niobate with sodium have maximum operating temperatures near 1300 K. Above these temperatures the materials may no longer be a piezoelectric material, might become chemically unstable, and could change crystal structure. The fatigue life of the piezo crystal is a moderately high risk issue and needs to be investigated thoroughly. Near-term testing is required to verify the maximum limits of the piezo crystal.

7.1.6. Housing construction

The transducer housing must be manufactured to withstand the harsh space environment. The housing is used as a protective containment for the piezoelectric element, electrical leads, absorbent backing, and wear plate. Materials such as nickel-based super alloys such as Inconel 600 will be considered because they are stable at high temperatures. Some sort of stainless steel may also be considered as a material choice. Defining a suitable housing construction material is considered to be low in risk.

8. Pressure Measurement Issues

One ultrasonic measurement technique was considered for development for space reactor gas pressure sensing. This technique is based on measuring ultrasonic signal amplitude change as a function of gas impedance.

8.1. Transducer element (piezoelectric)

A detailed discussion of piezoelectric transducers and their use in a space reactor application is provided in Section 5.1. In addition, to the information provided in Section 5.1, the following system attributes apply.

8.1.1. Standoff requirements

The standoff for the transducers should be the same material as the pipe or as close to the same material as possible. Having the standoff and the pipe be the same material or similar material will reduce the impedance mismatch and galvanic coupling as explained in previous sections. The goal is to have the impedance ratio equal to one or as close to one as possible. Keeping the impedance ratio near one will cause the least amount of signal reflected at the contact point. Since the pressure will be found from the amplitude measurement, keeping the signal loss to a minimum at the interfaces between the transducer, standoff, and pipe is imperative. A reference marker must be placed in the standoff to show changes in coupling between the transducer and standoff, and standoff and pipe wall. The reference signal amplitude will only be affected by changes in coupling and material. The ideal standoff length is predicted to be between 7.5 and 12.5 cm. Designing a suitable standoff is considered to be low risk.

8.1.2. Attachment/coupling of standoff & transducer to piping

A soft metal such as platinum can be used to attach the transducer to the standoff, and the standoff to the pipe. Platinum has a melting point of 2000 K and can withstand the high temperatures of the mission. In addition an Integral or "welded" joint can be used to attach the standoff to the pipe. The Integral or "welded" joint is used so that there will be minimal reflection or change in acoustic coupling between the standoff and the pipe wall. A near-perfect contact between the transducer and standoff,

and standoff and pipe is desired to limit the reflection of the ultrasonic signal. The attachment of the standoff and transducer to the pipe needs to be investigated thoroughly. This is moderate risk due to material compatibility concerns and uncertainties of acoustic effects at the integral joint.

8.1.3. Operation frequency

Frequency of the ultrasonic signal in each pulse will affect attenuation and reflective properties. A variety of frequencies will be analyzed and tested to obtain the best possible measurement sensitivity without interfering with other subsystems. As frequency of a piezoelectric transducer is simply based on the thickness of the piezoelectric element, this is considered to be low risk.

8.1.4. Temperature compatibility of transducers

Table 5.1.2.2-1 is a list of COTS piezoelectric elements whose operating temperatures range from 673 K to 1273 K with the majority of the listing showing operating temperatures above 800 K which is the target design temperature for the sensor system. Therefore, piezoelectric materials already exist that are temperature compatible with the defined space reactor application. Because several different elements are commercially available that are suitable for use in a space application, the risk associated with using a piezoelectric transducer for the space mission is low.

8.1.5. Housing construction

No significant housing issues are foreseen beyond those addressed in Section 5.1.1.

8.1.6. Materials compatibility of transducers and interface

Materials compatibility of the plate with the component of interest is of high concern. During the times when the sensor system is located on earth, dissimilar metals in contact with each other and a suitable electrolytic medium, such as moisture, will corrode due to galvanic coupling. This corrosion can degrade or confound the measurement, deteriorate the sensor to failure or, in the worst case, cause a component of the reactor system to fail. If possible, the plate should be made of the same material as that of the component to prevent galvanic coupling. Since the sensing element can have the same material composition as the component being measured, no risk is associated with this issue.

8.1.7. Fatigue life of piezoelectric crystal (at temperature)

Table 5.1.2.2-1 is a list of the COTS piezoelectric elements that are under consideration for a space application. Since the housing of the transducer will only reduce the amount of heat that the piezoelectric material will experience, the material must still withstand a significantly high temperature. As the maximum operating temperatures of the piezoelectric materials are approached, the materials will start to fatigue. Materials such as Aluminum Nitride, Langasite and Lithium Niobate with sodium have operating temperature near 1300K. Above these temperatures the materials will no longer be a piezoelectric material, might become chemically unstable, and could change crystal structure. The fatigue life of the piezo crystal is a moderate risk issue and needs to be investigated thoroughly. Near-term testing is required to verify the maximum limits of the piezo crystal.

8.2. Technique Development

8.2.1. Amplitude change sensitivity to gas pressure

As the pressure of a gas changes, its acoustic impedance will change as well. The ultrasonic pressure measurement concept takes advantage of this fact by detecting changes in the amplitude of the ultrasonic signal reflected from the pipe wall / gas interface as the energy enters the gas. Preliminary analysis indicates that, neglecting losses, a 7000 Pa change in gas pressure will result in

a 0.00015% change in reflected amplitude. As this is a very small change to detect, rigorous analyses and testing must be done to verify that amplitude changes will lie well above the noise floor of the instrumentation to the desired sensitivity of the instrument. This is a high risk issue.

8.2.2. Low pressure measurement limit

The system requirements and technique capabilities are unknown for ultrasonic pressure sensors at low pressures. Most of the work to date has been performed at higher pressures and it is unknown how the sensors will perform at low gas pressures in the 100-500 psi range. Since the space reactor application requirement is to monitor gas pressures from 0 to 300 psi, further testing and development is warranted with a moderate to high risk of failure.

9. Position Measurement Issues

One ultrasonic position measurement technique has been considered here for development for space reactor control element position indication. A linear and a rotary form of this technique are assessed due to the fact that the control element type has yet to be selected for the SNPP at the time of this report. Both forms are based on time-of-flight measurement of an acoustic pulse generated in a waveguide.

9.1. Common Issues for Linear and Rotary Position Measurement

The linear and rotary applications of ultrasonic position measurement have many similar issues, but there are issues that are unique to each case as well. The issues that are shared between the two are detailed in this section, followed by the issues specific to the linear application in Section 9.2, and the issues specific to the rotary application in Section 9.3

9.1.1. Permanent (Electro-) Magnet Marker

9.1.1.1. Field strength of marker

The magnetic marker must be of sufficient field strength to interact with the detector rod to produce a measurable acoustic signal. Different sizes and material grades can be chosen to meet field strength requirements, making this a low-risk issue. Also, magnets with higher intrinsic coerciveness will perform the best in long-term, high-temperature exposure.

9.1.1.2. Radiation/temperature sensitivity of marker

The permanent magnet marker will have to be of a high-Curie temperature material just as in the magnetostrictive transducer such that it does not lose magnetization at any point during the life of the mission. NdFeB magnets are the strongest for low temperature applications, but at 425 K and above, SmCo types will have stronger fields. An electromagnet can also be used.

Due to the fact that the position measurement is based on timing and not signal amplitude, minor loss of magnetic field strength may not be an issue. The sensor will function properly as long as the magnetic field is strong enough to produce an acoustic signal of sufficient amplitude to be detected by the transducer and conditioning electronics. Also, the use of an electromagnet instead of a permanent magnet may resolve any issues of field loss, along with limiting the effects of lifetime residual magnetization in the waveguide caused by a permanent magnet. However, the risk associated with using permanent magnets in the high-temperature environment is high.

9.1.2. Pulse Coil

9.1.2.1. Field strength required / turns per inch and current / Frequency

The pulse coil must create a field strong enough to generate a signal in the waveguide that is detectable by the transducer. This is determined by the number of turns around the waveguide and the amount of current supplied to them as described in Section 5.2.4.3 and is a low-risk issue. The pulse frequency can then be determined once the number of coils is known.

9.1.2.2. Conductor/Insulator Material

The conductor for the coil must be able to withstand high temperatures and also have as low of a thermal coefficient of resistance as possible. Copper or precious metal alloys are common high temperature conductors. A chrome or stainless steel cladding can also be used for added ruggedness. Ceramic coatings are typically used as insulation at high temperature.

9.1.2.3. Temperature sensitivity of coil

The concerns related to elevated temperature are the same as with the coil in the magnetostrictive transducer as described in Section 5.2.4.2. Again, the increased resistance in the coil at high temperatures causes a reduction in field strength, but it should not affect the timing measurement as long as there is the ability to generate a measurable signal in the waveguide. The coil in this sensor is many times larger so the increased resistance may provide a greater loss of magnetic field strength and is judged to be a moderate risk.

9.1.2.4. Attachment of coil to waveguide

The coil will be implemented as adjacent windings spanning the length of the waveguide. There will also be a protective sheath covering the waveguide/coil assembly. The magnet marker will travel the outside of this housing. This has been commercially accomplished so is therefore a low-risk issue.

9.1.3. Waveguide

9.1.3.1. Composition of waveguide

The waveguide must be composed of a magnetostrictive material that will demonstrate sufficient magnetostrictive strain with magnetic field interaction. Various materials have been developed with improved magnetostrictive properties, such as Remendur and Terfenol-D. In order to maintain the ability to generate acoustic signals in the detector rod, it is important that the magnetostrictive waveguide preserves its magnetic polarization in the high temperature and radiation environment and is a moderate risk. Irradiation testing is planned for waveguide material.

9.1.3.2. Degaussing

The degaussing of the position sensor waveguide is a very similar problem to that caused by the magnetostrictive transducer itself. When the permanent magnet marker is in one location for a period of time and moves to its next location, there is some residual magnetization in the waveguide at the initial location. To counteract this, a secondary bias coil in addition to the pulse coil can be wound around the waveguide. Prior to each position measurement, applying a DC pulse to this secondary coil will realign the magnetic dipoles of the waveguide to neutralize the residual magnetization. This is a simple solution with the only negative aspect being the additional cabling needed for the DC bias coil. Per work conducted at Penn State University, current requirements are in the range of 0.5 A for 15 ms, and the current level or duration can be varied depending on system needs. This technique has been successfully used in the NR program so is therefore a low-risk issue.

9.1.4. Transducer / Receiver

9.1.4.1. Frequency, Amplitude, Pulse Width

The transducer(s) used in position indication applications is used only for signal reception. Therefore the operating parameters must be designed in coordination with the pulse coil and magnet marker to be compatible. This is not an issue and has been done commercially for sensors of this type with much larger range.

9.1.4.2. Temperature compatibility

The transducer in the position indication system could potentially see temperatures in excess of 800 K, requiring a more robust design than what is currently available. Development of a high-temperature transducer is a moderate risk and the challenges associated with doing so are detailed in Section 5.2.

9.2. Linear Position Measurement Issues

9.2.1. Permanent (Electro-) Magnet Marker

9.2.1.1. Physical shape/size of marker

The magnet marker will be ring shape geometry with an inner diameter large enough to provide non-contact movement as it travels the length of the detector rod assembly for the full stroke of the control rod. Non-contact movement is necessary to provide a long lifetime of the position sensor. Outer diameter and thickness are the other variable dimensions and can be minimized by designs that are operated at the maximum energy product of the magnet (BH_{max}).

9.2.1.2. Attachment of marker to device

The magnetic marker must be attached to the control drive mechanism (CDM) lead-screw such that it is able to travel with the movement of the control rod/slider. Magnet attachments are commonly done with adhesives, but they are not suitable for the high-temperature vacuum environment. Any attachment, clamps, or mounting screws/holes cannot interfere with the magnetic field or material properties of the marker and should be made with a non-magnetic metal. Also, SmCo has the best temperature and radiation stability but is the most brittle, so this must be taken into account when mounting. However, there is low risk foreseen in engineering a proper attachment.

9.2.1.3. How to guide travel of marker along waveguide/pulse coil

Attaching the marker to the CDM lead-screw or some type of extension will provide linear motion of the marker through the entire range of movement. Attachment to a hollow lead-screw will allow the magnetic ring marker to traverse the detector rod as the lead-screw travels the outside of the rod. This minimizes the space occupied by the sensor and CDM when compared to a waveguide running adjacent to the lead-screw.

9.2.2. Waveguide

9.2.2.1. Attachment of waveguide to structure

The waveguide must be attached such that it maintains proper alignment allowing for linear travel of the magnet marker. The waveguide for position indication is much shorter than those described for temperature measurement (< 0.5 meters). It may be possible for the waveguide to be fully supported by its connection to the transducer and such an attachment might be necessary to allow for unobstructed motion of the magnet ring across the rod. However, this may not provide sufficient

alignment support during launch and throughout mission lifetime and there is a moderate risk in doing so. Also, attachments must not interfere with signal transmission as described in Section 5.2.5.3.

9.2.3. Transducer / Receiver

9.2.3.1. Number of Transducers

Linear position measurement is done with only one transducer which is needed for signal reception purposes only.

9.3. Rotary Position Measurement Issues

9.3.1. Permanent (Electro-) Magnet Marker

9.3.1.1. Physical shape/size of marker

The magnet marker for rotary position indication will be a horseshoe or semi-circular shape. It cannot be a closed ring, as in the linear application, to allow for 360° motion. Exact size and geometry will be chosen based on field strength and ease of implementation.

9.3.1.2. Attachment of marker to device

The marker can either be attached to the reflector drum itself, or to a rotating disc or shaft arm perpendicularly mounted to the rotating shaft of the CDM or other component of the CDM (such as a gear). Attachment to an arm or disc coupled to the shaft provides more mounting flexibility by the use of a shaft extension that can be varied in length. This reduces the impact of the sensor on the plant design and reduces the amount of magnetic interference potentially received from the CDM. Again, any fastening must be done with non-magnetic components and is not a risk.

9.3.1.3. How to guide travel of marker along waveguide/pulse coil

Attachment of the marker to the rotating drum or rotating shaft extension provides rotary movement of the marker with movement of the drum. The use of a shaft extension allows for the separation of the sensor and CDM component while still coupling to the rotary movement of the device. The radius of the waveguide (and the corresponding rotating disc or arm attachment) can also be varied to meet measurement resolution requirements. Assuming a linear sensitivity of 5 µm, a radius of 2.9 cm will provide resolution better than 0.01°.

9.3.2. Waveguide

9.3.2.1. Attachment of waveguide to structure

The waveguide must be attached such that it maintains its circular shape and its alignment with the CDM component of which it is measuring while creating a minimum of interference with signal transmission and is a moderate-risk issue. Waveguide attachments are described in Section 5.2.5.3.

9.3.3. Transducer / Receiver

9.3.3.1. Number of Transducers

Rotary position measurement has the option of being done with two transducers, both used for signal reception only. By placing a transducer at each end of the waveguide, both portions of the bidirectional pulse generated at the position of the marker can be detected. By making a measurement based on the two time-of-flight measurements, any changes of signal transmission properties in the waveguide over mission lifetime are nullified by correlating position measurement to

a ratio of the two received signals. Rotary position can also be measured with one transducer just as in the linear application if the additional mass of the second transducer and its cabling is too large.

10. References

- [1] Alderman, J.M. et al, *Study of the Radiation Damage of Nd-Fe-B Permanent Magnets*, Argonne National Laboratory, February 2002.
- [2] Babikov, O. I., *Ultrasonics and its Industrial Applications*, New York: Consultants Bureau, 1960.
- [3] Beyer, Robert T. and, Stephen V. Letcher, *Physical Ultrasonics*, New York: Academic Press, 1969.
- [4] Burnham, R., R. McCarey, O. Khrakovsky, L. Lynnworth, *Measurement of the Flow of Superheated Water in Blowdown Pipes at MP2 Using an Ultrasonic Clamp-On Method*, March 20, 2002. Internet Resource
- [5] *Design Guide*, Magnet Sales & Manufacturing Company, Inc, 2000.
- [6] Ensminger, Dale, *Ultrasonics (2nd Ed.)*, New York: Marcel Dekker, Inc., 1988.
- [7] Kim, Y., S-J. Song, S-S. Lee, J-K. Lee, and S-S. Hong, *A Study on the Couplant Effect in Contact Ultrasonic Testing*. Internet Resource
- [8] Mrasek, H., D. Gohlke, K. Matthies, and E. Neumann, *High Temperature Ultrasonic Transducers*, from NDTnet, September 1996, Vol. 1 No 9. Internet Resource
- [9] Sebastian, J., *Elevated Temperature Sensors for On-line Critical Equipment Health Monitoring*, Powerpoint Presentation, June, 9 2004. Internet Resource
- [10] *Magnetostriction: Basic Physical Elements*, MTS Sensors Group, 2001.
- [11] Mason, Warren P., *Physical Acoustics*, New York: Academic Press, 1964.
- [12] NDT Resource Center. Internet Resource
- [13] Povey, Malcolm J. W., *Ultrasonic Techniques for Fluids Characterization*, New York: Academic Press, 1997.
- [14] Ristic, Velimir M., *Principles of Acoustic Devices*, New York: John Wiley & Sons, 1983.
- [15] *Ultrasonic Technology and the Civilian Space Nuclear Program*, Lockheed Martin Missiles and Fire Control Presentation, March 2005.
- [16] WAPD-ATA(CDM)-513, September 1993.
- [17] Zelenka, Jiri, *Piezoelectric Resonators and their Applications*, Amsterdam: Elsevier, 1986.

- [18] Ultrasonic Flow Meter System Conceptual Design, ORNL/LTR/NR-PROM1/05-19, James E. Hardy et al, August 2005
- [19] Oak Ridge National Laboratory Sensor Technology Development Plan, ORNL/LTR/NR-JIMO/05-01, David Holcomb et al, dated April, 2005
- [20] Project Prometheus NRPCT Final Report , SPP-67110-0008/B-SE-0155

Enclosure 4

Position Indication Technology Evaluation

Jake Evans, *Bettis-Advanced Material System Integration*

Ryan Kristensen, *KAPL-Space Electrical Systems*

Rick Morgan, *Bettis-Space I&C Design*

This page intentionally blank

Table of Contents

1. POSITION INDICATION BASELINE REQUIREMENTS	5
2. EXTENSIBILITY	5
3. LINEAR VARIABLE DIFFERENTIAL TRANSFORMER	5
3.1. DESCRIPTION	5
3.2. FEASIBILITY	6
3.2.1. <i>Commercial state of the art</i>	6
3.2.2. <i>Level of development required</i>	7
3.2.3. <i>Jugular Issues</i>	7
3.3. DELIVERABILITY	7
3.3.1. <i>Development time required</i>	7
3.3.2. <i>Manufacturability</i>	7
3.4. CAPABILITY	7
3.4.1. <i>Sensitivity/accuracy/repeatability/resolution</i>	7
3.4.2. <i>Operation when located 60m from electronics</i>	8
3.4.3. <i>Physical measurement range – absolute position</i>	8
3.4.4. <i>Temperature range – effects and compensation requirements</i>	8
3.4.5. <i>Power source requirements</i>	9
3.4.6. <i>Testing – self calibration, etc.</i>	9
3.4.7. <i>Weight and size</i>	10
3.4.8. <i>Time response</i>	10
3.5. RELIABILITY	10
3.5.1. <i>Failure mechanisms – moving parts</i>	10
3.5.2. <i>Failure mitigation strategies</i>	11
3.5.3. <i>Environmental effects – radiation</i>	11
3.5.4. <i>NR/NASA Program experience</i>	11
3.6. IMPLEMENTATION CONCEPTS	11
3.6.1. <i>Sensor mounting methods</i>	11
3.6.2. <i>Sensor locations</i>	12
3.6.3. <i>Other engineering issues</i>	12
3.7. CABLING	14
3.8. ELECTRONICS AND ALGORITHMS	14
3.9. REFERENCES	16
4. RESOLVER	16
4.1. DESCRIPTION	16
4.2. FEASIBILITY	17
4.2.1. <i>Commercial state of the art</i>	17
4.2.2. <i>Level of development required</i>	17
4.2.3. <i>Jugular Issues</i>	17
4.3. DELIVERABILITY	18
4.3.1. <i>Development time required</i>	18
4.3.2. <i>Manufacturability</i>	18
4.4. CAPABILITY	18
4.4.1. <i>Sensitivity/accuracy/repeatability/resolution</i>	18
4.4.2. <i>Operation when located 60m from electronics</i>	18
4.4.3. <i>Physical measurement range – absolute position</i>	18
4.4.4. <i>Temperature range – effects and compensation requirements</i>	18
4.4.5. <i>Power source requirements</i>	19
4.4.6. <i>Testing – self calibration, etc.</i>	19
4.4.7. <i>Weight and size</i>	19
4.4.8. <i>Time response</i>	19
4.5. RELIABILITY	19

4.5.1.	<i>Failure mechanisms – moving parts</i>	19
4.5.2.	<i>Failure mitigation strategies</i>	19
4.5.3.	<i>Environmental effects – radiation</i>	19
4.5.4.	<i>NR/NASA Program experience</i>	20
4.6.	IMPLEMENTATION CONCEPTS	20
4.6.1.	<i>Sensor mounting methods</i>	20
4.6.2.	<i>Sensor locations</i>	21
4.7.	CABLING	21
4.8.	ELECTRONICS AND ALGORITHMS	21
4.9.	REFERENCES	22
5.	LINEAR AND ROTARY CAPACITIVE	22
5.1.	DESCRIPTION	22
5.2.	FEASIBILITY	23
5.2.1.	<i>Commercial state of the art</i>	23
5.2.2.	<i>Level of development required</i>	24
5.2.3.	<i>Jugular Issues</i>	24
5.3.	DELIVERABILITY	24
5.3.1.	<i>Development time required</i>	24
5.3.2.	<i>Manufacturability</i>	24
5.4.	CAPABILITY	24
5.4.1.	<i>Sensitivity/accuracy/repeatability/resolution</i>	24
5.4.2.	<i>Operation when located 60m from electronics</i>	25
5.4.3.	<i>Physical measurement range – absolute position</i>	25
5.4.4.	<i>Temperature range – effects and compensation requirements</i>	25
5.4.5.	<i>Power source requirements</i>	26
5.4.6.	<i>Testing – self calibration, etc</i>	26
5.4.7.	<i>Weight and size</i>	26
5.4.8.	<i>Time response</i>	27
5.5.	RELIABILITY	27
5.5.1.	<i>Failure mechanisms – moving parts</i>	27
5.5.2.	<i>Failure mitigation strategies</i>	27
5.5.3.	<i>Environmental effects – radiation</i>	28
5.6.	IMPLEMENTATION CONCEPTS	28
5.6.1.	<i>Sensor mounting methods</i>	28
5.6.2.	<i>Sensor locations</i>	28
5.7.	CABLING	28
5.8.	ELECTRONICS AND ALGORITHMS	28
5.9.	REFERENCES	29

Introduction

A continuous position indication of each of the reactivity control elements of the space nuclear power plant (SNPP) is required by the reactor Instrumentation and Control (I&C) system. The two types of reflector control elements currently under consideration by the NRPCT for the SNPP are sliders that move axially along the exterior of the reactor vessel adjacent to the core, and drums that rotate about a fixed axis parallel the region adjacent to the core.

Candidate technologies capable of measuring the linear or rotary displacement of a space reactor control slider or drum, respectively, are discussed below. These include linear variable differential transformers and capacitive sensors for linear displacement, and resolvers and capacitive sensors for rotary displacement. The focus on these technologies in particular is based on the findings of Reference (1). A discussion of ultrasonic-based position indication technology is provided separately in the ultrasonic technology evaluation in Enclosure (3).

1. Position Indication Baseline Requirements

The current baseline motion requirements being considered for a SNPP slider are an overall travel of 45cm at an accuracy of 0.5mm and a resolution of 0.05mm, and for a SNPP drum an overall angular movement of 360 degrees with an accuracy of 0.1 degrees and resolution of 0.01 degrees. The position detector will attach to the control element drive motor in a region immediately aft of the reactor radiation shield. The operational temperature of the detector should normally range from approximately 250K to 400K. The expected gamma dose and neutron fluence radiation levels at are of the order of 2×10^8 TID rads(Si) and 3.6×10^{15} nvt, respectively. The electronics for the position sensor is to be located approximately 60 meters from the sensor in a much reduced radiation field.

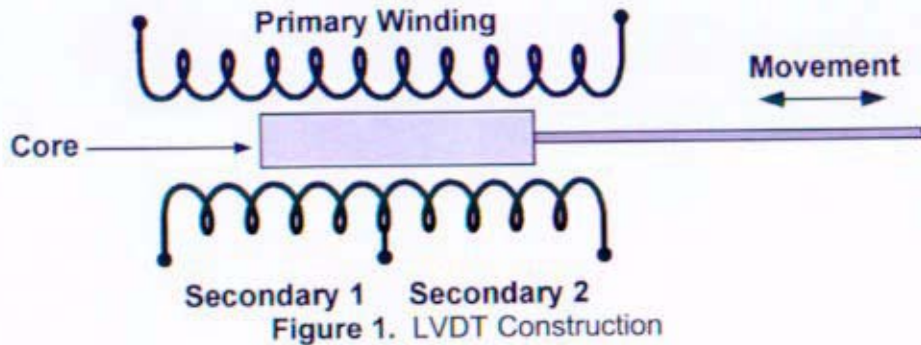
2. Extensibility

The position indication technologies identified in this submittal are directly extensible to a potential lunar power station application. A possible concern not associated with the original Jupiter mission could be the potential contamination of the position sensors by dust/debris infiltration, but appropriately engineered enclosures should mitigate this risk. The possibility of a reduced total radiation dose compared to the JIMO mission will ease sensor development and possibly allow the introduction of additional feasible position indication techniques.

3. Linear Variable Differential Transformer

3.1. Description

The linear variable differential transformer (LVDT) consists of a ferromagnetic core that passes through a three-winding transformer: a primary and two secondary windings. The primary winding is excited with a constant sine-wave current. Voltages measured in the two secondary windings differ in proportion to the inductive coupling provided by the ferromagnetic core. The difference in the secondary voltages is proportional to the linear position of the core. The ferromagnetic core is attached to a control element shaft and thus the control element's position is measured. A basic schematic of its construction is shown in Figure 1.



3.2. Feasibility

3.2.1. Commercial state of the art

LVDT's are a very mature linear position measurement technology. There are many examples of the LVDT devices working in harsh industrial environments including nuclear power plant applications. The capabilities of some of these meets or exceeds the requirements judged necessary for the Prometheus application. There are long-stroke LVDT's available with displacement ranges that meet the requirements of the Prometheus reactor position LVDT. There are others that currently meet the contemplated operational temperature range.. A rad-hard LVDT was developed for the SP-100 space reactor.. An SP-100 space reactor position LVDT was developed by Schaevitz Engineering Inc. in 1994. Schaevitz Engineering Inc. and RDP Electronics are suppliers of the harsh environment LVDTs. Current examples from their product line for high radiation, high temperature environments are compared against the SP100 LVDT and Prometheus requirements in Table 1.

Table 1: Comparison of Various LVDT Performance Data

	Schaevitz	RDP Electronics		SP100	Prometheus
	XS-ZTR	LIN256	ACT18500C		
Total Ionizing Dose (TID Rads)	1x10 ¹¹	1x10 ¹¹	--	--	2x10 ⁵
Neutron Fluence (nvt)	3x10 ²⁰	--	--	--	3.6x10 ¹⁵
Operating Temperature Range (K)	200-823	53-872	220-472	289-700	250-400K
Max. Non-Op. Temperature (K)	923	972	--	700	--
Measurement Range [Stroke] (mm)	25.4	25	470	127.0	450

3.2.2. Level of development required

As the results of Table 1 indicate, the provision of a LVDT position sensor for Prometheus would require an increase in the measurement range of the rad hard designs. The stroke capability of the commercial RDP ACT18500C unit suggests this is feasible. The temperature requirements for Prometheus are not significantly different from the specifications for available high temperature or high radiation devices. Some development may be necessary to combine the increased measurement range with the harsh radiation and temperature requirements. Current rad-hard designs could be modified to incorporate the technology of longer range designs. Findings of the SP-100 LVDT test report¹ suggest this is possible.

Temperature compatibility developments not only include a design that physically withstands high temperatures, but also provides compensation for variations in measurements due to changes in the physical characteristics of components that occur over the wide range of temperatures that the LVDT will experience. This may be accomplished by further materials and/or electronics development.

3.2.3. Jugular Issues

There are no jugular issues associated with implementation of an LVDT position indicator based on the most recent reactor power plant and thermal management models. The technology is well understood including those associated with temperature compensation and radiation. The biggest challenge associated with a LVDT could be the minimization of the mass and size of the sensing elements to meet the weight goals for the spacecraft.

3.3. Deliverability

3.3.1. Development time required

A task outline including design, simulation, fabrication, and testing included in the Sensor Technology Development Plan provided by ORNL² estimates three years until completion of full scope testing of a space-ready linear position measurement system.

3.3.2. Manufacturability

Accurate and consistent winding of the LVDT coils is the main manufacturing issue. This can be difficult depending on the conductor/insulator material in use and the winding arrangement. Winding arrangements are discussed later in section 6.3.2., but basically some arrangements are harder to implement in terms of consistent number density per unit length and radii of the turns. Symmetry is important to maintain measurement accuracy.

Accurate windings are also more easily constructed when a computer-controlled winding machine can be used. Some high temperature conductor materials (i.e. palladium) do not form good bonds with insulating material making them fragile and requiring hand winding. Stainless steel clad copper was found to work well for the SP-100 LVDT, and precise and repeatable windings were achieved through the use of a winding machine.

3.4. Capability

3.4.1. Sensitivity/accuracy/repeatability/resolution

LVDT sensitivity is expressed as millivolts of differential secondary signal per volt of primary excitation voltage per thousandth of an inch displacement and is on the order of 0.05 mV/V per 0.001" (25.4 μ m) for longer stroke designs. This translates to 10-50 mV per millimeter. Operating at a higher frequency allows for increased sensitivity.

LVDT's have very low nonlinearity typically equal to a maximum of 0.5% of full scale (0.225 mm), and a repeatability of 0.15 μm has been commercially achieved. The resolution of an LVDT is infinite and is limited by the accuracy and sensitivity of the signal conditioning electronics.

3.4.2. Operation when located 60m from electronics

Typically LVDT's are excited by large sinusoidal signals, e.g. 5Vrms at 1000Hz, that can be transmitted over long cable lengths without significant interference or attenuation. Assuming signal cabling is properly shielded and grounded, the effects of electromagnetic interference should be minimal.

3.4.3. Physical measurement range – absolute position

A SNPP control element position sensor must be able to identify the exact position of the element without reliance on the past history of control element travel. This ensures that losses of information resulting from power outages or electronic aberrations do not prevent identifying the absolute position of the control once power is restored. LVDT's provide an absolute measurement allowing for position measurements to be made in the event power is temporarily lost and restored.

3.4.4. Temperature range – effects and compensation requirements

LVDT's work best in a steady-state temperature environment because their accuracy is temperature dependent. In test applications using LVDT's with a 50 mm range in autoclaves at KAPL, measurement changes up to 1 mm have been observed when increasing from room temperature to 300°C. The LVDT's in this case are used for measuring changes in position at a steady elevated temperature, not absolute position, so no compensation techniques were used.

The largest shift in thermal sensitivity results from the thermal coefficient of resistance of the windings. As the primary coil resistance increases with temperature, the current in the coil decreases causing the magnetic flux to decrease. This results in a decreased voltage output and incorrect measurements. Other variations occurring with temperature are due to changes in magnetic properties of the core and dimensional changes. Possible electronic and signal conditioning techniques exist to compensate for temperature effects. These include high frequency excitation, constant current excitation, look-up table correction, and the sum-of-secondaries technique, which are explained below.

Using a higher excitation frequency reduces the need for temperature correction. At higher frequencies, the real part of the coil impedance decreases, thus limiting the effects of increased coil resistance with temperature. The LVDT developed for the SP-100 program exhibited 0.45% per 100°F temperature dependence at 10 kHz, and 1.4% at 2.5 kHz.¹ This corresponds to inaccuracies of several millimeters at maximum temperature.

Constant current excitation can be used for temperature compensation. As temperature rises causing a higher coil resistance, the current supplied can be forced to remain constant and ensure primary coil flux. This was used for the Halden Project LVDT, but without any report on results.³

A correction can be applied to the position measurements through the use of a look-up table. If the LVDT temperature is known (perhaps from an additional temperature sensor), a correction value can be applied to the measurement. A correction could also be obtained by correlating the LVDT temperature to the reactor outlet temperature. This estimate of LVDT temperature could be sufficient if the temperature dependence is small enough.²

The "sum of secondaries" technique can be used for signal conditioning to null the effects of temperature change. When using this technique, the sensor system output is a ratio of the difference in secondary voltages to the total sum of the secondary voltages. A block diagram of this can be seen in Figure 2. As temperature rises and causes a lower voltage output from each secondary, the ratios according to the core positions should remain the same. Another variation of this involves feedback control of the power source so that it varies the amplitude of the excitation signal to keep the sum of secondaries at a desired value. When using these techniques, the LVDT must be constructed such that the sum of the secondary voltages remains constant throughout the entire stroke of the sensor.⁴ Schaevitz's ZTR series LVDT's meet this requirement, but they still advise applying an additional correction by extrapolating from experimental data on measurement error with varying temperature.

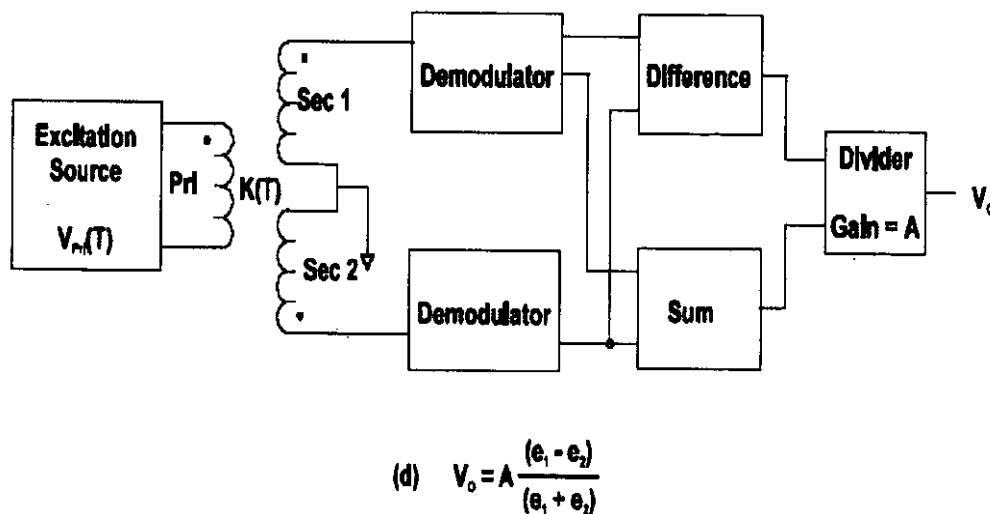


Figure 2. Sum-of-Secondaries Block Diagram

3.4.5. Power source requirements

LVDT's for high temperature applications require an AC source ranging from 50 mA at 400 Hz for constant current excitation to 3 Vrms at 10 kHz for high frequency excitation. Since LVDT's are inductive devices, sine wave excitation is strongly preferred over square wave. It is important that the DC component of the excitation be kept to a minimum, and a total harmonic distortion (THD) of less than 3% is generally acceptable. A low output impedance will also minimize variations in voltage due to changes in the LVDT primary impedance with different core positions.

3.4.6. Testing – self calibration, etc.

LVDT's have excellent null-position repeatability because this is the point where the voltage output is zero. Provided the two secondary coils experience the same temperature environment, the output value at null position should not change with varying temperature.

If other temperature correction methods prove to be inadequate, a dedicated temperature sensor for the LVDT could be used to obtain the actual temperature of the sensor to apply a correction factor via a look-up table. This is undesirable because of the added cabling and complexity. Since temperature

is being measured elsewhere on the spacecraft (Brayton cycle hot leg), it is possible to estimate the LVDT temperature based on correlation with other reactor temperatures. Both situations are undesirable because it is basing the function of the LVDT on the accuracy of another sensor, but may be the only way to apply measurement corrections for temperature compensation.

3.4.7. Weight and size

Standard LVDT's with a 15 cm range are 500 grams in mass. Additional temperature/radiation/EMI shielding is foreseen to increase the mass.

In general, LVDT's are a minimum of twice the desired measurement range in length. This gives enough clearance for the movement of a core adequately sized to provide the amount of inductive coupling necessary for accurate measurements. The winding arrangement of the secondaries (discussed in section 6.3.2.) can also increase or decrease the overall sensor length.

3.4.8. Time response

The frictionless movement of the LVDT allows for fast response of the sensor itself, limited by the inertial effects of the lightweight core. The time response of an LVDT system is usually limited by the characteristics of the signal conditioning electronics (i.e. the rise time of the amplifiers), and the excitation frequency. Typical responses are in the range of 250 Hz to 1000 Hz.

3.5. Reliability

3.5.1. Failure mechanisms – moving parts

The only moving part of an LVDT is the core, which is attached to the control rod. Movement of the core in the primary/secondary windings is non-contact which allows for a reliable, long-lifetime of the device. No bearings or lubrication are necessary.

Two potential points of failure were identified after the development of the SP-100 LVDT. The first was that the leadout wires were found to be fragile and needed improvement. The primary and secondary nickel leadout wires were actually combined into a single sheathed cable. This created a very rigid cable that was hard to route and made it hard to keep track of the primary and secondary cables. It was recommended that a separately sheathed, smaller diameter cable be used for each winding, which would also decrease the probability of crosstalk.

The second finding was later hypothesized to be the cause of device failure at high temperature. The coils of the LVDT were incased in glass thread insulation, which has a lower rate of thermal expansion than the coils. At high temperatures, the glass can act as a rigid, constrictive shell as the windings expand at a greater rate, and the insulation can then become damaged. This can result in a decrease in winding to winding resistance or even electrical shorts.

3.5.2. Failure mitigation strategies

The non-contact design of an LVDT can allow for high radial clearance between the core and its center bore to prevent sticking when the core is not moved for long durations in a high temperature vacuum environment. A coating of MoS₂ on the core and center bore will also prevent sticking.

Also, the open-ended housing design allows the LVDT to avoid damage if the moving core is temporarily over-extended out of the measurement range due to CDM malfunction or other conditions. Accurate measurements in the overshoot condition cannot be made, but the LVDT can remain unharmed until normal operating conditions resume.

Typically commercial products can withstand shock loads of the order of 1000 g shock for upto 10 ms and 20 g vibrations at frequencies upto 2 kHz.

3.5.3. Environmental effects – radiation

The LVDT must be able to withstand radiation from reactor and cosmic sources. The Halden Project LVDT exhibited neutron-fluence-related drift when subjected to high levels of radiation. There was a 3% linear increase in output voltage totaling 0.03 volts when two LVDT's were irradiated at $1.96 \cdot 10^{14}$ N/cm²/s to a total fluence of $7 \cdot 10^{19}$ N/cm². Two possible causes of the drift that were suggested but not verified were radiation induced swelling and crevice corrosion³. Note that this 3% drift occurred at a total fluence of several orders of magnitude greater than expected for the Prometheus reactor.

3.5.4. NR/NASA Program experience

The NR Program has significant experience with LVDT's for a wide variety of position measurement applications including ones with significant radiation and temperature levels. The design specifications for these applications, e.g. measurement ranges, accuracies, vibration, shock, etc., are similar to those being contemplated for the SNPP.

During the SP-100 program, NASA sponsored the development and test of an LVDT with a 5 inch range by Lucas Schaevitz Inc. that performed very well up to 700K (800°F), but was not recommended for higher temperatures after further tests at 810K (1000°F). The greater thermal expansion of the copper windings when compared to that of the glass insulation was hypothesized to be the cause of failure above 700K¹.

3.6. Implementation Concepts

3.6.1. Sensor mounting methods

Clamps, brackets, or mounting blocks can be placed over the LVDT housing at several locations to allow for mounting or screwing onto the plant in such a manner allowing for linear movement of the core inside the LVDT housing. Figure 3 shows two mounting methods. Clamps should be a non-magnetic, non-conductive material and must not be tightened to a point that deforms the internal winding geometry or core movement. If metal parts are used they should be symmetrically placed with respect to the center of the coil assembly. Also, because of the high levels of acceleration experienced during launch and other mission phases, end-to-end clamping will most likely be needed in addition to, or in place of, over-body clamping.

A threaded hole can be drilled into the moving core of the LVDT allowing for the moving control rod or slider to be screwed into it. The rod or any extension connected to the core must be non-magnetic such that it does not provide additional inductive coupling that interferes with the fields of the windings.

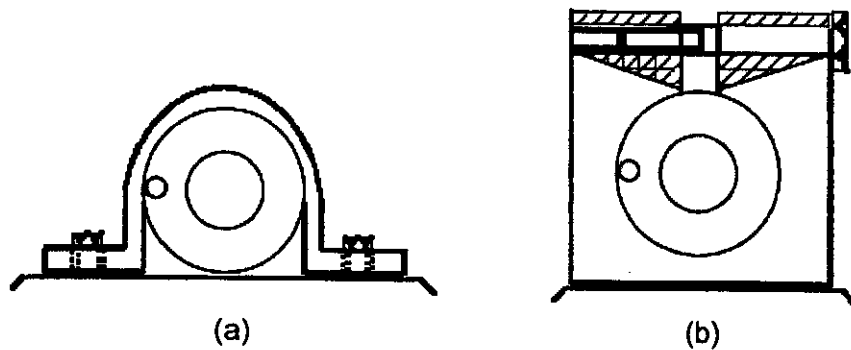


Figure 3. Head-on View of LVDT Mounting Methods. (a) Bracket, (b) Mounting Block.

3.6.2. Sensor locations

The sensor should be located in a position of lowest temperature and radiation with access to the rods to be measured. It should also be located away from motors and permanent magnets to avoid external inductive influences. A magnetically shielded housing can be used if this is a concern.

3.6.3. Other engineering issues

The high temperature and radiation environment experienced by the LVDT may require the use of materials not typically found in commercial designs. Table 2 includes the different materials used by the SP-100 and Halden Reactor Project LVDT's.

Table 2. LVDT Materials

	SP-100 LVDT	Halden Project LVDT
Core:	Vanadium Permendur	Low Carbon Chrome Steel
Bobbin:	Ceramic Mullite	Austenitic Stainless Steel
Coil Conductor:	Stainless Steel Clad Copper	Precious Metal Alloy
Coil Insulator:	Ceramic Coating	Ceramic Coating
Leads:	Nickel	28 AWG Nickel (MgO insulation)
Other:	Glass Thread Insulation Between Windings	Sprayed Aluminum Oxide Housing Insulation

An LVDT design issue that needs to be addressed is the arrangement of the secondary windings, especially if the sum-of-secondaries system is going to be used. If it is, the physical design of the LVDT must provide a constant sum of secondary voltages over the range of motion at any given temperature. This means that the number of turns per unit length of the LVDT remains constant throughout the entire stroke of the device with no concern for which secondary winding they belong to. If this requirement is not met, the sum-of-secondaries system becomes useless and measurements will be more temperature dependent. This is explained further in the following figures and descriptions of winding arrangements.

Non-overlap winding, non-constant turns (Figure 4a)

In this winding arrangement, the number of turns increases from the center outward for each secondary winding. This was the arrangement chosen for the SP-100 LVDT because it was easier to design and implement with symmetrical coils, and it produced a more linear output signal. This does not have a constant sum of secondary winding voltage.

Overlap winding (Figure 4b)

Overlap winding provides greater measurement range possibilities with smaller overall LVDT length. This is harder to implement with symmetrical coils and is more prone to having shorts occur between the secondaries because they do overlap. However, the sum of secondary voltages is constant.

Non-overlap winding, constant turns (Figure 4c)

Another arrangement with constant sum of secondary voltages consists of secondary windings that do not overlap and have a constant number of turns per unit length throughout the stroke of the device. The insulation between the secondaries must be of minimal width in order to preserve magnetic flux.

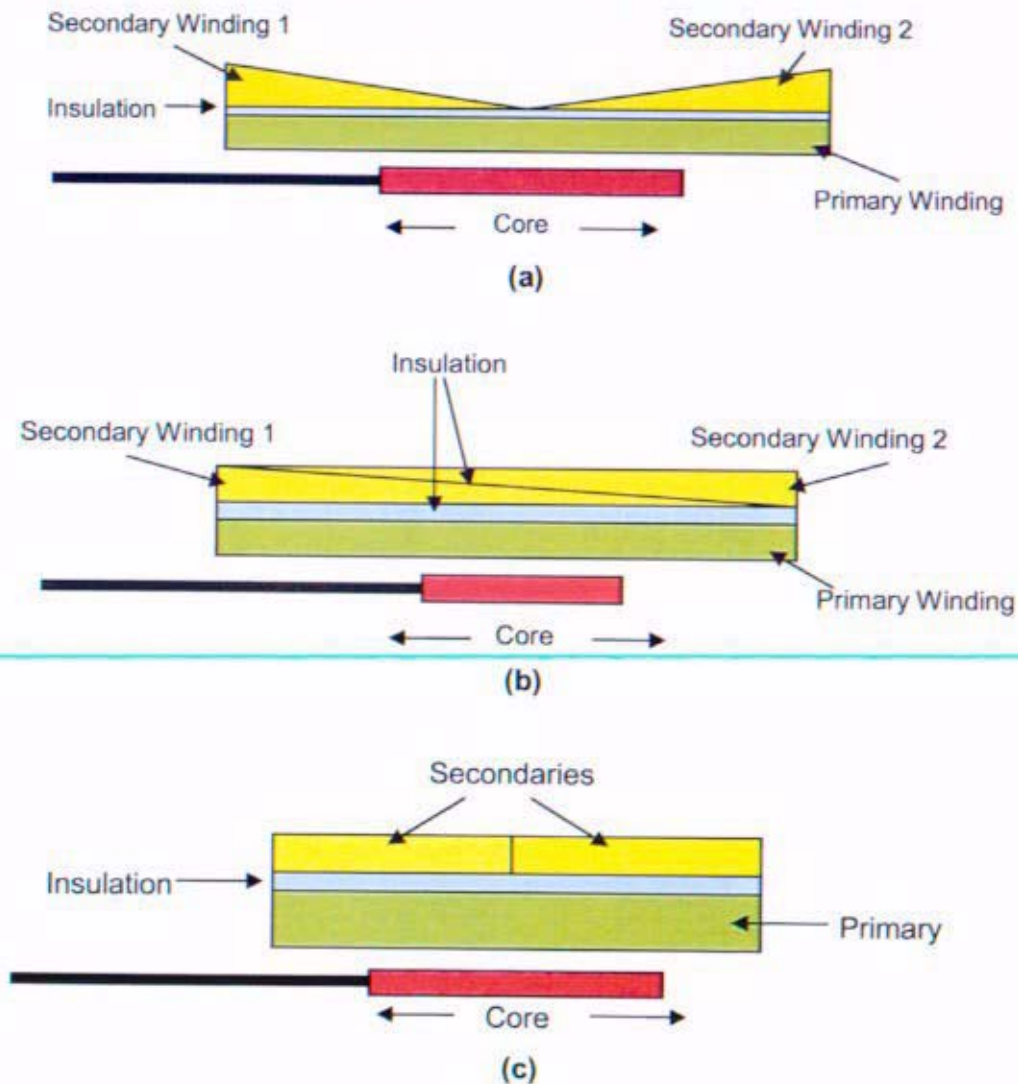


Figure 4. Top Half Cross Sections of Winding Arrangements (a) non-overlap, non-constant turns, (b) overlap, (c) non-overlap, constant turns.

A comparison of overall LVDT length versus winding arrangement is shown in Figure 5. For two example LVDT implementations, both with a measurement range of 16 cm, the differences between overlap and non-overlap windings are displayed. The core of an overlap design has the possibility of

being shorter in length and still inductively coupling with both secondary windings. The core of a non-overlap design must be longer to do so over the same measurement range, which increases the overall LVDT length. Further investigation and/or testing is required to determine the optimal dimensional ratios for designs of this range, but the possible advantage presented by overlap winding is still evident.

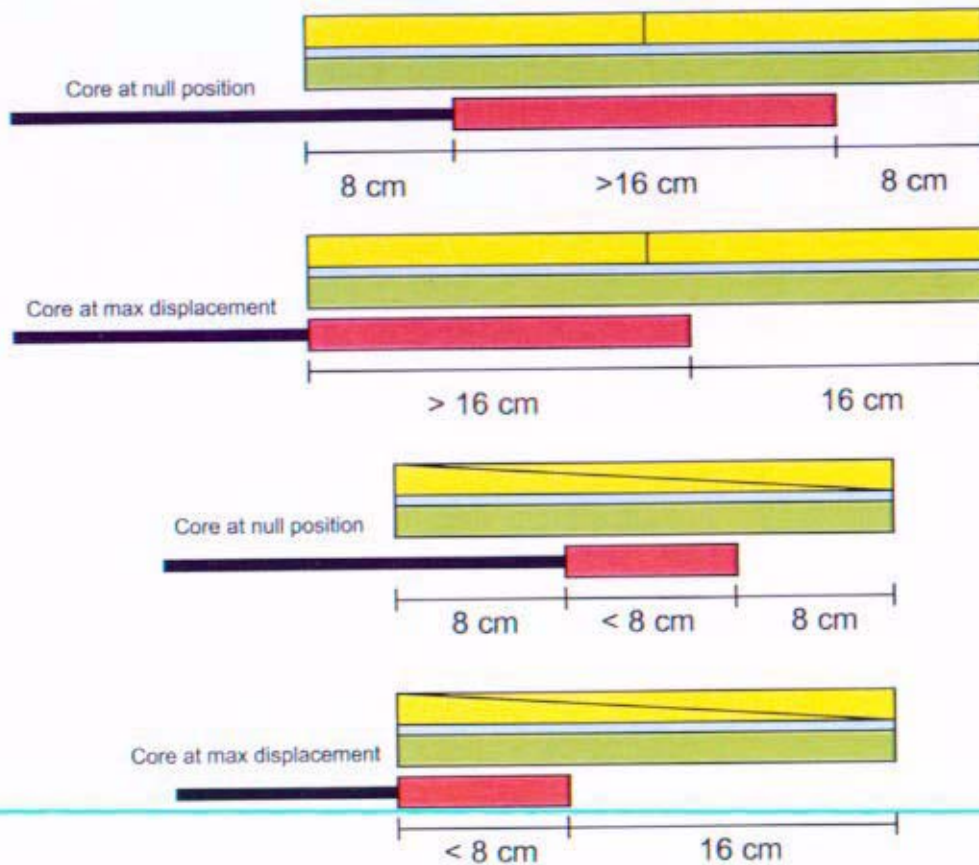


Figure 5. LVDT Length Comparison for Non-Overlap and Overlap Winding

3.7. Cabling

To properly implement a high temperature design with minimum crosstalk susceptibility, an LVDT will require three coaxial cables. 28 AWG nickel leadout cables are commonly used with high-temperature/rad-hard designs. Other cabling concerns are EMI shielding as the sensor cables will be in close proximity with the power cables running the length of the spacecraft 50m boom and their flexibility particularly during spacecraft deployment when boom temperatures near the lower end their expected range at 250K.

3.8. Electronics and Algorithms

LVDT's provide position measurements via a simple voltage measurement, but complexity increases with the use of temperature compensation techniques. Many of these techniques are accomplished electronically and were discussed in sections 4.4.1. - 4.4.4. The sum-of-secondaries is highly recommended for this application because of the large range of temperatures encountered. This creates output signals that are more independent of fluctuations in the excitation signal due to temperature variations. It requires one demodulator to generate a signal proportional to the difference

in secondary voltages, another to generate a signal proportional to the sum, and a divider to generate a ratio of the two which corresponds to the core position.

Arranging the secondaries in a series opposing configuration causes a 180° phase change of the AC signal as the core passes through the null position, so half of the possible core positions correspond to positive voltages, and the other half correspond to negative voltages.⁴ The resulting DC signal can be seen in Figure 6. The very low voltage signals when the core position is close to null are subject to interference from any high voltage cables in close proximity. A magnetic LVDT housing will provide additional EMI shielding in the immediate measurement location.

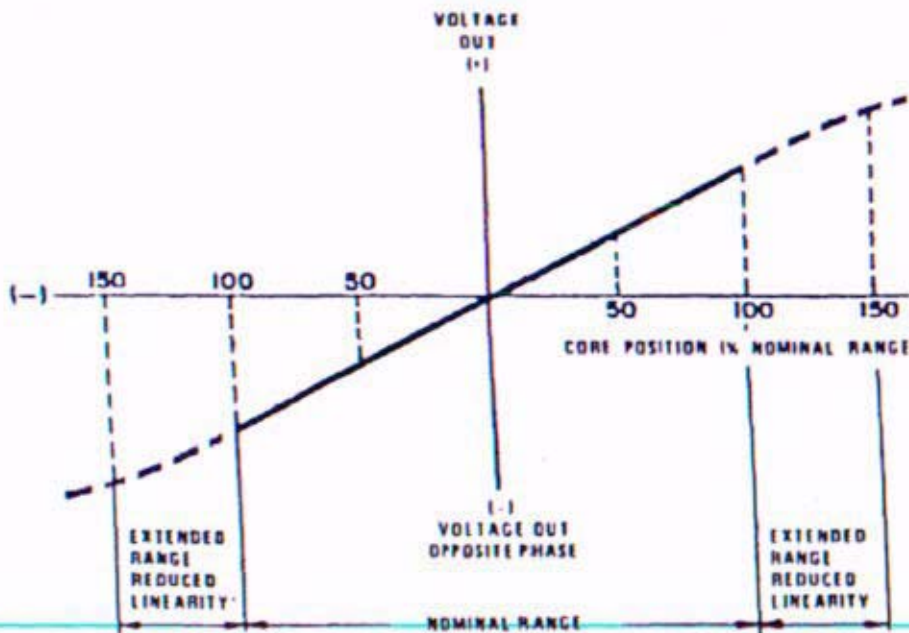


Figure 6. Difference of Secondary Voltages when in Series Opposing Configuration

3.9. References

1. JIMO Reactor Sensor Technology Development Plan, ORNL/LTR/NR-JIMO/05-01, January 2005
2. N. A. Meyer, "Control Drive Assembly Linear Position Sensor LVDT Bench Test," SP-100 Program. Information Request/Release, DOE/SF/16006- -T1194, Martin Marietta, January 1994.
3. "Sensor Technology Development Plan," ORNL/LTR/NR-JIMO/05-01, February 2005.
4. P. Gubel, "Reactor BR2," SCK-CEN Scientific Report, OECD Halden Reactor Project, 2002.
5. J. Szczyrbak and E. Schmidt, "LVDT Signal Conditioning Techniques," Lucas Control Systems, April 1997.

4. Resolver

4.1. Description

A resolver is an electromechanical transducer that measures the absolute rotational position of a rotating element, such as a shaft. As a circuit component, it functions as a variable coupling transformer. A resolver contains a one or two-phase primary and a two-phase secondary. The secondary windings are oriented at 90° , as are the primary windings. A sinusoidal input voltage will produce an output voltage with a magnitude that varies with the sine and cosine of the shaft angle (i.e. the input vector is resolved into its components). Energy can be transferred between the stator and rotor with slip rings and brushes or without any physical connections to the rotor via a circular rotary transformer (i.e. a brushless resolver). A typical brushless resolver cross section and schematic are shown in Figures 7 and 8.

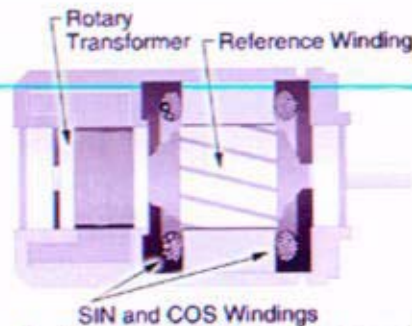


Figure 7. Brushless Resolver Cross Section¹

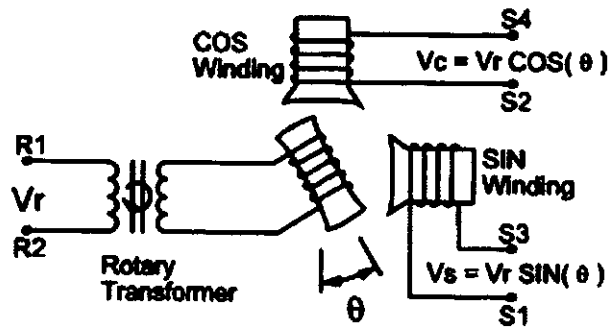


Figure 8. Brushless Resolver Schematic¹

4.2. Feasibility

4.2.1. Commercial state of the art

Resolvers have been used in rotary positioning systems for over 50 years including military, avionic, and industrial applications. Position measurement over a 360° range and in harsh environments is possible with resolvers. High temperature resolvers can carry ratings to 500K (220°C), but have limited potential above 500K. Radiation hardened resolvers have been developed to withstand total accumulated doses of 2×10^8 Rads gamma radiation. Resolvers have been developed to survive in a vacuum down to 10^{-9} Torr. Empire Magnetics, Inc. and MOOG Components Group, Inc. are two companies that have developed resolvers for use in space applications.^{2,3,4}

4.2.2. Level of development required

While resolvers have been developed to operate in high temperature, radiation, and vacuum environments, combining all of these conditions presents a difficult resolver design challenge. This challenge has been met before by resolver designs used in space applications, where all of the above conditions exist to some extent. However, there would be some additional development needed to meet the specific requirements presented by a space nuclear environment.

4.2.3. Jugular Issues

The maximum temperature rating of the resolver is limited to 500K, which is primarily governed by the winding insulation rating. High temperature magnet wire with a non-copper conductor and exotic insulation is required for applications over 500K. The inorganic insulation materials used in the high temperature magnet wire can crack and break when winding the fine wires found in most resolvers.

Many electrical parameter changes with temperature will have to be compensated, such as accuracy, electrical zero and phase shifts, transformation ratio, impedance, input current, input power, and null voltage changes.

4.3. Deliverability

4.3.1. Development time required

In Reference (1) ORNL estimates that a 3 year development effort will be necessary to prepare a prototype resolver based control element rotational position measurement system for integrated system testing.⁵

4.3.2. Manufacturability

Special cleaning, vacuum baking, extraction of contaminants, and sealing are some of the processes performed by experienced manufacturers of resolvers used in vacuum applications.

4.4. Capability

4.4.1. Sensitivity/accuracy/repeatability/resolution

Sensitivity is proportional to the output voltage and is expressed as a function of the shaft angle in mV/degree. Values can range from 35 to 450 mV/degree.

Accuracies of ± 5 arc min or better are achievable.

API Harowe, Inc. offers a resolver and resolver to encoder converter combination with a repeatability of 5 arc min.

Resolution of 5 arc min is attainable with a 12 bit resolver to digital converter.

4.4.2. Operation when located 60m from electronics

Assuming appropriately sized cabling properly shielded and grounded, EMI noise should not be a problem for a resolver based position sensor located upto 60m away from its electronics. However, for distances greater than 60m noise considerations may dictate lower impedance cables.

4.4.3. Physical measurement range – absolute position

Resolvers provide absolute rotational position measurement and units are available that measure over a 360° range.

4.4.4. Temperature range – effects and compensation requirements

Resolvers have been developed that operate as low as 250K (-20°C) and others as high as 500K.

Temperature changes above 25K can cause stresses and differential expansion in the lamination stack, windings, and hardware that affect the accuracy as much as a few arc minutes or the null voltage less than 1% per degree C. Also, minute mechanical changes with temperature can result in a shift of the electrical zero (i.e. when primary and secondary windings are perpendicular).

The resistive changes in the magnet wire due to its temperature coefficient can affect the phase shift, transformation ratio, impedance, input current, and input power.

The above temperature induced effects could be compensated for by characterizing their overall effect and applying a correction factor look-up table or a signal conditioning technique.

4.4.5. Power source requirements

Resolvers can be designed to operate with a sinusoidal input voltage from 0.5 to 115 Vrms over a frequency range of 60 Hz to 100 kHz.⁶

Input current is typically less than 100 mA, and input power is usually less than 1 W.

4.4.6. Testing – self calibration, etc.

The resolver may require an additional temperature sensor to apply accurate temperature compensation or may be able to be correlated with another system temperature measurement.

4.4.7. Weight and size

Most units are custom built and vary in size by application. Overall diameters can range from 2 to 20 cm, and lengths can range from 0.5 to 5 cm.

4.4.8. Time response

In general, shorter response times are achievable with higher operating frequencies.⁷

API Harowe, Inc. offers a resolver and resolver to encoder converter combination with a small step (1°) response time of 7 ms and a large step (179°) response time of 20 ms. These are maximum response time values that are arrived at with a 2 kHz operating frequency. The large step response time can be improved by almost a factor of 3 when operating the converter at 20 kHz. However, the small step response time sees little improvement when operating at 20 kHz, due to the bandwidth term in the settling time equation dominating the overall time response.⁸

4.5. Reliability

4.5.1. Failure mechanisms – moving parts

Inductively coupled brushless resolver life is limited only by its bearings and offers up to 10 times the life of units with traditional brushes or slip rings.⁹

Resolvers can fail from electrical shorts or open circuits in the windings.

4.5.2. Failure mitigation strategies

Bearing lubrication must be given considerable attention during the design of resolvers for use in environments with a vacuum, high temperature, and radiation exposure. Dry lubes such as MoS₂ are often used in vacuum environments where material outgassing can occur. Outgassing rates increase with temperature, and lubricant deterioration can increase with radiation over time. The ion implantation technique has been used to apply dry lubricants to instrument grade bearings for high precision applications.

Dielectric withstand voltage and insulation resistance tests should be performed to verify the integrity of the insulation system.

4.5.3. Environmental effects – radiation

See failure mitigation strategies above.

4.5.4. NR/NASA Program experience

Resolvers have been used on NASA's Cassini spacecraft.

4.6. Implementation Concepts

4.6.1. Sensor mounting methods

A stand alone brushless resolver is shown in Figure 9. This type of resolver can be mounted using screws entering the mounting face (1), attaching a flange bracket (2) to the mounting face, or securing a clamp (3) around its housing.

Coupling to the resolver shaft can be accomplished with a solid or bellows type coupling to another shaft or by using a gear arrangement.

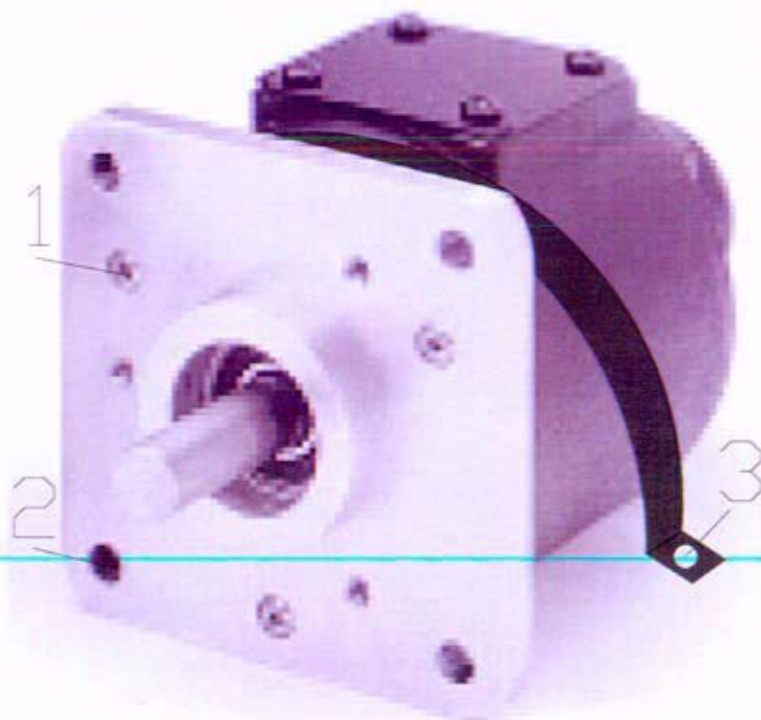


Figure 9. Stand Alone Brushless Resolver Mounting Options¹⁰

A pancake brushless resolver is shown in Figure 10. This type of resolver is supplied as separate stator and rotor assemblies. The stator assembly can be held in place using clamps that attach to the mounting grooves or flanges provided on the outside of the housing. The rotor assembly can be mounted adhesively, by using a keyway provided in the rotor bore, by clamping against the end of the hub, by set screws in tapped holes provided in the rotor hub, or by a combination of these methods.



Figure 10. Pancake Brushless Resolver¹¹

4.6.2. Sensor locations

Ideally, the resolver should be located in an area that minimizes the high temperature and radiation exposure.

4.7. Cabling

Typically, a low capacitance 6 conductor shielded cable consisting of 3 twisted-pairs is used for the resolver electrical connections.⁴

High temperature magnet wire with a non-copper conductor and exotic insulation has been developed for special applications to 500K..

4.8. Electronics and Algorithms

Resolvers require an AC signal source, and their analog output has to be converted to interface with digital systems.

Resolver to digital conversion is best performed using the tracking conversion technique to provide excellent noise immunity. A tracking converter looks at the ratio of the sine and cosine outputs of a rotor excited resolver. Distortion or amplitude variation in the excitation waveform appears equally on both the sine and cosine outputs, and its effect is cancelled out when looking at their ratio. Common mode rejection via the natural isolation of the resolver and the integration of the tracking loop used in the converter makes for a noise immune angular to digital conversion system.

A temperature compensation technique will need to be implemented in either the signal conditioning electronics or software to correct for electrical parameter changes with temperature.

4.9. References

1. http://www.amci.com/resolvers/what_is_resolver.asp
2. <http://www.polysci.com>
3. <http://www.moog.com>
4. <http://www.empiremagnetics.com>
5. "Sensor Technology Development Plan," ORNL/LTR/NR-JIMO/05-01, February 2005.
6. Joe Spetzer and Bill Ekhamel, "Things You Need to Know About Sizing and Applying Resolvers," Motion System Design, March 2001.
7. John Gasking, et al., "Synchro and Resolver Conversion," North Atlantic Industries, Inc., October 2001.
8. "Synchro/Resolver Conversion Handbook," Data Device Corporation, October 1994.
9. http://www.controlsocieties.com/resolver_application_data.shtml
10. "Heavy Duty Encoders, Resolvers, & Feedback Systems Product Guide," API Harowe, Inc.
11. "Synchro and Resolver Engineering Handbook," MOOG Components Group, Inc., December 2004.

5. Linear and Rotary Capacitive

5.1. Description

The principle of operation for linear and rotary capacitive displacement position sensing is the same electrically, but different with respect to sensor geometry and plate / dielectric movement. Therefore, the two technologies can be evaluated in one assessment.

Capacitive displacement position sensing can be best understood by first examining the parallel plate sensor configuration. The capacitance can be varied by changing the distance, the effective coupling area, or the dielectric medium between the plates (see Figure 11). Distance variation is suitable for measuring small displacements. Area and dielectric variation are more suitable for measuring larger displacements. A differential capacitance sensor configuration can be used to compensate for some types of sensor inaccuracies and environmental dependence (see Figure 12)¹. The sensing element is driven with an alternating current by an electronic circuit that demodulates the signal resulting from the sensing element capacitance change.

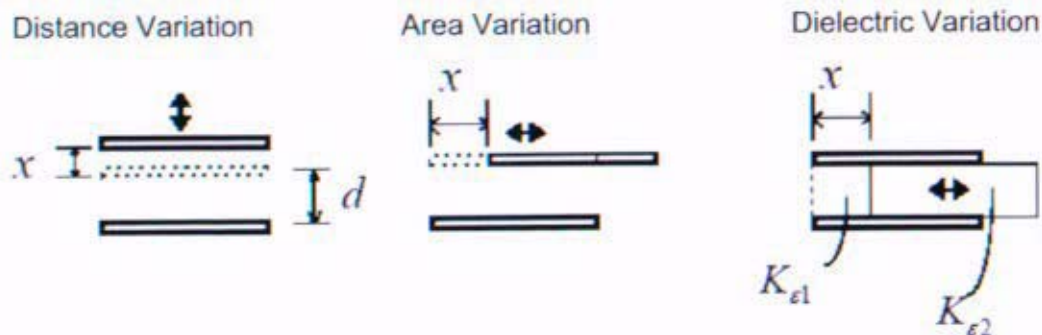


Figure 11. Parallel Plate Sensor Configurations²

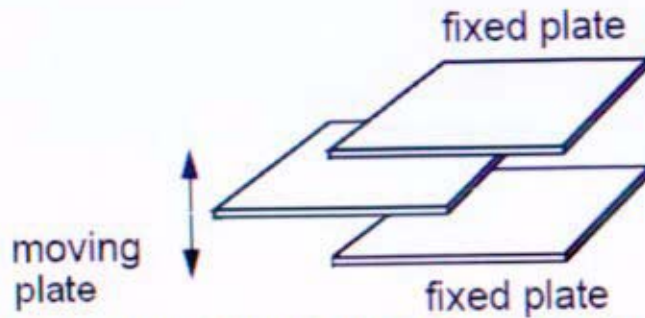


Figure 12. Parallel Plate Differential Sensor Configuration

5.2. Feasibility

5.2.1. Commercial state of the art

Rotary capacitive displacement position sensing has been used in radio frequency selection circuitry for years.³ Rotary position measurement over a 180° range using a similar concept is possible (see Figure 13). RDP Group is one company that has developed a rotary capacitive displacement transducer to operate over a 300° range.

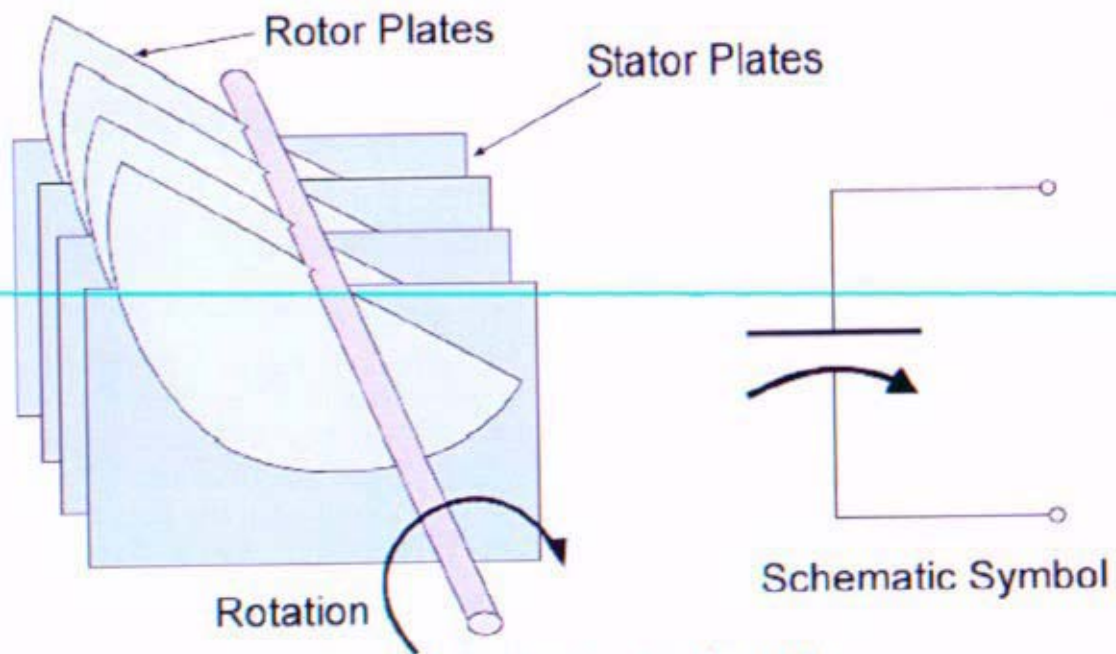


Figure 13. Rotary Capacitor Concept⁴

Linear capacitive displacement position sensing is commercially available from Ixthus Instrumentation for displacements up to 2 centimeters.⁵ However, for displacements on the order of tens of centimeters, there is nothing commercially available.

Capacitive displacement sensors can operate at up to 500K.^{5,6} Operation above 500K and in a radiation / vacuum environment is not currently commercially available.

5.2.2. Level of development required

The linear capacitive displacement position sensors available from Ixthus Instrumentation and Micro-Epsilon utilize the distance variation sensor configuration which is suitable for measuring small ranges. A sensor would need to be developed that utilizes the area or dielectric variation configuration to measure displacements on the order of tens of centimeters.

The rotary capacitive displacement position sensor available from RDP Group has a maximum operating temperature of 350K. A development effort would be needed to attempt to increase the temperature capability of this sensor or one of a similar design.

A linear or rotary capacitive displacement position sensor would require some additional development for operation in the high temperature, radiation, and vacuum conditions presented by a space nuclear environment.

5.2.3. Jugular Issues

The sensing plate separation must be kept small and well controlled to maximize the capacitance per unit volume and to minimize errors, respectively.

Static charge builds up on the insulators near the sensing plates due to triboelectric charging can cause an unwanted sensitivity to mechanical vibration.

Lubrication of moving sensor parts must be maintained under the space nuclear environment conditions which can cause lubricant material outgassing and deterioration.

The long term stability of the sensing plate and dielectric materials with time at temperature and radiation dose will need to be investigated.

5.3. Deliverability

5.3.1. Development time required

In Reference (5) ORNL estimated that a 3 year development effort will be necessary to prepare a prototype sensing system for the LVDT or resolver technologies⁴.based on the maturity and commercial availability of the technologies, particularly for radiation environments. In contrast, the limited availability and experience of capacitance position technologies, particularly in linear form, it is estimated that approximately 3.5 to 4 years would be needed to ready a linear or rotary capacitive displacement position measurement system for integrated system testing.

5.3.2. Manufacturability

A process to control the sensing plate spacing and cross axis tilt would be needed for linear or rotary capacitive displacement position sensors.

5.4. Capability

5.4.1. Sensitivity/accuracy/repeatability/resolution

Sensitivity is a function of the capacitance, excitation voltage, and excitation frequency. A linear sensor with a spiral geometry (see Figure 14) has a greater sensitivity than a parallel plate geometry

of equal volume at a given excitation voltage and frequency, due to its larger capacitance per unit volume.

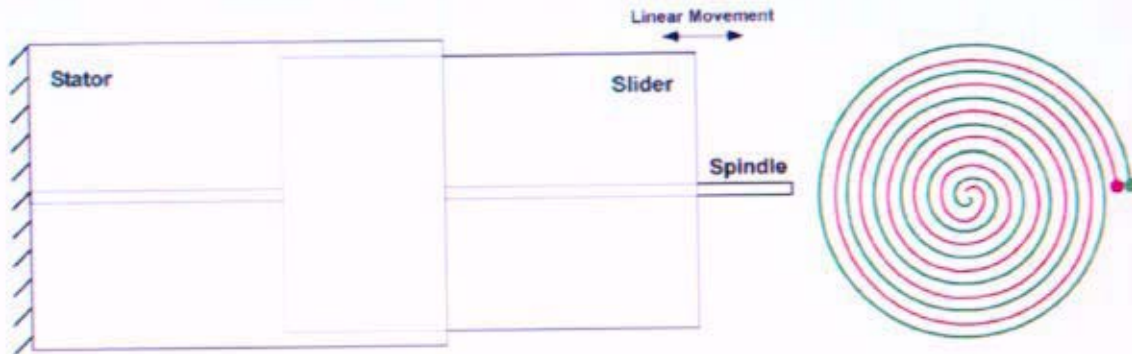


Figure 14. Spiral Wound Capacitor Concept⁴

In area variation sensor configurations, the mechanical accuracy of the electrode positions determines the final accuracy of the sensor system.⁷ This also applies for dielectric variation sensor configurations. Thus, the accuracy of these types of linear or rotary sensors is a function of the mechanical control on the sensing plate separation.

Micro-Epsilon claims that nanometer resolutions ($0.001 \mu\text{m}$) can be reached in the case of small measuring ranges with their capaNCDT series linear capacitive displacement measuring system.⁶ Repeatability for this type of sensor is typically less than 0.1% F.S.⁶

RDP Group has developed a rotary capacitive displacement transducer with a repeatability of 0.05% F.S. and resolution of 0.01% F.S.

5.4.2. Operation when located 60m from electronics

Sensitivity to cable capacitance and any other stray capacitance can be greatly reduced with a guard connection to a synchronous demodulator. A guard is a shield conductor that surrounds or is adjacent to the moveable sensing plate. In addition, the use of a guard reduces the effects of extraneous electromagnetic interference.

5.4.3. Physical measurement range – absolute position

Linear capacitive displacement sensors provide absolute linear position measurement, and units are available that measure over a range of several millimeters.

Rotary capacitive displacement sensors provide absolute rotational position measurement, and units are available that measure over a 300° range.

5.4.4. Temperature range – effects and compensation requirements

Capacitive displacement sensors have been developed that operate as low as 250K and others as high as 473K (200°C).

A differential capacitance sensor configuration can be used to first-order compensate for thermal expansion effects.⁹ This is achieved by configuring the amplifier circuit to generate a voltage

proportional to the ratio of the two capacitances formed by the three plate sensor. The capacitance ratio can then be arranged to track with temperature.

5.4.5. Power source requirements

Capacitive displacement sensors can be designed to operate with either sine or square wave excitation.

Excitation voltages of 5 to 500 Vp-p AC and a high impedance amplifier with a voltage noise of one or two nV per root Hz provide a high signal to noise ratio. The limit to the signal to noise ratio for capacitive sensors is the ratio of the excitation voltage to amplifier voltage noise.⁹

Excitation frequency should be reasonably high to minimize sensing plate impedance and low enough for easy signal conditioning circuit design. A frequency of 50 kHz is usually acceptably high.⁹

5.4.6. Testing – self calibration, etc.

Capacitive displacement sensors in general have good long-term stability.⁶ However, long-term stability of the sensor materials in a space nuclear environment would need further evaluation and/or testing.

5.4.7. Weight and size

Minimizing weight and size should be addressed by maximizing the capacitance per unit volume while providing some overlapping or underlapping of the sensor plate edges to reduce sensitivity to motion in unwanted axes.

The dimensions (mm) of one of RDP Group's rotary capacitive displacement sensors are shown in Figure 15.

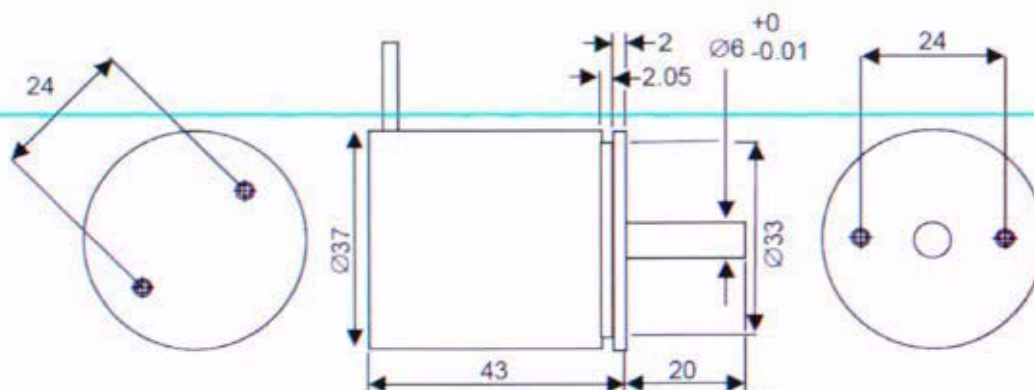


Figure 15. Type RCDT Dimensions¹⁰

Ixthus Instrumentation's larger range linear capacitive displacement sensor is 30 mm in diameter and 30 mm in length.

An area variation configuration concept for a linear capacitive displacement sensor is shown in Figure 16. This air dielectric concept has the disadvantage of requiring a large envelope to accommodate its length, which has to be at least two times the stroke, and area (not including a means to maintain plate separation) needed for the number of plates to maximize capacitance.

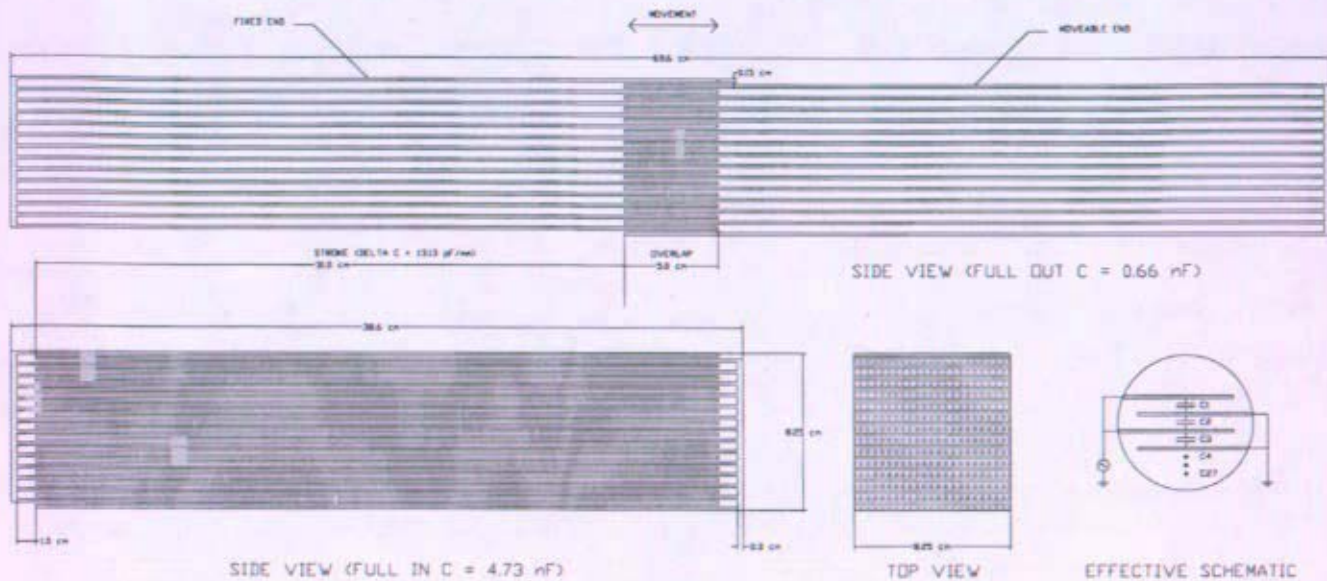


Figure 16. Parallel Plate Capacitor Concept

5.4.8. Time response

In Reference (5) ORNL indicated that response times of less than 1 ms for linear and rotary capacitive displacement sensors were achievable with an excitation frequency of several tens of kHz.⁴

5.5. Reliability

5.5.1. Failure mechanisms – moving parts

Rotary capacitive displacement position sensor life is limited by its bearings. Similarly, linear sensor life is limited by the means used to control the sensing plate spacing while allowing the plates to move freely.

Capacitive displacement position sensors can fail from electrical shorts between the sensor plates caused by triboelectric charging.

5.5.2. Failure mitigation strategies

Lubrication must be given considerable attention during the design of capacitive displacement sensors for use in environments with a vacuum, high temperature, and radiation exposure. Dry lubes such as MoS₂ are often used in vacuum environments where material outgassing can occur. Outgassing rates increase with temperature, and lubricant deterioration can increase with radiation over time. The ion implantation technique has been used to apply dry lubricants to instrument grade bearings for high precision applications.

Materials should be selected to minimize the triboelectric charge build-up when they are rubbed together.

5.5.3. Environmental effects – radiation

See failure mitigation strategies above.

Dielectric materials should be selected to be stable with respect to humidity which can be at a high level prior to launch. As most insulators expand with humidity, this can be detrimental to maintaining sensor plate spacing.

5.6. Implementation Concepts

5.6.1. Sensor mounting methods

The spiral wound capacitor linear sensor concept shown in Figure 4 can be mounted with the stator plate stationary and the slider plate attached to the component being moved.

The RDP Group rotary capacitive displacement position transducer can be mounted using clamps around its housing or with screws entering either of the housing faces (see Figure 5). Coupling to its shaft can be accomplished with a solid or bellows type coupling to another shaft or by using a gear arrangement.

5.6.2. Sensor locations

Ideally, the capacitive displacement sensor should be located in an area that minimizes the high temperature and radiation exposure while providing the best position indication of the component being moved.

5.7. Cabling

A low capacitance 3 conductor twisted shielded cable can be used for a differential capacitance sensor configuration. A concept for connecting to this type of sensor configuration is shown in Figure 7 with the three connection points identified.

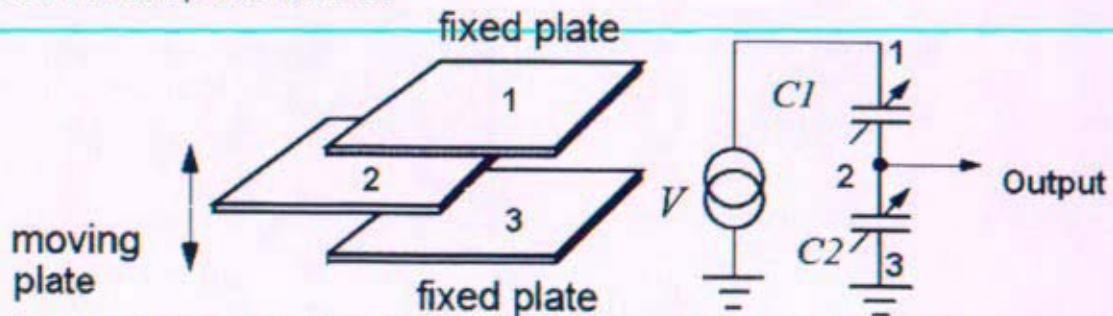


Figure 7. Differential Capacitance Sensor Connection Concept

5.8. Electronics and Algorithms

The change in AC drive signal that results from the change in the sensing element capacitance can be converted to a DC voltage with a few different circuits.

The sensing capacitance change could be used to determine the output frequency change of a free-running oscillator circuit. A frequency to voltage converter circuit can be used to convert the frequency change to a DC voltage amplitude change.

A variable DC voltage signal could also be obtained by converting the variable AC voltage signal from a variable capacitance and oscillator circuit through the use of a diode demodulator or synchronous demodulator.

The temperature sensitivity of the diode / diodes used in a diode demodulator circuit requires temperature compensation to obtain high accuracy signals. The temperature compensation can be implemented in software by applying a correction factor look-up table.

In a synchronous demodulator circuit, an electronic switch is used instead of a diode to avoid the errors associated with the change in the diode forward bias voltage which changes with temperature.

The signal conditioning circuit can be designed to output a variable DC voltage signal, so complex algorithms are not needed. However, the radiation tolerance of the signal conditioning circuit implementation would need to be investigated.

References

1. Larry K. Baxter, "Capacitive Sensors Design and Applications," The Institute of Electrical and Electronics Engineers, Inc., 1997.
2. "Motion - Transducer Presentation," McGill University Measurement Lab, March 2003.
3. <http://www.ee.polyu.edu.hk/staff/eencheun/WebSubject2/chapter1.htm>
4. "Sensor Technology Development Plan," ORNL/LTR/NR-JIMO/05-01, February 2005.
5. <http://www.ixthus.co.uk/ft-sensors.htm>
6. http://www.connectingindustry.com/news_story.asp?story_id=15498
7. Ferry N. Toth, "A design methodology for low-cost, high-performance capacitive sensors," Delft University Press, 1997.
8. David S. Nyce, "Linear Position Sensors Theory and Application," John Wiley & Sons, Inc., 2004.
9. Larry K. Baxter, "Capacitive Sensors," July 2000 (<http://www.capsense.com/capsense-wp.pdf>).
10. "Technical Manual Rotary Displacement Transducer Type RCDT," RDP Group.

This page intentionally blank

Enclosure 5

Neutron Flux Sensor Technology Evaluation

John Boyle, *KAPL-Space Electrical Systems*

Michael Corcoran, *KAPL-Space Electrical Systems*

Clint Geller, *Bettis-Advanced Material System Integration*

Harvey Mikesell, *Bettis-Space I&C Design*

Edward Pheil, *KAPL-Shielding*

Robert Vareha, *Bettis-Space I&C Design*

October 13, 2005

This page intentionally blank

Table of Contents

1.	ABSTRACT	5
2.	OVERVIEW	5
2.1.	GENERAL GOALS	5
2.1.1.	Range	5
2.1.2.	Size	5
2.1.3.	SNPP and Space Environment	5
2.1.4.	Location.....	6
2.1.5.	Duration.....	6
2.1.6.	Electronics.....	6
3.	BACKGROUND.....	6
3.1.	INTRODUCTION	6
3.2.	PROPORTIONAL COUNTERS.....	6
3.2.1.	Functional Description	6
3.2.2.	BF ₃ Proportional Counters	7
3.2.3.	³ He Proportional Counters	7
3.2.4.	The Wall Effect.....	8
3.2.5.	¹⁰ B-lined Proportional Counters.....	8
3.3.	ION CHAMBERS.....	8
3.4.	FISSION CHAMBERS.....	9
3.5.	SILICON CARBIDE NEUTRON DETECTORS.....	10
4.	RESEARCH OF NEUTRON DETECTOR TECHNOLOGIES.....	12
4.1.	INTRODUCTION	12
4.2.	FUNCTIONAL GUIDELINES	12
4.2.1.	Detector Sensitivity	12
4.2.1.1.	Approach to Criticality	12
4.2.1.2.	Power Operation.....	13
4.2.1.3.	Operational Temperature.....	13
4.2.1.4.	Vibration and Shock.....	13
4.2.1.5.	Correlation between Sensor Measurement and Reactor Flux	13
4.2.2.	Measurement Electronics Location and Survival.....	13
4.3.	STATE OF THE ART SURVEY	13
4.3.1.	Fission Chambers-Counters.....	13
4.3.1.1.	Micro fission counters	14
4.3.1.2.	ORNL ultrahigh sensitivity fission counter.....	14
4.3.1.3.	ORNL high temperature high sensitivity fission counter.....	14
4.3.2.	Ion Chambers.....	14
4.3.2.1.	Boron-10 coated ion chamber.....	14
4.3.2.2.	Boron-10 trifluoride or helium-3 ion chambers	14
4.3.3.	Self-Powered Neutron Detectors (SPNDs).....	14
4.3.4.	Self-Powered Gamma Detectors (SPGDs).....	15
4.3.5.	Silicon Carbide Detectors	15
4.3.6.	Measurement Electronics	15
4.3.7.	Cabling.....	15
4.3.8.	Suppliers.....	15
4.4.	TECHNOLOGY CANDIDATE EVALUATION.....	15
4.4.1.	Reliability	16
4.4.2.	Support Requirements (Cabling, Electronics Complexity).....	16
4.4.3.	Location Viability.....	16
4.4.4.	Range (Startup, Power Range, Mode Switchover).....	16
4.4.5.	Lifetime, Burn-up, Graceful Degradation.....	16

4.4.6.	<i>Pre-Start Orbital Temperatures and Temperature Cycles</i>	16
4.4.7.	<i>Current Level of Maturity</i>	16
4.5.	DEVELOPMENT NEEDS	17
4.5.1.	<i>Engineering and Materials Challenges</i>	17
4.5.2.	<i>Health Monitoring and Extended Capabilities</i>	17
4.5.3.	<i>Testing and Qualification</i>	17
4.6.	DEVELOPMENT PLAN	17
4.6.1.	<i>Major Requirements for Space Implementation</i>	17
4.6.2.	<i>Prototype Hardware Testing</i>	17
4.6.3.	<i>System Modeling</i>	17
4.6.3.1.	Control interface	17
4.6.3.2.	Health assessment and fault diagnostics	17
4.6.3.3.	Degradation mechanisms	18
4.6.3.4.	Production testing	18
4.6.3.5.	Manufacturing Recommendation	18
4.6.4.	<i>Backup Approaches</i>	18
5.	ARRANGEMENT OF FISSION CHAMBERS FOR NUCLEAR INSTRUMENTATION	18
5.1.	INTRODUCTION	18
5.2.	INSIDE-OF-SHIELD POSITIONING	18
5.3.	COMMERCIAL OFF THE SHELF	19
5.4.	ADDITIONAL ISSUES	19
6.	DETECTOR TECHNOLOGY EVALUATION	22
6.1.	INTRODUCTION	22
6.2.	DETECTOR EVALUATION MATRIX	23
6.3.	SOURCE, INTERMEDIATE, AND POWER RANGE OPERATIONS	24
6.4.	TEMPERATURE RANGE	24
6.5.	STATE OF THE ART (EXCLUDING HIGH-TEMPERATURE PERFORMANCE)	24
6.6.	SIGNAL STRENGTH	24
6.7.	GAMMA DISCRIMINATION	25
6.8.	DETECTOR SIZE	25
6.9.	DURABILITY / LIFE	25
6.10.	VOLTAGE PLATEAU / SATURATION REGION	25
6.11.	OPERATING VOLTAGE	25
6.12.	REQUIRED FILL GAS	25
6.13.	SPECIAL CHARACTERISTICS	26
6.14.	THERMAL NEUTRON CROSS-SECTION (DETECTOR EFFICIENCY)	26
6.15.	CONCLUSION	26
7.	EXTENDIBILITY TO A LUNAR POWER STATION	27
8.	ASSESSMENT AND TECHNOLOGY RECOMMENDATION	27
9.	REFERENCES	28

1. Abstract

The purpose of the neutron flux detector evaluation is to identify the best neutron flux sensing technology for a Space Nuclear Power Plant (SNPP) reactor application. The evaluation report begins with an overview of requirements for the neutron detector as it relates to the space reactor application. The background and research sections describe the theory of operation for the various detector candidates, and summarize the neutron detector technology development plan completed by Oak Ridge National Laboratory (ORNL). The evaluation section includes a parameter matrix weighing the detector candidates against prioritized performance criteria to establish a rank of preference for going forward. The resulting recommendation is to continue the primary focus on implementing fission chamber technology, while completing research on ion chambers and silicon carbide detectors to better determine their viability. The extendibility of this evaluation to a potential lunar power station is also discussed, and the current work in fission chamber development is described at the end of the report.

2. Overview

The space nuclear power plant may require the measurement of reactor power based upon the neutron flux. Its uses may include: shutdown verification, assembly and pre-launch confirmation, initial criticality, low power and high power physics testing, reactor startups and shutdowns, detection of abnormal conditions requiring reactor protection or power adjustments, and steady state operations and transitions at power.

2.1. General Goals

2.1.1. Range

It is desired to identify a single neutron flux detector capable of measuring reactor flux over the entire range of the reactor operation, approximately 10 decades of flux, from shutdown prior to initial criticality to full power operation. The full power (100%) thermal neutron flux is currently estimated at 1×10^9 neutrons/cm²-sec. To achieve this large dynamic range in a single detector will require that the detector operate in a pulse-counting mode at low levels and in a continuous current mode at higher levels.

2.1.2. Size

The mass and size of the detector should be as small as possible to minimize its impact on spacecraft power plant I&C system weight, as well as the reactor plant architecture, arrangement, and structure, etc.

2.1.3. SNPP and Space Environment

The SNPP will be a compact, fast reactor with a highly enriched uranium core and without moderating materials. The reactor coolant will be a He-Xe gas. There will be a shield between the reactor and remainder of the plant and spacecraft.

The neutron flux sensing system must be able to withstand the harsh conditions of the reactor plant and the space environment. The reactor plant temperatures external to the reactor coolant boundary may be near 1200 K (for refractory metal pressure vessel and piping) or 900 K (for super alloy metal pressure vessel and piping). The temperatures of the shield are contemplated to be less than 800 K. The temperature range behind the shield will be 300-500 K.

2.1.4. Location

The detector is to be located external to the core. It may be located forward, within, or behind the reactor shield.

2.1.5. Duration

The neutron flux detector should be capable of long term operation in a harsh plant and space environment without significant degradation. The deep space missions require a reactor plant capable of 15 years of operation. A neutron detector that will last the life of the plant in good operational condition is desired.

2.1.6. Electronics

The neutron flux sensor electronics are to be located in the electronics vault. This location significantly reduces the radiation from both the space environment and the reactor that the electronics must tolerate without failure. The electronics will have to meet environmental requirements of the SNPP application including shock and vibration, electromagnetic interference, and radiation exposure (currently set to 1 MRad TID).

3. Background

3.1. Introduction

In order to more fully understand the benefits and pitfalls of the leading candidate technologies, the NRPCT has reviewed various texts other than those referenced by the ORNL Sensor Technology Development Plan. The following sections serve as a summary of those texts as they relate to the candidates for SNPP neutron detectors – proportional counters, ion chambers, fission chambers, and silicon carbide detectors.

3.2. Proportional Counters

3.2.1. Functional Description

Normal operations of proportional counters, ion chambers, and fission chambers are based on the collection of charges created by ionization within a fill gas through the application of an electric field. Free neutrons from the reactor provide the incident radiation that enters the detector and ionizes the gas, and the charges collect on the electrodes of the applied electric field. The associated instrumentation measures the collected charge, typically either in the form of a set of pulses for lower neutron flux levels (i.e., source to intermediate ranges) or as a DC current for higher flux (i.e., intermediate to power ranges). The supplied voltage for the detector's electric field restores the charge on the electrodes to the original condition.

The major difference in the function of proportional counters as compared to other types is the use of *gas multiplication*. The phenomenon of gas multiplication originates with the direct ionization of the gas by the incident neutrons. Given a large enough electric field (i.e., high applied voltage) and a fill gas that willingly relinquishes electrons, the free electrons from the initial direct ionization have sufficient energy to produce an *avalanche* of additional ionization proportional to the applied bias voltage. The avalanche terminates when all free electrons have been collected at the counter anode, which is typically a fine wire suspended within a hollow cylindrical cathode. The avalanche effectively amplifies the charge represented by the original ion pairs created within the gas. This charge amplification reduces demands on external amplifiers and improves the signal-to-noise ratio of the detector output. Thus, gas multiplication enables the application of proportional counters for detecting

smaller levels of neutron flux, as seen in the source range, than ion chambers can detect. The operating point for a proportional counter is generally selected such that the count rate is invariant under constant-source conditions for variations in applied voltage, i.e. a plateau.

The proportional counter typically operates over the first five decades of flux detection, from 1 to 10^5 neutrons/cm²-sec. In the intermediate and power ranges, the pulses will occur too close together and pile up, becoming indistinguishable. Signal resolution is lost in such a state of saturation. The proportional counter cannot be operated in the power range without lowering the supplied voltage to reduce the gas multiplication, and switching the instrument from pulse mode to current mode.

Because the operation of the proportional counter strongly depends on the fill gas, the detector's performance is very sensitive to gas purity and composition. For instance, gas multiplication relies on the speedy migration of free electrons rather than low-mobility negative ions, so the fill gas must not have a strong electron attachment. Furthermore, to maintain a linear proportionality between the initial ionization and the resultant pulse amplitude (i.e., a consistent *multiplication factor M*), the proportional counter requires a stable voltage bias and a fill gas that remains pure and true to its design. A residual effect of gas multiplication is the release of photons by previously-excited gas molecules that lack enough energy to ionize. The fill gas will often include a small percentage of *quench gas*, like methane (CH₄), to absorb these photons that can trigger additional ionization and lead to loss of proportionality. The most common general-purpose proportional gas used is P-10, with 90% argon and 10% methane. However, proportional counters employed for thermal neutron detection typically use one of the following gases: BF₃, ³He, or Ar-N₂.

3.2.2. BF₃ Proportional Counters

The boron trifluoride (BF₃) proportional counter, along with the helium-3 (³He) proportional counter, uses the fill gas as both the target of the direct ionization and the proportional gas. The boron-10 reaction [¹⁰B + ¹n → ⁷Li + ⁴α] is the most popular reaction in slow neutron detection, primarily due to the abundance of enriched boron and the high Q-value (energy released in the reaction) of 2.310 MeV. High Q-value is important for discriminating against lower-energy pulses from gamma rays, thus filtering the output to reflect only the neutron radiation. The voltage supply for BF₃ proportional counters ranges from 2000 V to 3000 V; the high operating voltage can lead to spurious counts from leakage currents or vibration. Previous BF₃ counters have been temperature limited to 423 K, as gas impurities develop at higher temperatures to decrease pulse amplitude and, moreover, resolution. Also, BF₃ performs poorly as a proportional gas at higher pressure (above 1 atm).

3.2.3. ³He Proportional Counters

The ³He proportional counter employs a neutron reaction [³He + ¹n → ³H + ¹p] that carries a higher thermal neutron cross section (5330 barns) than the ¹⁰B reaction (3840 barns). The higher cross section benefits the detector's sensitivity, as the incident neutrons are more likely to react with the helium atoms. This fact, combined with the ³He counter's improved capabilities at high pressure, makes it a good choice for maximum sensitivity applications. However, the helium reaction's smaller Q-value of 0.764 MeV adds difficulty in discriminating neutron-induced pulses from gamma-induced pulses. Like the BF₃ counters, the ³He counter requires high voltage (2000-3000 V) that can cause counting inaccuracies or insulation issues. ³He proportional counters have demonstrated operating temperatures up to 523 K; high temperatures generally increase the pulse amplitude and decrease the pulse height resolution. Materials development is needed to increase the temperature capabilities of any proportional counter. The most typical cause of failure of the ³He counter is eventual gas contamination.

3.2.4. *The Wall Effect*

These detectors, BF_3 and ^3He , that depend on the fill gas for the primary neutron reaction, are subject to the detrimental *wall effect*, which prevents the full kinetic energy (Q-value) of the reaction from translating to the charge induced on the electrodes. The two products of the reaction repel in opposite directions, making it likely that one of the products will hit the detector wall. The resultant energy deposited in the gas will vary down to the energy of the product with the smallest Q-value. Specifically, the 2.3-MeV boron reaction in BF_3 counters can reduce to 0.84 MeV from the lithium product, and the 0.76-MeV helium reaction in ^3He counters can reduce to 0.19 MeV from the hydrogen product. Consequently, the smaller pulses are difficult to distinguish from low-amplitude gamma-induced pulses, and this restricts the detector's resolution. The wall effect is best counteracted by enlarging the detector diameter and thus the entire detector size, to allow the reaction products more room to deposit their energy in the gas. Raising the gas pressure also reduces the wall effect, although higher pressure requires higher voltage to maintain proportionality.

3.2.5. *^{10}B -lined Proportional Counters*

As opposed to gas-reaction detectors like BF_3 and ^3He proportional counters, the boron-lined proportional counter incorporates a ^{10}B coating inside the detector cylinder as the target of the direct ionization from the incident neutrons. Since this design does not depend on the fill gas reacting with the neutrons, a more suitable proportional gas can be selected. Noble gases, with a small percentage of quench gas, serve well as proportional gases due to their resistance to chemical degradation. 99% argon with 1% nitrogen is a common fill gas. An additional benefit of the boron-lined counter is the reduced operating voltage, typically 1500 V. The disadvantage of the ^{10}B -lined counter is the reduction of energy released per neutron interaction, a phenomenon similar to, but seemingly worse than, the wall effect in gas-reaction detectors. Since the interactions occur in the coating, only one reaction product is released per interaction. The maximum energy released will be the initial kinetic energy of an alpha (α) particle (1.47 MeV), but the actual energy will vary down to zero, depending on the location of the neutron within the coating thickness. Because of this variation in pulse energy, the ^{10}B -lined counter has less long-term counting stability than BF_3 counters. In addition, gamma-ray discrimination is inferior to BF_3 counters because the average energy released per interaction is much less.

3.3. *Ion Chambers*

Ion chambers and proportional counters can have similar construction and use similar ionization concepts for neutron detection. For instance, ion chambers typically contain a thin coating of boron on the electrodes of the neutron-detecting volume, just like ^{10}B proportional counters. The two detector types differ mostly in what range of neutron flux they are designed and operated to measure. As described in the previous section, proportional counters utilize a strong neutron-reactive target material and a high applied voltage to generate an ionization avalanche, amplifying the original ionization created by the incident radiation. Proportional counters typically operate in a *proportional region* of the voltage range, where the amplitude of the pulse output increases in direct proportion to the original ionization. This proportional-region voltage provides the energy necessary for multiplication, to output a measurable signal for even small flux levels, like those in the source range.

In contrast, the voltage applied to an ion chamber is reduced to a region of *ion saturation*, large enough to collect the full direct-ionization charge without the recombination of ions, yet smaller than the threshold for gas multiplication. The measurable output from an ion chamber is usually a direct steady-state current, produced by the drift of positive and negative ions in the electric field. Because this drift is intermittent and random at lower neutron flux, the current is too small for adequate

measurement in the source range. To compete with a proportional counter at this level, pulse output from an ion chamber is possible, but at very low amplitudes (10^{-5} V) that require complex pre-amplification and pulse processing. However, the ion chamber offers an advantage at higher flux when output pulses from a proportional counter are too close together, a condition called *pulse pile-up* that destroys the signal resolution. At these levels, corresponding to the intermediate and power ranges of flux, the ion chamber current supplies a true indication of the ions formed by the incident radiation, and at a much lower applied voltage. Even as the applied voltage must be increased at higher irradiation rates to guarantee the ion saturation, the supply typically remains below 1500 V, considerably lower than BF_3 counters. Furthermore, as long as the ion chamber's operating voltage stays within the saturation range, small voltage variations do not affect the output as they do in the proportional counter. So for the benefits inherent in each technology, proportional counters are used in pulse mode for source range detection, and ion chambers are used in current mode for intermediate and power range detection.

Unlike the pulse size deviation available in proportional counters to discriminate against gamma-induced ionization, the current output from a basic single-volume ion chamber combines neutron and gamma detection components. The neutron flux in the power range is large enough to dwarf the gamma effect on the detection output, but in the intermediate range the gamma component can be as much as or greater than the neutron component. Compensated ion chambers (CICs) resolve this problem by including an additional electrode in another gas volume, equivalent in size but without neutron-reactive target material (i.e., no boron lining), so that the ionization due to gamma radiation is equal in both volumes. The electrodes are biased to cancel out the gamma component in the resultant signal current, leaving only the measured neutron interactions.

The fact that ion chambers are usually operated in current mode allows more flexibility in the selection of fill gas. While the operation of detectors in pulse mode depends on the fast collection of electron charges at the anode, current mode lets the detector gather negative charges either as free electrons or as lower-mobility negative ions. Therefore, the fill gas can be chosen to meet other requirements, like stability over time. A denser gas like argon is often used to increase the ionization density for improved sensitivity. Helium combined with nitrogen is also employed in some ion chambers. Just like proportional counters, high-temperature materials for ion chambers would require development.

3.4. Fission Chambers

When compared to other neutron detector types, the overwhelming characteristic of the fission chamber is the high Q-value, or the energy release per neutron reaction. While the boron reaction that is popular in proportional counters and ion chambers releases a maximum energy of 2.8 MeV, each neutron-induced fission contributes 200 MeV, of which approximately 160 MeV appears as kinetic energy of the fission fragments. This large energy release results in higher-amplitude output signals, providing benefits in gamma discrimination, noise suppression, and low-flux (i.e., source-range) sensitivity.

Fission counters and fission chambers are structurally the same, the name distinction simply describing pulse output (for counters) versus current output (for chambers). The detector uses a fissile material (typically enriched ^{235}U -based) coated on the active walls of the electrodes as the target for neutron interaction. The sequence of radiation-ionization-collection is identical to that of a boron-lined detector. As the fission occurs in the wall coating, the fragments move away in opposite directions, so one of the two typically enters the gas for potential ionization. The actual kinetic energy of the fission fragment leaving the coating depends on the depth at which the reaction occurs, but the energy spectrum double-peaks at 100 MeV and 70 MeV for thin coatings. Increased deposit

thickness will increase the neutron detection efficiency, but will decrease the average energy release at the same time. The energy loss limits the practical deposit thickness to about 2-3 mg/cm². To counteract this limitation, fission chambers can be constructed with multiple active volumes, each with fissile deposits, to increase the sensitivity.

The highly-enriched ²³⁵U deposited in the fission chamber is naturally alpha and gamma radioactive, resulting in a small background ionization rate and subsequent output noise. Normally, the small size of this noise in relation to the fission-induced output enables discrimination based on amplitude in pulse mode, and can be neglected in the higher flux levels of current mode. The alpha activity limits the practical size of a detection volume to a compromise between the shorter range of the fission fragments (typically a few centimeters) and the longer range of the alpha particles. This helps to optimize the ratio of gas ionization from neutron-induced fissions to gas ionization from alphas. In contrast with light charged particles, heavy fission fragments release more of their energy to the gas near the beginning of their motion, so the available travel distance can be smaller to further reduce the alpha-triggered ionizations.

The necessary applied voltage for a fission counter or chamber typically ranges from 300 to 800 V, significantly less than for proportional counters and ion chambers. The operating voltage is set to a sufficient level - within a *plateau* region for pulse mode, or a *saturation* region for current mode - so the detector output will not fluctuate with small voltage changes. This range is also set high enough for ionization without significant recombination, yet low enough to avoid major gas multiplication.

As is the case with ion chambers, the ionization in a fission-based neutron detector is not dependent on the specific characteristics of the fill gas. Argon with nitrogen is a commonly used fill gas; argon is a stable, noble gas with dense ionization properties. High-temperature stability and contamination of the fill gas are still concerns with fission chambers as with the other gas-filled detectors. Some high-temperature fission chambers have been developed, but may require further verification or enhancement.

3.5. Silicon Carbide Neutron Detectors

Solid-state semiconductor neutron detectors represent an attractive alternative to gas-filled counters and chambers. Silicon Carbide (SiC) is the semiconductor material of choice for neutron detectors, due to this material's large *band gap* energy. The band gap is the energy difference between low-energy valence-band electrons that help define a crystal's lattice, and high-energy conduction-band electrons that are free to migrate through the crystal. A "wide" band gap in a semiconductor is large enough to provide protection to the material structure from high temperature and radiation, yet small enough to reasonably conduct electricity as a semiconductor, not an insulator. SiC's band gap (3.25 eV) is much "wider" than that of other traditional semiconductors like silicon (1.14 eV) and germanium (0.77 eV). Therefore, SiC is the better semiconductor candidate for the high-temperature, high-radiation environment of a space reactor.

The SiC neutron detector is commonly designed as a collection of a hundred or more silicon carbide diodes connected together in one or more electrical arrays within a protective housing. The sensitive elements of the detector are the SiC diodes covered with a ⁶LiF neutron-converter foil. (Note: A different foil material may be necessary to withstand the high temperature of the space reactor application.) The incident thermal neutrons ionize the lithium atoms in the foil through the ⁶Li(n,α)³H reaction. The alpha particles are blocked by a thin aluminum layer, but the tritons (³H) pass through the aluminum and the SiC diode while depositing energy and creating electron-hole pairs. Due to a voltage bias of 30 to 80 V applied across the diode, the electrons and holes collect at the electrodes,

Pre Decisional – For Planning and Discussion Purposes Only

and the charge is measured as a current pulse. One key consideration in the design of the diode semiconductor element is to limit the thickness of the active detection area to prevent the tritons from coming to rest and producing radiation damage there.

The Q-value of the ${}^6\text{Li}(n,\alpha){}^3\text{H}$ reaction in the SiC neutron detector ${}^6\text{LiF}$ foil is 4.78 MeV, which is larger than both the ${}^{10}\text{B}$ reaction Q-value and the ${}^3\text{He}$ reaction Q-value. The ${}^6\text{Li}$ reaction has a smaller cross section (940.7 barns) and subsequent lower efficiency than these other reactions, but this helps to limit displacement damage in the detector. Plus, SiC detectors can be fabricated with materials that produce lower neutron activation than traditional detectors, for less radiation exposure to personnel.

SiC detectors are of specific interest because of the ability of their semiconductor elements to operate in harsh temperature and radiation environments. This capability contrasts sharply with that of semiconductor radiation detectors based on silicon and germanium. The wide band gap of the SiC diode allows the device to develop radiation-induced signals in high temperature environments without thermally-generated noise. While Si and Ge based elements can have significant noise issues near room temperature, satisfactory operation of SiC detectors has been documented to 355K. Performance at the temperatures contemplated for the space reactor detectors, however, has not been shown. The SiC diode has been shown to be very effective in the radiation environment of reactor plants. Careful design of the sensitive elements, by shielding them from alpha particles with a thin aluminum layer and by having a thin-enough diode-depleted region such that tritons do most of their damage beyond the active region, gives a detector lifetime that can potentially be much longer than traditional detectors. An SiC neutron detector that had been previously irradiated with a fast fluence of up to $1.3 \times 10^{16} \text{ cm}^{-2}$ showed thermal neutron response characteristics indistinguishable from a non-irradiated detector.

Another major advantage of SiC neutron detectors is their significantly different response to neutron and gamma radiations. This difference allows the detector instrumentation to completely separate gamma rays and neutron-induced pulses on the basis of pulse height. This capability makes gamma compensation and lead shielding for gamma unnecessary, unlike the provisions made for gas-filled detectors.

The SiC detector offers the ability to operate over multiple ranges to cover the entire range of reactor operation from startup to full power in pulse mode. The comparatively low operating voltages, faster charge-collection times, and compact sensing element sizes compared to the gas-filled detectors, allow this form of operation. Pulse-mode operation of silicon carbide from startup to full power eliminates the need for the permissive overlap checks between the source, intermediate, and power range detectors. The nuclear instrument for the SiC detector can be designed to accommodate a single type of wide range detector with switchable sensitivity. This offers the unique ability to vary the number and type of the diode elements sensed within the detector as a function of the reactor power level, or as a function of element location over the length of the detector. The former allows the detector sensitivity to be adjusted as reactor power increases to linearize the instrument output over the reactor operating range, while the latter facilitates the measurement of the reactor axial power profile.

The performance of prototype SiC neutron detectors configured as ex-core reactor power monitors for pressurized water reactors (PWRs) has been tested under approximate PWR conditions, as described in References 4, 5, and 6. Source, intermediate, and power range prototype SiC detectors were designed to have neutron sensitivities similar to the gas-filled proportional counters and ion chambers used for these ranges. The prototypes were comprised of SiC Schottky diode arrays

equipped with ${}^6\text{LiF}$ converter layers to deliver the appropriate thermal neutron sensitivities. The test results showed highly linear proportional responses to neutron flux for each of the three ranges. Furthermore, as long as the SiC neutron detector was not exposed to a fast fluence of greater than $1.3 \times 10^{16} \text{ cm}^{-2}$, the detector exhibited stability in a voltage plateau beyond a bias voltage of about 20 V. For this reason, the detector was operated at a bias voltage of 30 V.

The main disadvantage of silicon carbide neutron detectors is its limited sensitivity at low neutron flux levels. This results from the small size of the individual diode elements and their finite capacitance. In order to achieve enough surface area for adequate sensitivity, a sufficient number of SiC diodes must be wired in parallel, which creates a capacitance issue. For example, the source-range prototype from the described test employed a total of 282 2.5-mm-diameter diodes among 10 axial locations, to reach a sensitivity of 0.3 (counts/s)/nv. When the full 282-diode array was measured in parallel, the high capacitance exceeded the capabilities of the charge-sensitive preamplifiers, leading to a degradation of the pulse height spectrum. To counteract the capacitance effect, measurements were made from one of the 10 axial locations alone to remain within the capabilities of the preamplifiers, which resulted in reduced source range sensitivity.

Despite the many apparent advantages of this detector technology, many questions remain about the SiC neutron detector's viability for the SNPP. SiC detector technology is highly developmental; significant design, manufacturing, testing, and qualification efforts remain to be accomplished before its sustained long-term performance in a power reactor application can be assured. Moreover, the SiC detectors would have to meet the high temperature, flux, fluence, range of operation, and lifetime requirements specific to the SNPP application.

4. Research of Neutron Detector Technologies

4.1. Introduction

NRPCT contracted ORNL to perform research on potential sensing technologies for measurement of reactor power and to suggest the ones with the best potential for meeting the demands of a space reactor plant. This work was to evaluate technologies and recommend a technology development plan for a detector that encompassed the full spectrum of reactor operation from shutdown (prior to initial criticality) to full power operation, that provided for a single detector type to cover the full range of operation, that could withstand the harsh conditions of the space and reactor environment, and that could last the entire mission. The results of this ORNL work were provided in Reference (1). The following is a summary of ORNL's reactor power sensor technologies evaluation.

4.2. Functional Guidelines

4.2.1. Detector Sensitivity

4.2.1.1. Approach to Criticality

U^{235} produces almost no spontaneous neutron emission. Observation of subcritical multiplication in a clean, highly enriched core without a neutron source will depend on environmental radiation from the sun and intergalactic radiation. These highly variable and generally low intensity sources for trigger neutrons make observation of startup problematic. Specific detector sensitivity varies with reactor design, with detector aspect ratio, with detector orientation to the reactor core, control element position, the reactor neutron spectra, and the moderator surrounding the detector. On these bases, a high sensitivity detector is required.

4.2.1.2. Power Operation

Neither boron-based nor uranium-based flux detectors will have significant burn-up. Assuming the reactor is not shutdown after its initial ascent to power, and operates for 15 full-power years, with a flux at the front of the shield estimated at 1×10^9 neutrons/cm²/sec, the detector low energy fluence will equal 5×10^{17} neutrons/cm².

4.2.1.3. Operational Temperature

Forward of the shield, the operational temperature may be as low as 500 K and as high as 1150 K, with the possible exception of some transient situations. Aft of the shield, temperatures should be less than 600 K.

4.2.1.4. Vibration and Shock

The detector must handle launch vibration. Most industrial detectors are currently built to standards that would meet this criterion.

4.2.1.5. Correlation between Sensor Measurement and Reactor Flux

For a fission counter detector in the Jovian radiation environment, the energetic proton and electron flux induces fission events that generate competing signals to reactor-flux-induced fissions. This effect is only marginally significant, i.e., < 5% of the total fissions, for a moderator-covered fission counter aft of the shield in the worst (Europa) environment. For flux detectors located within and behind the reactor shield, physical changes in the reactor shielding over the lifetime of the plant can impact the correlation between the measured signal and the calculated reactor power. The volumetric expansion of LiH under irradiation would be an example of this type of change. Periodic calorimetric calibrations can compensate for shielding changes of this type.

4.2.2. Measurement Electronics Location and Survival

The location of the electronics in the vault at the rear of the spacecraft will result in a cable between 30 and 50 meters from the sensing detector. A high voltage bias must be supplied to the detector at levels between 500 V (fission chambers) and 1500 V (boron ion chambers). Fission counters generate large signal pulses caused by the fission energy dissipated in the ionization of the detector gas (80 to 100 MeV), allowing the lower bias voltages. Boron chambers generate 1.5-MeV pulses and require *gas multiplication* to generate sufficient ionization and pulse size.

The fidelity of the charge pulses generated by a detector, i.e., the sharpness of their edges and their duration, is a strong function of the capacitance in the detection system and the input impedance of the electrical instrument. Cabling capacitance and instrument impedance mismatches reduce the sharpness and the peak value of the pulses. A preamplifier is commonly used to reduce this signal degradation. The cable capacitance forms a feedback circuit element that can act to destabilize and degrade the preamplifier performance (i.e., response time, noise immunity, and bandwidth) of the instrument. The closer the preamplifier is to the detector, the higher the fidelity of the pulse signals and the performance of the instrument.

4.3. State of the Art Survey

4.3.1. Fission Chambers-Counters

A conventional fission chamber, or fission counter, is an ion chamber with an interior surface that has been coated with a fissionable isotope. The principle advantage of this type of detector is the large signal produced by fission reactions as compared to competing types of ionizations. This allows

unambiguous measurement of low levels of neutron flux in relatively intense background radiation environments. Also, fission chamber technology has been studied and commercially applied for roughly 50 years. One disadvantage of the fission chamber is that its thermal neutron detection efficiency is limited to roughly 0.5% for a typical design. Another issue is that the typical fill gas, 90% Ar – 10% N₂, contains nitrogen that can form nitride compounds with some wall materials at high temperatures.

4.3.1.1. Micro fission counters

Miniature fission chambers are used in-core in light water reactors for local flux measurements. Due to their small size and consequent low efficiency they are not of interest outside of the core.

4.3.1.2. ORNL ultrahigh sensitivity fission counter

ORNL developed a prototype fission counter to provide sensitive detection for fast neutrons (> 2 MeV). The primary limitation for its use in this mission is its size – a mass of 17 kg and a neutron-sensitive surface area of 5 m².

4.3.1.3. ORNL high temperature high sensitivity fission counter

ORNL developed this fission counter with a thermal neutron sensitivity of ~10 cps/nv and the ability to measure flux from source range through power range. The detector has been shown to operate to ~800 K. Its components are fabricated from Inconel™-600 and it uses high-temperature alumina insulators. The outer shell actually houses a set of 19 fission chambers to counteract limitations in detector count rate.

4.3.2. Ion Chambers

4.3.2.1. Boron-10 coated ion chamber

Boron-10 coated ion chambers are typically employed in current mode for reactor flux measurement because the individual pulses generated from neutron interactions are hard to distinguish from gamma-induced pulses. However, pulse mode would be required for low reactor power because the low energy release of the boron ionizations will not generate measurable current. The principle advantage of a ¹⁰B-based detector is higher detector efficiency in pulse mode than for fission chambers of the same area.

4.3.2.2. Boron-10 trifluoride or helium-3 ion chambers

³He and BF₃ detectors have similar characteristics as ¹⁰B-lined ion chambers. They, too, have higher detector efficiency in pulse mode than for fission chambers of the same area. As an improvement on the boron-lined detectors, the gas multiplication that occurs within these detectors provides better pulse height resolution. One major issue with these detectors is their typical use of an additive quench gas containing hydrocarbons or fluorine, which break down in high radiation doses. The chemical reactivity of fluorine also poses a long-term corrosion concern, so the ³He detector owns this advantage over the BF₃ detector. However, activated charcoal has been used to absorb contaminants in BF₃ tubes, so carbon composite BF₃ detectors are of interest for long-term survival testing.

4.3.3. Self-Powered Neutron Detectors (SPNDs)

SPNDs generate very small output signals that are impractical for an extended transmission through a noisy environment. For example, the thermal neutron sensitivity for a vanadium-wire SPND is 5×10^{-23} amps/nv_{th}/cm, which is too low for application out-of-core, or even in-core during startup.

Pre Decisional – For Planning and Discussion Purposes Only

4.3.4. Self-Powered Gamma Detectors (SPGDs)

The physical structure, operation, strengths, and limitations of SPGDs are almost identical to those of SPNDs. As with SPNDs, the sensitivity of SPGDs is too low.

4.3.5. Silicon Carbide Detectors

Silicon carbide-based neutron detectors are just emerging from the experimental stage. They show potential for very high-speed pulse detection. They have demonstrated operation at ~625 K and fast fluence of 10^{17} neutrons/cm². Their principle disadvantage is their lack of sensitivity due to size limitation, which is related primarily to diode capacitance. A large number of neutron-converter diodes would be required to boost the sensitivity to an adequate level, and the accumulation of capacitance from these diodes hinders the output signal. A lumped-element transmission-line configuration for these detectors has not been demonstrated on a useful scale. In addition, the small amplitude and duration of the neutron-induced pulses would require a preamplifier close to the detector.

4.3.6. Measurement Electronics

In general, the measurement electronics technologies are well-known and should not limit the reactor power measurement. However, the SNPP application will require development of custom electronics that are qualified for space.

To monitor the entire flux range from source to power, two signal processing candidates are considered: a one-time switchover from pulse mode to current mode, or a single-mode wide-range amplifier channel.

4.3.7. Cabling

For temperatures less than 1000 K, mineral-insulated, metal-sheathed cable is commercially available. The main cabling concerns include flexibility, joints, and insulation in the high-temperature area, as well as impedance matching. Temperatures above 1000 K may require precious-metal sheathing and conductors, and high-purity packed-powder alumina insulation.

4.3.8. Suppliers

GE Reuter-Stokes, IST Sensing, and Thermo Electron have all indicated an interest in partnering with ORNL to develop higher temperature fission chambers. GE Reuter-Stokes and IST also supply low-temperature ion chambers.

4.4. Technology Candidate Evaluation

As described in the previous sections, fission chambers, ¹⁰B-lined ion chambers, and ³He detectors without hydrogenous or fluorine-based quench gases are potential candidates for reactor flux monitoring. In the fore-of-shield location, a fission counter is recommended, and a ³He-Ar detector is the second choice. Due to their larger pulse sizes, fission counters are preferred for pulse mode long-cable applications like SNPP reactor startup. In the aft-of-shield location, it may be possible to use a commercially-available, high-temperature, high-sensitivity fission chamber encased in a neutron moderator. The second choice for aft-of-shield deployment is to replicate the fore-of-shield fission counter. Ion chambers are not strong candidates for aft-of-shield deployment due to the large amount of background counts from the Jovian environment.

Fore-of-shield detectors have advantages over aft-of-shield detectors: larger ambient flux for source-range measurement and independence from shield variance. However, the milder temperature and radiation aft-of-shield environment may accommodate commercial detectors for power-range

measurement. A detector design for the high temperature fore-of-shield area requires in-depth study of materials candidates.

4.4.1. Reliability

Detector properties and design attributes that raise reliability concerns include contamination, carbon-based structure unknowns, joint stresses, current ground loops, and high voltage stresses. Fission chambers (~500 V) use lower operating voltage than ion chambers (~1500 V) use.

4.4.2. Support Requirements (Cabling, Electronics Complexity)

A fission chamber requires a power supply of ~500 V capable of sourcing up to 25-mA current. Transmission line fission counters require one signal line for each end; one line also provides the bias voltage. A common signal ground is also required. All of the detector conductors need to be housed within a shield ground. The cable characteristic impedance needs to be matched to those of the detector and, if applicable, the preamplifier. Standard nuclear instrumentation pulse processing electronics are recommended.

4.4.3. Location Viability

MCNP simulations indicate that small changes in the sensor locations do not significantly impact the sensor selection or design variables. Backing the detector away from the reactor greatly increases the sensitivity required for startup monitoring. Placing a detector within the shield would lower the temperature but may significantly complicate the shield fabrication.

4.4.4. Range (Startup, Power Range, Mode Switchover)

The detection system is required to function over roughly ten orders of magnitude in neutron flux. A full-range detector would require a signal processing switch from pulse mode to current mode as the reactor power increases. Assuming no reactor restarts, only one mode switch would be required. An alternative system would include a fore-of-shield detector working in tandem with an aft-of-shield detector to cover the entire flux range. An aft-of-shield detector would not likely operate at low reactor power, so it could remain in pulse mode and not require a mode switch. Also, an aft-of-shield detector would likely activate before its complementary fore-of-shield detector would be required to switch to current mode.

4.4.5. Lifetime, Burn-up, Graceful Degradation

The flux level in either location should not cause a significant burn-up in the neutron detectors. The detectors should function throughout the mission.

4.4.6. Pre-Start Orbital Temperatures and Temperature Cycles

Pre-start orbital temperatures and temperature cycles should not overly stress fission chambers. However, system qualification should include low-temperature thermal cycling.

4.4.7. Current Level of Maturity

Very high temperature (i.e., fore-of-shield) neutron detectors are at a low technological maturity level. Significant development activity is required before either carbon or precious metal fission counters will be capable of space deployment. Moderate sensitivity and temperature aft-of-shield sensors are available commercially.

4.5. Development Needs

4.5.1. Engineering and Materials Challenges

Development of a carbon-based prototype fission chamber is required to confirm the validity of using carbon composite materials. The alternative precious-metal material must be evaluated for coating with uranium oxide and sealing against sapphire at high temperatures. Many uncertainties must be resolved.

4.5.2. Health Monitoring and Extended Capabilities

Bias current is typically a good indication of the health of the device. Often, simply lowering the bias voltage of a poorly functioning device will extend its lifetime.

4.5.3. Testing and Qualification

Materials, components, and prototype testing are required. Apart from electrical characterization electronics, a vacuum furnace, a shaker table, and a neutron source are the principle test devices.

4.6. Development Plan

4.6.1. Major Requirements for Space Implementation

The prime development attributes required for the SNPP neutron detector include: durability in high temperature, endurance through the mission's life, and sensitivity for monitoring reactor startup. Reliability for extended time at high temperature will be evaluated, although the development period is too short for full time-at-temperature testing.

4.6.2. Prototype Hardware Testing

Developed detectors and their instrumentation will be tested in prototypic pre-launch and active reactor environments. The equipment will be evaluated in response to temperature, radiation, vacuum, vibration, electromagnetic interference, and proximity to structural materials like refractory alloys. Initial device environmental testing should be performed in a vacuum furnace with a small neutron dose and with either natural or depleted uranium coating, to reduce the radioactivity and hence the cost. If the initial phase of environmental testing proves successful, higher flux testing will be required to provide more prototypic stress on the fission chambers.

4.6.3. System Modeling

4.6.3.1. Control interface

The control system will need to record and correlate measurements from several detectors simultaneously, assess the health of the sensors, reduce the bias voltage of degrading sensors while changing the sensor response function, and provide an indication of the reactor power to the reactor control logic.

4.6.3.2. Health assessment and fault diagnostics

Bias current is a useful indication of the health of the device. If required, alternate methods of calculating reactor power from temperatures and flow can be used as periodic reference measurements to gauge the performance of the neutron detectors and to provide for possible recalibration. Redundant devices should be used as references to monitor sensor degradation and to provide graceful degradation in the event of a detector failure. Control logic algorithms can provide fault detection and diagnostics.

4.6.3.3. Degradation mechanisms

Failure mechanisms for high-temperature fission chambers can include: loss of electrical isolation between anode and cathode, fill gas leaking, anode corrosion, uranium layer flaking, mechanical joint failure, and support electronics failure.

4.6.3.4. Production testing

Individual components of the detector system should be environmentally tested to uncover deficiencies in material or process quality. Overall system evaluation should include end-to-end performance demonstration, electromagnetic compatibility testing, vibration testing, and full-channel validation.

4.6.3.5. Manufacturing Recommendation

GE Reuter-Stokes, IST Sensing, and Thermo Electron all have extensive backgrounds in reactor instrumentation. Any of the three would be a reasonable vendor choice.

4.6.4. Backup Approaches

ORNL's recommended approach is to aggressively pursue the carbon-based fission chamber technology development while maintaining a parallel development effort on a precious-metal-based fission chamber. In-shield lower-temperature fission chambers provide a viable alternative. Another strategy is to combine sacrificial high-efficiency detectors near the reactor core for startup monitoring and aft-of-shield fission chambers for higher reactor power measurement.

5. Arrangement of Fission Chambers for Nuclear Instrumentation

5.1. Introduction

Fission chambers are envisioned to be placed in three general locations: Fore-of-shield (FOS), Inside-of-shield (IOS), and Aft-of-shield (AOS). Placement of the fission chambers has been investigated FOS and IOS. In the FOS region, the desired location for these instruments is within the fixed radial reflector as shown above. In the IOS region, the desired location for these instruments is around the centerline region of the shield, within the CDM penetrations.

5.2. Inside-of-Shield Positioning

As shown above, there are three notional orientations for the IOS fission chambers. In IOS (A), the long edge of the fission chambers is directed radially outward from the centerline of the shield. This orientation provides a very intuitive means for the wire harness to exit the shield, and provides a symmetrical setup for each of the four fission chambers. In IOS (B), the fission chambers are located much like they are FOS. This orientation is also symmetrical and does not remove any of the center region of the shield. Since the detectors are towards the outside of the shield, there will be less neutron flux, which might increase the sensitivity requirements for the IOS fission chambers. With this setup, however, it may be more difficult to route the connected wiring. Finally, in the IOS (C) setup, four detectors are placed side by side in the center of the shield. This orientation is not symmetric and uses some of the shield in the center region. For these reasons, this is not the ideal orientation for the IOS fission chambers.

5.3. Commercial off the Shelf

One major challenge is positioning the fission chamber in a region where a commercial off the shelf fission chamber can operate in the ambient temperature. Both Centronic and Photonis produce high temperature instruments. The FC538 by Centronic is capable of operating in an environment of 823 K, while Photonis produces both the CFUC06 and CFUE32 which are capable of operating to 873 K.

Leading High Temperature Commercial off the Shelf Fission Chamber Specifications					
	Maximum Temperature	Neutron Flux Range	Fluence Exposure Limit (Thermal)	Diameter	Length
<i>Photonis CFUC06</i>	873 K	Pulse 1 to 10^5 n.cm ⁻² .s ⁻¹	2×10^{19} n.cm ⁻²	4.8 cm	37.2 cm
<i>Photonis CFUE32</i>	873 K	Pulse, Fluctuation, Current 10^3 to 10^8 n.cm ⁻² .s ⁻¹ 10^7 to 3×10^{12} n.cm ⁻² .s ⁻¹ 10^9 to 10^{13} n.cm ⁻² .s ⁻¹	2×10^{19} n.cm ⁻²	0.7 cm	15 cm
<i>Centronic FC538</i>	823 K	Pulse 20 to 2×10^5 n.cm ⁻² .s ⁻¹ 5.6 to 5.6×10^5 n.cm ⁻² .s ⁻¹	Unknown	4.75 cm	55.1 cm

There is no one fission chamber which satisfies the high temperature requirements, flux range capabilities, and fluence exposure limits. At this point it is unclear if any of commercial off the shelf fission chamber would be able to endure the fluence exposure in the fixed radial reflector.

Temperature and Neutron Flux Environment of Fission Chamber Locations			
	Temperature	Neutron Flux	Fluence Exposure *
<i>Fixed Radial Reflector</i>	850 K	1.16×10^{11} n.cm ⁻² .s ⁻¹	4.4×10^{19} n.cm ⁻²
<i>Fore Shield – Centerline</i>	405 K	1.00×10^{11} n.cm ⁻² .s ⁻¹	3.8×10^{19} n.cm ⁻²
<i>Fore Shield – Outside Radius</i>	405 K	4.75×10^{10} n.cm ⁻² .s ⁻¹	1.8×10^{19} n.cm ⁻²
<i>Aft of Shield</i>	400 K	9.50×10^6 n.cm ⁻² .s ⁻¹	3.6×10^{15} n.cm ⁻²

* based on a 12 year mission

5.4. Additional Issues

One of the issues with placing the fission chambers FOS and IOS is that shielding is removed to accommodate the detectors. This may or may not be an issue, as the fission chambers are absorbing neutrons. If additional shielding is necessary, it must be added such that it avoids both the CDM shaft penetrations and the coolant piping. In the same regard, the wiring harnesses connected to the detectors must also avoid the CDM shaft penetrations and coolant piping.

Figure 1: General Arrangement of FOS and IOS Neutron Detectors

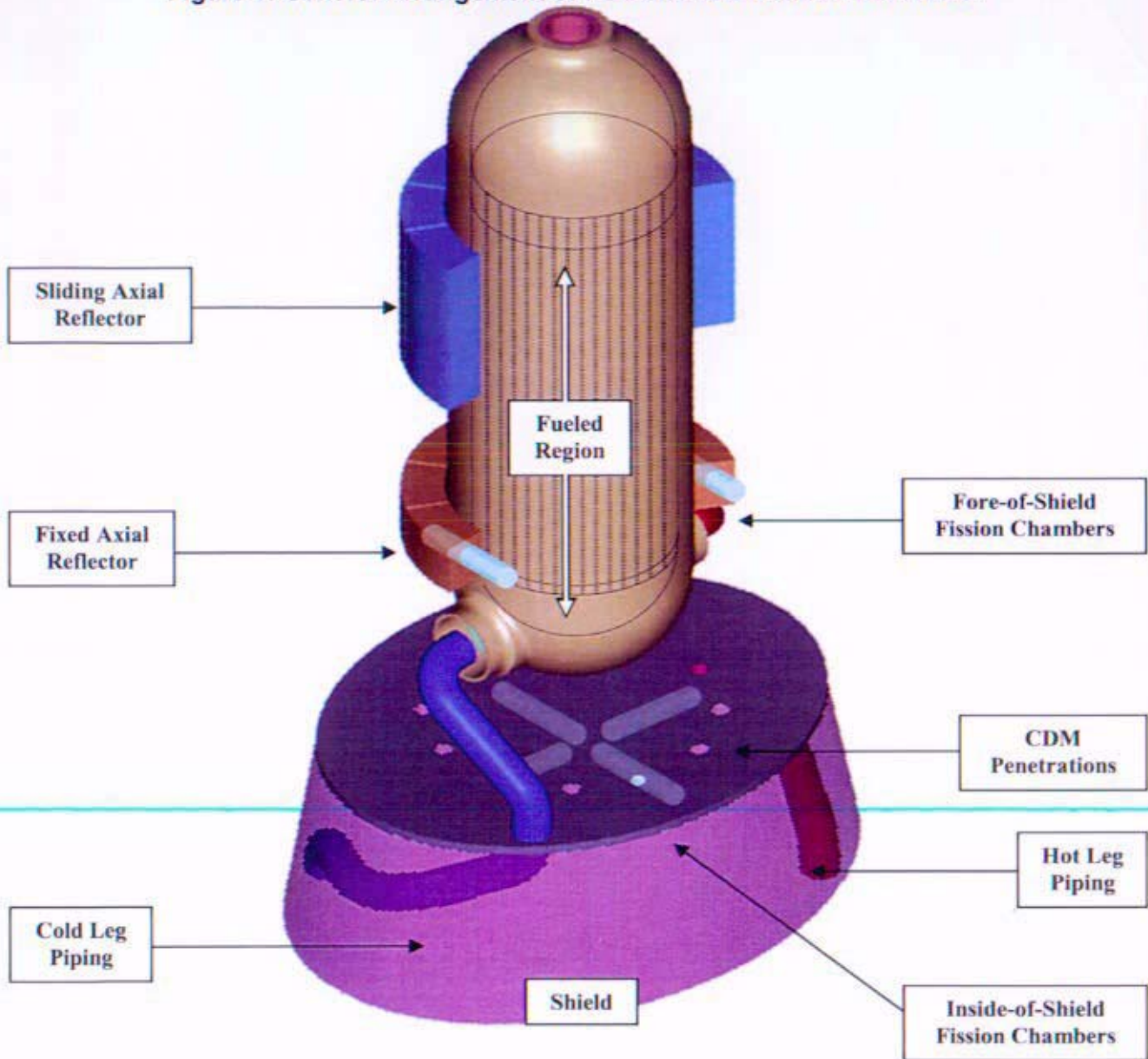
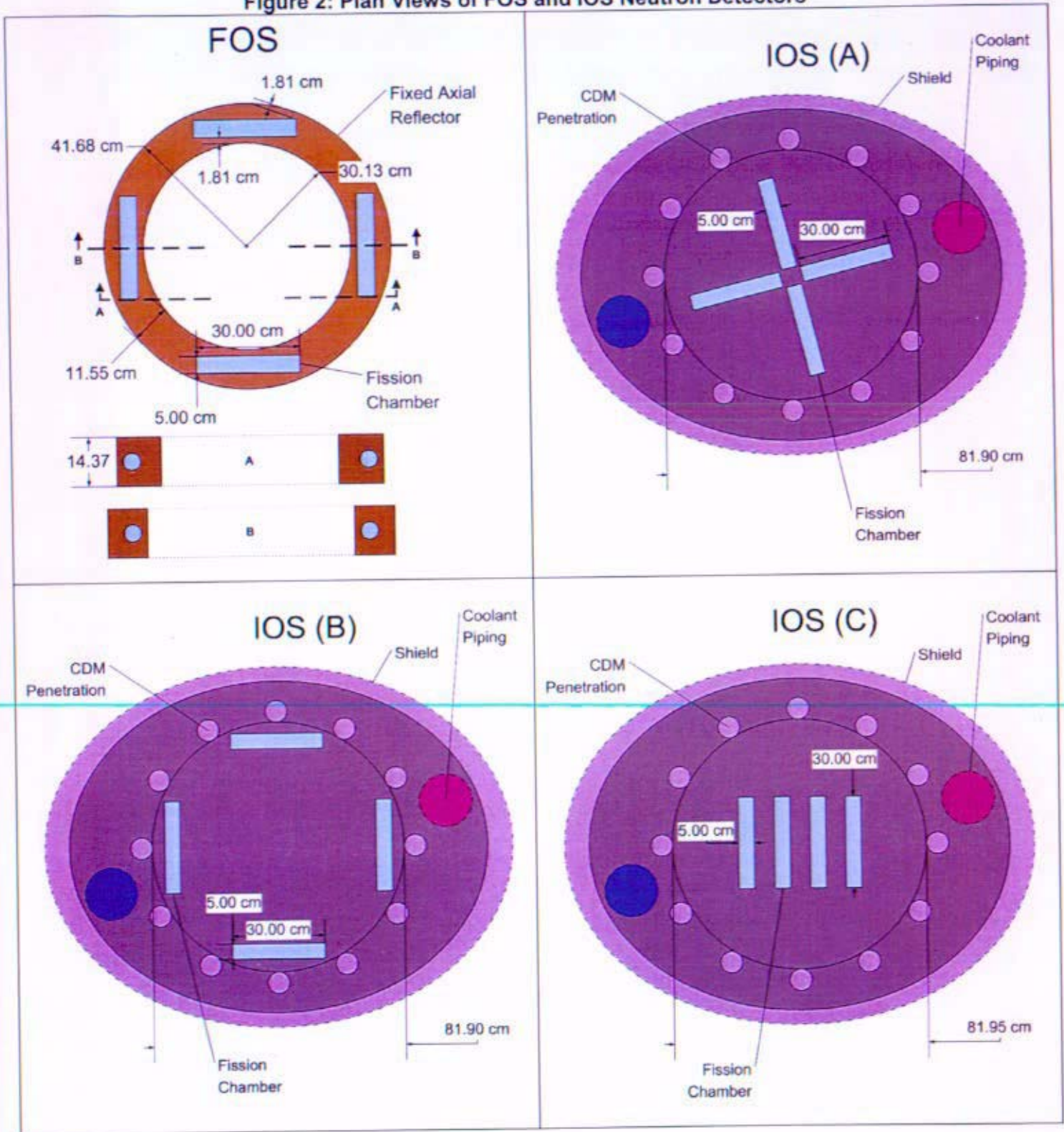


Figure 2: Plan Views of FOS and IOS Neutron Detectors



6. Detector Technology Evaluation

6.1. Introduction

The information gathered in the ORNL Sensor Technology Development Plan and from the background material described above is compiled in the following Evaluation Matrix. This chart rates the types of neutron flux detectors against the evaluation criteria, also providing the support information found in the research. The "Design Parameters" listed in the left column depict the major characteristics that distinguish between the candidate detectors and their applicability to the SNPP. Each "Design Parameter" is weighted by importance (10 = highest importance), and the weight factor is multiplied by the rating (0 through 5, 5 = highest rating) for each detector type. The weighted scores are summed to award each detector type a total score, listed along with its percentage of the full score possible. Some descriptions of the "Design Parameters", along with justification for their assigned weights, are offered in the sections following the matrix.

6.2. Detector Evaluation Matrix

Design Parameter	Weight (1-10)	BF ₃ Proportional Counter	Rating (0-5)	Weighted Score	¹⁰ He Proportional Counter	Rating (0-5)	Weighted Score	¹⁰ B-lined Proportional Counter	Rating (0-5)	Weighted Score	Normal ¹⁰ B-lined Ion Chamber	Rating (0-5)
Source Range Operation	10	Pulse mode operation, i.e., counts each neutron reaction. Operates over 5 decades.	5	50	Pulse mode operation, i.e., counts each neutron reaction. Operates over 5 decades.	5	50	Pulse mode operation, i.e., counts each neutron reaction. Operates over 5 decades.	5	50	Detector operates in either Mean Square Voltage or current mode. Source range signal levels in either mode too small for measurement.	0
Intermediate Range Operation	10	With pulse mode operation, the proportional counter instrument output saturates.	0	0	With pulse mode operation, the proportional counter instrument output saturates.	0	0	With pulse mode operation, the proportional counter instrument output saturates.	0	0	Detector operates in MSV mode. Current varies over approximately 5 decades. Gamma compensation is necessary.	4
Power Range Operation	10	With pulse mode operation, the proportional counter instrument output saturates.	0	0	With pulse mode operation, the proportional counter instrument output saturates.	0	0	With pulse mode operation, the proportional counter instrument output saturates.	0	0	Detector operates in DC current mode. Linear operation over approximately 2 decades.	5
Temperature Range	10	Previous counters limited to 423 K.	2	20	Previous operation demonstrated to 523 K.	3	30	Typical temperature range for COTS detectors 223 K to 373 K.	2	20	Typical temperature range for COTS detectors 223 K to 373 K.	2
State of the Art (excluding high temperature performance)	9	Technology well understood.	5	45	Technology well understood.	5	45	Technology well understood.	5	45	Technology well understood.	5
Signal Strength	8	Boron Q-value ~ 2.3 MeV, higher than helium. Gas multiplication amplifies the signal.	4	32	Low Q-value (0.764 MeV), but gas multiplication increases the signal.	3	24	Boron Q-value ~ 2.3 MeV, but neutron interactions occur in the wall coating, so energy release will vary from 0-1.47 MeV.	3	24	Neutron interactions occur in the wall coating, so energy release will vary from 0-1.47 MeV. Good levels for typical current-mode application.	4
Gamma Discrimination	7	High Q-value and gas multiplication strongly benefit the neutron vs gamma amplitude ratio.	4	28	Low Q-value (0.764 MeV) hinders gamma filtering.	2	14	Inferior to BF ₃ counters because average energy released per interaction is much less.	3	21	Compensated Ion Chambers (CICs) cancel out the gamma component.	5
Detector Size	7	Larger diameter required to reduce the wall effect, increase average ionization, improve resolution.	1	7	Larger diameter required to reduce the wall effect, increase average ionization, improve resolution.	1	7	Comparable to or smaller than gas-target counters (no wall effect).	2	14	Diameter typically smaller than proportional counters.	3
Durability / Life	7	Gas purity is the key; contamination may limit detector life. Fluorine may corrode detector structures. Charcoal can remove gas poisons and extend life.	1	7	Typical cause of failure is elemental gas contamination. Charcoal can remove gas poisons and extend life.	3	21	Due to variation in pulse energy, less long-term counting stability than BF ₃ counters. But fill gas can be more stable.	2	14	Fill gas can be chosen for long-term stability.	3
Voltage Plateau / Saturation Region	7	Detector operation in proportional region. Plateau sensitivity (count rate/unit voltage at constant flux) near constant.	4	28	Detector operation in proportional region. Plateau sensitivity (count rate/unit voltage at constant flux) near constant.	4	28	Detector operation in proportional region. Plateau sensitivity varies slightly with voltage from wall effect.	2	14	Detector operation in ion saturation region. Plateau sensitivity near constant.	4
Operating Voltage	8	Typical bias voltage 2000-3000 V. High voltage across insulating elements in detector and cable increase susceptibility to noise.	2	12	Typical bias voltage 2000-3000 V. High voltage across insulating elements in detector and cable increases susceptibility to noise.	2	12	Typical bias voltage ~1500 V. Moderate noise susceptibility.	3	18	Typical bias voltage ~1500 V. Moderate noise susceptibility.	3
Required Fill Gas	5	BF ₃ rectified - good for gas multiplication, but not chemically inert (fluorine is corrosive), some nonlinearity as a proportional gas. Quench gas life concern.	1	5	Helium is required. Helium is a stable, noble gas. Quench gas life concern.	3	15	Good proportional gas can be selected. Helium and Argon are common choices (inert gases, non-reactive). Quench gas life concern.	4	20	Good, stable, proportional gas can be selected. Argon is common choice (inert). Quench gas life concern.	4
Special Characteristics	6	Higher pressure gas reduces wall effect, but requires higher voltage, and hinders proportionality.	2	10	Higher pressure gas reduces wall effect, but requires higher voltage, and hinders proportionality.	2	10	Boron-coated detectors are well-established.	3	15	Boron-coated detectors are well-established.	3
Thermal Neutron Cross-Section (Detector Efficiency)	4	Good cross section (3840 barns).	4	16	Very high cross section (5330 barns).	5	20	Good cross section (3840 barns).	4	16	Good cross section (3840 barns).	4
Total Scores				280			278			271		
Possible Score	106			526			525			525		
% of Full Score				50%			53%			52%		

Weighted Score	Full Range ⁶³ Blind Ion Chamber	Rating (0-5)	Weighted Score	SiC Diode Detector	Rating (0-5)	Weighted Score	Fission Counter / Chamber	Rating (0-5)	Weighted Score
0	Pulse mode operation with detector biased as proportional counter. Operates over 5 decades.	4	40	Pulse mode operation. Highly linear proportional response to neutron flux. (0.3 counts/s/nv)	4	40	Detector operates in pulse mode without gas multiplication. High reaction energy generates large number of ionization pairs for large single pulse amplitudes	5	50
40	Detector operates in MSV mode. Current varies over approximately 5 decades. Gamma compensation is necessary.	4	40	Pulse mode operation. Highly linear proportional response to neutron flux. (2 x 10 ⁴ counts/s/nv)	4	40	Detector operates in MSV mode. Approximately 5 decades of operation. Neutron induced pulses result in much greater charge than gamma allowing gamma compensation.	5	50
50	Detector operates in DC current mode. Linear operation over approximately 2 decades.	5	50	Pulse mode operation. Highly linear proportional response to neutron flux. (1 x 10 ⁴ counts/s/nv)	4	40	Detector operates in DC current mode. Linear operation over approximately 2 decades.	4	40
20	Typical temperature range for COTS detectors 223 K to 373 K	2	20	Operation to 355 K demonstrated.	2	20	Operation to 800 K demonstrated.	4	40
45	Detector technology well understood, but integration of proportional and ion chamber performance into one is required.	3	27	Significant research and development required.	2	18	Technology well understood.	5	45
32	Good levels for typical current-mode application. Potential gas multiplication would amplify low-flux signals.	4	32	Lithium Q-value of 4.78 MeV, higher than both boron and helium, but no gas multiplication.	3	24	High Q-value (200 MeV) dwarfs other detectors. However, dense ionization in fission material introduces non-linearity in amplitude, reduces the signal.	5	40
35	Compensated Ion Chambers (CICs) cancel out the gamma component.	5	35	Gamma ray and neutron induced pulses are separable on the basis of pulse height.	4	28	High Q-value (200 MeV) offers high pulse amplitude, so gamma is negligible.	4	28
21	Diameter typically smaller than proportional counters.	3	21	Each detector, consisting of 8 to 30 diodes, consumes ~ 1.5 cm ² . (Note that 8 to 10 detectors are used for each range configuration.)	5	35	Size of detection volume is limited by alpha range and fission material thickness. Can be enlarged through multiple detection volumes, for increased sensitivity.	3	21
21	Fill gas can be chosen for long-term stability. Counting stability may be an issue with varying voltage.	3	21	Degradation of active region prevented by shielding alpha particles, and allowing tritons to do most of their damage beyond the active region. No fill gas concerns.	4	28	Fill gas can be chosen for long-term stability. Good counting stability.	4	28
28	Detector operation in ion saturation region. Plateau sensitivity near constant.	4	28	Solid state diode detector operated in reverse bias mode forming depletion layer whose thickness varies with bias voltage. Count sensitivity constant with voltage.	5	35	Detector operated in ion saturation region. Plateau sensitivity constant.	5	35
18	Multi-range high voltage bias supply required. In proportional operation, typical bias voltage ~2000-3000 V. In ion saturation operation, typical bias voltage ~1500 V.	1	6	Typical bias voltage 20 - 80 V. Noise susceptibility TBD.	5	30	Typical bias voltage ~500 V. Low noise susceptibility.	4	24
20	Good, stable, proportional gas can be selected. Argon is common choice (inert). Quench gas life concern.	4	20	No fill gas is required.	5	25	Good proportional gas can be selected. Argon is common choice (inert). Quench gas life concern.	4	20
15	Boron-coated detectors are well-established. May require more complex, massive voltage supply.	3	15	Pulse mode operation from startup to full power prevents overlap or permissive traps. Power gradients can be obtained because each axial location is independently addressable.	3	15	Full-range detection is available without significant modifications.	4	20
16	Good cross section (3840 barns)	4	16	Moderate cross section (941 barns)	3	12	Moderate cross section (200-2000 barns within the thermal neutron range)	3	12
381			371			380			453
525			525			525			525
69%			71%			74%			89%

6.3. Source, Intermediate, and Power Range Operations

The first three parameters in the evaluation matrix – source, intermediate, and power range operations – are distinguishing features between the detector types. As a whole, however, they represent the entire charter of the neutron detector within the SNPP system. The ability of the neutron detector to measure the low neutron flux escaping from the reactor before initial criticality is of paramount importance to the Prometheus project. Other methods of gauging reactor activity (i.e., temperature) at this early stage would seemingly be unable to deliver the necessary resolution. The sensor used to control the fast-fission reactor through the delicate startup process must be sensitive to small flux changes within the source and intermediate ranges, and provide a corresponding, discernible output.

While source and intermediate range operations are crucial for reactor startup, the detector's capability in the power range is important as well, although other control parameters (i.e., temperature and flow) should be available near full power. One major challenge of developing a full-flux-range neutron detector lies in the need to provide output signals, at both low and high flux, with adequate resolution to capture the desired step change in reactor power. Current mode is the traditional signal process applied during power range operation because pulse pile-up at high counting rates severely damages the resolution of pulse output. Available ion chambers and fission chambers will provide current mode sensitivity, while proportional counters will not. However, further study may uncover possibilities for a "hybrid" chamber that can provide the necessary sensitivity in both pulse and current modes, perhaps by modifying the detector's operating parameters (i.e., voltage).

6.4. Temperature Range

The temperature range in which the neutron detectors are expected to operate is rated equal in importance to their performance in operation as a sensor technology driver. The high temperature of the fast fission reactor at full power results in structural temperatures in the reactor reflector and radiation shield of approximately 1000K and 800K. Alternately, these structures are expected to be near 250K during startup. The neutron detectors located near or within these structures must be capable of withstanding these environmental temperatures.

All of the detector types included in this evaluation require some development to find optimum materials and fill gases for this high-temperature application. ORNL has described some work already begun in these areas for fission chamber technology.

6.5. State of the Art (excluding high-temperature performance)

The amount of potential development needed to implement a particular detection technology for the SNPP application is a major factor in the evaluation. Previous knowledge and operating history of a candidate device provides valuable confidence in the probability of its success. Developing new ideas may result in a better solution, but requires investments of time and money. The development of high-temperature capabilities for these candidates is omitted from this parameter, as it stands alone as a separate critical item.

6.6. Signal Strength

The amplitude of the output signal is critical to the Prometheus project, in the desire to avoid placing preamplifier electronics near the neutron detector. However, the need for a strong output signal does not outweigh the fundamental requirement for detector sensitivity throughout the flux range. The Q-value (energy release) of the initial nuclear reaction that defines each candidate detector largely contributes to the signal it generates.

6.7. Gamma Discrimination

Proper control information from the neutron detector requires that the conditioned output signal reflect the charge accumulated from only neutron interactions within the detector. Therefore, other interactions, primarily gamma-induced (plus some natural alpha radioactivity in fission chambers), must either be separable from the desired signal or negligible in amplitude comparison. Gamma discrimination represents a major facet of maintaining signal resolution through the entire detection range.

6.8. Detector Size

Component mass and dimensions are to be minimized if possible for the SNPP, to ease launch and deployment. Signal strength is considered a more important parameter because it prevents the addition of preamplifier electronics and corresponding shielding, which would probably add considerably more mass than any practical size increase in the detector.

6.9. Durability / Life

The neutron flux detector should be capable of long term operation in a harsh plant and space environment without significant degradation. The deep space missions require a reactor plant capable of 15 years of operation. A neutron detector that will last the life of the plant in good operational condition is desired. Some typical failure mechanisms of neutron detectors include corrosion of the electrodes and breakdown / contamination of the fill gas. A moderate amount of these conditions may alter the response of a detector without full failure, but the sensor must maintain a discernible sensitivity, perhaps through the aid of some automated recalibration procedure, to be considered effective.

6.10. Voltage Plateau / Saturation Region

A "flat" response to voltage fluctuation within the operating region is a significant asset to a neutron detector for preventing signal discrepancies or degradation. This operating region is called a *plateau* for pulse-mode operation and *saturation* for current-mode operation, and it represents the voltage range in which the detector sensitivity stays constant for a given flux. If the detector is functioning within a wide and level plateau region, the probability for long-term stable output increases.

The previous four design parameters – gamma discrimination, detector size, durability/life, and voltage plateau/saturation region - are all considered relatively equal in importance and thus are given equal rating. In essence they represent the middle tier of evaluation criteria, in between the top absolute priorities and the bottom less-crucial characteristics.

6.11. Operating Voltage

Lower requirements for operating voltage benefit the overall plant with respect to cabling and insulation specifications. Supplying higher voltage to the neutron detectors heightens the concern for leakage current and overall physical deterioration of the sensor. However, the overall power draw is hardly affected, as the resultant current is very small.

6.12. Required Fill Gas

All of the detector types in this evaluation matrix contain a fill gas for ionization and consequent charge collection. Depending on the reactivity and the purity of the fill gas, as well as the specific requirements for an included quench gas, the long-term viability of these gaseous detectors is a concern that will be mitigated through testing.

6.13. Special Characteristics

This design parameter is included to describe some advantage or disadvantage specific to each neutron detector type.

6.14. Thermal Neutron Cross-Section (Detector Efficiency)

The thermal neutron cross-section of the resident target material in the detector represents the likelihood that an incident neutron will react with the material and, therefore, be counted. This design trait characterizes the sensor's natural ability to detect neutrons, and it affects many of the other parameters that have already been mentioned. In order to prevent multiplying its effect on the overall evaluation, it is given a lower weight. Other conditions, such as the operating voltage and the quantity of target material, contribute to the neutron detector's efficiency.

6.15. Conclusion

As illustrated in the results listed at the bottom of the evaluation matrix, the fission chamber rates the highest of all detector types against the desired criteria, receiving 86% of a full possible score. The silicon carbide detector rates second with 74%, while a proposed full-range ^{10}B -lined ion chamber rates a close third with 71%.

The ratings given to the silicon carbide detector are based on test data and development information, not on application history like the other candidates. Therefore, further investigation and development are required to verify the potential for applying this technology to the SNPP.

The fission chamber possesses some major advantages over the traditional ion chamber:

- The fission chamber releases roughly 70-100 MeV of energy per neutron reaction to the fill gas, triggering ample ionization for high-amplitude pulse output at low flux levels. The ion chamber releases roughly 1.5 MeV of energy per neutron reaction to the fill gas, and does not utilize gas multiplication for signal strength like a proportional counter does. Therefore, the ion chamber is not well suited for source-range pulse-mode measurement, while the fission chamber is capable of monitoring flux from source range to power range.
- The voltage saturation region of the fission chamber is very flat over a wide range, providing long-term counting stability. The response to voltage changes is not as flat in the ion chamber's saturation region, which is also not as wide a voltage range.
- The voltage bias required by the fission chamber (~500 V) is much smaller than any alternative, including the ion chamber (~1500 V). This promotes longer life of components and more stable sensor operation over time.

The proportional counters evaluated in the matrix fall far behind the fission chamber and the ion chamber, simply because their traditional design lacks the ability to provide an output with discernible resolution at higher flux levels. Once the pulse count of a proportional counter reaches a high rate, the pulses occur too close together to distinguish between them and measure the corresponding rate of neutron incidence. Furthermore, the gas multiplication inherent in the counter increases the pulse amplitude, so the pulse overlap causes the amplitudes to severely pile up, along with gamma-induced pulses which increase at high flux levels. The recognizable relationship between the neutron radiation input and the pulse signal output is lost.

One thought that has been generated in the midst of this evaluation is the idea of a "hybrid" ion chamber, capable of supporting full-range flux monitoring. This option is included in the evaluation matrix as a "Full Range ^{10}B -lined Ion Chamber." Such a detector would require sufficient gas

multiplication for measurable pulse output in the source range, yet be able to reduce that multiplication factor for current-mode use in the power range. The practical method for controlling the ion multiplication would be an adjustable voltage bias – high voltage for pulse mode, lower voltage for current mode. Another control possibility might include reducing the gas pressure at higher flux. Beyond the question of an effective output signal lies other issues with proportional counters, mostly degradation and corrosion issues with fill gases (BF₃ especially.) These may be avoided by pursuing a ¹⁰B-lined chamber; however, its source range sensitivity may not perform as well as the gas-target detectors. The potential for a workable solution for a neutron detector without fissionable material deserves some further investigation of these ideas.

7. Extendibility to a Lunar Power Station

In the event that Project Prometheus becomes focused on installing the SNPP as a lunar power station, the results of this evaluation generally remain the same. After considering what design traits may be altered, the justification for using a fission chamber neutron detector is still valid. The operating temperature range may be adjusted, but will still require development of high-temperature devices regardless of the detector type. The observable neutron flux may change due to shielding differences, but will still require a full-range detector with close to the same 9 or 10 decades of sensitivity, which the fission chamber will provide most effectively. Furthermore, assuming that any SNPP mission plan will wish to minimize the necessary mass, the fission chamber provides the strongest output signal for transmission to a remote instrumentation vault, thus the best chance for avoiding an external preamplifier with additional shielding. While the pursuit of fission chamber technology remains the likely front-runner for a lunar-based case, the secondary options – silicon carbide detectors and full-range ion chambers – also retain their viability and should be investigated further.

8. Assessment and Technology Recommendation

A study of the available neutron detector technologies has generally confirmed ORNL's primary recommendation, which is to pursue the development of a fission chamber to measure reactor flux for the Prometheus project. Fission chamber technology offers the best neutron detection performance over the full range of reactor power. It requires a smaller voltage bias than other gas-filled detector candidates for reduced demand on components. Furthermore, it provides a sizeable output level at both low and high flux. These design traits make the fission chamber the most viable candidate for successful neutron flux monitoring.

While the primary candidate for neutron detector development for a SNPP application will remain, for some time, the fission chamber technology, two other alternative technologies showed significant potential and further study may be warranted in any future space endeavor with nuclear power. Silicon carbide neutron detection offers many of the same benefits as the fission chamber technology, but in addition, offers significant savings in mass and volume, a low bias voltage, and simplified signal processing compared to all the gas chamber technologies. Its high temperature and source range sensitivity issues still remain to be addressed in the development of this technology. Refining the idea of a full-range "hybrid" ion chamber that combines the operation of boron based proportional counters and ion chambers into a single detector may also warrant consideration. While it appears substantially more complex in the areas of detector design, signal processing, and bias voltage, it does offer the possibility of full range detector performance without the fissile material coating. Evaluations of both of these technologies may be warranted along with the fission chamber based approach for the next space reactor plant concept.

9. **References**

1. JIMO Reactor Sensor Technology Development Plan, ORNL, January 2005
2. Glenn F. Knoll, *Radiation Detection and Measurement*, 2nd edition, Wiley, New York, 1989.
3. Bettis Atomic Power Laboratory, *The Neutron Detector Handbook*, date unknown.
4. Ruddy, F.H., Slides from "Silicon Carbide Semiconductor Radiation Detectors." October 2000.
5. Ruddy, F.H. et al. "Nuclear Reactor Power Monitoring Using Silicon Carbide Semiconductor Radiation Detectors." *Nuclear Technology*, Vol. 140, November 2002.
6. Ruddy, F.H. et al. "Demonstration of an SiC Neutron Detector for High-Radiation Environments." *IEEE*, Vol. 46, No. 3, March 1999.
7. Ruddy, F.H. et al. "The Fast Neutron Response of Silicon Carbide Semiconductor Radiation Detectors." *Nuclear Science Symposium Conference Record, 2004 IEEE*, Volume 7, Date: 16-22 Oct. 2004, Pages: 4575-4579.

THIS PAGE INTENTIONALLY BLANK

Enclosure 6

RTD / Thermocouple Technology Evaluation

John Boyle, *KAPL-Space Electrical Systems*
David Bullen, *Bettis-Advanced Material System Integration*
Clint Geller, *Bettis-Advanced Material System Integration*
Ryan Kristensen, *KAPL-Space Electrical Systems*
Joe Rossman, *Bettis-Space I&C Design*
Camille Linton, *Bettis-Space I&C Design*

This page intentionally blank

Acronyms

CANEL	Connecticut Advanced Nuclear Engineering Laboratory
DBTT	Ductile-to-Brittle Transition Temperature
GE	General Electric Company
GEHTIL	GE Valley Forge SP-100 High Temperature Voltage Insulator Laboratory
HIP	Hot Isostatic Press
ID	Inside Diameter
JNT	Johnson Noise Thermometry
NERVA	Nuclear Engine for Rocket Vehicle Application
OD	Outside Diameter
RTD	Resistance Temperature Detector
SNPP	Space Nuclear Power Plant
TC	Thermocouple
TCR	Temperature Coefficient of Resistivity
WHC	Westinghouse Hanford Company

For brevity and clarity, all elemental and chemical compounds are referred to with their chemical formula.

Preface

The report presents a discussion of resistance temperature detector (RTD) and thermocouple (TC) options for use as temperature sensors in the Prometheus space nuclear power plant (SNPP). The content includes a discussion of the important design and materials issues. The report was intended to be a continuously updated document, a central repository for new information as it was evaluated and integrated into the temperature sensor decision. Since the project was discontinued before the evaluation could be completed, several issues received little or no analysis. In these cases, the work that remained to be done was described at the end of the respective section. This report is concluded with an extensive bibliography that lists papers and publications that may be of interest to future RTD / TC designers. Many, but not all, of these papers were reviewed during the evaluation.

THIS PAGE INTENTIONALLY BLANK	2
ACRONYMS	3
PREFACE	3
1. REACTOR COOLANT TEMPERATURE MEASUREMENT REQUIREMENTS	7
2. ISSUES COMMON TO RTDS AND TCS	7
2.1. SHEATH MATERIALS.....	7
2.1.1. <i>Melting and Evaporation</i>	7
2.1.2. <i>Recrystallization and Phase Change</i>	8
2.1.3. <i>Fabricability</i>	8
2.1.3.1. Process Environment.....	8
2.1.3.2. Ductility / Formability.....	9
2.1.3.3. Weldability / Brazability.....	10
2.1.3.4. Cold End Sealing.....	11
2.1.4. <i>Thermal Expansion</i>	11
2.1.5. <i>External Environmental Effects</i>	12
2.1.5.1. Reactor Generated Radiation.....	12
2.1.5.2. Coolant, Crud, and Fission Product Generated Radiation.....	12
2.1.5.3. The Jovan Environment.....	12
2.1.5.4. The Lunar Environment.....	12
2.1.5.5. The Martian Environment.....	13
2.1.5.6. The Ground Test Reactor Environment.....	13
2.1.6. <i>Binary Alloying</i>	13
2.1.7. <i>Oxygen Solubility, Diffusion, and Reactions</i>	13
2.1.8. <i>Compatibility with Other Plant Materials</i>	18
2.1.9. <i>Specific Materials</i>	18
2.1.9.1. Mo, ODS-Mo, TZM, Mo-41 to 47Re.....	18
2.1.9.2. Re.....	18
2.1.9.3. Ta, T-111, ASTAR-8111C, Ta-10W.....	19
2.1.9.4. Nb, Nb-1Zr, FS-85, PWC-11.....	19
2.1.9.5. V, V-4Cr-4Ti, V-5Cr-5Ti.....	19
2.1.9.6. Pt and Pt-Rh Alloys.....	19
2.1.9.7. W, W-25 to 26Re.....	19
2.1.9.8. Superalloys: MAR-M-247, IN718, Nimonic PE-16, Nimonic 263, Hastelloy XR, Haynes 230.....	19
2.2. INSULATOR MATERIALS.....	20
2.2.1. <i>Insulator Type</i>	20
2.2.2. <i>Oxide Stability</i>	20
2.2.3. <i>Compactability and Sinterability</i>	20
2.2.4. <i>Specific Materials</i>	20
2.2.4.1. Y ₂ O ₃	20
2.2.4.2. Sc ₂ O ₃	21
2.2.4.3. ThO ₂	22
2.2.4.4. BeO.....	22
2.2.4.5. La ₂ O ₃	23
2.2.4.6. HfO ₂	23
2.2.4.7. ZrO ₂	23
2.2.4.8. Al ₂ O ₃	23
2.2.4.9. MgO.....	24
2.2.4.10. SiO ₂	24
2.3. GENERAL PHYSICAL DESIGN ISSUES.....	24
2.3.1. <i>Heat Transfer</i>	24
2.3.2. <i>Joints between Sensors and Cables</i>	25
2.3.3. <i>Wire Dimensions</i>	25

2.3.4.	<i>Mounting</i>	25
2.3.5.	<i>Cover Gas</i>	28
2.3.6.	<i>Insulation</i>	30
3.	RESISTANCE TEMPERATURE DETECTORS	31
3.1.	OPERATION.....	31
3.1.1.	<i>Sensor Electrical Configuration</i>	31
3.2.	ISSUES.....	32
3.2.1.	<i>Resistivity</i>	32
3.2.2.	<i>Temperature Coefficient of Resistivity</i>	33
3.2.3.	<i>Coil Design</i>	34
3.3.	CANDIDATE ELEMENTS	34
3.3.1.	<i>Overview</i>	34
3.3.2.	<i>Thermoelement Materials</i>	34
3.3.2.1.	Re	35
3.3.2.2.	W, AKS-W, and W-Re alloys.....	35
3.3.2.3.	Mo, ODS-Mo, TZM, and Mo-Re alloys.....	35
3.3.2.4.	Ta, T-111, ASTAR-8111C, and Ta-W alloys.....	35
3.3.2.5.	Nb, Nb-1Zr, FS-85, PWC-11.....	35
3.3.2.6.	Rh.....	35
3.3.2.7.	Ir and Ir-Rh alloys	35
3.3.2.8.	Pt, ODS-Pt, and P-Rh alloys.....	36
3.3.2.9.	Ru.....	36
	Studies of Ruthenium and its alloys as a RTD thermoelement should be performed.	36
3.3.2.10.	Hf.....	36
3.3.2.11.	V.....	36
3.3.2.12.	Cr.....	36
3.4.	INSULATORS, SHEATHS, SEALS, AND CABLING	36
4.	THERMOCOUPLES	36
4.1.	THERMOCOUPLE OPERATION.....	36
4.2.	SENSOR CONFIGURATION	36
4.3.	CANDIDATE ELEMENTS	37
4.3.1.	<i>Type K</i>	37
4.3.2.	<i>Type N</i>	38
4.3.3.	<i>Type R, S, B and other Pt/Rh variants</i>	38
4.3.4.	<i>Ir-Rh variants</i>	40
4.3.5.	<i>Type C</i>	40
4.3.6.	<i>Mo vs. W</i>	44
4.3.7.	<i>Nb-1Zr vs. Mo and Mo-5Nb vs. Nb-40Mo</i>	44
4.4.	FABRICATION PROCESS.....	44
5.	IN-SITU CALIBRATION OPTIONS	44
5.1.	JOHNSON NOISE THERMOMETRY	45
5.2.	BUILT-IN MELT STANDARDS	46
5.3.	REMOTE MERCURY THERMOMETER	48
6.	CONCLUSION	48
6.1.	RESISTANCE TEMPERATURE DETECTORS.....	48
6.2.	THERMOCOUPLES	50
6.3.	THE EXPANDED TD / TC PERFORMANCE ENVELOPE	50
7.	BIBLIOGRAPHY	50

INTRODUCTION

One of the primary parameters required for operation of a nuclear reactor is the temperature of its coolant. It is commonly measured at key locations around the coolant loop to monitor and control reactor plant operations. The space nuclear power plant, as currently conceived, is to be a high temperature, gas cooled reactor with baseline inlet and outlet temperatures of 890 and 1150K, respectively at full reactor power. In addition, there are other locations around the loop with temperatures as low as 500K to be measured. This report considers the application of a resistance temperature detector (RTD) and thermocouple (TC) technologies to the measurement of these temperatures. As the reactor coolant outlet temperature is the most challenging parameter resulting from the impact of this high temperature on the sensor materials and attachments, and as it is generally considered to be an essential parameter for reactor control, this report focuses on the challenges of this parameter, in particular.

1. Reactor Coolant Temperature Measurement Requirements

The current baseline requirements being considered for a SNPP reactor coolant outlet temperature sensor range of 100K to 1300K with a nominal temperature of 1150K at full power, an accuracy of +/- 5K and a resolution of +/- 1K. The reactor outlet piping passes from the reactor vessel, through a radiation shield, to the power conversion equipment. The reactor coolant hot leg piping is to be insulated over this entire length. The notional location for the temperature sensor is just aft of the shield to minimize sensor and cabling radiation levels. Ideally the reactor coolant outlet temperature sensor would be immersed in the coolant flow stream to measure its temperature most accurately and with the smallest delay. Realistically the sensor will be housed in a well inserted into the outlet piping or attached to the piping external surface. The expected gamma dose and neutron fluence radiation levels at this location are of the order of 2×10^8 TID rads(Si) and 3.6×10^{15} n/cm², respectively. All the electronics for the sensor are to be located approximately 50 meters from the sensor in a much reduced radiation field. The temperature sensor must have a continuous service life of more than 1 decade without maintenance and preferably without calibration. This requirement suggests that the drift of the device with high temperature operation must remain strictly bounded such that the device meets its accuracy requirement throughout its service.

2. Issues Common to RTDs and TCs

RTDs and Thermocouples share many common design and materials issues. This section discusses the common issues in a general sense with more specific details in Sections 3 and 4.

2.1. Sheath Materials

2.1.1. Melting and Evaporation

The most basic requirement of any material used in an RTD or TC is that it be able to withstand the system temperature without melting or evaporating. Table 2-1 lists, for several pure elements, the melting temperature and the temperature required to maintain 1mmHg vapor pressure over the surface. The high temperature refractory metals are strong candidates for both thermoelement wires and sheaths. The properties of other elements are also important because they are generally present as alloying components and impurities. Some materials, such as Cr, have a relatively high vapor pressure, which must be carefully considered in design decisions. The lanthanides were not included

in this list because they are very rare, little is known about them, and they are generally very soft (similar to Pb), which limits their usefulness.

2.1.2. Recrystallization and Phase Change

In order to create a useful sensor geometry, the sheath material must be mechanically worked. This causes refinement of the crystal structure, which promotes recrystallization at elevated temperatures. In most refractory materials, grain growth leads to impurity concentration at the grain boundaries, embrittlement of the sheath, and a greater potential for failure. The initiation of recrystallization in the sheath is a function of the amount of cold work performed on the material, its microstructure, and impurity levels. Generally speaking, more highly worked materials begin to recrystallize at a lower temperature but embedded precipitates can hinder this.

Phase changes in materials and alloys are also important. In pure materials, changes from one crystal structure to another can occur at specific temperatures with a corresponding change in material volume. This can result in mechanical stresses in the system. In alloys, temperature changes can lead to changes in solubility and microstructure, which also have an impact on the performance of the material.

A detailed evaluation of the recrystallization and phase change behavior of various sheath materials would be the next step in the characterization.

References

[1] *ASM Handbook, Volume 2: Properties and Selection of Nonferrous Alloys and Special-Purpose Materials*, ASM International, 1990.

2.1.3. Fabricability

2.1.3.1. *Process Environment*

For ease of manufacture and cost, it is generally desirable to select RTD and TC materials that may be fabricated using existing, proven methods, without significant process development or modification. As a result, the sheath material should be capable of being formed and modified in an easily controlled environment. Air is the most preferred environment, followed by inert gas, and lastly vacuum. The following sections discuss other material related issues to fabricability.

Table 2-1. Melting temperatures and temperatures required to reach 1mmHg vapor pressure for common metals and semiconductors with melting temperatures above 1500K. Lanthanides (Gd, Tb, Dy, Ho, Tm, Er, Lu), transuranics (Cm), and non-naturally occurring elements (Tc) are not included.

Element	Melting temperature (K)	Temp req. to reach 1mmHg vapor pressure	
		Abs. Temp (K)	as a % of T_m (%)
C	3823	3586	93.80%
W	3650	3990	109.32%
Re	3450	3767	109.19%
Os	3318	3221	97.08%
Ta	3269		
Mo	2895	3102	107.15%
Nb	2740		
Ir	2683	3103	115.65%
Ru	2583	2946	114.05%
Hf	2500		
Rh	2239	2803	125.19%
V	2163	2563	118.49%
Cr	2130	1883	88.40%
Zr	2125	2459	115.72%
Pt	2045	2873	140.49%
Th	2023	2915	144.09%
Ti	1933	2453	126.90%
Pd	1827	1743	95.40%
Sc	1812		
Fe	1808	1787	98.84%
Y	1796		
Co	1768	2183	123.47%
Ni	1726	2073	120.10%
Si	1683	1724	102.44%
Be	1551	1793	115.60%

2.1.3.2. Ductility / Formability

For both thermoelements and sheath materials, ductility is required so that the sensor can be swaged to a smaller diameter, annealed, and bent (at room temperature) to conform to the plant geometry during installation. Ductility is also important for resisting vibration during launch and orbital maneuvers.

Refractory metals and alloys are candidates for both the sheath and thermoelement. Pure Ta and Nb are very ductile at room temperature and are easily formed with conventional methods at room temperature. Typically, they are formed in the annealed condition and have characteristics similar to mild steel (but are more prone to galling, tearing, and seizing). Ta and Nb have high solubilities for interstitial contaminants, as shown in Table 2-2, allowing them to retain their properties with relatively large impurity percentages. In general, absorption of impurities results in considerable strengthening

and loss of ductility at low temperatures. At high temperatures, both metals can absorb enough oxygen to destroy their room temperature ductility. Since room temperature ductility is necessary for the final fabrication step (bending to conform to plant piping), high temperature processing should be minimized or eliminated unless it can be done in an inert or vacuum environment.

Table 2-2. Estimated solubilities (in ppm) of interstitial contaminants C, N, O, and H in four refractory metals [2].

Interstitial	Nb	Ta	Mo	W
C	100	70	<1.0	<0.1
N	300	1000	1.0	<0.1
O	1000	300	1.0	1.0
H	9000	4000	0.1	N.D

Pure Mo and W are far less ductile. They have a very low solubility for interstitial contaminants, a characteristic that can lead to grain boundary embrittlement. This failure mode begins with the metal absorbing a large concentration of contaminants at high temperature where they are more soluble. When the metal is cooled, the solubility drops and the interstitials are forced out of the grains to the grain boundaries where they accumulate. This can result in oxide and carbide films that limit plastic flow. Warm working below the recrystallization temperature breaks up the films and produces an anisotropic fibrous grain structure. The addition of Re greatly improves the room temperature ductility of both Mo and W.

Pure Re is ductile, even down to 0K, but cannot be machined by conventional methods. Re oxidizes catastrophically in air above 600°C because its oxide (Re_2O_7) vaporizes at 363°C. When hot-worked at temperatures below 363°C, the oxide diffuses to the grain boundaries and causes grain boundary embrittlement [1]. In addition, its strain hardening rate is 3.5 times that of W or Mo. As a result, Re is limited to low levels of cold working (10-20%) with frequent anneals in a vacuum, inert, or reducing environment (such as H_2). Re can be rolled, swaged, forged, and wire drawn[1].

A detailed analysis of refractory metal ductility, the effects of contaminants, and recrystallization conditions would be the next step in the characterization of the ductility and formability of materials for the RTD or TC sheath.

References

- [1] *ASM Handbook, Volume 2: Properties and Selection of Nonferrous Alloys and Special-Purpose Materials*, ASM International, 1990.
- [2] D.T. Hoelzer, A.F. Rowcliffe, S.J. Zinkle, "Critical Review Of Solubility, Diffusivity, and Metallurgical Effects In Group V And VI Metals," ORNL Draft report, ORNL/LTR/NR-JIMO/04-01.

2.1.3.3. Weldability / Brazability

The ability to weld or braze refractory metals to themselves, other refractories, and superalloys is essential to produce sheath assemblies. Pure Ta and Nb are very ductile at room temperature and are easily formed and joined with conventional methods. Welding must be done in a good vacuum to exclude impurities that lead to grain boundary embrittlement of the weld zone. Re can be welded, soldered and brazed by conventional means. Welding should be done in an inert atmosphere or vacuum to preserve ductility [1]. W and Mo can be electron-beam welded with poor results, and are generally brazed or mechanically joined whenever possible. Table 2-3 shows the joint efficiency of welds in various refractory metals.

A detailed analysis of dissimilar refractory metal joining and joining to superalloys would be the next step in the characterization of the weldability and brazability of materials for the RTD or TC sheath..

Pre Decisional – For Planning and Discussion Purposes Only

Table 2-3. Weld joint efficiency for welds in various refractory metals. Joint efficiency is a measure of the strength of the joint as compared to the strength of the original material.

Material	Best case weld joint efficiency
Nb	>75%
Ta	>75%
Mo	<50%
W	<50%

References

[1] *ASM Handbook, Volume 2: Properties and Selection of Nonferrous Alloys and Special-Purpose Materials*, ASM International, 1990.

2.1.3.4. Cold End Sealing

RTDs and TCs have a hot end where the sensor is located and a cold end where the leads exit the sheath. This end of the sheath must be sealed to prevent the entry of contaminants from the environment into the sheath and prevent the loss of sheath cover gas to the environment. Previous studies [1] have found that the effects of contaminants diffusing into a TC from the cold end can completely mask the effects of microstructural change and transmutation on the sensor output. In general, the seal must be hermetic, electrically insulating, and able to withstand the temperature of its environment. In some cases, the cold end seal can be integrated into the structure that is used to couple the sensor leads to a cable.

An examination of glass-to-metal seals and ceramic-to-metal seals, as well as a review of sealing methods used in previous TC development projects would be the next step in the characterization of the end sealing of the RTD or TC sheath.

References

[1] P. Bliss and S. Fanciullo, "High Temperature Thermometry at Pratt and Whitney Aircraft-CANEL," PWAC-462, Pratt and Whitney Aircraft, Connecticut Aircraft Nuclear Engine Lab, 1 June 1965.

2.1.4. Thermal Expansion

There are two manifestations of thermal expansion and contraction in the sensor and each has an effect on reliability. For slow temperature changes along the length of the sheath, differences in longitudinal expansion and contraction between the sheath, insulator, and thermoelements can introduce strains that may cause the thermoelements to break or read erroneously due to strain-induced resistance changes. Large differences in thermal expansion coefficient between the sheath and insulation can also lead to radial expansion or contraction and a loss of contact between internal components. For fast changes in temperature, radial temperature gradients can also cause gaps or insulator compression even if the materials are well matched.

A gathering of thermo-mechanical property data, an analysis of various thermoelement/insulator/sheath combinations, and an exploration of potential stress mitigation methods would be the next step in the characterization of the thermal expansion of the RTD or TC sheath.

2.1.5. External Environmental Effects

2.1.5.1. *Reactor Generated Radiation*

The reactor is a source of thermal, epithermal, and fast neutrons. Neutron irradiation can cause a change in temperature sensor performance via transmutation, displacement damage, and ionization. The magnitude of the effect is a function of the neutron velocity, neutron flux density, material absorption cross-section, exposure time, and half-life of the transmuted isotopes. Generally speaking, the lower the neutron speed, the greater the probability of its absorption. Fortunately, the location of the sensors in the plant is expected to reduce the potential for neutron-induced effects. The aft-of-shield fluence in the region of the sensors is expected to be less than 3.6×10^{15} n/cm². Given that the atomic density of most metals under consideration is in the range of $4\text{-}7 \times 10^{22}$ atoms/cm³, even if every neutron is absorbed and results in transmutation, the percentage of transmuted elements will be very low. For example, in a wire with a 0.001in diameter, if every neutron is captured, the transmutation will be on the order of 0.004%-0.007.5%. This is not expected to be enough to cause significant drift in mechanical properties, thermoelectric potentials, or electrical resistivity. The total radiation dose also corresponds to displacement damage levels on the order of 10⁻²dpa. This level of damage is not expected to cause significant microstructural evolution in sensor materials.

Gamma radiation is also generated by the reactor and can affect sensor performance. Gamma absorption in a material generates heat and is proportional to the material density. Sensor element heating can result in an elevated temperature reading that is not representative of the actual system temperature (this is the operating principle of the gamma thermometer). Maximum gamma dose rates aft-of-shield are expected to be on the order of 2rad/sec. This dose is not expected to create significant gamma heating in RTDs and TCs that are in good thermal contact with the component or structure they are measuring.

References:

[1] B-MT(SMAT)-005, Space Materials Plan, issued 4April05.

2.1.5.2. *Coolant, Crud, and Fission Product Generated Radiation*

In addition to radiation from the reactor, there will also be radiation generated by the activated coolant and particulates formed from plant materials and activated in the core. These materials circulate throughout the primary system, plate out on internal piping surfaces, and decay over time. If a fuel cladding leak occurs, fuel and fission products will also circulate through the coolant system with similar effects. The neutron, gamma, and beta dose from these sources has not yet been evaluated.

2.1.5.3. *The Jovan Environment*

Radiation in the Jovan environment is expected to take the form of high energy electrons and protons, heavy ions, and gammas and cosmic rays from deep space. Little is known about the effects of these fluxes on sensor materials or assemblies. It is assumed that charged particle bombardment of insulating materials may lead to some level of electrical conductivity, charge buildup, and internal discharge that could cause damage. The magnitude of these problems remains to be explored.

References:

[1] B-MT(SMAT)-005, Space Materials Plan, issued 4April05.

2.1.5.4. *The Lunar Environment*

A detailed characterization of lunar environment and its effect on RTD and TC sheath materials and components would be necessary for SNPP moon application..

2.1.5.5. The Martian Environment

A detailed characterization of lunar environment and its effect on RTD and TC sheath materials and components would be necessary for SNPP Mars application.

2.1.5.6. The Ground Test Reactor Environment

Although details of the ground test reactor environment are not yet available, it is probable that the reactor will be operated in a vacuum or inert atmosphere. In either case, it is probable that the oxygen, nitrogen, and carbon content of this environment will be significantly higher than the mission environment. To ensure a successful test, the sheath must be capable of surviving and protecting the thermoelements in this environment.

A detailed evaluation of the ground test reactor environment, and the performance of sheath materials in that environment, would be necessary to support such an application.

2.1.6. Binary Alloying

One of the most significant interactions between sensor materials is the interdiffusion and alloying of component materials. When one sensor material alloys with another, the most significant impact is the alteration of the alloy's melting temperature. Table 2-4 lists the minimum eutectic temperature of various binary alloys that can be formed from sensor materials. This is the minimum melting temperature of the binary system and represents one temperature limit on systems employing a given combination of materials.

An examination of data related to inter-diffusion rates and mechanisms of the above combinations would be the next effort to characterize this material behavior.

2.1.7. Oxygen Solubility, Diffusion, and Reactions

Although many potential contaminants are present in the sheath, O is the most abundant. The presence of oxygen in the insulator creates potential problems for the sheath and thermoelements. There is a risk that the oxide formed by the sheath or thermoelement metal will be more thermodynamically stable than the insulator oxide. This can lead to oxygen in the insulator being gettered by the thermoelement wires or sheath material, leaving behind the pure base metal in the insulator. The result is oxide formation in the sheath and alloying of the sheath material with the insulator base metal.

One way to evaluate the potential for adverse oxide reactions is to examine the Gibbs free energy of formation of the oxides that can form from sheath and insulator metals. Figure 2-1, Figure 2-2, and Figure 2-3 show the Gibbs free energy of formation of several oxide insulator materials as well as metals that may be present in the sheath. The Gibbs free energy is the amount of energy liberated in the formation of each oxide at the temperature specified. For oxide insulator materials, lower the values (more negative) result in a more stable oxide. For sheath and thermoelement metals, the higher the value, the more resistant to oxidation.

Table 2-4. Minimum eutectic temperatures (in K) of potential binary alloys that can form from sensor materials. An X indicates that the two elements are completely solid solution soluble, thus the minimum melting temperature is generally the lower of the two elements [1,2].

	Al	Si	Ni	Fe	Pt	Zr	Cr	V	Rh	Hf	Ru	Ir	Nb	Mo	Ta	Re
T _m	933		1723	1800	2042		2133	2199	2239							
W	933	1673	1723	1798	2042	2008	X	X	2239		2478		X	X	X	3098
Re	933	1398		1800	2042	1866	2133	2173			X		2708	2778	2963	
Ta	933		1593	1623	2033	2093	1973	2199	2013				X	X		
Mo	933			1723	2042	1823	X	X	2213		2228		X			
Nb	933	1573	1443	1645	1973	2013		X	1773							
Ir							1953									
Ru	933		1726	1800	2042		1883									
Hf	933			1573			1783									
Rh			X		X		1748	1793								
V	933	1663	1473	1743	1993	1493	X									
Cr	933	1608	1618	1780	1773											
Zr	933	1628	1233	1220	1452											
Pt	930	1103		1800												
Fe	928	1463	1713													
Ni	913	1237														
Si	850															

References

- [1] *Binary Alloy Phase Diagrams*, Second Ed., Thaddeus B. Massalski, ed., ASM International, 1990.
- [2] *Smithells Metals Reference Book*, Eric Brandes, ed. Butterworths, New York, NY, 1983.

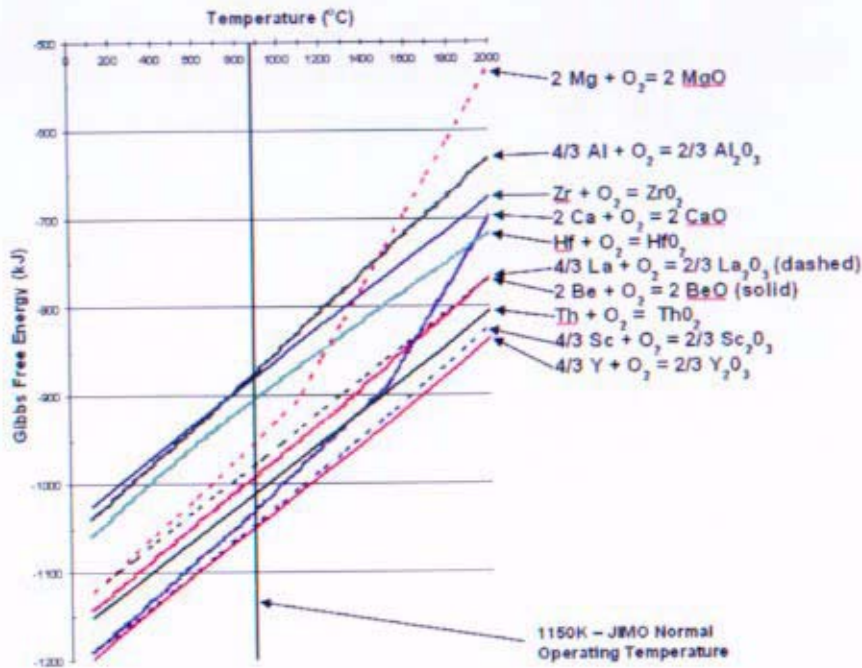


Figure 2-1. Gibbs free energy of formation (per mol O₂) of several potential oxide insulator materials [2].

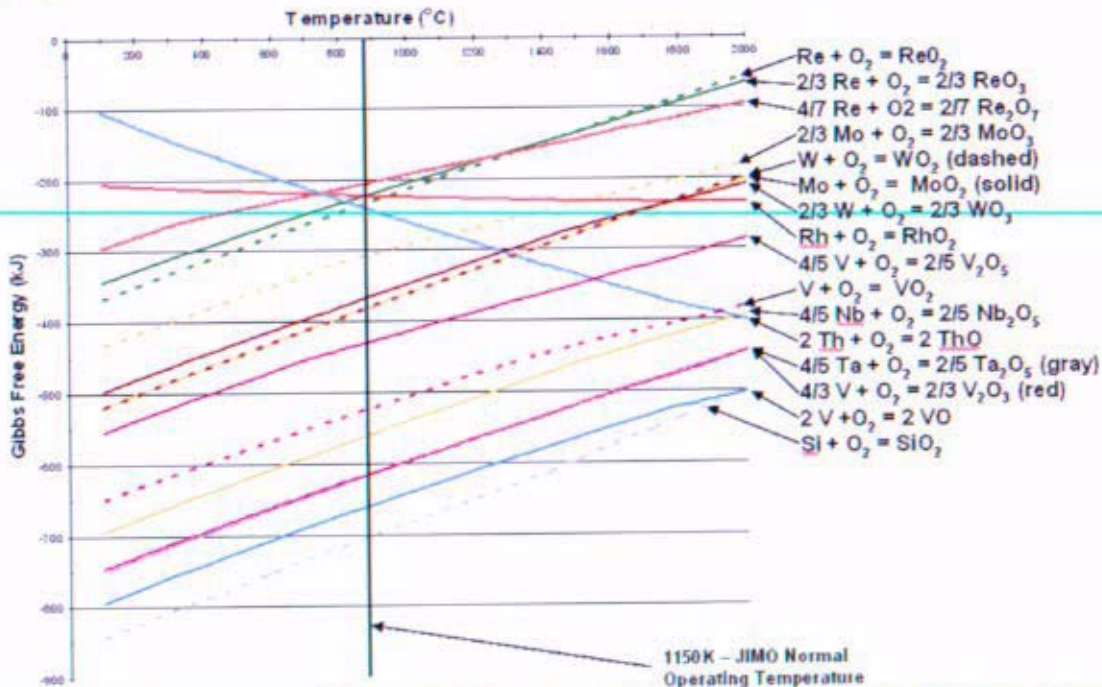


Figure 2-2. Gibbs free energy of formation (per mol O₂) of several oxides formed from RTD and TC materials [2].

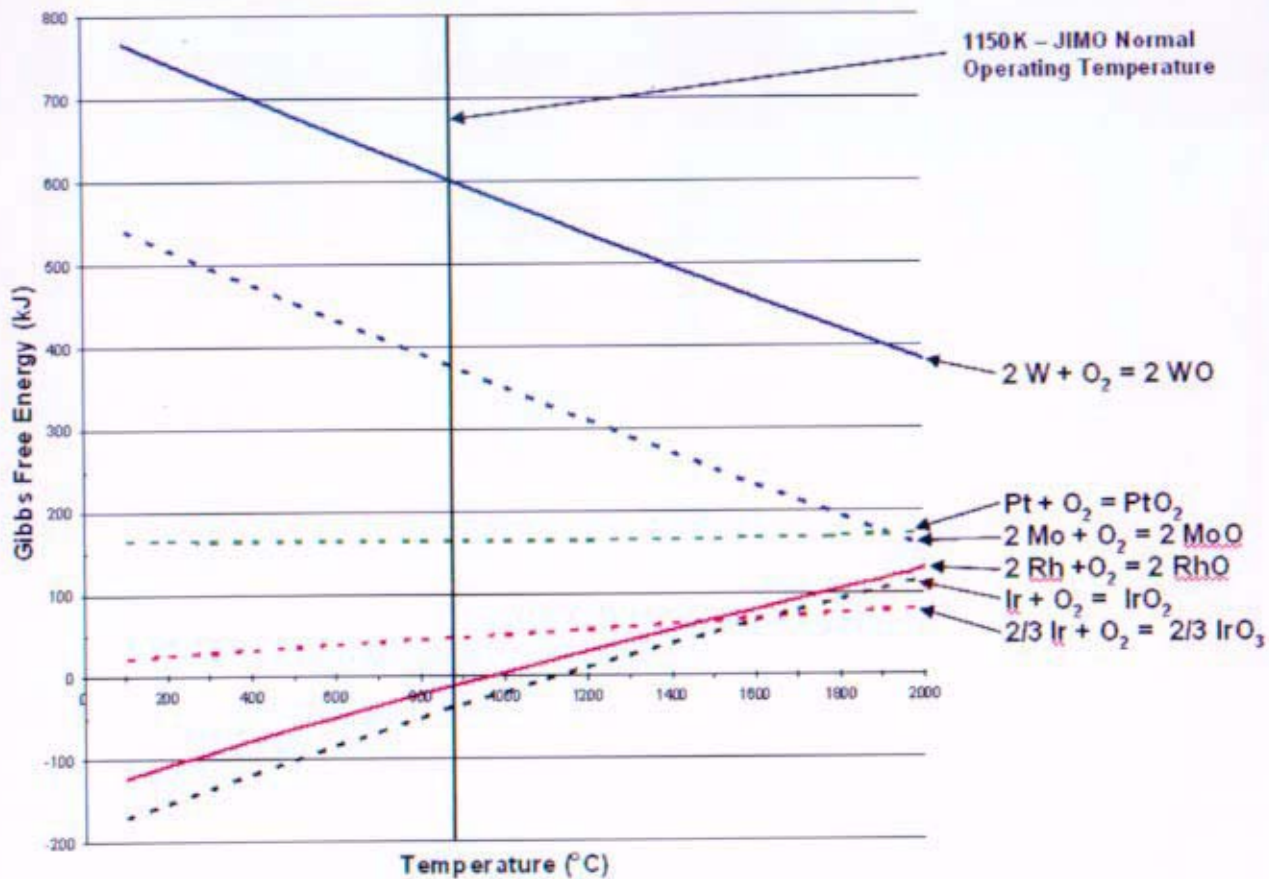


Figure 2-3. Gibbs free energy of formation (per mol O₂) of several oxides formed from RTD and TC thermoelement materials [2].

Table 2-5 lists values from the tables above at 300K and 1150K at 1atm pressure and in a vacuum. Vacuum values are presented to hint at the possible shifts in chemical equilibrium in the event of a sheath cover gas leak.

Table 2-5. Gibbs free energy of formation at specific temperatures [2].

Reaction	300K, 1atm	1150K, 1atm	300K, Vac	1150K, Vac
$2 W + O_2 = 2 WO$	783	602	697	271
$2 Mo + O_2 = 2 MoO$	556	374	470	44
$Pt + O_2 = PtO_2$	166	163	166	163
$2/3 Ir + O_2 = 2/3 IrO_3$	19	46	105	376
$2 Rh + O_2 = 2 RhO$	-134	-11	-48	263
$Ir + O_2 = IrO_2$	-186	-39	-100	291
$4/7 Re + O_2 = 2/7 Re_2O_7$	-307	-204	-224	32
$2/3 Re + O_2 = 2/3 ReO_3$	-355	-222	-269	108
$Rh + O_2 = RhO_2$	-204	-222	-204	-222
$Re + O_2 = ReO_2$	-379	-234	-294	97
$Th + O_2 = ThO_2$	-86	-239	-171	-569
$2/3 Mo + O_2 = 2/3 MoO_3$	-445	-308	-360	-79
$2/3 W + O_2 = 2/3 WO_3$	-509	-366	-424	-43
$Mo + O_2 = MoO_2$	-532	-380	-446	-53
$W + O_2 = WO_2$	-534	-382	-448	-51
$4/5 V + O_2 = 2/5 V_2O_5$	-567	-429	-482	-99
$V + O_2 = VO_2$	-663	-524	-577	-261
$4/5 Nb + O_2 = 2/5 Nb_2O_5$	-706	-560	-621	-230
$4/3 V + O_2 = 2/3 V_2O_3$	-759	-615	-673	-284
$4/5 Ta + O_2 = 2/5 Ta_2O_5$	-764	-617	-679	-287
$2 V + O_2 = 2 VO$	-807	-660	-722	-329
$Si + O_2 = SiO_2$	-856	-704	-771	-323
$4/3 Al + O_2 = 2/3 Al_2O_3$	-1055	-874	-969	-343
$Zr + O_2 = ZrO_2$	-1040	-879	-954	-549
$Hf + O_2 = HfO_2$	-1078	-904	-992	-573
$2 Mg + O_2 = 2 MgO$	-1138	-952	-1053	-2
$4/3 La + O_2 = 2/3 La_2O_3$	-1135	-978	-1050	-499
$2 Be + O_2 = 2 BeO$	-1158	-991	-1073	-358
$2 Th + O_2 = 2 ThO$	-1164	-1010	-1078	-680
$2 Ca + O_2 = 2 CaO$	-1207	-1029	-1121	-147
$4/3 Sc + O_2 = 2/3 Sc_2O_3$	-1203	-1045	-1117	-568
$4/3 Y + O_2 = 2/3 Y_2O_3$	-1213	-1049	-1128	-635

The subject of oxygen interaction with refractory and high temperature materials is very broad. The next effort in this material area would be to evaluate oxygen solubility, diffusion rates, transport mechanisms, and oxide stability and volatilization conditions in potential RTD/TC materials. In addition, models should be investigated that characterize metal diffusion through oxide grains, along grain boundaries, and surfaces.

Pre Decisional – For Planning and Discussion Purposes Only

References

- [1] P. Bliss, S. Franciullo, "High Temperature Thermometry at Pratt and Whitney Aircraft-CANEL," PWAC-462, Pratt and Whitney Aircraft, Connecticut Aircraft Nuclear Engine Lab, 01 Jun 1965.
 [2] Data assembled from databases and calculations performed using FACTSAGE.

2.1.8. Compatibility with Other Plant Materials

At a minimum, sensor sheath must be compatible with the pipe that the RTD or TC is attached. In addition, it should also be compatible with the other plant materials that can diffuse through the pipe wall. At the time of this writing, the most promising pipe concept was a nickel superalloy with a refractory metal liner. The pipe and liner were to be separated by an insulation of perhaps refractory oxide or superalloy foam. In addition, in the event that a fuel cladding leak occurs, fuel and fission product materials would also circulate through the core and create compatibility issues. A partial list of potential plant and core materials is given in Table 2-6. Compatibility between these materials and the sheath material remains to be evaluated.

Table 2-6. Composition of various potential plant structural alloys.

Structural Alloy Name	Composition
Haynes 230	Ni-22Cr-14W-2Mo-0.5Mn-0.4Si-0.3Al-0.1Cr-0.02La
Alloy In617	Ni-22Cr-11Co-9Mb
Hastelloy X	Ni-22Cr-18Fe-9Mo-1.5Co-0.6W-0.1C
Nimonic PE-16	Ni-33Fe-16.5Cr-3.3Mo-1.2Ti-1.2Al
ASTAR-811C	Ta-8W-1Hf-0.7Re-0.025C
FS-85	Nb-26Ta-10W-1Zr
	Ta-10W
	Mo-47.5Re
	Ti-6Al-4V
	SiC

2.1.9. Specific Materials

This section describes the characteristics of various classes of materials used as sheath materials, including the examination of both refractory and non-refractory metals as well as important alloys of these materials.

2.1.9.1. *Mo, ODS-Mo, TZM, Mo-41 to 47Re*

The molybdenum and molybdenum alloys should be one class of materials to be studied.

2.1.9.2. *Re*

Re has several properties that make it a candidate for a sheath material, as well as several properties that are cause for concern. Re easily withstands the operating temperature and is highly ductile at all temperatures. It does not form a carbide, implying some resistance to C contamination from superalloy components it may be in contact with. The enthalpy of formation of ReO_2 , ReO_3 , and Re_2O_7 is far less negative than the insulators under consideration, indicating chemical compatibility with those materials. Unfortunately, in the presence of free oxygen, Re oxidizes catastrophically above 600°C to Re_2O_7 , which immediately vaporizes. The oxide can also cause grain boundary embrittlement. This is a concern for operation in ground test reactor because a high vacuum may not be possible and oxygen may be a significant contaminant. Re components are sometimes coated with Ir to protect them from high temperature oxidation resistance. The cost of pure Re parts is generally very high because of the rarity of the metal and its high work-hardening rate.

2.1.9.3. *Ta, T-111, ASTAR-8111C, Ta-10W*

Tantalum and its alloys represent a class of materials that should be evaluated.

2.1.9.4. *Nb, Nb-1Zr, FS-85, PWC-11*

The composition of several candidate Nb alloys is given in Table 2-7. In addition to these alloys, several Nb-Ta mixtures are available for special applications.

Table 2-7. Composition of several industrially important Nb alloys.

Alloy	Composition
Nb	Nb
Nb-1Zr	Nb-1Zr
FS-85	Nb-27Ta-10W-1Zr
PWC-11	Nb-1Zr-0.1C

Nb has frequently been called upon as structural and pressure boundary material for use in reactors because of its compatibility with liquid metals. Nb is not attacked by most liquid metals and the addition of Zr allows the alloy to getter O from the liquid metal and prevent it from diffusing into, and embrittling, the base Nb. For sensor applications, only the pure metal is a potential candidate. It has been shown in several studies [1,2] that Zr will reduce Al_2O_3 , SiO_2 , and MgO insulators. It has been observed that, when a Nb-1Zr sheath is used with Al_2O_3 insulation, the reduction of Al_2O_3 occurs in conjunction with the formation of Nb_3Al intermetallic phases and ZrO_2 precipitates in the sheath. A similar reaction occurs for many insulator materials except MgO. Mg is insoluble in Nb, thus only the ZrO_2 precipitates form. For this reason, any alloy containing Zr is unacceptable for use as a sheath material unless it is clad with a barrier layer.

References

- [1] "Fabrication of SP-100 High Temperature Sensor Attachment," GE SP-100 Program Information Request 1027, Dated 1/16/92.
[2] Fornwalt, D.E., Gourley, B.R., Manzione, A.V., "A Study of the Compatibility of Selected Refractory Metals with Various Ceramic Insulation Materials," Pratt and Whitney Aircraft Division, CNLM-5942, 30Nov1964.

2.1.9.5. *V, V-4Cr-4Ti, V-5Cr-5Ti*

Vanadium and its alloys represent a class of materials to be studied.

2.1.9.6. *Pt and Pt-Rh Alloys*

Platinum and its alloys represent a class of materials to be studied.

2.1.9.7. *W, W-25 to 26Re*

Tungsten and its alloys represent a class of materials to be studied.

2.1.9.8. *Superalloys: MAR-M-247, IN718, Nimonic PE-16, Nimonic 263, Hastelloy XR, Haynes 230*

The superalloys represent a class of materials to be studied.

2.2. Insulator Materials

2.2.1. Insulator Type

Many material classes can be used to insulate electrical systems. These include polymers, fibrous ceramics, hard-fired ceramics, gases, vacuum, oil, mica, etc. Of these materials, polymers and oils are not an option due to the high temperatures reached by the sensor. An inert gas may work except that a structure would still be required to mechanically support and separate the conductors from each other in the small sheath diameter. Vacuum insulated systems suffer from the same problem as well as having an unobstructed path between materials for evaporative transport. Even mica is not suitable because it will decompose by calcination in the range of 600°C-900°C.

At the highest plant temperatures, only hard-fired oxide ceramic insulation will properly insulate the thermoelement wires. As indicated by Figure 2-1, several insulator materials may be chemically suitable as insulation. Those materials are discussed in detail below.

2.2.2. Oxide Stability

Oxides are formed by chemical reaction that generally begins with a gaseous source of oxygen. A reduction in the oxygen partial pressure over the oxide surface can drive this process in reverse (via LeChatelier's Principle). This can drive the material off stoichiometry and liberate elemental oxygen and base metal reactants, especially if the sheath or thermoelement material participates in the reaction at high temperature. It is also possible that low melting point suboxides may be formed, resulting in volatilization. These issues must be considered when considering the insulator materials and cover gas used.

2.2.3. Compactability and Sinterability

If hard-fired ceramics are to be used to insulate the system, it is important that those materials have good compacting and sintering properties. This will allow them to be formed into bead compacts, crushed in the sheath during the swaging process, and possibly sintered at high temperature.

An evaluation of the sintering properties of common ceramic insulators would be the next effort in the characterization of the compactability and sinterability of the insulating materials.

2.2.4. Specific Materials

2.2.4.1. Y_2O_3

Y_2O_3 was briefly considered as insulation for the SP-100 program[3]. This decision was based on a GE demonstration that Y_2O_3 was chemically very stable (lowest enthalpy of formation of all oxides) and could even be safely immersed in liquid Li without reaction. For SP-100, it was important that oxygen from the insulator not be reduced by the Li in the liquid metal loops. Later testing by WHC indicated that the electrical resistivity of Y_2O_3 was two orders of magnitude lower than Al_2O_3 at SP-100 temperatures and decreased further with high temperature aging (1000 to 2000 hours at 1100°C in the WHC test). Long term conductivity testing of Y_2O_3 at GEHTIL also showed that its conductivity was unstable at 1100°C and that it fluctuated with varying voltage [2]. The researchers surmised that these effects were caused by impurities. Resistivity may also be a function of temperature and oxygen partial pressure. Changes in either parameter cause small deviations in stoichiometry that, in turn, establishes a concentration of electronic charge carriers [1]. Due to its low and unstable insulating capability, Y_2O_3 was dropped from SP-100 consideration. Although GE planned further testing of higher purity material, no results have been uncovered in the literature.

Limited materials compatibility testing was performed using simulated thermocouples consisting of W-5Re/W-26Re TC wires, loose fitting Y_2O_3 insulation, a Nb-1Zr sheath, and He fill gas [3]. After furnace aging at 1375K for 819 hours, no interaction between the insulator and wires was noted and they were judged to be fully compatible.

In a separate study [4], both commercial and spectrographic grades of Y_2O_3 were tested in a Nb-1Zr sheath with W-5Re and W-26Re wires. The sheath was swaged to ensure good contact between the materials. Samples were annealed at 1090, 1310, and 1540C for 200, 500, and 1000 hours. No reactions were noted for any time-temperature combination when spectrographic grade Y_2O_3 was used. When commercial grade Y_2O_3 was used, a 2.5 μ m thick reaction zone of Nb_3Si_5 formed in the sheath, presumably as a result of the 300ppm Si impurity in the Y_2O_3 insulator. There was no interaction between the insulator and wires in any experiment.

References

- [1] High Temperature Oxides: Part 2, Oxides of Rare Earths, Titanium, Zirconium, Hafnium, Niobium, and Tantalum, ed. Allen Alper, Academic Press, New York, 1970.
- [2] "Fabrication of SP-100 High Temperature Sensor Attachment," GE SP-100 Program Information Request 1027, Dated 1/16/92.
- [3] R.C. Knight, N.S. Cannon, "SP-100 Reference Temperature Sensor Summary Report," Westinghouse Hanford Company, WHC-SP-1080, Rev. 0, April 1994.
- [4] Fornwalt, D.E., Gourley, B.R., Manzione, A.V., "A Study of the Compatibility of Selected Refractory Metals with Various Ceramic Insulation Materials," Pratt and Whitney Aircraft Division, CNLM-5942, 30Nov1964.

2.2.4.2. Sc_2O_3

In the context of a space nuclear power system, the most significant use of Sc_2O_3 has been as an electrically insulating spacer in the thermionic converters of the TOPAZ-II reactor [1], as shown in Figure 2-4. In this device, Sc_2O_3 spacers were used to separate a Mo-W clad, UO_2 fuel plate from a Mo thermionic collector. In this application, the Sc_2O_3 spacer was in contact with the fuel plate and a Nb ring. After an investigation of many insulator materials, the researchers selected Sc_2O_3 over the next best material (Al_2O_3) for the spacer because, in addition to suitable insulating properties, it provided the best chemical resistance to cesium vapor and ignited cesium plasma during operation at 1800°C. Experiments showed that it had a lifetime under these conditions of several orders of magnitude greater than Al_2O_3 ($\sim 10^6$ hours vs. 2500 for Al_2O_3) as defined by the mass loss rate (via vaporization) during operation. Material compatibility studies were not performed.

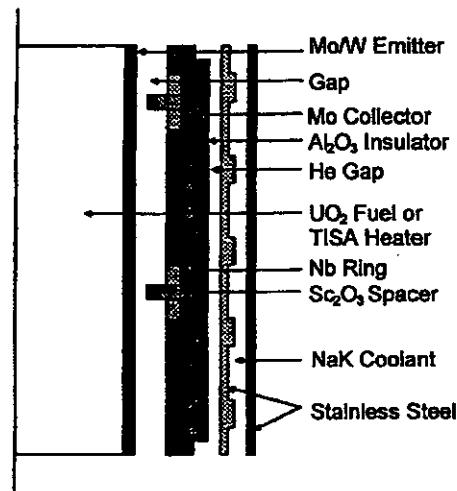


Figure 2-4. Thermionic converter cell of the TOPAZ-II reactor using a Sc₂O₃ spacer.

Although Sc₂O₃ looks extremely chemically stable from the perspective of Gibbs free energy, there is very little engineering data available outside the thermionic application. There are also very few vendors capable of providing the raw material and sintered compacts needed for further development.

References

[1] A.S. Gontar, M.V. Nelidov, Yu.V. Nikolaev, L.N. Schulepov, "Fuel Elements of Thermionic Converters," Sandia National Laboratories, SAND97-0071, Jan 1997.

2.2.4.3. ThO₂

ThO₂ was considered as a ceramic insulator in the NERVA project largely due to its extremely high melting point of 3220°C. Unfortunately, ThO₂ is an n-Type semiconductor whose conductivity changes radically with changes in temperature, environment, and composition. The addition of stabilizers such as Ca or Y can lead to O anion vacancies and ionic conductivity, similar to the mechanisms that make ZrO₂ conductive. Finally, all of the 12 isotopes of Th are radioactive, many of which decay by alpha and beta emission. This raises serious safety, contamination, and administrative barriers to its use.

References

[1] High Temperature Oxides: Part 2, Oxides of Rare Earths, Titanium, Zirconium, Hafnium, Niobium, and Tantalum, ed. Allen Alper, Academic Press, New York, 1970.

2.2.4.4. BeO

BeO was chosen to insulate the thermocouples that monitored the core temperature of the NERVA reactor [1]. The NERVA reactor was intended to operate at temperatures approaching 2500°C for durations on the order of minutes to an hour. Although the melting point of BeO is not as high as other refractory ceramics, it has the highest electrical resistivity of any material in that operating range [3]. BeO also has a thermal conductivity on par with many high conductivity metals. Unfortunately, BeO presents a significant health hazard (it causes pulmonary granulomatosis), making it difficult to work with safely. For this reason, it was eliminated from consideration as an insulator in the SP-100 thermocouple design.

Compatibility testing of BeO insulation has been performed [2] using a Nb-1Zr sheath and W-5Re and W-26Re wires. The sheath was swaged to ensure good contact between the materials. Samples were

annealed at 1090, 1310, and 1540C for 200, 500, and 1000 hours. When spectrographic grade materials were used, there was no evidence of interaction between any material combination. When commercial grade BeO was used (which had a 300ppm Si impurity), an intermetallic reaction zone formed between the insulator and sheath. The zone consisted of 5-10 μ m thick layer of Nb₃Si₅. In addition, a ZrO₂ precipitate formed in the sheath.

References

- [1] A. W. Hoppe, P. J. Levine, "Status of High Temperature Thermometry for the NERVA Reactor," Westinghouse Astronuclear Laboratory.
- [2] Fornwalt, D.E., Gourley, B.R., Manzione, A.V., "A Study of the Compatibility of Selected Refractory Metals with Various Ceramic Insulation Materials," Pratt and Whitney Aircraft Division, CNLM-5942, 30Nov1964.
- [3] Ryshkewitch, E., "Oxide Ceramics: Physical Chemistry and Technology," Academic Press, New York, 1960.

2.2.4.5. La₂O₃

2.2.4.6. HfO₂

HfO₂ is sometimes offered as a non-toxic alternative to BeO by thermocouple companies. Compatibility testing of HfO₂ insulators with W-5Re/W-26Re wires and a Nb-1Zr sheath was performed by WHC [1]. After 1007 hours at 1600°C, the inside surface of the sheath became pitted and HfO₂ began to sinter to the sheath surface. The W-26Re wire surface became very rough, embedded with HfO₂ particles, and its grain boundaries were enriched with Re and contained Nb (indicating transport from the sheath to the wires). These adverse reactions between HfO₂ and the specified wire and sheath materials lead to HfO₂ being rejected as a potential insulator for the SP-100 program.

References

- [1] R.C. Knight, N.S. Cannon, "SP-100 Reference Temperature Sensor Summary Report," Westinghouse Hanford Company, WHC-SP-1080, Rev. 0, April 1994.

2.2.4.7. ZrO₂

ZrO₂ has an enthalpy of formation similar to Al₂O₃ indicating chemical stability in the oxide form. Pure ZrO₂ has an electrical resistivity of 10¹³-10¹⁴ ohm-cm at room temperature that drops to 10⁷-10⁸ ohm-cm at 1000°C. Unfortunately, pure ZrO₂ is mechanically unstable and must be stabilized by the addition of another cubic crystal oxide, typically of lower valency. This leads to the liberation of O ions in the lattice that are free to conduct charge. Electrical resistivities as low as 10²-10³ ohm-cm have been reported in stabilized ZrO₂.

References

- [1] Ryshkewitch, E., "Oxide Ceramics: Physical Chemistry and Technology," Academic Press, New York, 1960.

2.2.4.8. Al₂O₃

Al₂O₃ is the most common material used for RTD and TC insulation, and was the final choice for the SP-100 RTD and TC insulator material. It is abundant, easy and safe to work with, inexpensive, and is backed by a wealth of engineering data.

Compatibility of Al₂O₃ in TC applications was demonstrated by Pratt and Whitney [1]. The test involved Al₂O₃ TC insulation in a Nb-1Zr sheath with W-5Re and W-26Re wires. The sheath was swaged to ensure good contact between the materials. Due to contaminants in the insulator material, three grades were used: Al₂O₃-2Si, Al₂O₃-0.5Si, and spectrographic Al₂O₃. Samples were annealed at

1090, 1310, and 1540C for 200, 500, and 1000 hours. In all tests, the Si impurity in the $\text{Al}_2\text{O}_3\text{-2Si}$ diffused into the sheath material to form an intermetallic layer of Nb_3Si_5 . The $\text{Al}_2\text{O}_3\text{-0.5Si}$ formed this layer only sporadically, and the Al_2O_3 did not form it at all. In the 1090 and 1310C tests of all three grades, reduction of the insulator created Al that also diffused into the sheath to form layers of Nb_2Al and Nb_3Al under the Nb_3Si_5 to a maximum depth of $25\mu\text{m}$. At 1540C, the 200 and 500 hour samples revealed that the Al and O diffused into the sheath and preferentially formed Al_2O_3 , instead of ZrO_2 , precipitates. The 1000 hour samples indicated that the Al_2O_3 had redissolved.

There is a significant body of literature on Al_2O_3 ceramic insulation. The next action in this area would be a more detailed evaluation of its electrical and sintering properties.

References

[1] Fornwalt, D.E., Gourley, B.R., Manzione, A.V., "A Study of the Compatibility of Selected Refractory Metals with Various Ceramic Insulation Materials," Pratt and Whitney Aircraft Division, CNLM-5942, 30Nov1964

2.2.4.9. *MgO*

MgO is a common high temperature TC insulator. Compatibility testing of commercial grade MgO insulation has been performed [1] using a Nb-1Zr sheath and W-5Re and W-26Re wires. The commercial grade material had 2000ppm Si impurity. The sheath was swaged to ensure good contact between the materials. Samples were annealed at 1090, 1310, and 1540C for 200, 500, and 1000 hours. After the anneals, all samples exhibited a 2.5-5 μm deep reaction zone in the sheath surface consisting of Nb_3Si_5 , presumably from the Si contamination in the insulator. A sample using spectrographic grade MgO was annealed for 1000 hours at 1310C. During the test, some Mg was reduced, contributing to an oxygen concentration of 4400ppm and the formation of ZrO_2 precipitates in the sheath. There was no evidence of Mg diffusion into the sheath, probably due to the extremely low solubility of Mg in Nb. MgO is hygroscopic and easily absorbs water from the atmosphere so a dry atmosphere is required for fabrication.

There is a significant body of literature on MgO ceramic insulation. The next action would be a more detailed evaluation of Mg chemical and mechanical effects on sheath materials.

References

[1] Fornwalt, D.E., Gourley, B.R., Manzione, A.V., "A Study of the Compatibility of Selected Refractory Metals with Various Ceramic Insulation Materials," Pratt and Whitney Aircraft Division, CNLM-5942, 30Nov1964.

2.2.4.10. *SiO₂*

SiO_2 is known from previous compatibility studies [1] to react with several important sheath materials. In these experiments, the Si was a contaminant in the insulation and formed silicides in the metal sheath. This released oxygen to the sheath environment, allowing it to form oxides with the sheath metal.

References

[1] Fornwalt, D.E., Gourley, B.R., Manzione, A.V., "A Study of the Compatibility of Selected Refractory Metals with Various Ceramic Insulation Materials," Pratt and Whitney Aircraft Division, CNLM-5942, 30Nov1964.

2.3. General Physical Design Issues

2.3.1. Heat Transfer

The design of the RTD or TC must accommodate the following heat transfer considerations:

- i. The sensor must be adequately thermally connected to the pipe to ensure that the sensing element reaches the pipe temperature.

Pre Decisional – For Planning and Discussion Purposes Only

- ii. Heat losses from the pipe via the sensor sheath must not significantly alter the pipe temperature.
- iii. For RTDs, the entire sensing coil must reach the sensing-point temperature. For TCs, the junction must reach the sense point temperature and must cool to the reference temperature *before connections are made to other materials*.
- iv. The sensor design must have a satisfactory transient response time. This may require the use of *thinner sheaths and insulators, and potted coils in RTD designs*.
- v. For RTD designs, self heating must be minimized to prevent erroneous temperature measurements.

In the SP-100 program reference temperature sensor [1], the TC sheath was to be diffusion bonded to a Nb block with a V bonding layer. The Nb block was to be hot isostatically bonded to a Nb-1Zr block that itself is bonded to a boss of the side of the reactor vessel. This configuration was to have maintained a sensor time constant of less than 8 seconds, the SP-100 sensor criteria.

For the Prometheus reactor, a ten second time constant has been defined as a target. Unlike the single-wall pipe, liquid metal cooled SP-100 concept, the Prometheus reactor is anticipated to have an insulated double wall to contain a gas phase coolant. *These design issues introduce several sources of thermal resistance that may make small response time constants unobtainable. The impact of this pipe design on temperature sensing, particularly its accuracy and response times, must be fully evaluated.*

References

[1] "Updated GFS Requirements and Design Description," Attachment to PIR 1810-D5-1056, General Electric, May 1992.

2.3.2. Joints between Sensors and Cables

In all sensor designs, it is probable that the materials and construction methods employed in the sensor will be different from those employed in the cable leads. *This will necessitate a transition between the sensor and cable that can become a point of failure. A detailed evaluation of related material fabrication, electronic, joining, venting, and gas sealing issues for this joint is necessary.*

2.3.3. Wire Dimensions

A detailed study of signal stability and drift, grain growth and failure, heat transfer, and material interdiffusion in small wires is necessary as part of the RTD and TC designs.

2.3.4. Mounting

In the SP-100 design, the sensor was sheathed in pure Nb. The sheath was bonded to a Nb block using a V diffusion assistance layer and HIPed at 1200°C and 200psi for 3 hours [1] (this process as developed but never demonstrated in a full scale sensor assembly). The Nb block was then HIP bonded to a Nb-1Zr block at 1450°C and 15,000psi for 1 hour. *Due to the anticipated plant differences between the Prometheus design and the SP-100 design other mounting options may be necessary.*

For the sensor to function properly, the TC junction or RTD coil must be heated to the temperature of the component being monitored. The goal of the measurement is to sense fluid temperature. If the sensor is attached to the side of the pipe, the best performance it can deliver is to measure the pipe

temperature. If the pipe-in-pipe geometry is adopted, an accurate model will have to be developed that relates superalloy pipe temperature to the fluid temperature.

The ideal installation for both TCs and RTDs is to have a well in the pipe. From the standpoint of material compatibility, the well material probably does not impact the sensor design since an insert can be used to block interaction between the sheath and well.

Since a superalloy well may not have enough strength in a full T_{Hot} well installation, a refractory metal well may be called for. The well will have to be attached to the pipe in a way that does not transport excessive heat to the pipe. It will also have to penetrate the insulation in a way that does not result in a thermal hot spot on the outer pipe. One option for setting up such a refractory metal well is illustrated in Figure 2-5 below.

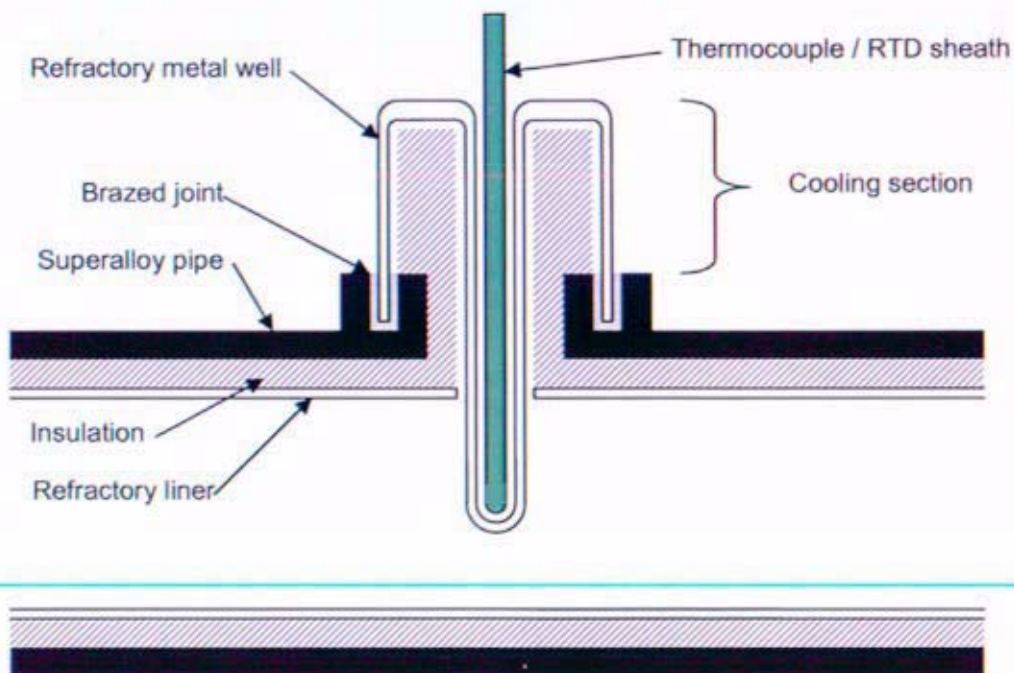


Figure 2-5. One method of creating a refractory metal well for use in an insulated pipe design. This method avoids creating a hot spot on the superalloy pipe and relies on a brazed joint as a pressure boundary.

Because the reactor outlet piping using the pipe-in-pipe concept delivers coolant from the reactor outlet to the Brayton machine turbine inlet without a significant loss of heat or temperature reduction, the measurement of the coolant temperature could notionally occur at the inlet. The turbine housing may be made of a cast nickel alloy material capable of withstanding the high reactor coolant outlet temperatures without significant creep. This could allow the incorporation of a cast dry well into the turbine inlet housing that overcomes many of the problems associated with the reactor outlet piping well. However, with this approach the well must be located a sufficient distance upstream of the turbine to ensure that the expansion of the coolant in this region does not effect the accuracy of the temperature measurement. This alternative is shown in Figure 2-6.

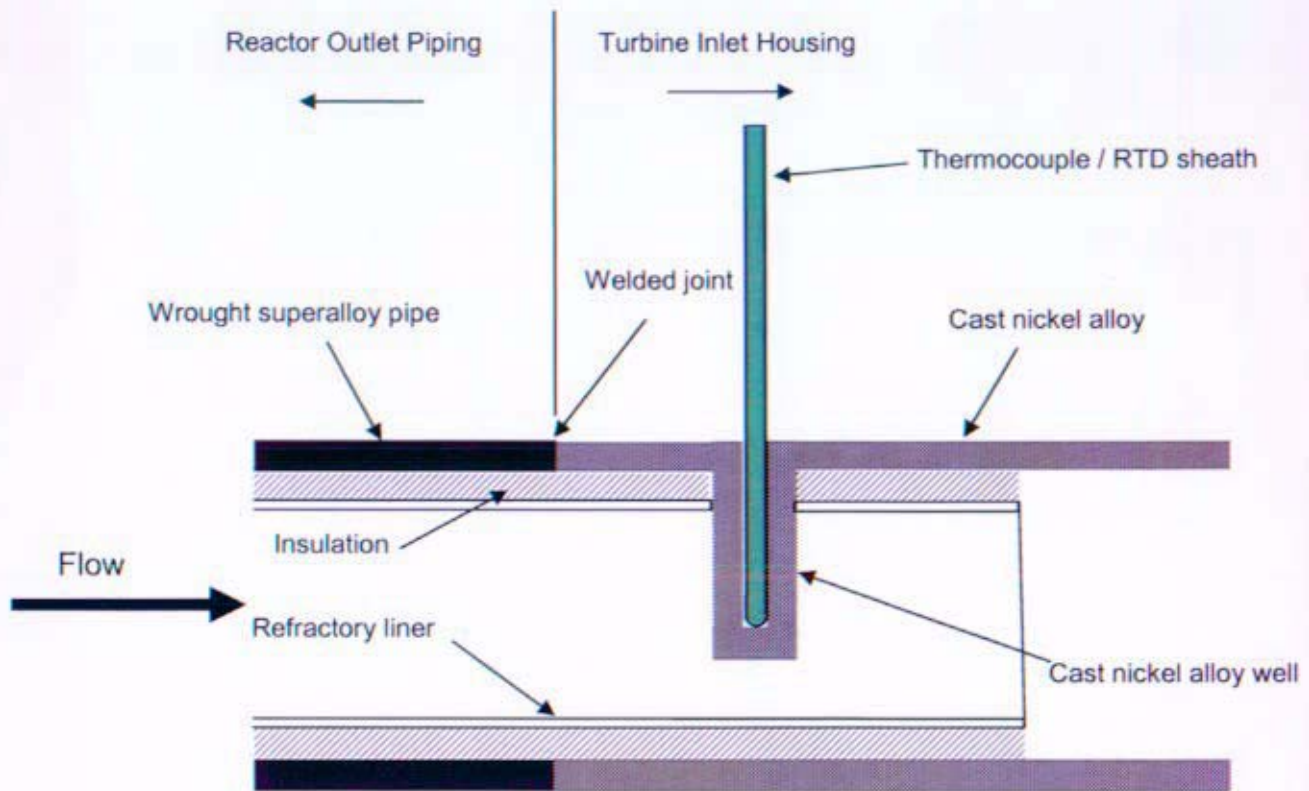


Figure 2-6. A cast turbine inlet dry well. The cast superalloy is assumed to be capable of high temperature performance. The pipe and housing weld is insulated from the high temperature coolant and located sufficiently far from this well to ensure the weld and the wrought piping material temperatures remain below 900K.

A third solution could be to strap the RTD/TC to the pipe wall. This solution is illustrated in Figure 2-below. In this option, the sheath is embedded in a material that is mechanically fixed or welded to the pipe. If the attachment block is strapped or otherwise mechanically attached to the pipe, it could be made out of a barrier material to prevent interaction between the sheath and pipe. If the block is welded to the pipe (and thus made of similar material), a separate barrier sleeve can be used around the sensor sheath to prevent interactions.

The advantage of this design is the avoidance of a piping penetration and weldment for a RTD/TC well, which potentially has a greater risk for boundary failure and gas coolant leakage than the piping itself. The principle disadvantage is the pipe internal insulation would have a much slower response time and the reactor coolant temperature must be extrapolated from the measured piping surface temperature with added uncertainty. The attachment block can be backed with thermal insulation to help it follow the wall/gas temperature more accurately but there is a danger that the superalloy pipe under the block will be overheated.

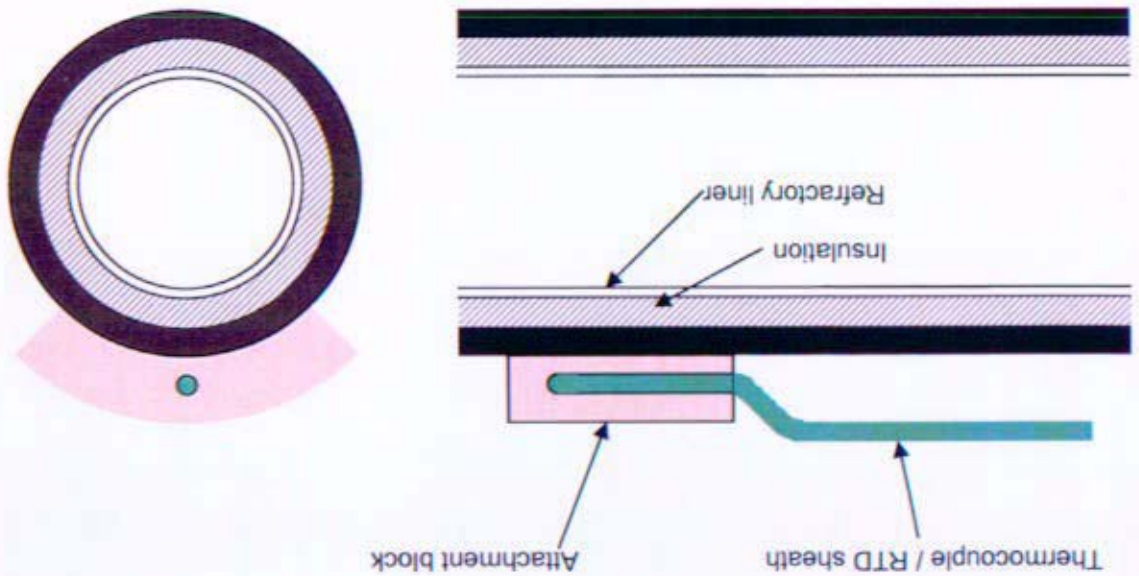


Figure 2-7. Method of attachment of a TC or RTD to a pipe sidewall.

Welding the RTD/TC sheath to the pipe is probably the worst option. Welding would require that the sheath be made of a material compatible with the pipe and would expose the sensing element to extremely high temperatures that could damage it. The weld-joint would provide the lowest thermal time constant between the pipe and sensor but at high cost. Diffusion bonding the sheath to the attachment block and welding or fixturing that block to the pipe could be an alternative to welding if a suitable material combination can be identified.

2.3.5. Cover Gas

A cover gas, or backfill gas, is any gas contained in the TC or RTD sheath. There are several important reasons for using a cover gas. In designs that use loose, uncompact insulation or insulation beads, a cover gas increases the thermal conductivity between the element and sheath. This reduces the response time of the sensor, especially when the principle mechanism of heat transfer is conduction at lower reactor coolant temperatures. The cover gas can also reduce material interactions by providing a barrier to direct, evaporative transport from one surface to another at high temperature. In addition, some materials require a gas partial pressure above their surfaces to remain stable. These conditions are particularly important when the sensor is operated at high temperature.

These advantages come with added risk. There are several ways that the cover gas can be lost to the space environment. If the sensor design requires the gas for proper functioning, its loss may lead to sensor failure. The cover gas may be lost through a leak caused by launch or thermal stresses. It may also be lost by leakage through grain boundaries in the metallic sheath or diffusion through the sheath material. Leak rates for small molecule gases such as He can be particularly large and must be evaluated. The presence of a trapped gas in the sheath also places a hoop stress on the sheath [1].

Pre Decisional – For Planning and Discussion Purposes Only

References
[1] "Fabrication of SP-100 High Temperature Sensor Attachment," GE SP-100 Program Information Request 1027, Dated 1/16/92.

In the highest temperature regions, this stress may be enough to cause dimensional creep or even sheath failure.

The need to prevent loss of the cover gas necessitates the need for a cold end seal on the sensor sheath. Depending on the device design, this may require glass-to-metal bonding, ceramic-to-metal bonding, polymer sealants, or ceramic paste technology. For operation in air, the seal is still necessary to prevent oxygen from diffusing down the sheath and causing failure of the sheath and thermoelement. In previous studies [2], sheaths have suffered complete radial failure (a "bamboo split") in as little as 3500 hours at 1339K by this mechanism. Such a failure is shown in Figure 2-6. Early in this work, epoxy cold end seals were used but proved unreliable.



Figure 2-6. A high temperature TC test fixture consisting of multiple TCs passing through a pressure boundary and terminating in an isothermal block. Most of the TCs have suffered a "bamboo split" failure due to oxygen diffusion into the sheath through the unsealed cold end. Reproduced from [3].

Potential cold end sealing techniques for the RTD/TC sheaths require study. Similarly the effects of different cover gasses requires further investigation.

References

- [1] R.C. Knight, N.S. Cannon, "SP-100 Reference Temperature Sensor Summary Report," Westinghouse Hanford Company, WHC-SP-1080, Rev. 0, April 1994.
- [2] P. Bliss and S. Fanciullo, "High Temperature Thermometry at Pratt and Whitney Aircraft-CANEL," PWAC-462, Pratt and Whitney Aircraft, Connecticut Aircraft Nuclear Engine Lab, 1 June 1965.

Pre Decisional – For Planning and Discussion Purposes Only

[3] P. Bliss, S. Franciullo, "High Temperature Thermometry at Pratt and Whitney Aircraft-CANEL," PWAC-462, Pratt and Whitney Aircraft, Connecticut Aircraft Nuclear Engine Lab, 01 Jun 1965.

2.3.6. Insulation

Oxide ceramic insulation for high temperature RTDs and TCs can take four forms: sintered, hard-fired beads, loose powdered insulation, cured ceramic paste insulation, and compacted insulation. Loose powder insulation is uncommon because it is difficult to load the powder into the sheath and maintain uniform wire spacing.

Hard-fired beads are a common insulation form. In this method, the two or four sensor wires are threaded through uniformly spaced holes in a ceramic cylinder. The cylinders may have flat ends or cupped ends that allow the beads to nest together. This wire and insulator assembly fits in the sheath with enough clearance for easy insertion and sheath bending.

Compacted insulation starts with the use of crushable beads, similar to the more compacted, hard-fired ceramic beads. The sensor is fabricated by threading the wires through the beads, loading the assembly into a sheath, and swaging the assembly to a smaller diameter. This crushes the beads while retaining the relative location of the wires with respect to each other. This is another common assembly method.

Evidence suggests that the used of beads alone may not be adequate. Homewood [1] used homogeneity tests to show excess contamination of a Pt-Rh TC at regions where the SiO₂ insulation beads butted together (each bead was 4 in. long over a 48 in. length of TC). For this reason, the general practice is to backfill the gaps in the insulation system with powder insulation.

Each insulation form should be evaluated based for their heat transfer, vibration, and mechanical deformation characteristics.

References

[1] C. F. Homewood, "Factors Affecting the Life of Platinum Thermocouples," *Temperature: Its Measurement and Control in Science and Industry*, Reinhold Publishing Corporation, New York, 1941.

3. Resistance Temperature Detectors

There are three general RTD thermoelement concepts: wire-wound, thin film, and ceramic. In wire wound RTDs, the conductor is a thin wire that is wound into a coil or around an insulating bobbin. This is, by far, the most common type and is the type described in this report. The thermoelement in thin film RTD is a thin metallic film or wire deposited and patterned on an insulating substrate. It is commercially available RTD with an increasing share of the market due in large part to its ease of manufacture and lower cost. Neither a wire wound RTD nor a thin film RTD currently exist capable of meeting the temperature sensor requirements. There are few applications demanding such high temperature service for such a long period of time without significant drift, and so their application is generally found at temperatures less than 1000K. For high temperature applications both forms of the RTD are subject to significant drift mechanisms induced by the thermal environment, including composition changes, differential thermal expansion between the element and its substrate, and grain growth. To overcome these challenges, Reference [1] suggested the development of a bulk ceramic RTD made entirely of a single material that would theoretically eliminate the differential thermal expansion as a drift mechanism. This concept represents the final RTD type, the ceramic RTD.

While both the wire-wound and the thin film devices are subject to the same issues, the latter is considered to be more severely affected. For this reason, the evaluation herein focuses on the wire-wound form of the RTD. The basic operation of the RTD including the various methods of measurement are described. Some of the salient issues associated with high temperature implementation are enumerated. Finally, some of the potential material systems for the device are discussed.

In References [1] and [2] presents further discussions of the SNPP reactor coolant temperature sensing using a RTD technology. The former compares RTDs against a number of other temperature technologies, detailing many of the features and challenges of each. Reference [2] proposes design processes for both the wire-wound and the ceramic RTDs and suggests conceptual designs and materials for the prototypes of each type.

References

- [1] JIMO Reactor Sensor Technology Development Plan, ORNL/LTR/NR-PROM1/05-01, January 2005
- [1] Resistance Temperature Detector Conceptual Design for Space Nuclear Power Systems, ORNL/LTR/NR-PROM1/05-11, June 2005.

3.1. Operation

A resistance temperature detector (RTDs) is thermoelectric element whose material resistance is a significant function of the element temperature, such that as the temperature of the element increases, the RTD resistance correspondingly increases. This change in resistance is typically sensed as an imbalance in a resistive Wheatstone bridge, one leg of which is formed by the RTD element, and results in an output proportional to its temperature.

3.1.1. Sensor Electrical Configuration

RTDs can be connected to signal processing electronics via three different configurations: 2-wire, 3-wire, and 4-wire. The configurations differ in the lead wire compensation they provide, but all three require a precision power supply to supply current to the coil and precision analog-to-digital conversion to provide a voltage value that can be mapped to temperature.

Pre Decisional – For Planning and Discussion Purposes Only

The 2-wire configuration is the simplest and lightest layout but has a lead resistance that is inserted in parallel with the sensor resistance. Changes in lead resistance due to temperature, drift, or damage are superimposed on the resistance of the sensing coil, leading to temperature error. Lead resistance error can be partially mitigated by minimizing the lead resistance (shorter leads and/or thicker wire) or pre-measurement and subtraction from the total sensor resistance. Signal processing presents no significant challenges with this sensor configuration.

In the 3-wire configuration, a wire is placed in parallel with one of the two leads and its resistance is inserted as compensation in the measurement bridge. If the third lead has the same resistance as the original two, this compensates for the lead resistance (assuming no current is drawn for the bridge voltage measurement) and only the coil resistance is measured. An extra wire is required by this approach resulting in a small increase in mass.

In the 4-wire configuration, two pairs of wires are used to separately provide current to, and measure the resistance of, the sensor coil. Assuming a high impedance voltage measurement system, the system is insensitive to differences in lead wire resistance, thus removing a large source of error. The two additional wires necessary to implement this approach represent a small increase in cabling mass compared to the 2-wire scheme.

3.2. Issues

3.2.1. Resistivity

For wire-wound RTDs, the raw resistivity of the conductor plays a critical role in the design by dictating the size of the sensing coil. In general, thicker wires make for more robust high temperature sensors because they are mechanically stronger and require a longer time to become compromised by microstructural changes and impurity diffusion. Unfortunately, thick wires have lower resistance than thin wires and require larger coils to develop the same resistance. This makes the sensor larger and limits its installation options. The design preference is for a material with the highest possible resistivity. Figure 3-1 shows the resistivity vs. temperature of 13 pure refractory metals.

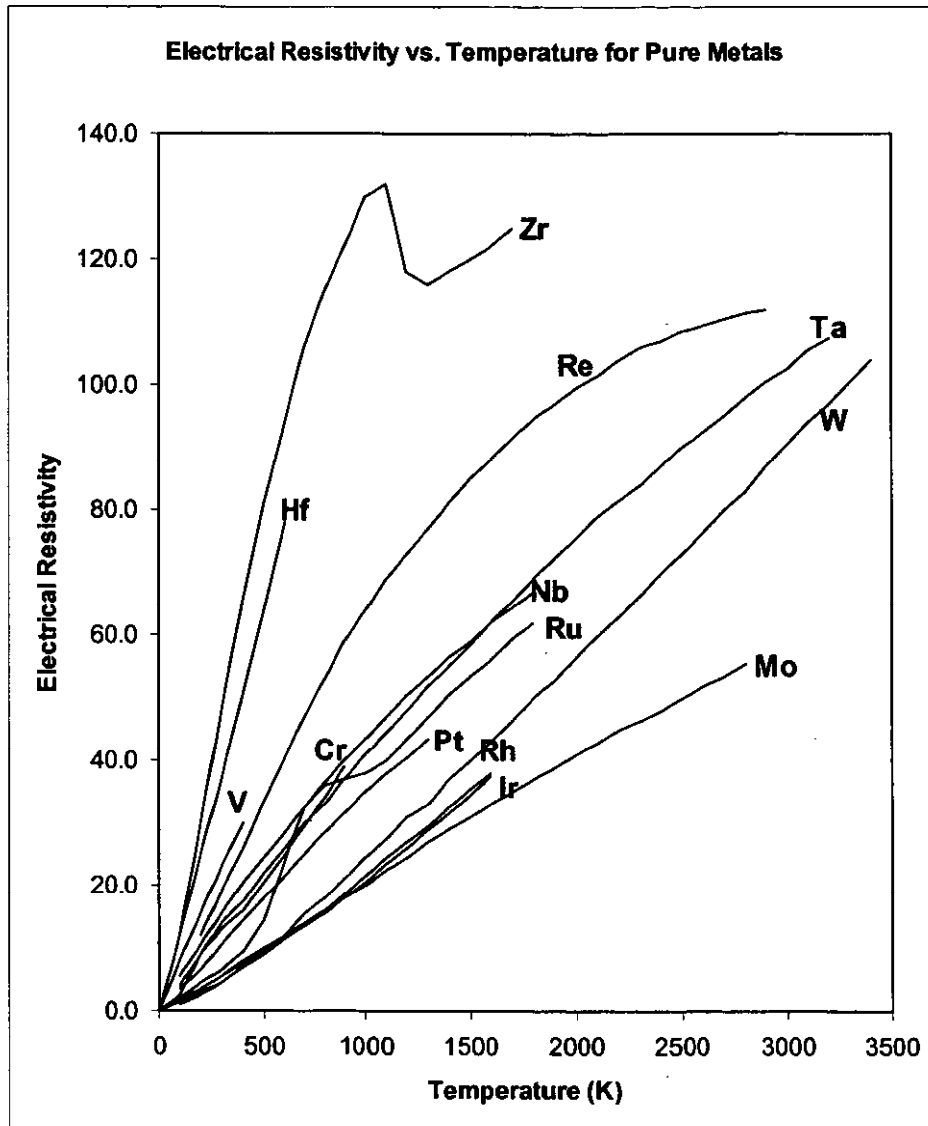


Figure 3-1. Electrical resistivity vs. Temperature for candidate RTD element materials.

3.2.2. Temperature Coefficient of Resistivity

The temperature coefficient of resistivity (TCR) is a measure of the change in electrical resistivity of a material with temperature. This property is the basis of RTD operation. The standard definition of TCR assumes that the value is not a function of temperature. Although this is true for many materials, there are some materials with high resistance values that do not have a constant TCR over the operating range. If the non-linearity can be linearized, this may not be a problem for the sensor's design.

In both linear and non-linear resistivity behavior, the important question is whether resistivity drift can be recharacterized using a single-point calibration. For example, assume a material with a linear resistivity vs. temperature relationship. Irradiation and time-at-temperature effects will alter its calibration. If the altered resistivity vs. temperature relationship is still linear, then the new relationship

can be found with a single point calibration and the *assumption* that the resistivity goes to zero at 0K. If, instead, the material becomes non-linear, or a non-linear material changes in an unpredictable way, then multipoint recalibration is necessary. The design preference is for a material possessing a high TCR that does not drift due to irradiation and temperature effects, or remains linear if it does.

3.2.3. Coil Design

Wire RTDs can be wound in one of several different configurations. Each configuration has different sensitivities to vibration, thermal and mechanical strains, and induced magnetic fields. The designs also differ in their thermal response times and ease of fabrication.

3.3. Candidate Elements

3.3.1. Overview

Throughout the plant, the baseline operating temperatures at full power around the loop are expected to vary from 379K (secondary water return from the radiators) to 1150K (reactor hot leg temperature). It is also possible that the reactor could experience temperature transients of as much as 115K (10%) above the average temperature for periods of up to several hours. The sensor must be capable of withstanding these transients. In addition, the plant is expected to experience temperatures as low as 250K during the orbital/coast period prior to initial startup. The need for temperature measures at various locations whose temperatures differ significantly suggest that more than one RTD design may be appropriate. Moreover, the severity of the temperatures at the inlet and outlet to the reactor and at the inlet to the power conversion system, i.e., the turbine inlet of a Brayton machine may require a particularly robust device, while the temperatures at the remaining locations are significantly moderated and may allow the use of existing RTD technology and materials.

It should also be noted that there are RTD device developmental considerations which may mandate a higher temperature design than that suggested by the maximum reactor coolant temperature at the intended loop location. The ability to perform testing on the prototype RTD designs, such as accelerated life testing, may mandate a high temperature tolerance to avoid the potential for catastrophic failures.

3.3.2. Thermoelement Materials

Due to the system temperatures possible, the material candidates for the coil are limited to the high temperature metals and their alloys. It is good engineering practice to use materials with melting temperatures at least several hundred degrees Kelvin above the maximum expected temperature. Using 2000K as an arbitrary cutoff, the possible materials include W, Re, Os, Ta, Mo, Nb, Ir, Ru, Hf, Tc, Rh, V, Cr, Zr, Pt, Th, and many of their alloys.

Of these materials, several can be immediately eliminated from serious consideration due to various disqualifying aspects. Th is a radioactive heavy element that has isotopes that undergo alpha and beta decay, thus presenting safety, contamination, and administrative barriers to its use. Zr is known to reduce many potential oxide insulators at the operating temperature. Tc is not naturally occurring, and Os has an oxide, OsO₄, that is toxic and boils at 130°C. Work underway at the time of project discontinuation included an examination of the remaining materials for use as RTD thermoelements.

3.3.2.1. *Re*

The general properties of Re as a sheath material are discussed in section 2.1.9.2. In addition to these properties, Re is also known to have a high recrystallization temperature compared to the other refractories and a longer rupture life than W at temperatures up to 2800°C. Both properties are advantages for thermoelement designs because a major failure mode of thermoelements is grain boundary bridging across the thermoelement cross section.

3.3.2.2. *W, AKS-W, and W-Re alloys*

W is commonly used as a filament material because it offers high strength at extremely high temperatures. W is initially ductile at room temperature, but becomes brittle after its first recrystallization. The ductile-to-brittle transition temperature of W is also a function of grain size with DBTT dropping as grain size decreases below 0.1mm. The addition of Re in percentages of 1% to 26% substantially increases room temperature ductility.

W oxidizes in air to WO_3 [1]. The enthalpies of formation of WO , WO_2 , and WO_3 suggest that W will not reduce any of the insulator oxides under consideration. At temperatures above 800°C, WO_3 evaporation rates can be substantial.

One potentially valuable W alloy is AKS-W. This alloy is processed from a powder that contains the W, Si, Al, and K constituents. After sintering and drawing, the wire is annealed at high temperature, which allows the Al and Si, both of which are soluble in W, to diffuse to the wire surface and evaporate. The K is not soluble. During the drawing process, K inclusions are drawn into long bubbles, which pinch off to form grain-pinning regions. The result is an elevated recrystallization temperature and superior strength and creep resistance at high temperatures.

References

[1] S. W. H. Yih, C. T. Wang, "Tungsten: Sources, Metallurgy, Properties, and Applications," Plenum Press, New York, 1979.

3.3.2.3. *Mo, ODS-Mo, TZM, and Mo-Re alloys*

Studies of Molybdenum and its alloys as a RTD thermoelement should be performed.

3.3.2.4. *Ta, T-111, ASTAR-8111C, and Ta-W alloys*

Studies of Tantalum and its alloys as a RTD thermoelement should be performed.

3.3.2.5. *Nb, Nb-1Zr, FS-85, PWC-11*

Restrictions on the use of Nb and its alloys in thermoelements are similar to the restrictions for their use in sheaths. Specifically, Nb alloys with Zr are incompatible with many of the insulators under consideration. See section 2.1.9.4 for additional discussion on this topic. Since Zr is the most common alloying component in Nb, only pure Nb is a thermoelement option.

3.3.2.6. *Rh*

Studies of Rhodium and its alloys as a RTD thermoelement should be performed.

3.3.2.7. *Ir and Ir-Rh alloys*

Studies of Iridium and its alloys as a RTD thermoelement should be performed.

3.3.2.8. Pt, ODS-Pt, and P-Rh alloys

Studies of Platinum and its alloys as a RTD thermoelement should be performed.

3.3.2.9. Ru

Studies of Ruthenium and its alloys as a RTD thermoelement should be performed.

3.3.2.10. Hf

Studies of Hafnium and its alloys as a RTD thermoelement should be performed.

3.3.2.11. V

Studies of Vanadium and its alloys as a RTD thermoelement should be performed.

3.3.2.12. Cr

Studies of Chromium and its alloys as a RTD thermoelement should be performed.

3.4. Insulators, Sheaths, Seals, and Cabling

Analysis of several RTD / TC shunt resistance models for evaluating minimum insulation thicknesses is required. Other aspects of the design, such as transitions between different high and low temperature sheathing concepts and cold end sealing should also be studied.

4. Thermocouples

4.1. Thermocouple Operation

TC voltage is generated in the temperature gradient section of the sensor, with the junction serving as the common reference point for both legs. In TC design, a large Seebeck voltage with a large temperature coefficient is most desirable. It is also desirable for the voltage have a linear one-to-one relationship with temperature that is constant with time/temperature history. If TCs are present in the system, a reference temperature and reference temperature sensor are also required. The reference temperature sensor is typically a precision RTD.

4.2. Sensor Configuration

TCs can be fabricated in several configurations. The most common design is the ungrounded design where the two thermoelements of different materials are electrically insulated from the sheath at all points. This design reduces the level of electrical noise picked up by the sheath that is coupled to the output signal. Since the junction is insulated from the sheath, it increases the sensor response time compared to a grounded design. It also minimizes problems resulting from different thermal expansion coefficients between the wires and sheath. In the grounded design, the junction is in contact with the end of the sheath. This results in a comparatively rapid response time, increases the potential for electrical noise coupling into the sensor, and raises the risk of thermal expansion problems. A variation of this design involves a single wire run through the sheath and connected to the end such that the sheath acts as the second material. For the Prometheus SNPP, a two-conductor, ungrounded design appears most appropriate.

4.3. Candidate Elements

4.3.1. Type K

The Type K element consists of a positive leg of Ni-10Cr (Chromel) and a negative leg of Ni-5AlSi (Alumel). Its temperature range is about 73K (-200C) to 1523K (1250°C). Use in vacuum and low oxygen conditions should be avoided. The Alumel leg is magnetic.

Type K TCs were tested for 10,000 hours at between 1339K and 1366K by Pratt and Whitney [1]. The TCs were composed of 24 gage, ungrounded thermoelements (grounded elements may form a low melting point eutectic with the Nb-1Zr sheath), preformed Al_2O_3 insulators, and 22 mil wall thickness Nb-1Zr sheaths. After assembly, the thermoelements were backfilled with dry Ar and swaged to a diameter of 3.175mm (0.125 inch). The TCs were tested in an environment of 3-5psig Ar. During two rounds of testing, encompassing 20 TCs total, the largest drift noted was -1.45% (-20.5 K) and none of the TCs failed during the test.

Post test analysis indicated several metallurgical effects. Nitrogen contaminants in the furnace environment resulted in the formation of Nb_2N in the sheath outer surface. On the inner surface of the sheath, Nb_2Al , Nb_3Al , and Nb_5Si_3 were detected, indicating reduction of the Al_2O_3 insulator by the Zr in the sheath, and/or dissolution of the thermoelement wires. O_2 from the insulator formed ZrO_2 in the bulk sheath material. Grain growth in the Alumel wire was described as excessive. In both elements, grain growth resulted in grain boundaries that grew across the wire thickness. In two TCs that became grounded during the fabrication process, no eutectic was formed with the sheath materials.

The standard PW-CANEL thermocouple design was an ungrounded, Nb-1Zr sheathed, Al_2O_3 insulated design as shown in Figure 4-1 [2]. A Ta plug was used at the end to prevent the contamination of the hot end cap weld with O_2 from the insulator (the weld was in contact with liquid Li outside the sheath). A Ta foil barrier was installed between the insulator and sheath in the hottest region to prevent the diffusion of Ni from the thermoelements into the sheath. Ni contamination of the Nb sheath can drop its melting temperature from 2469°C (2732K) to 1175°C (1448K) at 69.5at% Ni. This is less than the 1204°C (1477K) system that the design is intended to service. In contrast, Ni contamination of the Ta liner will drop the liner's melting temperature to only 1350°C (1623K) at 64at% Ni. Diffusion of Ta into the Nb sheath will only raise the alloys melting temperature.

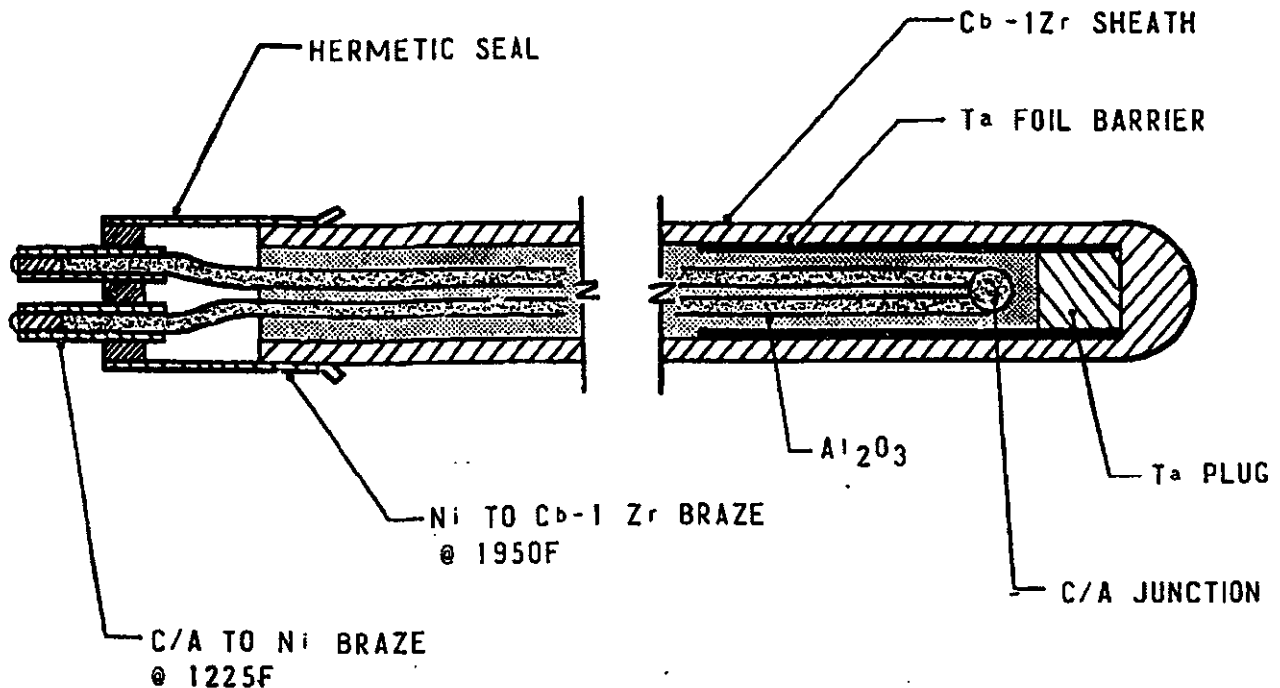


Figure 4-1. The Pratt and Whitney-CANEL type K thermocouple design for high temperature (2200F), long duration (>10,000 hours) thermometry applications. This design is swaged. C/A refers to Chromel/Alumel. Cb refers to Columbium, an early name for Niobium. Reproduced from [2].

References

- [1] S. Fanciullo, "Drift and Endurance Testing of Chromel/Alumel, W-5Re/W-26Re and Mo/W-26Re Thermocouples at 1950F to 2000F for 10,000 hours," PWAC-454, Pratt and Whitney Aircraft, Connecticut Aircraft Nuclear Engine Lab, 23 Feb 1965.
- [2] P. Bliss, S. Fanciullo, "High Temperature Thermometry at Pratt and Whitney Aircraft-CANEL," PWAC-462, Pratt and Whitney Aircraft, Connecticut Aircraft Nuclear Engine Lab, 01 Jun 1965.

4.3.2. Type N

The Type N element consists of a positive leg of Ni-14Cr-1.5Si (Nicrosil) and a negative leg of Ni-4.5Si-0.1Mg (Nisil). Its temperature range is 3K(-270C) to 1573K(1300°C). Type N TCs were still under investigation when the project ended.

4.3.3. Type R, S, B and other Pt/Rh variants

Type R and S thermocouples use a pure Pt negative leg and a Pt-13Rh or Pt-10Rh positive leg respectively. Both have a temperature range of 273K (0C) to 1723K (1450°C). Type B thermocouples have a positive leg of Pt-30Rh and a negative leg of Pt-6Rh. Its temperature range is 273K (0C) to 1973K (1700°C).

Operation of Pt/Rh thermocouples in a vacuum environment (surrounding the elements) is not recommended because of the potential for element cross-contamination. This occurs when the Rh evaporates from one element, condenses on the other, and diffuses into it [2]. This reduces the compositional difference between the two and reduces the thermoelectric output. In addition, at temperatures above 1373K (1100°C), the Pt and Rh volatilize at a different rate (Rh is faster), which also leads to compositional changes [3]. Volitization can be detected by the presence of metallic

Pre Decisional – For Planning and Discussion Purposes Only

crystals inside the insulator bore. To reduce the effect of evaporation, Rh can be added to the negative leg and the Rh content of the positive leg increased. Pt-1Rh vs. Pt-10Rh is useable up to 1873K (1600°C), Pt-5Rh vs. Pt-20Rh is useable up to 1973K (1700°C), Pt-6Rh vs. Pt-30Rh (Type B) is useable up to 1973K (1700°C), and the Pt-20Rh vs. Pt-40Rh is useable up to 2073 (1800°C). In addition to slowing the rate of cross-contamination, the addition of Rh provides some solid solution strengthening at high temperature. Above 1033K (760°C), Pt and Rh are completely soluble in each other. Below this temperature, they are completely insoluble at Rh concentrations between ~4wt% and ~85wt%.

In general, Pt thermocouples are noted for their ability to operate at high temperatures in air and other oxidizing environments. Still, operation at high temperature in air for long durations can result in oxidation of the Rh component and decalibration. At temperatures below 673K (400°C), oxidation does not occur. At temperatures between, 673K (400°C) and 873K (600°C) the Rh component of the alloy can oxidize to Rh_2O_3 . This lowers the positive potential of the thermoelement due to the loss of Rh from the alloy. At temperatures above about 1273K (1000°C), the oxide reverts to the pure metal and the thermoelement voltage is largely restored.

Grain growth in the pure Pt element is also a problem at high temperatures. A 90% cold worked Pt wire can be completely annealed at 673K (400°C) in 1 hour. As the grains grow, impurities that collect at the boundaries are concentrated since the grain boundary area is reduced. When these brittle grain boundaries cross the wire thickness, the wire can easily fracture at that point. To minimize the chance of fracture, the element should be designed to minimize stresses and vibration in the wire. Elements that are annealed to large grain sizes are also more susceptible to contamination [2].

There are two options for improving the mechanical properties of pure Pt. The first is the use of a form of composite cold-worked Pt called fibro-Pt [5]. In this material, a tube of cast Pt is filled with highly cold-worked Pt strands. The tube is then swaged and annealed down to the final wire size. The result is a composite of Pt with an elongated grain structure and improved creep strength over pure Pt. Compared with Pt-Rh alloys, Fibro-Pt has similar creep strength to Pt-5Rh but less strength than Pt alloys with more Rh.

Another option for strengthening pure Pt is to use oxide dispersion strengthened (ODS) Pt. ODS-Pt is a form of Pt that is strengthened by the inclusion of Y_2O_3 or ZrO_2 precipitates. The precipitates retard grain growth at high temperature and increase wire lifetime.

The Pt-Rh TC has been around since 1886 and some long lifetime experiments have been performed as far back as 1939 indicating multiple year performance in stationary installations. In one set of experiments performed at the New Jersey Zinc Company [1], six Pt-13Rh TCs were exposed to 1563K (1290°C) for 23800 hours (2.7 years). One of the TCs was exposed for an additional period for a total of 27500 hours (3.1 years). All TCs survived the temperature run and were found to read within 6K (6°C) to 9K (9°C) of the standard calibration for Type R TCs at the end of the run suggesting a drift of approximately 2.2K/year to 2.9K/year.

The construction of the TCs consisted of 0.56mm diameter wires inserted in a circular, double bore SiO_2 insulator with a bore diameter of 1mm and OD of 8.5mm. The insulator/thermoelement assembly was inserted in a primary protection tube made of Al_2O_3 that had an ID of 14mm and OD of 19mm. The primary protection tube was inserted in one of two 25.4mm holes in a secondary Al_2O_3 protection tube that had an outer dimension of 50.8mm x. 88.9mm. The other 25.4mm hole in the secondary protection tube was used to periodically insert a calibration TC to verify the device under test. The

large differences between wires and insulators minimized the stresses transmitted between surfaces and permitted air to circulate throughout the device. This was necessary to maintain a high O₂ partial around the SiO₂ insulator, preventing it from being reduced and releasing Si, which is readily absorbed by the thermoelements.

Although not the specific focus of the test, data has been collected for unsheathed, Type R TCs operating for 10,000 hours at 1339K to 1366K [1]. In this experiment, Al₂O₃ insulated, unsheathed, 0.635mm wire, Type R TCs were used as temperature references for the testing of other TC types. During the test, the Type Rs drifted negatively and suffered localized melting. The author hypothesized that the melting was caused by the absorption of Si in the Pt-13Rh element, leading to the formation of a low melting point eutectic. The silicon was believed to have been a contaminant in the Al₂O₃ retort that the experiment was carried out in. In a separate experiment carried out in a 310 stainless steel retort, the thermoelements suffered Mn contamination.

Si is particularly harmful to Pt. When alloyed with Pt, Si forms a eutectic with a melting temperature of about 1073K (800°C). It is also almost completely insoluble in Pt and segregates to the grain boundaries. The presence of the eutectic at the grain boundaries enhances the sliding of those boundaries and leads to wire failure.

Beyond Pt-Rh alloys, there are several other Pt alloys of note. Pd vs. Pt-15Ir TCs have a maximum temperature of around 2533K (1260°C) and are used in jet engine atmospheres. The Au-40Pd vs. Pt-10Ir can be used up to 1273K (1000°C) in air without calibration drift.

References

- [1] S. Fanciullo, "Drift and Endurance Testing of Chromel/Alumel, W-5Re/W-26Re and Mo/W-26Re Thermocouples at 1950F to 2000F for 10,000 hours," PWAC-454, Pratt and Whitney Aircraft, Connecticut Aircraft Nuclear Engine Lab, 23 Feb 1965.
- [2] E. D. Zysk, "Platinum Metal Thermocouples," Temperature: Its Measurement and Control in Science and Industry, Vol. 3, Charles. M. Herzfeld, editor-in-chief, Reinhold Publishing Corporation, New York, 1962.
- [3] C. F. Homewood, "Factors Affecting the Life of Platinum Thermocouples," Temperature: Its Measurement and Control in Science and Industry, Reinhold Publishing Corporation, New York, 1941.
- [4] B. Brenner, "Changes in Platinum Thermocouples Due to Oxidation," Temperature: Its Measurement and Control in Science and Industry, Reinhold Publishing Corporation, New York, 1941.
- [5] J. S. Hill "Fibro Platinum for Thermocouple Elements," Temperature: Its Measurement and Control in Science and Industry, Vol. 3, Charles. M. Herzfeld, editor-in-chief, Reinhold Publishing Corporation, New York, 1962.

4.3.4. Ir-Rh variants

The Ir vs. Rh-40Ir TC is good to 2273K (2000°C). Ir volatilizes faster than Rh at elevated temperatures, therefore a shift to Ir-40Rh vs. Rh-40Ir may result in a more stable TC. Ir is embrittled in H environments so it should not be operated at high temperatures in H. Additional information on this TC type was being sought when the project ended.

References

- [1] E. D. Zysk, "Platinum Metal Thermocouples," Temperature: Its Measurement and Control in Science and Industry, Vol. 3, Charles. M. Herzfeld, editor-in-chief, Reinhold Publishing Corporation, New York, 1962.

4.3.5. Type C

The Type C thermocouple consists of a positive element of W-5Re and a negative leg of W-26Re. Its temperature range is 273K (0°C) to 2593K (2320°C). This thermocouple design was selected for the SP-100 project and studied extensively for the space reactor application.

Type C TCs were tested for 10,000 hours (1.14 years) at between 1339K and 1366K by Pratt and Whitney [1]. The TC's were composed of 24 gage, grounded thermoelements, preformed Al_2O_3 insulators, and 22 mil wall thickness Nb-1Zr sheaths. After assembly, the thermoelements were backfilled with dry Ar and swaged to a diameter of 3.175mm (0.125 inch). The TC's were tested in an environment of 3-5psig Ar. During two rounds of testing, encompassing 16 TCs total, the largest drift noted was -0.55% (-7.5 K) and none of the TC's failed during the test.

Post test analysis indicated several metallurgical effects. Nitrogen contaminants in the furnace environment resulted in the formation of Nb_2N in the sheath outer surface. On the inner surface of the sheath, Nb_2Al , Nb_3Al , and Nb_5Si_3 were detected, indicating reduction of the Al_2O_3 insulator by the Zr in the sheath. O_2 from the insulator formed ZrO_2 in the bulk sheath material. The thermoelement wires themselves were good condition and no contamination was noted.

Compatibility studies [2] of Ta sheath material, W-5Re and W-26Re thermoelement wires, and insulators made of ThO_2 , Y_2O_3 , BeO, MgO, and Al_2O_3 have been performed at 1363K (1090°C), 1583K (1310°C), and 1813K (1540C) for 200, 500, and 1000 hours. The sheath was swaged to ensure good contact between the sheath, insulator, and wire materials. No reactions were noted for any time-temperature-material combination tested.

A W vs. W-26Re thermocouple was selected as the optimal design for the NERVA reactor. The NERVA reactor was developed for nuclear thermal propulsion. In this device, H_2 was pumped through a graphite-moderated core where it was heated to high temperatures and expelled through a nozzle at high velocity to produce thrust. From a materials selection perspective, the presence of C in the core strongly impacted the design. At high temperatures, C will alloy with the Mo sheath, resulting in a suppression of its melting temperature by 673K (400°C). This problem was mitigated by CVD coating the hot end of the Mo sheath with W to slow the diffusion of C into the sheath. The final design is illustrated in Figure 4-2. The design consists of a W coated Mo sheath and vitrified BeO insulation (probably stabilized with <1% MgO) and a Mo plug at the end. The cooler regions of the TC were sheathed with stainless steel and insulated with compacted MgO. The connection between the two sections was made with a stainless steel adapter that was overlapped and brazed to both sections.

In a later design, shown in Figure 4-3, the sheath was further protected by a Ta outer sheath. Ta was chosen because it has the highest melting temperature of all the refractory metals in the presence of C and is the most ductile as well. In this design, the inner Mo sheath is left uncoated and the outer Ta sheath is CVD coated with W, in this case to slow the diffusion of H into the Ta, which leads to embrittlement of the Ta.

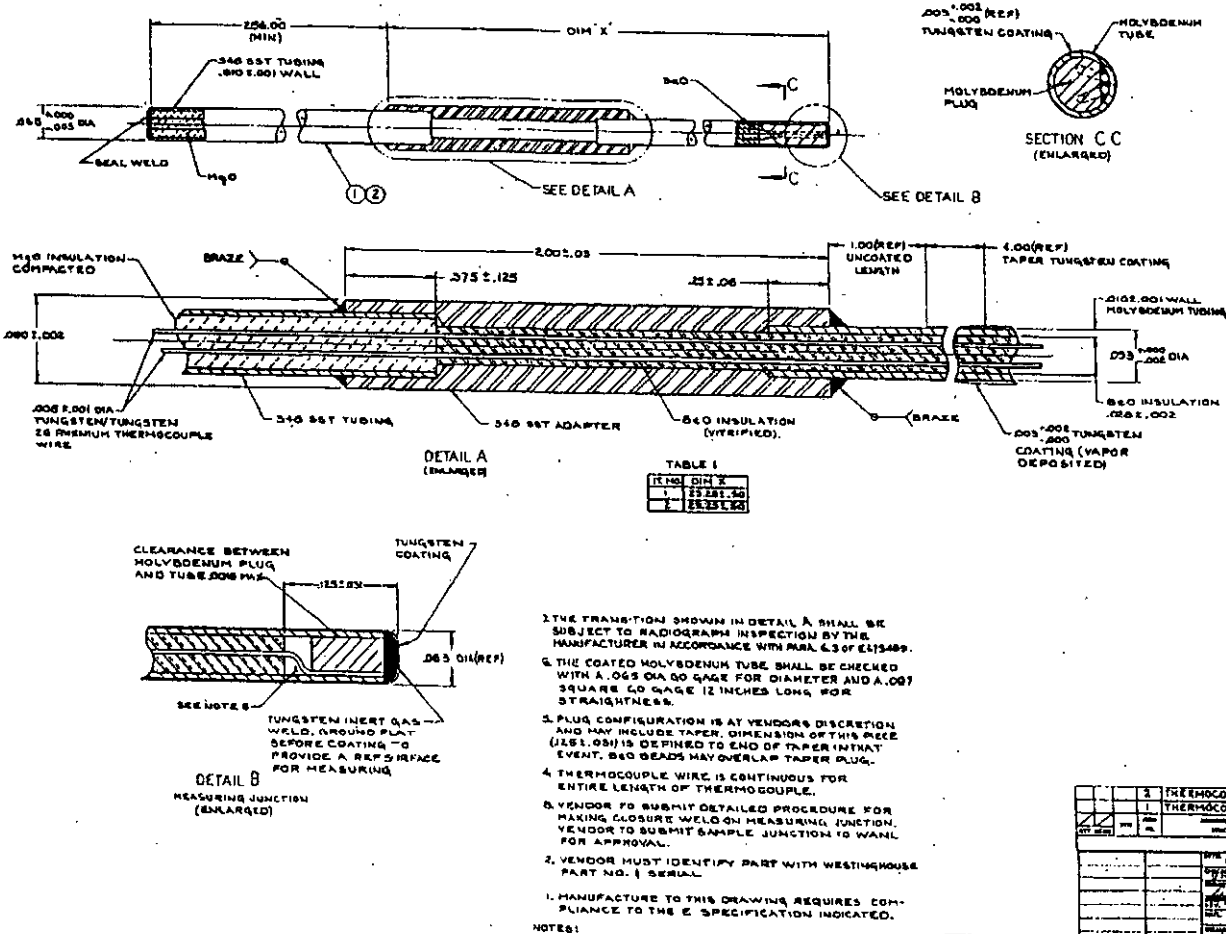


Figure 4-2. A W vs. W-26Re thermocouple developed for the NERVA reactor. The sensing end of the thermocouple is BeO insulated with a Mo sheath. The Mo sheath is further coated with a thin layer of W at its very end. The cool end of the TC is MgO or BeO insulated and uses a stainless steel sheath.[3]

4.3.6. Mo vs. W

TCs with legs of Mo and W should withstand temperatures up to the melting point of Mo around 2903K (2630°C). In theory, a combination of microstructurally modified materials, such as ODS-Mo vs. AKS-W, should produce a robust, high temperature TC. Unfortunately, the Mo vs W combination suffers an emf reversal around 1073K-1173K (800°C-900°C) where it stops decreasing and begins increasing [2]. As a result, the sensitivity of the sensor is lowest at temperatures around the plant operating temperature and the temperature-emf relationship is not one-to-one.

An alternative to the Type C TC is Mo/W-26Re. Mo/W-26Re TCs were tested for 10,000 hours (1.14 years) at between 1339K and 1366K by Pratt and Whitney [1]. The TC's were composed of 24 gage, grounded thermoelements, preformed Al₂O₃ insulators, and 22 mil wall thickness Nb-1Zr sheaths. After assembly, the thermoelements were backfilled with dry Ar and swaged to a diameter of 3.175mm (0.125 inch). The TC's were tested in an environment of 3-5psig Ar. During two rounds of testing, encompassing 7 TCs total, the largest drift noted was -0.90% (-12.3 K) and none of the TC's failed during the test. Post test analysis indicated several metallurgical effects, all of which were the same as for the similar experiment carried out on Type C TCs above.

References

- [1] S. Fanciullo, "Drift and Endurance Testing of Chromel/Alumel, W-5Re/W-26Re and Mo/W-26Re Thermocouples at 1950F to 2000F for 10,000 hours," PWAC-454, Pratt and Whitney Aircraft, Connecticut Aircraft Nuclear Engine Lab, 23 Feb 1965.
[2] F.R. Caldwell, "Thermocouple Materials," National Bureau of Standards Monograph 40, 1 March 1962.

4.3.7. Nb-1Zr vs. Mo and Mo-5Nb vs. Nb-40Mo

4.4. Fabrication Process

In the effort to produce robust, long-life, low-drift thermocouples, material purity and process quality must be a primary concern. The processes of the Pratt and Whitney and SP-100 for TC fabrication show two approaches to meeting these challenges. exemplify these concerns.

5. In-Situ Calibration Options

It should be a the goal of the RTD and TC design is to provide a drift free device, particularly for the high temperature reactor coolant locations at the inlet and outlet to the reactor and at the power conversion turbine inlet. It is commonly considered that typical thermocouple sensors that are exposed to high temperatures for long durations tend to drift out of calibration for a variety of reasons. These include sensing element strain, creep, diffusion, corrosion, material migration, and/or transmutation. Similarly for RTDs operated at the upper end of their temperature design envelop in which material changes are induced. However, it is also recognized that RTDs operated within moderate temperature envelopes can exhibit nearly drift free performance, and this should be the requirement for any advanced RTD/TC development effort.

Recognizing that the research and development effort for the high temperature RTD or TC may not be able to entirely eliminate the thermally induced drift problem, the possibility of remote recalibration of a SNPP temperature sensor should be considered. This section discusses several options for performing in-situ calibration of sensing elements after they are installed in the system and inaccessible.

5.1. Johnson Noise Thermometry

Johnson Noise Thermometry (JNT) is a method of temperature measurement using an RTD that takes advantage of the inherent thermal noise measured across a resistive sensor. The temperature can be calculated using knowledge of the measured mean squared noise voltage across the sensor, the measured sensor resistance, and the bandwidth over which the voltage is measured. The measurement equation for this technique is provided below. Note that other techniques utilizing noise voltage and noise current are possible that do not depend on sensing element resistance.

$$T = \frac{\overline{V}_{JNT}^2}{4 \cdot R \cdot k_b \cdot \Delta f}$$

where T is temperature (K), \overline{V}_{JNT}^2 is mean squared noise voltage (V^2), R is sensor resistance (ohm), k_b is Boltzmann's constant, and Δf is measurement bandwidth.

In practical terms, the amplifier gain needs to be known and stable. Second, the amplifier band pass and filtering effects of connection cabling must be well known within the required measured accuracy. Finally, the resistance of the sensor must be independently and accurately measured. This is usually accomplished through a parallel 4-wire Wheatstone bridge measurement of the thermoelement resistance.

The signals measured in noise thermometry are small; a thermometer with a 100 Ω sensor at 300K and a bandwidth of 100kHz produces a noise a signal of about 0.4 μ Vrms. Thus, the elimination of extraneous sources of noise and demonstration of their absence is one of the recurring issues in noise thermometry.

A second problem is the long measurement time. Because the thermometer measures noise, its output fluctuates about its expected value. To achieve an uncertainty equivalent to 3 mK a thermometer with a 100kHz bandwidth operating at 300K must integrate for a minimum of 27 hours. For industrial applications, the measurement time is less of a limitation, an uncertainty of 1K at 1000K requires 10 seconds.

Because of the small signals and the wide bandwidths employed in Johnson Noise Thermometry, the rejection of electromagnetic interference (EMI) is a major concern. In sensitive applications, battery power is used to eliminate the possibility of EMI from a power converter. In every case, good shielding methods are required to prevent EMI and radio frequency interference (RFI).

The sensor should ideally be a four terminal resistor element such as a standard RTD. The four-wire system as previously discussed has the ability to cancel noise and separate the signal from lead interference. In contrast, a two wire lead sensor has noise transmitted on the same signal lines as interfering noise.

The Johnson noise thermometer appears to be a viable solution for temperature measurement assuming low EMI, accurate signal amplifiers, and a stable measured known sensor resistance. There are amplifiers, power supplies and interconnecting cabling that will meet the requirements for the JNT.

5.2. Built-In Melt Standards

In this calibration scheme, a metal melt standard and reference RTD is included in the sensor package as illustrated in Figure 5-1. This method is based on the method used by NIST to create prime standard temperature sensors that are used to calibrate other sensors.

This calibration scheme is based on the known (and ideally unchanging) melting/freezing temperature of a pure metal. During normal plant operations, the gas temperature is below the freezing temperature of the melt standard. To perform a single point calibration of the reference RTD, the heater is activated and used to melt the melt standard. When the heater is turned off, the melt standard cools and the temperature of the standard is monitored by the reference RTD. At the freezing point, the temperature of the system stabilizes as latent heat is liberated. Signal processing methods are used to identify this plateau in the temperature-time curve and the reference RTD resistance is pegged to the known freezing temperature of the melt standard. The second reference point for the reference RTD is absolute zero, where its resistance goes to zero.

Once the reference RTD is calibrated, it is used to calibrate the operational temperature sensor. For this to occur, the plant must operate at steady temperature long enough for both the operational sensor and the standard to reach thermal equilibrium. Once this occurs, the two sensors are compared and the calibration curve for the operational sensor adjusted to match the reference RTD. This can be done at other temperatures as well if plant operations afford the opportunity.

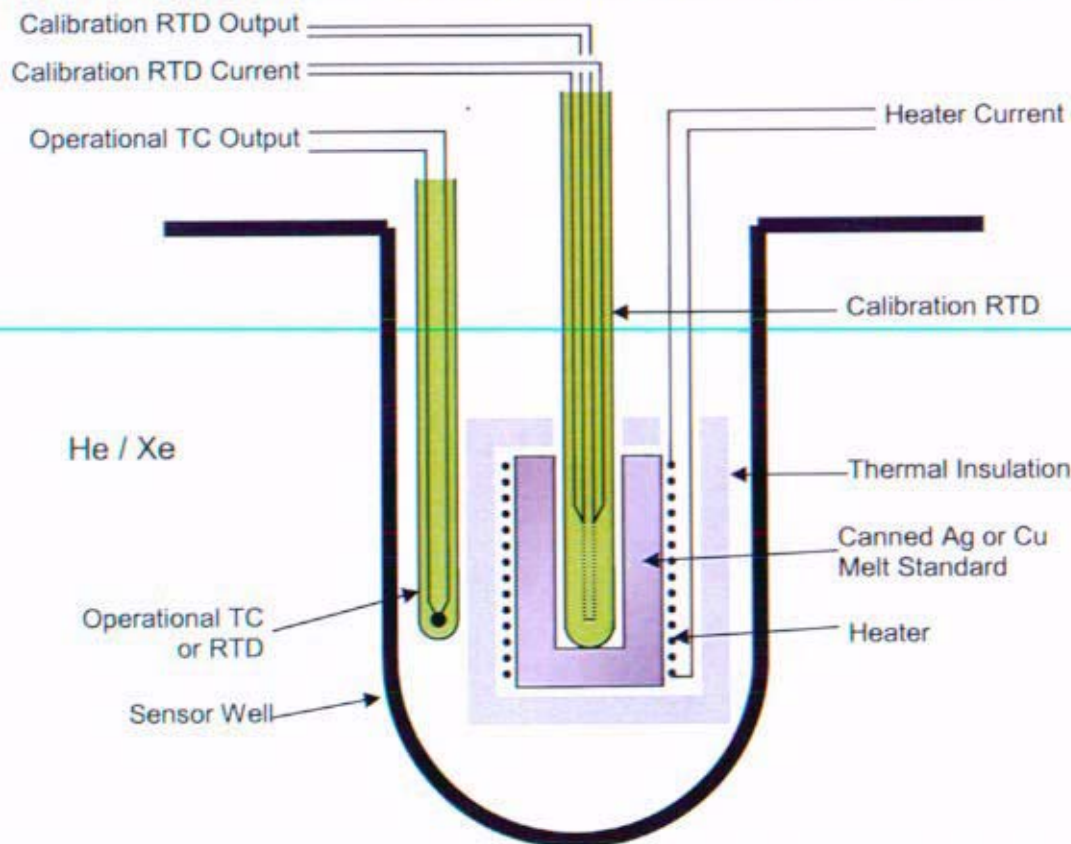


Figure 5-1. Built-in melt standard for in situ calibration of temperature sensors.

The melt standard is selected such that its melting temperature is above the operating temperature of the plant but not high enough to damage a sensor at the melting temperature. It must also be compatible with the sensor materials. A list of potential melt standards is given in Table 5-1.

Table 5-1. Possible melt standards for single-point calibration at temperatures above plant temperature (1150K).

Standard	Melting Temperature (K)	Temp Above Plant Temp (K)
Ge	1210	60
Ag	1235	85
Nd	1283	133
Au	1337	187
Cu	1358	208
Mn	1517	367

Use of the melt standard recalibration scheme will require additional components in the sensor well. If a TC is used as the reference sensor, the standard will require a separate heating coil to melt the standard. If an RTD is used, as illustrated in Figure 5-1, the RTD coil can be used to melt the standard by self-heating at a high current level. Although simpler, this option is not recommended because it requires the sensor to be exposed to even higher temperatures than the melt standard temperature. A separate heating coil is recommended for both RTDs and TCs. Of course, the system will also require a capsule of the melt standard material installed in the sensor assembly.

From a heat transfer perspective, the melt standard concept optimization must be balanced against the sensor's need for accuracy and response time. In a single sensor system (the reference sensor is also used as the operational temperature sensor and there is no second operational sensor), the optimal configuration would be to insulate the operational sensor and melt standard such that a minimal heat input can warm and melt the melt standard. Unfortunately, this configuration also results in a large sensor time constant because the sensor is not thermally well connected to the plant. In order to achieve a suitable response time, the sensor must be mounted in a configuration that is thermally well connected to the system it measures. Thus, the plant becomes a large heat sink on the calibration system. This increases the power required to melt the standard and leads to large temperature gradients that are the source of calibration error. For a single sensor system, the solution to this problem is to design the sensor/standard for heat transfer symmetry and predictability, both of which make the resulting measurement more accurate. A drawing of a self-calibrating TC concept is shown in Figure 5-2.

For a two sensor system (one reference and one operational, as shown in Figure 5-1), one sensor is designed for calibration, then used to calibrate the other sensor when the plant is operating under steady state conditions. In this configuration, the time constant of the operational sensor is minimal because the well can change temperature much faster than the insulated melt-standard. In addition, the reference sensor/melt standard can be designed in a way that provides slow, repeatable melting and freezing of the melt standard for high accuracy.

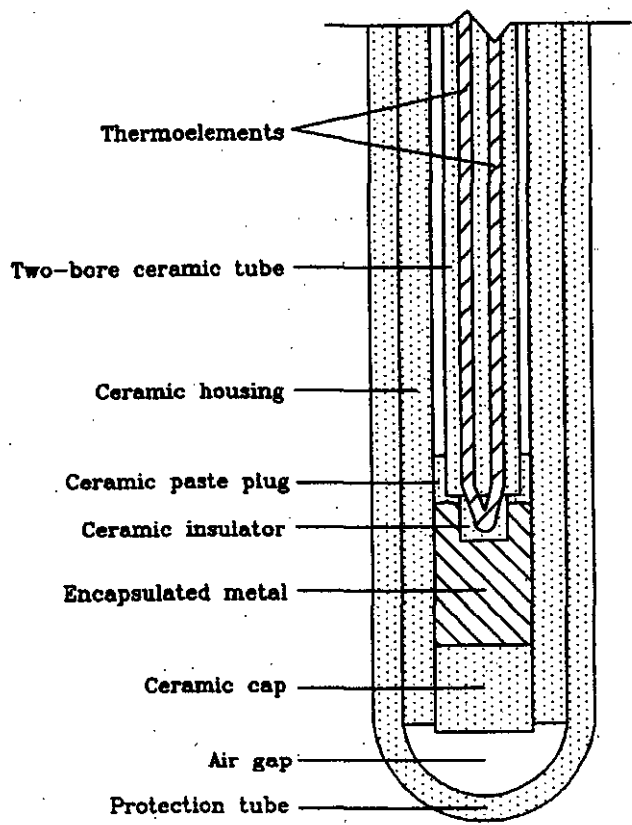


Fig. 1. Cross sectional view of self-calibrating thermocouple.

Figure 5-2. A drawing of a self-calibrating TC concept. In this case, the encapsulated metal is an alloy that is designed to melt on the way up to the operating temperature of the system. This provides a melt plateau to which the sensor output can be compared.

5.3. Remote Mercury Thermometer

In this method, a large Hg (or other liquid metal) bulb is placed at the sensing point and a filled-solid pipe is run from the reservoir back to the instrument vault. In the vault, the movement of Hg through an evacuated standpipe, or against a spring-loaded plunger, is monitored with an absolute position sensing system (optical, electrical, etc.). This system would give a ballpark absolute temperature measurement with no electrical components or insulators forward of the boom. It essentially converts a temperature measurement problem into a position measuring problem.

6. Conclusion

6.1. Resistance Temperature Detectors

The wire-wound RTDs technology appears to have the capability of fulfilling the requirements for a SNPP reactor coolant temperature measurement application. This conclusion is based on the general understanding of the challenges involved in the technology and the necessary adjustments in design, materials, processes, and fabrication appear to be well understood and tractable.

Selection of the right material system for reactor coolant RTDs, particularly for the high temperature locations requires significant study. However, it is possible to identify some of the key ideas that should govern their choice. The materials must withstand the application temperature, they must be internally and externally compatible with each other and the rest of the plant, and they must survive with predictable drift for the mission duration.

The materials must be selected as a system. Although there are many possible combinations, several materials can be eliminated based on previous research. For sheath materials, most Nb alloys (but not pure Nb) can be eliminated because of the reducing potential of the Zr alloy component. W and its alloys can be eliminated because of the difficulty in fabricating components from this material. For insulators, Y_2O_3 is known to have an unstable resistivity at high temperatures, ZrO_2 becomes a conductor when stabilized by lower valency materials, the Si in SiO_2 has detrimental alloying effects in several materials, BeO is toxic to work with, and HfO_2 reacts with some thermoelement materials at high temperature.

Based on the above candidate eliminations, and previous research, several materials have emerged as strong candidates for RTD construction. For the sheath, Mo and Ta are strong refractory candidates. With a suitable liner, a Ni-superalloy may also work, especially if used with a superalloy thermoelement. For operation in the high oxygen environment of the ground-based test facility, a Pt/Rh alloy sheath or outer cladding is called for because of its outstanding resistance to oxidation at high temperatures.

For the insulation, Al_2O_3 , Sc_2O_3 , and MgO are the prime candidates. Although chemically and electrically an excellent candidate, Sc_2O_3 may be difficult to obtain in the desired forms due to its small usage base. Of the remaining two, fabrication may be the key discriminator. MgO has superior compactability but absorbs moisture from the environment. Al_2O_3 is more difficult to compact but does not uptake contaminants from the environment when exposed during fabrication.

For the thermoelement, very little published information is available on materials other than Pt and Ni in RTD applications. As a result, the suitability of various materials must be determined from their use in TCs. High temperature survivability for 1.14 years at temperatures between 1400K-1563K has been demonstrated with W, W-26Re, Mo, Pt, and Pt-13Rh thermocouples. These materials should all be candidates for the RTD thermoelement. Related alloys such as Mo-41Re and Mo-47Re are also strong candidates. In addition, the Type K TC materials, Ni-10Cr and Ni-5AlSi, may be suitable if an appropriate liner is used inside sheath to block the interdiffusion of these materials.

Assuming that the coolant-carrying pipe is a Ni-superalloy, the current research suggests that the following system will perform well at 1150K: a Mo sheath, Al_2O_3 insulation, and a Mo or W-26Re thermoelement. The RTD would use beaded insulation that is backfilled with loose Al_2O_3 powder to increase thermal conductivity and reduce vibration of the internal components. The sheath would be backfilled with He gas and sealed with a sintered Al_2O_3 plug that is brazed in place to provide a hermetic seal. The 4-wire, coil-in-insulator design should be used to provide the truest voltage signal possible and the maximum mechanical support to the element. The element can be connected to the pipe with a conformal Ta pipe clamp that thermally connects the sensor to the system while blocking the diffusion of Ni and O between the two systems.

The above configuration has elements that are similar to the designs used in the SP-100 and Pratt and Whitney-CANEL nuclear aircraft projects, both of which are backed up with long-term drift and survival studies. For this reason, a RTD device developed based on these designs should be a considered along with others alternatives as the development is pursued.

Pre Decisional – For Planning and Discussion Purposes Only

Due to the simplicity and maturity of RTD technology, the developmental work should be fairly straight forward, the predominate initial activities being materials studies (of which there is a high level of confidence in success) and RTD element design work to minimize thermal stress and the response time constant.

6.2. Thermocouples

Selection of a materials system for TCs is done with much the same logic as RTDs. The selection of the sheath and insulator is constrained in the same ways as it is for RTDs, leading to the same preference: a Mo sheath and beaded/loose fill Al_2O_3 insulation. The choice of thermoelement is based on previous long-term studies. Both the Type C (W-5Re vs. W-26Re) and Type R (Pt vs. Pt-13Rh) TCs have been tested for >10k hours. For this sheath and insulator material, both are viable candidates for a TC design although the Type C will probably provide better drift performance. The improved drift performance of the Type C is due to the higher melting temperature of the thermoelements and the fact that both elements contain Re, thus reducing the effect of Re interdiffusion. Backfilling, sheath sealing, and mounting of this TC design should be the same as for the RTD above. The only other difference is the requirement for the addition of a reference temperature RTD for the cold end of the sheath. Since this is the cold end of the sheath, a precision Pt RTD should provide suitable accuracy and lifetime for this application. As with the RTDs, the simplicity and maturity of TC technology means that development work for this sensor is limited to materials compatibility studies and thermal design work.

6.3. The Expanded TD / TC Performance Envelope

Although the Prometheus SNPP requires survival of the sensor suite for approximately 12 years at 1150K in a pristine vacuum environment, there are other conditions to consider when evaluating the sensor design. During the development of the plant, a ground test reactor was expected to be developed. The environment that this reactor would have operated in would have been of considerably lower vacuum with significant contamination by oxygen, nitrogen, and water vapor. In addition to the primary mission, the sensor suite must also survive this environment.

Other potential operating environments include the low earth orbit (primarily atomic oxygen contamination), the lunar surface (hard vacuum with oxide dust), and the Martian surface (CO_2 and iron oxides). These other environments may require a reevaluation of the plant concept, which may result in a higher temperature design.

The sensor concepts discussed here have focused on the Prometheus SNPP application to the Jupiter environment. However, they are extensible to other environments. The primary change required to match the sensor to the environment is to switch the outer sheath to a less reactive material such as Re or clad it with a less reactive metal such as Pt. With respect to potential increases in operating temperature, all the RTD and TC designs above have been operated to at least 1475K for upto 3 years. Their temperature range is expected to cover all of the reasonable plant configurations that may be implemented for these new missions.

7. Bibliography

The remainder of this report is composed of a list of references that may be relevant to the development of high-temperature, long-lifetime RTD and TC temperature sensing systems. The references are categorized by source for easy retrieval. This list was included for future reference since many of the sources are not widely indexed. This list supplements the SP-100 Nuclear Space Power Source Book, DOE/TC/90001-T1, and the SP-100 Technical Summary Report, Vol. 3: Bibliography, JPL D-11818.

Pre Decisional – For Planning and Discussion Purposes Only

1. Conferences and Symposiums

1.1. Temperature: Its Measurement and Control in Science and Industry

1.1.1. Volume 1 (1939)

Brenner, B., "**Changes in Platinum Thermocouples Due to Oxidation,**" presented at Temperature: Its Measurement and Control in Science and Industry, pp. 1281-3, Fairchild, Hardy, Sosman, Wensel, ed., Reinhold Publishing Corporation, New York, NY, 1941.

Homewood, C.F., "**Factors Affecting the Life of Platinum Thermocouples,**" presented at Temperature: Its Measurement and Control in Science and Industry, pp. 1272-80, Fairchild, Hardy, Sosman, Wensel, ed., Reinhold Publishing Corporation, New York, NY, 1941.

1.1.2. Volume 2 (1954)

No papers of consequence to the project.

1.1.3. Volume 3 (1961)

Hill, J.S., "**Fibro Platinum for Thermocouple Elements,**" presented at Temperature: Its Measurement and Control in Science and Industry, Vol. 3, Part 2, pp. 157-60, sponsored by the American Institute of Physics, proceedings published by Reinhold Publishing Corporation, New York, NY, 1962.

Lachman, J.C., McGurty "**The Use of Refractory Metals for Ultra High-Temperature Thermocouples,**" presented at Temperature: Its Measurement and Control in Science and Industry, Vol. 3, Part 2, pp. 177-87, sponsored by the American Institute of Physics, proceedings published by Reinhold Publishing Corporation, New York, NY, 1962.

Franks, E., "**High Temperature Thermocouples Using Nonmetallic Members,**" presented at Temperature: Its Measurement and Control in Science and Industry, Vol. 3, Part 2, pp. 189-94, sponsored by the American Institute of Physics, proceedings published by Reinhold Publishing Corporation, New York, NY, 1962.

Zysk, E.D., "**Platinum Metal Thermocouples,**" presented at Temperature: Its Measurement and Control in Science and Industry, Vol. 3, Part 2, pp. 135-56, sponsored by the American Institute of Physics, proceedings published by Reinhold Publishing Corporation, New York, NY, 1962.

Levy, G.F., Fouse, R.R., Sherwin, R., "**Operation of Thermocouples Under Conditions of High Temperature and Nuclear Radiation,**" presented at Temperature: Its Measurement and Control in Science and Industry, Vol. 3, Part 2, pp. 277-82, sponsored by the American Institute of Physics, proceedings published by Reinhold Publishing Corporation, New York, NY, 1962.

Browning, W.E., Miller, C.E., "**Calculated Radiation Induced Changes in Thermocouple Composition,**" presented at Temperature: Its Measurement and Control in Science and Industry, Vol. 3, Part 2, pp. 271-6, sponsored by the American Institute of Physics, proceedings published by Reinhold Publishing Corporation, New York, NY, 1962.

Bennett, R.L., Rainey, W.T., McClain, W.M., "**Drift Studies on Chromel-P-Alumel Thermocouples in Helium Atmospheres,**" presented at Temperature: Its Measurement and Control in Science and Industry, Vol. 3, Part 2, pp. 289-94, Herzfeld, C.M., ed., Reinhold Publishing Corporation, New York, NY, 1962.

Zysk, E.D., "**Platinum Metal Thermocouples,**" presented at *Temperature: Its Measurement and Control in Science and Industry*, Vol. 3, Part 2, pp. 135-56, Herzfeld, C.M., ed., Reinhold Publishing Corporation, New York, NY, 1962.

Levy, G.F., Fouse, R.R., Sherwin, R., "**Operation of Thermocouples under Conditions of High Temperature and Nuclear Radiation,**" presented at *Temperature: Its Measurement and Control in Science and Industry*, Vol. 3, Part 2, pp. 277-82, Herzfeld, C.M., ed., Reinhold Publishing Corporation, New York, NY, 1962.

Hill, J.S., "**Fibro Platinum for Thermocouple Elements,**" presented at *Temperature: Its Measurement and Control in Science and Industry*, Vol. 3, Part 2, pp. 157-60, Herzfeld, C.M., ed., Reinhold Publishing Corporation, New York, NY, 1962.

Franks, E., "**High-Temperature Thermocouples Using Nonmetallic Members,**" presented at *Temperature: Its Measurement and Control in Science and Industry*, Vol. 3, Part 2, pp. 189-94, Herzfeld, C.M., ed., Reinhold Publishing Corporation, New York, NY, 1962.

Kelly, M.J., Johnston, W.W., Baumann, C.D., "**The Effects of Nuclear Radiation on Thermocouples,**" presented at *Temperature: Its Measurement and Control in Science and Industry*, Vol. 3, Part 2, pp. 265-9, Herzfeld, C.M., ed., Reinhold Publishing Corporation, New York, NY, 1962.

Lachman, J.C., "**The Use of Refractory Metals for Ultra High-Temperature Thermocouples,**" presented at *Temperature: Its Measurement and Control in Science and Industry*, Vol. 3, Part 2, pp. 177-87, Herzfeld, C.M., ed., Reinhold Publishing Corporation, New York, NY, 1962.

Evans, J.P., Burns, G.W., "**A Study of Stability of High Temperature Platinum Resistance Thermometers,**" presented at *Temperature: Its Measurement and Control in Science and Industry*, Vol. 3, Part 1, pp. 313-8, Herzfeld, C.M., ed., Reinhold Publishing Corporation, New York, NY, 1962.

Berry, R.J., "**The Stability of Platinum Resistance Thermometers at Temperatures up to 630°C,**" presented at *Temperature: Its Measurement and Control in Science and Industry*, Vol. 3, Part 1, pp. 301-11, Herzfeld, C.M., ed., Reinhold Publishing Corporation, New York, NY, 1962.

Bradley, D., Entwistle, A.G., "**Anomalous Electrical Resistance Effects in Small Diameter Platinum and Platinum-Rhodium Resistance Elements at Temperatures in Excess of 1000°C in a Gaseous Environment,**" presented at *Temperature: Its Measurement and Control in Science and Industry*, Vol. 3, Part 1, pp. 319-25, Herzfeld, C.M., ed., Reinhold Publishing Corporation, New York, NY, 1962.

Anderson, A.R., Stickney, T.M., "**The Use of Ceramic Resistance Thermometers as Temperature Standards above 2300°R,**" presented at *Temperature: Its Measurement and Control in Science and Industry*, Vol. 3, Part 2, pp. 361-7, Herzfeld, C.M., ed., Reinhold Publishing Corporation, New York, NY, 1962.

1.1.4. Volume 4 (1971)

Goodier, B.G., Fries, R.J., Tallman, C.R., "**High Temperature Core Thermocouple Development for the Nuclear Rocket Engine Program (ROVER),**" presented at *Temperature: Its Measurement and Control in Science and Industry*, Vol. 4, Part 3, pp. 1959-65, sponsored by the American Institute of Physics, proceedings published by Instrument Society of America, 1972.

Fitts, R.B., Miller, J.L., Long, E.L., "**Observations on Tungsten-Rhenium Thermocouples Used In-Reactor in (U, Pu)O₂ Fuel Pins,**" presented at *Temperature: Its Measurement and Control in Science and Industry*, Vol. 4, Part 3, pp. 1951-58, sponsored by the American Institute of Physics, proceedings published by Instrument Society of America, 1972.

Heckelman, J.D., Kozar, R.P., "**Measured Drift of Irradiated and Unirradiated W3%Re/W25%Re Thermocouples at a Nominal 2000K,**" presented at Temperature: Its Measurement and Control in Science and Industry, Vol. 4, Part 3, pp. 1935-49, sponsored by the American Institute of Physics, proceedings published by Instrument Society of America, 1972.

Burns, G.W., Hurst, W.S., "**Studies of the Performance of W-Re Type Thermocouples,**" presented at Temperature: Its Measurement and Control in Science and Industry, Vol. 4, Part 3, pp. 1751-66, sponsored by the American Institute of Physics, proceedings published by Instrument Society of America, 1972.

Anderson, T.M., Bliss, P., "**Tungsten-Rhenium Thermocouples Summary Report,**" presented at Temperature: Its Measurement and Control in Science and Industry, Vol. 4, Part 3, pp. 1735-46, sponsored by the American Institute of Physics, proceedings published by Instrument Society of America, 1972.

Liermann, J., Tarassenko, S., "**Temperature Measurement on Nuclear Fuel Elements,**" presented at Temperature: Its Measurement and Control in Science and Industry, Vol. 4, Part 3, pp. 1903-14, Plumb, H.H., ed., Instrument Society of America, Pittsburgh, PA, 1972.

Burley, N.A., "**Nicrosil and Nilil: Highly Stable Nickel-Base Alloys for Thermocouples,**" presented at Temperature: Its Measurement and Control in Science and Industry, Vol. 4, Part 3, pp. 1677-1695, Plumb, H.H., ed., Instrument Society of America, Pittsburgh, PA, 1972.

Bliss, P., "**Fabrication of High-Reliability Sheathed Thermocouples,**" presented at Temperature: Its Measurement and Control in Science and Industry, Vol. 4, Part 3, pp. 1797-1803, Plumb, H.H., ed., Instrument Society of America, Pittsburgh, PA, 1972.

Darling, A.S., Selman, G.L., "**Some Effects of Environment on the Performance of Noble Metal Thermocouples,**" presented at Temperature: Its Measurement and Control in Science and Industry, Vol. 4, Part 3, pp. 1633-1644, Plumb, H.H., ed., Instrument Society of America, Pittsburgh, PA, 1972.

Selman, G.L., "**On the Stability of Metal Sheathed Noble Metal Thermocouples,**" presented at Temperature: Its Measurement and Control in Science and Industry, Vol. 4, Part 3, pp. 1833-40, Plumb, H.H., ed., Instrument Society of America, Pittsburgh, PA, 1972.

Swartzlander, E.E., "**Comparison of Temperature Sensors for Space Instrumentation,**" presented at Temperature: Its Measurement and Control in Science and Industry, Vol. 4, Part 3, pp. 2337-45, Plumb, H.H., ed., Instrument Society of America, Pittsburgh, PA, 1972.

Carpenter, F.D., Sandefur, N.L., Grenda, R.J., Steibel, J.S., "**EMF Stability of Chromel/Alumel and Tungsten-3%Rhenium/Tungsten-25%Rhenium Sheathed Thermocouples in a Neutron Environment,**" presented at Temperature: Its Measurement and Control in Science and Industry, Vol. 4, Part 3, pp. 1927-34, Plumb, H.H., ed., Instrument Society of America, Pittsburgh, PA, 1972.

Aarset, B., Kjaerheim, G., "**In-Core Applications and Experience with Thermocouples in the Halden Boiling Water Reactor,**" presented at Temperature: Its Measurement and Control in Science and Industry, Vol. 4, Part 3, pp. 1889-902, Plumb, H.H., ed., Instrument Society of America, Pittsburgh, PA, 1972.

Zysk, E.D., Robertson, A.R., "**Newer Thermocouple Materials,**" presented at Temperature: Its Measurement and Control in Science and Industry, Vol. 4, Part 3, pp. 1697-734, Plumb, H.H., ed., Instrument Society of America, Pittsburgh, PA, 1972.

Glawe, G.E., Szaniszlo, A.J., "**Long-Term Drift of Some Noble- and Refractory-Metal Thermocouples at 1600K in Air, Argon, and Vacuum,**" presented at Temperature: Its Measurement and Control in Science and Industry, Vol. 4, Part 3, pp. 1645-62, Plumb, H.H., ed., Instrument Society of America, Pittsburgh, PA, 1972.

Toenshoff, D.A., Zysk, E.D., "**Material Preparation and Fabrication Techniques for the Production of High Reliability Thermocouple Devices,**" presented at Temperature: Its Measurement and Control in Science and Industry, Vol. 4, Part 3, pp. 1791-6, Plumb, H.H., ed., Instrument Society of America, Pittsburgh, PA, 1972.

Shepard, R.L., Hyland, R.F., "**Equivalent Circuit Modeling of Insulator Shunting Errors in High Temperature Sheathed Thermocouples,**" presented at Temperature: Its Measurement and Control in Science and Industry, Vol. 4, Part 3, pp. 1841-53, Plumb, H.H., ed., Instrument Society of America, Pittsburgh, PA, 1972.

Carr, K.R., "**Testing of Ceramic Insulator Compaction and Thermoelectric Inhomogeneity in Sheathed Thermocouples,**" presented at Temperature: Its Measurement and Control in Science and Industry, Vol. 4, Part 3, pp. 1855-66, Plumb, H.H., ed., Instrument Society of America, Pittsburgh, PA, 1972.

Gray, W.T., Finch, D.I., "**Accuracy of Temperature Measurement,**" presented at Temperature: Its Measurement and Control in Science and Industry, Vol. 4, Part 3, pp. 1381-92, Plumb, H.H., ed., Instrument Society of America, Pittsburgh, PA, 1972.

Foster, R.B., "**A Fixed Point Calibration Procedure for Precision Platinum Resistance Thermometers,**" presented at Temperature: Its Measurement and Control in Science and Industry, Vol. 4, Part 3, pp. 1403-14, Plumb, H.H., ed., Instrument Society of America, Pittsburgh, PA, 1972.

Droege, J.W., Schimek, M.M., Ward, J.J., "**Chemical Compatibility in the Use of Refractory Metal Thermocouples,**" presented at Temperature: Its Measurement and Control in Science and Industry, Vol. 4, Part 3, pp. 1767-79, Plumb, H.H., ed., Instrument Society of America, Pittsburgh, PA, 1972.

Evans, J.P., "**High Temperature Platinum Resistance Thermometry,**" presented at Temperature: Its Measurement and Control in Science and Industry, Vol. 4, Part 2, pp. 899-906, Plumb, H.H., ed., Instrument Society of America, Pittsburgh, PA, 1972.

Chattle, M.V., "**Platinum Resistance Thermometry up to the Gold Point,**" presented at Temperature: Its Measurement and Control in Science and Industry, Vol. 4, Part 2, pp. 907-18, Plumb, H.H., ed., Instrument Society of America, Pittsburgh, PA, 1972.

Sawada, S., Mochizuki, T., "**Stability of 25 Ohm Platinum Thermometer up to 1100°C,**" presented at Temperature: Its Measurement and Control in Science and Industry, Vol. 4, Part 2, pp. 919-26, Plumb, H.H., ed., Instrument Society of America, Pittsburgh, PA, 1972.

Anderson, R.L., "**The High Temperature Stability of Platinum Resistance Thermometers,**" presented at Temperature: Its Measurement and Control in Science and Industry, Vol. 4, Part 2, pp. 927-34, Plumb, H.H., ed., Instrument Society of America, Pittsburgh, PA, 1972.

Dutt, M., "Practical Applications of Platinum Resistance Sensors," presented at Temperature: Its Measurement and Control in Science and Industry, Vol. 4, Part 2, pp. 1013-8, Plumb, H.H., ed., Instrument Society of America, Pittsburgh, PA, 1972.

1.1.5. Volume 5 (1982)

Schley, R., Metauer, G., "Thermocouples for measurements under conditions of high temperature and nuclear radiation," presented at Temperature: Its Measurement and Control in Science and Industry, Vol. 5, Part 2, pp. 1109-13, Schooley, J.F. ed., American Institute of Physics, New York, NY, 1982.

1.1.6. Volume 6 (1992)

Cannon, N.S., Knight, R.C., "SP-100 W/Re thermocouple calibration techniques," presented at Temperature: Its Measurement and Control in Science and Industry, Vol. 6, Part 1, pp. 613-6, sponsored by the American Institute of Physics, proceedings published by American Institute of Physics, 1992.

Wilkins, S.C., "Characterization and material-compatibility tests of molybdenum/niobium thermocouples," presented at Temperature: Its Measurement and Control in Science and Industry, Vol. 6, Part 1, pp. 627-30, sponsored by the American Institute of Physics, proceedings published by American Institute of Physics, 1992.

Daneman, P.E., "Thermocouple calibration standard," presented at Temperature: Its Measurement and Control in Science and Industry, Vol. 6, Part 1, pp. 575-7, Schooley, J.F., ed., American Institute of Physics, New York, NY, 1992.

Burley, N.A., "N-Clad-N' A novel integrally sheathed thermocouple: Optimum design rational for ultra-high thermoelectric stability," presented at Temperature: Its Measurement and Control in Science and Industry, Vol. 6, Part 1, pp. 579-84, Schooley, J.F., ed., American Institute of Physics, New York, NY, 1992.

Bentley, R.E., "Thermoelectric behavior of Ni-based ID-MIMS thermocouples using the Nicrosil-plus sheathing alloy," presented at Temperature: Its Measurement and Control in Science and Industry, Vol. 6, Part 1, pp. 585-90, Schooley, J.F., ed., American Institute of Physics, New York, NY, 1992.

Bentley, R.E., "Optimizing the thermoelectric stability of SI-MIMS type K thermocouples by adjusting the levels of Mn and Al," presented at Temperature: Its Measurement and Control in Science and Industry, Vol. 6, Part 1, pp. 591-4, Schooley, J.F., ed., American Institute of Physics, New York, NY, 1992.

Wang, T.P., Bediones, D., "10,000 hr stability test of type K, N, and a Ni-Mo/Ni-Co thermocouple in air and short-term tests in reducing atmospheres," presented at Temperature: Its Measurement and Control in Science and Industry, Vol. 6, Part 1, pp. 595-600, Schooley, J.F., ed., American Institute of Physics, New York, NY, 1992.

Burns, G.W., et al., "New reference function for platinum-10% rhodium versus platinum (type S) thermocouples based on the ITS-90. Part 1: Experimental procedures," presented at Temperature: Its Measurement and Control in Science and Industry, Vol. 6, Part 1, pp. 537-40, Schooley, J.F., ed., American Institute of Physics, New York, NY, 1992.

Burns, G.W., et al., "**New reference function for platinum-10% rhodium versus platinum (type S) thermocouples based on the ITS-90. Part 2: Experimental procedures.**" presented at Temperature: Its Measurement and Control in Science and Industry, Vol. 6, Part 1, pp. 541-6, Schooley, J.F., ed., American Institute of Physics, New York, NY, 1992.

Guthrie, W.F., et al., "**Statistical analysis of type S thermocouple measurements on the International Temperature Scale of 1990.**" presented at Temperature: Its Measurement and Control in Science and Industry, Vol. 6, Part 1, pp. 547-52, Schooley, J.F., ed., American Institute of Physics, New York, NY, 1992.

Rosch, W., Fripp, A., Debnam, W., Sorokach, S., Simchick, R., "**Damage of fine diameter platinum sheathed type R thermocouples at temperatures between 950 and 1100°C.**" presented at Temperature: Its Measurement and Control in Science and Industry, Vol. 6, Part 1, pp. 569-74, Schooley, J.F., ed., American Institute of Physics, New York, NY, 1992.

Reed, R.P., "**Thermoelectric inhomogeneity testing: Part 1-Principles.**" presented at Temperature: Its Measurement and Control in Science and Industry, Vol. 6, Part 1, pp. 519-30, Schooley, J.F., ed., American Institute of Physics, New York, NY, 1992.

Yamamoto, T., Tamura, Y., Kawate, Y., "**Experimental studies and an estimation model for shunting errors of sheathed thermocouples.**" presented at Temperature: Its Measurement and Control in Science and Industry, Vol. 6, Part 1, pp. 607-12, Schooley, J.F., ed., American Institute of Physics, New York, NY, 1992.

McGhee, J., Henderson, I.A., Michalski, L., Eckersdorf, K., Sankowski, D., "**Dynamic properties of contact temperature sensors: I Thermokinetic modeling and the idealized temperature sensor.**" presented at Temperature: Its Measurement and Control in Science and Industry, Vol. 6, Part 1, pp. 1157-62, Schooley, J.F., ed., American Institute of Physics, New York, NY, 1992.

McGhee, J., Henderson, I.A., Michalski, L., Eckersdorf, K., Sankowski, D., "**Dynamic properties of contact temperature sensors: II Modeling, characterization, and testing of real sensors.**" presented at Temperature: Its Measurement and Control in Science and Industry, Vol. 6, Part 1, pp. 1163-68, Schooley, J.F., ed., American Institute of Physics, New York, NY, 1992.

Ronsin, H., et al., "**Assessment of microcrucible fixed points for thermocouple calibration through an international comparison.**" presented at Temperature: Its Measurement and Control in Science and Industry, Vol. 6, Part 1, pp. 1061-66, Schooley, J.F., ed., American Institute of Physics, New York, NY, 1992.

Strouse, G.F., "**NIST implementation and realization of the ITS-90 over the range 83K to 1235K: Reproducibility, stability, and uncertainties.**" presented at Temperature: Its Measurement and Control in Science and Industry, Vol. 6, Part 1, pp. 169-74, Schooley, J.F., ed., American Institute of Physics, New York, NY, 1992.

Wang, K.H., Cui, C.M., Wang, T., "**New thermocouple ceramet protection tubes for high-temperature melt thermometry.**" presented at Temperature: Its Measurement and Control in Science and Industry, Vol. 6, Part 1, pp. 631-5, Schooley, J.F., ed., American Institute of Physics, New York, NY, 1992.

Levine, P.D., Mellons, B.E., Schneider, W., "**Development of a stand-alone calibration for long stem SPRTs.**" presented at Temperature: Its Measurement and Control in Science and Industry, Vol. 6, Part 1, pp. 405-8, Schooley, J.F., ed., American Institute of Physics, New York, NY, 1992.

Nicholas, J.V., "Thermodynamic behaviour of platinum resistivity," presented at Temperature: Its Measurement and Control in Science and Industry, Vol. 6, Part 1, pp. 383-8, Schooley, J.F., ed., American Institute of Physics, New York, NY, 1992.

Arai, M., Sakurai, H., "Development of industrial platinum resistance sensors for use up to the gold point," presented at Temperature: Its Measurement and Control in Science and Industry, Vol. 6, Part 1, pp. 439-42, Schooley, J.F., ed., American Institute of Physics, New York, NY, 1992.

Ruffino, G., Coppa, P., de Santoli, L., Castelli, A., Cornaro, C., "A platinum resistance thermometer for exploration of the Titan atmosphere," presented at Temperature: Its Measurement and Control in Science and Industry, Vol. 6, Part 1, pp. 409-13, Schooley, J.F., ed., American Institute of Physics, New York, NY, 1992.

Nubbemeyer, H.G., "High-temperature platinum resistance thermometers and fixed-point cells for the realization of the ITS-90 in the range 0°C to 961.78°C," presented at Temperature: Its Measurement and Control in Science and Industry, Vol. 6, Part 1, pp. 199-202, Schooley, J.F., ed., American Institute of Physics, New York, NY, 1992.

Lin, J.H., Tsai, S.F., Chou, Y.H., Yeh, T.I., "Experiences with high-temperature platinum resistance thermometry to the silver point," presented at Temperature: Its Measurement and Control in Science and Industry, Vol. 6, Part 1, pp. 401-3, Schooley, J.F., ed., American Institute of Physics, New York, NY, 1992.

Strouse, G.F., Mangum, B.W., Pokhodun, A.I., Moiseeva, N.P., "Investigation of high-temperature platinum resistance thermometers at temperatures up to 962°C, and, in some cases, 1064°C," presented at Temperature: Its Measurement and Control in Science and Industry, Vol. 6, Part 1, pp. 401-3, Schooley, J.F., ed., American Institute of Physics, New York, NY, 1992.

Ruppel, F.R., "Evaluation of the self-calibrating thermocouple as a front end to a smart temperature measurement system," presented at Temperature: Its Measurement and Control in Science and Industry, Vol. 6, Part 1, pp. 637-42, Schooley, J.F., ed., American Institute of Physics, New York, NY, 1992.

1.1.7. Volume 7 (2002)

Boltovets, N.S., et al., "New Generation of Resistance Thermometers Based on Ge Films on GaAs Substrates," presented at Temperature: Its Measurement and Control in Science and Industry, Vol. 7, Part 1, pp. 399-404, Ripple, D.C., ed., American Institute of Physics, New York, NY, 2003. AIP Conference Proceedings Volume 684.

Courts, S., Swinehart, P.R., "Review of Cernox™ (Zirconium Oxy-Nitride) Thin-Film Resistance Temperature Sensors," presented at Temperature: Its Measurement and Control in Science and Industry, Vol. 7, Part 1, pp. 393-8, Ripple, D.C., ed., American Institute of Physics, New York, NY, 2003. AIP Conference Proceedings Volume 684.

Arai, M., Kawata, A., "Properties of a High-Temperature Platinum Resistance Thermometer up to 1350°C," presented at Temperature: Its Measurement and Control in Science and Industry, Vol. 7, Part 1, pp. 381-5, Ripple, D.C., ed., American Institute of Physics, New York, NY, 2003. AIP Conference Proceedings Volume 684.

Xing, C., "Development of Metal Sheathed Secondary Standard and Precision RTD Thermometers at Temperatures up to 960°C and 1,100°C," presented at Temperature: Its Measurement and Control

in Science and Industry, Vol. 7, Part 1, pp. 375-80, Ripple, D.C., ed., American Institute of Physics, New York, NY, 2003. AIP Conference Proceedings Volume 684.

Arai, M., Kawata, A., Imamura, T., Kinoshita, K., "**Platinum-Sheathed High-Temperature Platinum Resistance Thermometers for Use up to 1200°C,**" presented at Temperature: Its Measurement and Control in Science and Industry, Vol. 7, Part 1, pp. 357-61, Ripple, D.C., ed., American Institute of Physics, New York, NY, 2003. AIP Conference Proceedings Volume 684.

Yamazawa, K., Arai, M., "**Measurement of Insulation Resistance for the Development of High Temperature Platinum Resistance Thermometers with a Guard Electrode,**" presented at Temperature: Its Measurement and Control in Science and Industry, Vol. 7, Part 1, pp. 363-8, Ripple, D.C., ed., American Institute of Physics, New York, NY, 2003. AIP Conference Proceedings Volume 684.

Ancsin, J., "**Oxidation of Platinum Resistance Thermometers,**" presented at Temperature: Its Measurement and Control in Science and Industry, Vol. 7, Part 1, pp. 345-9, Ripple, D.C., ed., American Institute of Physics, New York, NY, 2003. AIP Conference Proceedings Volume 684.

Zhao, M., Li, X., Chen, D., "**Experimental Study of Different Filling Gasses on the Stability of Metal-Sheathed Standard Platinum Resistance Thermometers,**" presented at Temperature: Its Measurement and Control in Science and Industry, Vol. 7, Part 1, pp. 339-44, Ripple, D.C., ed., American Institute of Physics, New York, NY, 2003. AIP Conference Proceedings Volume 684.

Batagelj, V., Bojkovski, J., Drnovsek, J., Pusnik, I., "**Influence of SPRT Self-Heating on Measurement Uncertainty in Fixed Point Calibration and Calibration by Comparison,**" presented at Temperature: Its Measurement and Control in Science and Industry, Vol. 7, Part 1, pp. 315-20, Ripple, D.C., ed., American Institute of Physics, New York, NY, 2003. AIP Conference Proceedings Volume 684.

Boguhn, D., Augustin, S., Bernhard, F., Mammen, H., Tischler, M., "**Application of Binary Alloys in Miniature Fixed-Point Cells as Secondary Fixed Points in the Temperature Range from 500°C to 660°C,**" presented at Temperature: Its Measurement and Control in Science and Industry, Vol. 7, Part 1, pp. 249-54, Ripple, D.C., ed., American Institute of Physics, New York, NY, 2003. AIP Conference Proceedings Volume 684.

Belevtsev, A.V., Karzhavin, A.V., Ulanowsky, A.A., "**Stability of a Cable Nicrosil-Nisil Thermocouple under Thermal Cycling,**" presented at Temperature: Its Measurement and Control in Science and Industry, Vol. 7, Part 1, pp. 453-6, Ripple, D.C., ed., American Institute of Physics, New York, NY, 2003. AIP Conference Proceedings Volume 684.

Walker, J., Cassidy, G., "**Development of a New Thermocouple for Harsh Environments,**" presented at Temperature: Its Measurement and Control in Science and Industry, Vol. 7, Part 1, pp. 457-61, Ripple, D.C., ed., American Institute of Physics, New York, NY, 2003. AIP Conference Proceedings Volume 684.

Ode, J., Douji, S., Ogawa, M., "**High-Temperature Characteristics of Ultra-Fine, Mineral-Insulated Type K Thermocouples,**" presented at Temperature: Its Measurement and Control in Science and Industry, Vol. 7, Part 1, pp. 463-7, Ripple, D.C., ed., American Institute of Physics, New York, NY, 2003. AIP Conference Proceedings Volume 684.

Jahan, F., Ballico, M., "**A Study of the Temperature Dependence of Inhomogeneity in Platinum-Based Thermocouples,**" presented at Temperature: Its Measurement and Control in Science and Industry, Vol. 7, Part 1, pp. 469-74, Ripple, D.C., ed., American Institute of Physics, New York, NY, 2003. AIP Conference Proceedings Volume 684.

Halawa, M., Megahed, F., El-Aziz, Y.A., Ammar, M.M. "**Performance, Thermoelectric Homogeneity and Stability of Au/Pt and Pt-10%Rh/Pt Thermocouples,**" presented at Temperature: Its Measurement and Control in Science and Industry, Vol. 7, Part 1, pp. 475-80, Ripple, D.C., ed., American Institute of Physics, New York, NY, 2003. AIP Conference Proceedings Volume 684.

Gotoh, M., "**Thermoelectric Scanning Study of Pt/Pd and Au/Pt Thermocouples up to 960°C with a Pressure Controlled Sodium Heat-Pipe,**" presented at Temperature: Its Measurement and Control in Science and Industry, Vol. 7, Part 1, pp. 481-4, Ripple, D.C., ed., American Institute of Physics, New York, NY, 2003. AIP Conference Proceedings Volume 684.

Ogura, H., et al., "**Effects of Heat Treatment on the Inhomogeneity of the Pt/Pd Thermocouple at the Cu Freezing Point,**" presented at Temperature: Its Measurement and Control in Science and Industry, Vol. 7, Part 1, pp. 485-9, Ripple, D.C., ed., American Institute of Physics, New York, NY, 2003. AIP Conference Proceedings Volume 684.

Reed, R.P., "**The Effect of Interrogating Temperature Profile in the Seebeck Inhomogeneity Method of Test (SIMOT),**" presented at Temperature: Its Measurement and Control in Science and Industry, Vol. 7, Part 1, pp. 491-6, Ripple, D.C., ed., American Institute of Physics, New York, NY, 2003. AIP Conference Proceedings Volume 684.

Schuh, W., Frost, N., "**Improving Industrial Thermocouple Temperature Measurement,**" presented at Temperature: Its Measurement and Control in Science and Industry, Vol. 7, Part 1, pp. 497-501, Ripple, D.C., ed., American Institute of Physics, New York, NY, 2003. AIP Conference Proceedings Volume 684.

Karzhavin, A.V., Belevtsev, A.V., Ulanowsky, A.A., "**A Method for Testing the Quality of Cable Thermocouple Junctions,**" presented at Temperature: Its Measurement and Control in Science and Industry, Vol. 7, Part 1, pp. 503-6, Ripple, D.C., ed., American Institute of Physics, New York, NY, 2003. AIP Conference Proceedings Volume 684.

Reed, R.P., "**Possibilities and Limitations of Self-Validation of Thermoelectric Thermometry,**" presented at Temperature: Its Measurement and Control in Science and Industry, Vol. 7, Part 1, pp. 507-12, Ripple, D.C., ed., American Institute of Physics, New York, NY, 2003. AIP Conference Proceedings Volume 684.

Wei, Z., Weixin, C., "**Researching the Platinum versus Palladium Thermocouple in the Range 419.527°C to 1084.62°C,**" presented at Temperature: Its Measurement and Control in Science and Industry, Vol. 7, Part 1, pp. 513-17, Ripple, D.C., ed., American Institute of Physics, New York, NY, 2003. AIP Conference Proceedings Volume 684.

Kim, Y-G., Gam, K.S., Kang, K.H., "**Fabrication of Small Copper Sealed-Cells for Thermocouple Calibration,**" presented at Temperature: Its Measurement and Control in Science and Industry, Vol. 7, Part 1, pp. 519-22, Ripple, D.C., ed., American Institute of Physics, New York, NY, 2003. AIP Conference Proceedings Volume 684.

Jahan, F., Ballico, M., "**The 'Mini-Coil' Method for Calibration of Thermocouples at the Palladium Point,**" presented at Temperature: Its Measurement and Control in Science and Industry, Vol. 7, Part 1, pp. 523-8, Ripple, D.C., ed., American Institute of Physics, New York, NY, 2003. AIP Conference Proceedings Volume 684.

Zvizdic, D., et al., "Estimation of Uncertainties in Comparison Calibration of Thermocouples," presented at Temperature: Its Measurement and Control in Science and Industry, Vol. 7, Part 1, pp. 529-34, Ripple, D.C., ed., American Institute of Physics, New York, NY, 2003. AIP Conference Proceedings Volume 684.

Liedberg, H.G., "Traceability of Surface Temperature Measurements Using Contact Thermometers," presented at Temperature: Its Measurement and Control in Science and Industry, Vol. 7, Part 1, pp. 535-40, Ripple, D.C., ed., American Institute of Physics, New York, NY, 2003. AIP Conference Proceedings Volume 684.

Sloneker, K.C., Polsky, D.N., Zhagrov, A., Lutsenko, V., "High-Resolution Differential Thermocouple Measurements Using an Improved Noise Cancellation and Magnetic Amplification Technique," presented at Temperature: Its Measurement and Control in Science and Industry, Vol. 7, Part 2, pp. 997-1002, Ripple, D.C., ed., American Institute of Physics, New York, NY, 2003. AIP Conference Proceedings Volume 684.

Hashemian, H.M., "Verifying the Performance of RTDs in Nuclear Power Plants," presented at Temperature: Its Measurement and Control in Science and Industry, Vol. 7, Part 2, pp. 1057-1062, Ripple, D.C., ed., American Institute of Physics, New York, NY, 2003. AIP Conference Proceedings Volume 684.

Cessac, K.J., "Reducing Thermowell Conduction Errors in Gas Pipeline Temperature Measurement," presented at Temperature: Its Measurement and Control in Science and Industry, Vol. 7, Part 2, pp. 1093-6, Ripple, D.C., ed., American Institute of Physics, New York, NY, 2003. AIP Conference Proceedings Volume 684.

Barberree, D.A., "Dynamically Self-Validating Contact Temperature Sensors," presented at Temperature: Its Measurement and Control in Science and Industry, Vol. 7, Part 2, pp. 1097-102, Ripple, D.C., ed., American Institute of Physics, New York, NY, 2003. AIP Conference Proceedings Volume 684.

1.2. Industrial Temperature Measurement Symposium

Ludtka, G.M., Kollie, T.G., Anderson, R.L., Christie, W.H., "Performance of Chromel Versus Alumel and Nicrosil Versus Nisil Thermocouple Assemblies in Vacuum and Argon Between 1000° and 1200°C.," presented at the Industrial Temperature Measurement Symposium, pp. 5.01-5.19, 1984.

1.3. Space Nuclear Power Systems

1.3.1. 1984

Anderson, J.L., Oakes, L.C., "Instrumentation and Controls Evaluation for Space Nuclear Power Systems," Space Nuclear Power Systems 1984, Vol. 1, pp. 109-114, El-Genk, M.S. and Hoover, M.D., ed., Orbit Book Company, Malabar, FL 1985.

1.3.2. 1985

No papers of consequence to the project.

1.3.3. 1986

No papers of consequence to the project.

1.3.4. 1987

No papers of consequence to the project.

1.3.5. 1988

Wilkins, S.C., "Low Cross-Section Mo-Nb Thermocouples for Nuclear Application: The State-of-the-Art," Space Nuclear Power Systems 1988, Vol. 9, pp. 481-6, El-Genk, M.S. and Hoover, M.D., ed., Orbit Book Company, Malabar, FL 1989.

Oakes, L.C., Shepard, R.L., "Johnson Noise Thermometer for High Radiation and High Temperature Environments," Space Nuclear Power Systems 1988, Vol. 9, pp. 487-93, El-Genk, M.S. and Hoover, M.D., ed., Orbit Book Company, Malabar, FL 1989.

1.3.6. 1989

Roberts, M.J., Blalock, T.V., Shepard, R.L., "Application of Johnson Noise Thermometry to Space Nuclear Reactors," Space Nuclear Power Systems 1989, Vol. 10, pp. 87-93, El-Genk, M.S. and Hoover, M.D., ed., Orbit Book Company, Malabar, FL 1992.

Olthoff, J.K., Hebner, R.E., "Metrology Requirements of Future Space Power Systems," Space Nuclear Power Systems 1989, Vol. 10, pp. 95-101, El-Genk, M.S. and Hoover, M.D., ed., Orbit Book Company, Malabar, FL 1992.

1.3.7. 1990

Bond, J.A., deLorenzi, H.A., "Development of a High Voltage Insulator Assembly for SP-100," Space Nuclear Power Systems 1990, pp. 248-54, El-Genk, M.S. and Hoover, M.D., ed., 1990.

Will, F.G., deLorenzi, H.A., Janora, K.H., "Electrical Conductivity and Ionic Transference Measurements on Single Crystal Alumina," Space Nuclear Power Systems 1990, pp. 255-60, El-Genk, M.S. and Hoover, M.D., ed., 1990.

deLorenzi, H.A., Will, F.G., "A Mathematical Model of the Electrical Conductivity of Single Crystal Alumina," Space Nuclear Power Systems 1990, pp. 261-6, El-Genk, M.S. and Hoover, M.D., ed., 1990.

Roberts, M.J., Blalock, T.V., Shepard, R.L., "Tuned-Circuit Johnson Noise Thermometry," Space Nuclear Power Systems 1990, pp. 918-23, El-Genk, M.S. and Hoover, M.D., ed., 1990.

1.3.8. 1991

Ryan, R., Shukla, J., Long, J., Gilliland, K., "JNT Multiplexer and Analog Input Processor," Space Nuclear Power Systems 1991, pp. 1105-12, El-Genk, M.S. and Hoover, M.D., ed., 1991.

1.3.9. 1992

Knight, R.C., Greenslade, D.L., "Irradiation Testing of a Niobium-Molybdenum Developmental Thermocouple," Space Nuclear Power Systems 1992, pp. 594-603, El-Genk, M.S. and Hoover, M.D., ed., 1992.

1.3.10. 1993

No papers of consequence to the project.

1.3.11. 1994

Wu, W.Y., Patuwathavithane, C., Zee, R.H., "Radiation Induced Conductivity in Ceramics Insulators for Thermionic Systems," Space Nuclear Power and Propulsion 1994, pp. 1147-52, El-Genk, M.S., ed., 1994.

1.3.12. 1995

No papers of consequence to the project.

1.4. Symposium on Refractory Alloy Technology for Space Nuclear Power Applications

Ambrus, J., "**Origin and Organization of the SP-100 Program,**" proceedings of The Symposium on Refractory Alloy Technology for Space Nuclear Power Applications, Oak Ridge National Laboratory, 10-11 August 1983, ed. Cooper, R.H, and Hoffman, E.E., January 1984.

Truscello, Vincent C., "**SP-100 Program Overview,**" proceedings of The Symposium on Refractory Alloy Technology for Space Nuclear Power Applications, Oak Ridge National Laboratory, 10-11 August 1983, ed. Cooper, R.H, and Hoffman, E.E., January 1984.

Cooper, R.H., "**Potential Refractory Alloy Requirements for Space Nuclear Power Applications,**" proceedings of The Symposium on Refractory Alloy Technology for Space Nuclear Power Applications, Oak Ridge National Laboratory, 10-11 August 1983, ed. Cooper, R.H, and Hoffman, E.E., January 1984.

Hoffman, E.E., "**Refractory Alloy Component Accomplishments From 1963 to 1972,**" proceedings of The Symposium on Refractory Alloy Technology for Space Nuclear Power Applications, Oak Ridge National Laboratory, 10-11 August 1983, ed. Cooper, R.H, and Hoffman, E.E., January 1984.

DeVan, J.H., DiStefano, J.R., Hoffman, E.E., "**Compatibility of Refractory Alloys with Space Reactor System Coolants and Working Fluids,**" proceedings of The Symposium on Refractory Alloy Technology for Space Nuclear Power Applications, Oak Ridge National Laboratory, 10-11 August 1983, ed. Cooper, R.H, and Hoffman, E.E., January 1984.

Buckman, R.W., "**A Review of Tantalum and Niobium Alloy Production,**" proceedings of The Symposium on Refractory Alloy Technology for Space Nuclear Power Applications, Oak Ridge National Laboratory, 10-11 August 1983, ed. Cooper, R.H, and Hoffman, E.E., January 1984.

Hagel, W.C., Shields, J.A., Tuominen, S.M., "**Processing and Production of Molybdenum and Tungsten Alloys,**" proceedings of The Symposium on Refractory Alloy Technology for Space Nuclear Power Applications, Oak Ridge National Laboratory, 10-11 August 1983, ed. Cooper, R.H, and Hoffman, E.E., January 1984.

Yang, L., Gulden, T.D., Watson, J.F., "**CVD Refractory Metals and Alloys for Space Nuclear Power Application,**" proceedings of The Symposium on Refractory Alloy Technology for Space Nuclear Power Applications, Oak Ridge National Laboratory, 10-11 August 1983, ed. Cooper, R.H, and Hoffman, E.E., January 1984.

Christopher, J.D., "**Machining Refractory Alloys-An Overview,**" proceedings of The Symposium on Refractory Alloy Technology for Space Nuclear Power Applications, Oak Ridge National Laboratory, 10-11 August 1983, ed. Cooper, R.H, and Hoffman, E.E., January 1984.

Lessmann, G.G., "**Welding of Refractory Alloys,**" proceedings of The Symposium on Refractory Alloy Technology for Space Nuclear Power Applications, Oak Ridge National Laboratory, 10-11 August 1983, ed. Cooper, R.H, and Hoffman, E.E., January 1984.

Young, W.R., "**Refractory Alloy Component Fabrication,**" proceedings of The Symposium on Refractory Alloy Technology for Space Nuclear Power Applications, Oak Ridge National Laboratory, 10-11 August 1983, ed. Cooper, R.H, and Hoffman, E.E., January 1984.

Conway, J.B., "**Mechanical and Physical Properties of Refractory Metals and Alloys**," proceedings of The Symposium on Refractory Alloy Technology for Space Nuclear Power Applications, Oak Ridge National Laboratory, 10-11 August 1983, ed. Cooper, R.H, and Hoffman, E.E., January 1984.

Wiffen, F.W., "**Effects of Irradiation on Properties of Refractory Alloys with Emphasis on Space Power Reactor Applications**," proceedings of The Symposium on Refractory Alloy Technology for Space Nuclear Power Applications, Oak Ridge National Laboratory, 10-11 August 1983, ed. Cooper, R.H, and Hoffman, E.E., January 1984.

Harms, W.O., "**Summary of Key Needs for Further Research and Development on Refractory Alloys for Space Nuclear Power Applications**," proceedings of The Symposium on Refractory Alloy Technology for Space Nuclear Power Applications, Oak Ridge National Laboratory, 10-11 August 1983, ed. Cooper, R.H, and Hoffman, E.E., January 1984.

1.5. Miscellaneous

Rempe, J.L., "**High Temperature Thermocouples for In-Pile Applications**," proceedings of the 11th International Topical Meeting on Nuclear Reactor Thermal-Hydraulics (NURETH-11), 2-6 October 2005.

Devold, H., "**Irradiation Performance of Gamma Thermometers Relative to Neutron Detectors**," proceedings of a Specialists' Meeting on In-Core Instrumentation and Reactor Assessment, Fredrikstad, Norway, 10-13 October 1983.

Romslo, K., Moen, O., "**RADCAL Gamma Thermometer: A Promising Device for Accurate Local Fuel Power Measurements in Light Water Reactors**," proceedings of a Specialists' Meeting on In-Core Instrumentation and Reactor Assessment, Fredrikstad, Norway, 10-13 October 1983.

Tsuyuzaki, N., Ishii, T., Tanaka, I., Sagawa, H., Iwai, T., Itami, H., "**Reliability of Thermocouples Experienced in the JMTR**," proceedings of a Specialists' Meeting on In-Core Instrumentation and Reactor Assessment, Fredrikstad, Norway, 10-13 October 1983.

Tavener, J.P., Southworth, D., Ayres, D., Davies, N., "**Industrial Measurements with Very Short Immersion**," Source unknown.

Ruppel, F.R., "**Modeling A Self-Calibrating Thermouple for Use in a Smartj Temperature Measurement System**," Source unknown.

2. Journal Papers

Wood, Van E., "**Thermal Neutron Transmutation Effects on W/W-26Re Thermocouples**," Journal of Applied Physics, Vol. 38, No. 1, pp. 1756-8, March 15, 1967.

3. Commercial Technical Reports

3.1. Pratt and Whitney Aircraft – CANEL

Hahn, H.R., "**Thermocouple Transient Investigation**," TIM-258, Pratt and Whitney Aircraft, 10 May 1956.

Hahn, H.R., "**Capsule Thermocouple Investigation**," CNLM-1757, Pratt and Whitney Aircraft, 19 June 1959.

Tarasewich, A., "Summary of Preirradiation Testing for a Thermocouple Calibration Capsule Mockup," CNLM-3696, Pratt and Whitney Aircraft, 5 June 1961.

Butler, E.N., "Inpile Capsule for Thermocouple Calibration: PW 25 Series," TIM-694, Pratt and Whitney Aircraft - CANEL, 22 June 1961.

Fanciullo, S., "Irradiation Test of Various Thermocouple Connectors," TIM-700, Pratt and Whitney Aircraft - CANEL, 16 August 1961.

Butler, E.N., "Inpile Capsule for Thermocouple Calibration: PW 25 30 Series," TIM-713, Pratt and Whitney Aircraft - CANEL, 23 May 1962.

Fanciullo, S., "Thermocouple Development, Lithium-Cooled Reactor Experiment," PWAC-422, Pratt and Whitney Aircraft - CANEL, 5 March 1964.

Fanciullo, S., "Drift and Endurance Testing of Chromel/Alumel, W-5Re/W-26Re and Mo/W-26Re Thermocouples at 1950F to 2000F for 10,000 Hours," PWAC-454, Pratt and Whitney Aircraft - CANEL, 23 February 1965.

Bliss, P., Fanciullo, S., "High Temperature Thermometry at Pratt and Whitney Aircraft-CANEL," PWAC-462, Pratt and Whitney Aircraft - CANEL, 1 June 1965.

3.2. Rockwell International - Energy Technology Engineering Center

Schmidt, G. L., "SNAP 10A Test Program," Energy Technology Engineering Center, Rockwell International, September 1988

3.3. Westinghouse

3.3.1. Westinghouse Advanced Energy Systems

Bajaj, R., "Operating Instructions for Ultra-High Vacuum Annealing Tests for the SP-100 Program," OI-SPGES-002, Advanced Energy Systems, Westinghouse Electric Corporation, 8 June 1988.

Buckman, R.W., "Operation of Vacuum Furnaces for Pressurized Tube Creep/Lithium-Filled Capsule Exposure," SP-GES-89-2187, Advanced Energy Systems, Westinghouse Electric Corporation, 4 April 1990.

3.3.2. Westinghouse Astronuclear

Hoppe, A.W., Levine, P.J., "Status of High Temperature Thermometry for the NERVA Reactor," Westinghouse Astronuclear Laboratory, internal report.

Sheer, I., Marlett, R.A., "KIWI B-5 Thermocouple Instrumentation," WANL-TMI-338, Westinghouse Astronuclear Laboratory, 24 October 1962.

Ramp, R.L., "Thermocouple, Resistance Thermometer and Strain Gage Transducer Development Plans and Candidate Transducer Data Sheets for Inclusion Into NERVA Instrumentation Data Book," WANL-TME-257, Westinghouse Astronuclear Laboratory, 19 January 1963.

Murray, T.P., "High Temperature Thermocouples for NRX," WANL-TME-582, Westinghouse Astronuclear Laboratory, 4 November 1963.

Gilmour, G.A., "Effect of NRX-A3 Installation on In-Core Thermocouple Accuracy and Response Time," WANL-TME-1019, Westinghouse Astronuclear Laboratory, 28 October 1964.

Malinchak, R.M., "Non-Nuclear Qualification Test on Station 45 Thermocouple Design for NRX-A4 In-Core Application," WANL-TME-1208, Westinghouse Astronuclear Laboratory, 6 July 1965.

Rich, R.B., "Non-Nuclear Evaluation Tests on the Support Block and Cluster Exhaust Gas Thermocouple Designs for NRX Application," WANL-TME-1252, Westinghouse Astronuclear Laboratory, 23 August 1965.

Dunn, W.F., "NERVA High Temperature Thermocouple Insulator Development," WANL-TME-1405, Westinghouse Astronuclear Laboratory, 1 March 1966.

3.3.3. Westinghouse Hanford Company

Cannon, C.P., "2200C Thermocouples for Nuclear-Reactor-Fuel Centerline-Temperature Measurements," HEDL-SA-2639-FP, Hanford Engineering Development Laboratory, Westinghouse Hanford Company, March 1982

Knight, R.C., Greenslade, D.L., "Irradiation Testing of a Niobium-Molybdenum Thermocouple," WHC-SA-1256-FP, Westinghouse Hanford Company, October 1991.

Cannon, N.S., Knight, R.C., "SP-100 W/Re Thermocouple Calibration Techniques," WHC-SA-1258, Westinghouse Hanford Company, January 1992.

Knight, R.C., Cannon, N.S., "SP-100 Reference Temperature Sensor Summary Report," WHC-SP-1080, Westinghouse Hanford Company, April 1994.

3.4. Atomics International

Dearborn, K.R., "Flexure Tests of a Helically Coiled Thermocouple," NAA-SR-MEMO-4717, Atomics International, 8 December 1959.

Whitlock, D.L., "S8DS Gridplate Hydraulics-Thermocouple Insertion," NAA-SR-MEMO-8817, Atomics International, 29 July 1963.

McCarty, W.K., "Status Report - Thermocouple Evaluation Program," NAA-SR-MEMO-9685, Atomics International, 25 March 1964.

Babbe, E.L., "Increasing Thermocouple Reliability for In-Pile Experiments," NAA-SR-10511, Atomics International, 20 April 1965.

Staub, D.W., "SNAP 10A Summary Report," NAA-SR-12073, Atomics International, 25 March 1967.

3.5. General Electric

Otwell, R.L., "Non 1E Thermocouple Temperature Sensor Equipment Specification for the SP-100 Nuclear Assembly Test: Revision A," DOE/SF/16006-T908, General Electric Company, 7 February 1991.

Kjaer-Olsen, C.G., "Evaluate Thermocouple Performance," DOE/SF/16006-T926, General Electric Company, 28 March 1991.

3.6. Aerojet-General

Samuelson, R.D., "Thermocouple Reference Junction Recommendations for NERVA Flight Applications," RN-TM-0594, Aerojet-General Corporation, 3 December 1969.

4. Government Technical Reports

4.1. Oak Ridge National Lab

Cooper, R.H., Harms, W.O., "Engineering Data Bases for Refractory Alloys," CONF-8509153-2, Oak Ridge National Laboratory, 1985.

Hoelzer, D.T., Speakman, S.A., "Recovery and Recrystallization Behavior of Nb-1Zr," ORNL/LTR/NR-JIMO/04-07 – Draft, Aug 04.

Enclosure 7

Optical Pyrometry Technology Evaluation

Ray Blasi, *Bettis-Advanced Material System Integration*

Clint Geller, *Bettis-Advanced Material System Integration*

Ryan Kristensen, *KAPL-Space Electrical Systems*

Harvey Mikesell, *Bettis-Space I&C Design*

Audra Rice, *KAPL-Space Electrical Systems*

Joe Rossman, *Bettis-Space I&C Design*

Ken Wenzel, *Bettis-Space I&C Design*

This page intentionally blank

Table of Contents

EXECUTIVE SUMMARY	5
1.1 WAVEGUIDE PYROMETRY	5
1.1.1 <i>Principal Engineering Challenges of Waveguide Pyrometry</i>.....	7
1.1.1.1 Waveguide Performance Stability (temperature and radiation effects)	7
1.1.1.2 Hot Leg Interface Issues	11
1.1.1.2.1 Surface Configuration.....	12
1.1.1.2.2 Cavity Configuration	13
1.1.1.2.2.1 Surface Mounted Cavity	15
1.1.1.2.2.2 Imbedded Cavity.....	15
1.1.1.3 Sensor Electronics.....	15
1.1.1.3.1 Electrical Interface.....	18
1.1.1.3.2 Radiation Tolerance	18
1.1.1.3.3 Ambient Temperature.....	19
1.1.1.3.4 Electromagnetic Compatibility (EMC)	19
1.1.1.4 Measurement Techniques	21
1.1.1.4.1 Single Wavelength Method.....	21
1.1.1.4.2 Dual Wavelength Pyrometry Schemes	22
1.1.1.4.3 Multi-Waveband Methods.....	22
1.1.1.4.4 Total Broadband Method.....	23
1.1.2 <i>Drift Correction Methods</i>.....	23
1.1.2.1 <i>In Situ</i> Recalibration Options.....	23
1.1.2.2 Expert System Software	27
1.1.3 <i>Extensibility to Other Space Missions</i>	28
1.1.4 <i>Summary Assessment of Development Prospects</i>.....	28

This page intentionally blank

Executive Summary

- Radiation thermometry is a remote temperature measurement method that works with lightweight and flexible dielectric waveguides. The waveguide may not need to experience the primary coolant temperature, although an implementation could involve a blackbody cavity in direct thermal contact with the hotleg pipe. Commercial pyrometry systems usually do not require black body cavities and some routinely are used with surfaces having emissivity values as low as 0.02. Nevertheless the potential advantages and drawbacks of a black body cavity for a Prometheus application need to be evaluated further. Shielding a nickel based superalloy external skin from the primary coolant temperature may also require some sort of an insulated well. Electromagnetic interference (EMI) from the high frequency power cabling is also eliminated as an issue.
- Pyrometry systems with *in situ* recalibration capability have been employed successfully in industry for applications such as metal processing where surface emissivity values change unpredictably. A vendor claims that some deployed systems have operated over ten years without maintenance. However, additional optical components and increased circuit complexity are involved with this recalibration capability. Because of electronics vulnerability, adapting such a recalibration system for space applications would engender moderate to high risk, depending on the radiation profile. Expert system pyrometry implementations also have been commercially available since 1997 that search for wavelength bands in which the dependence of the spectral emissivity is linear, and contain logic that can discriminate narrow spectral features (such as those caused by radiation induced effects in fiber optics) and exclude selected data from consideration (see subsection 1.1.1.5.2). The former approach requires more hardware components, whereas the latter is algorithmically more complex and may require greater computational resources. Both approaches pose challenges but appear promising.
- Several satisfactory options likely exist for sufficiently radiation hardened waveguides to support aft-of-shield pyrometry applications for space missions with radiation profiles up to and including those as severe as the Jupiter Icy Moons Orbiter (JIMO) mission.
- Depending upon mission specifics, the necessary electronics components to support a space pyrometry system may require a level of radiation hardness not readily attainable with today's off-the-shelf, rad-hard components. While this statement may be generally true of JIMO mission electronics requirements, some pyrometry components such as the photon-to-electron converters and signal amplifiers may be especially vulnerable. Rational prospects exist for meeting this challenge, but the risk of failure also is significant.
- A lunar surface or other space mission with reduced charged particle radiation background would tend to reduce development risks associated with a pyrometric temperature measurement system.

1.1 Waveguide Pyrometry

Of the alternative temperature measurement methods currently under consideration within the NRPCT for space applications pyrometry is the only potentially non-contacting technique, although the practicality of implementing such a system without engineering a well on the periphery of the coolant envelope has not as yet been demonstrated.

In contact temperature measurement methods, intimate thermal contact must be maintained between the signal conduit and the surface whose temperature is to be measured. This contact must be maintained without compromising the integrity or properties of the mechanical waveguide or electrical leads in question, and without diffusing the signal conduit into the test surface to such a degree that their interface becomes indistinct and the signal no longer is confined to the lead. Consequently, material interactions between the signal lead and the target surface, including interface embrittlement concerns, are always issues for contact temperature measurement techniques.

As generally implemented, optical pyrometry is a remote technique involving two different materials, both of which are interfaced with vacuum. (Vacuum indicates the absence of material, not necessarily the absence of issues.) Another potentially important difference between candidate techniques is that optical and/or IR waveguides do not suffer from electrical interference from other sensor cables, data transmission cables or power cables in their vicinity.

Optical pyrometry is widely employed in industry for monitoring surface temperatures in material and chemical processing lines where contact temperature measurement techniques are either inconvenient or completely impractical. Certain applications in the steel industry are a case in point. There pyrometric methods are used routinely to ascertain the temperature of molten metal as it moves through the production process. In such applications, surface emissivity values can change rapidly and often. Nevertheless at least two vendors market apparently successful commercial pyrometry systems designed to cope with unpredictably changing emissivity values through *in situ* recalibration schemes. One of these vendors, Pyrometry Instrument Co., based in Northvale, NJ, claims that several of their units are still in regular use more than ten years after having been installed, and without maintenance during that period. IR thermometry is used in numerous other industries, including safety-critical aerospace applications such as health monitoring of jet engines.

To date no experience exists with optical pyrometry under radiation conditions approaching that specified for the JIMO Mission, i.e., up to 2.0 GRad (equivalent in Si) of total ionizing dose and 6×10^{15} neutrons per square centimeter fast fluence immediately aft of the primary shield (decreasing sternward) on sensor components exterior to the electronics vault; and 1 MRad (equivalent in Si) total ionizing dose and a damage displacement dose of 6×10^{11} neutrons per square centimeter (1 MeV equivalent in Si) on electronic components residing within the shielded vault. Concerns raised by the presence of such a radiation field include: a) darkening of the optical waveguides; b) increased noise, reduced sensitivity, and/or systematic drift in the optical diode of the photosensor, the transimpedance amplifier and the analog-to-digital conversion electronics; and c) interrupts and faults in the processing and memory electronics due to energetic charged particles. While some of these issues are common to all the temperature measurement methods currently entertained, photosensors are inherently radiation sensitive because they are designed specifically to sense radiation, and pyrometry systems likely require a higher gain amplification circuit than most competing methods. Spot shielding could be considered for especially sensitive electronic components, though the effectiveness of such additional shielding against either fast neutrons or Bremsstrahlung from extremely energetic heavy ions could be limited. It is not yet clear what aspects of current, emissivity-correcting pyrometric technology would survive such an environment (e.g., the analog circuitry used to compensate for changing photodiode dark current) and which aspects of the technology would need to be reinvented. Of the three great challenges posed by the JIMO Mission profile: harsh radiation fields, prolonged exposure to high temperatures, and inaccessibility (making maintenance effectively impossible), the first would be significantly mitigated by an increasingly likely shift to a moon-based ground power

mission, or even to a Mars based mission. Such a shift thus would favor a proven, non-contact thermometry technique whose biggest unknown would be radiation tolerance.

1.1.1 Principal Engineering Challenges of Waveguide Pyrometry

The principal engineering challenges associated with waveguide pyrometry for a JIMO mission are judged to be: waveguide performance stability; signal processing (HW/SW) issues; radiation hardening of photosensors; and successfully implementing an on-board drift compensation option.

1.1.1.1 Waveguide Performance Stability (temperature and radiation effects)

"Browning" of optical waveguides due to the creation of radiation-induced defects (such as color centers) is a potentially life-limiting process for a pyrometric temperature measurement system operating in a radiation environment. Three generic types of waveguides are available for pyrometry applications, in increasing order of development risk: solid core waveguides; hollow core waveguides; and photonic crystal waveguides. Hollow core waveguides are especially rad-hard, because signals are transmitted primarily in vacuum, but suffer from large signal losses when bent even through a relatively large radius. Photonic crystal waveguides are arrays of small, closely spaced fibers ordered in such a manner as to enhance, or to block transmission in prescribed bands of wavelength. In such crystals signals are transmitted by the evanescent waves existing in the interstices between parallel fibers and within their outer skins. The utility of photonic crystals in a radiation environment is determined by the properties of the building block material(s) of which specific photonic crystal are constructed, their geometric arrangement and the precision with which adjacent fibers are aligned. The NR Program has been studying the use of optical waveguides for terrestrial sensor and data transmission applications in radiation fields more intense than that expected on the JIMO mission. In some of these more demanding applications, hollow waveguides and photonic crystals are still being considered as alternatives to solid core fibers, the adequacy of whose radiation resistance remains in doubt. However, for JIMO-type applications, there appear to be several core fiber materials with sufficient radiation resistance and offering lower development risk to serve. In fact, even in more demanding terrestrial applications, there appear to be promising core fiber materials with sufficient radiation hardness to satisfy mission requirements. A moon or Mars based pyrometry application would appear to offer even less incentive than a JIMO application to pursue hollow core or photonic crystal waveguide development, unless pyrometry applications forward of the reactor shield are contemplated. The remainder of this section, however, will focus on material alternatives for solid core waveguides appropriate for applications aft of the reactor shield.

The decision as to which waveguide material to employ cannot be divorced from decisions as to which and how many waveband(s) at which to collect signals. At 1150K, the spectral radiance of a gray body is maximum at a wavelength of approximately 2.5 microns, well into the infrared range of electromagnetic radiation. However, it is not essential that a pyrometry system employ the portion of the emission spectrum near the Wien wavelength. In fact, other considerations may militate against using the portion of the emission spectrum near the maximum spectral radiance. Commercial vendors of pyrometry equipment tend to prefer wavelengths in or near the visible range for which silicon, or sometimes gallium arsenide photodiodes can be employed. The fundamental bandgap energy of the semiconducting material of which a photodiode is constructed prescribes the maximum wavelength [minimum photon energy] of electromagnetic radiation to which the diode will be sensitive. The maximum electromagnetic wavelength that can be absorbed by a material is given by the approximate formula: $\lambda_{\max} \cong 1.24/E_{\text{gap}}$, where E_{gap} is in eV, and λ_{\max} is in microns. Hence, the maximum absorption wavelength for several possible diode materials, Si, Ge, GaAs, and InAs, will be 1.107,

1.851, 0.886, and 3.543 microns, respectively, at 300K, growing slightly larger at higher temperatures. However, diode dark current correlates inversely with bandgap and with material purity.

Other photon-to-electron technologies discussed in subsections 1.1.1.3 and 1.1.1.4 also favor silicon based devices, because it offers the lowest noise, greatest stability, greatest temperature tolerance, and minimum cooling requirements. GaAs photodiodes are actually more radiation tolerant than silicon diodes because their unirradiated minority carrier lifetimes are less influenced by impurity – based (so called Shockley – Reed – Hall) carrier recombination processes. However, silicon diodes can be made less sensitive to irradiation by increasing the dopant concentrations in the active layers of the diode. This is a trade which also shortens the minority carrier diffusion length and increases the dark current more towards levels typical of binary III-V semiconductors like GaAs.

For the above reason, the portion of the electromagnetic spectrum below approximately 1.1 microns tends to be the most heavily utilized for pyrometry. Within this wavelength range, or others, one or more distinct sensing windows can be established by means of optical filters. If a gray body target undergoes a uniform shift in spectral emissivity, the magnitude of the shift can be factored out of a temperature determination by ratioing the signals collected from each window. If a *non*-gray body target undergoes a *non*uniform spectral emissivity shift in service, recourse to multiple wavebands can enable an improved temperature estimate under certain conditions. Multiband schemes generally either work on line-of-sight optics without waveguides, or assume that the characteristics of the waveguide being used, which is usually removed from and cooler than the target, do not change over time. In many application environments this would be an eminently reasonable assumption, but not necessarily in a radiation field. To employ a multiple band pyrometry scheme together with an optical waveguide in a reasonably harsh radiation environment, one would either need to know in advance how the waveguide properties will change, or one would need a reliable *in situ* recalibration scheme capable of determining such changes independently of possible simultaneous changes in the emissivity of the target surface. The impact on a temperature determination of expected shifts in waveguide characteristics due to radiation can be minimized through judicious choice of waveguide materials and wavebands. By avoiding certain wavelength ranges, the browning problem can be significantly mitigated. (The greatest relief, of course, results with silica fibers from strictly minimizing the degree of initial water contamination.) Waveguide materials that exhibit no appreciable transmission changes in a useable set of wavebands obviously are preferred, although the only hard and fast requirement is that their transmittance remains in the acceptable range. Transmission losses as high as 50%, and perhaps greater, over 60 meters are likely to be tolerable.

The known irradiation performance of several prospective solid core optical fiber materials is summarized in Table 1.1.1.1-1. For transmission over distances of 60 meters or more at visible wavelengths, high purity silica is likely a good choice, even for the demanding JIMO mission service conditions. The presence of hydroxyl ions in irradiated silica is associated with the development of an absorption band near 1.38 microns (1380 nm). Brichard *et al* have identified γ -induced hydrogen diffusion as the principal source of hydroxyl absorption band formation in silica optical fibers exposed in nuclear reactors [1.1.1.1.-1]. However, while producing a vibrational band at 1380 nm, the presence of hydroxyl may somewhat suppress color center formation, another optical loss mechanism, at 850 nm [1.1.1.1.-2]. At 850 nm, some silica fiber sample types subject to mixed neutron and γ radiation in the BR-2 reactor exhibited less than 4 dB signal loss (about a 60% loss) per meter after 200 GRad TID and $> 1.3 \times 10^{20}$ n/cm²[1.1.1.1-2]. Scaled linearly to a TID of 2.0 GRad, this represents about a 0.6% loss per meter, or a 30.3% signal loss in 60 meters. However, even 10 mils of aluminum would reduce environmental charged particle TID by 90%. Hence TID values on the order of 0.5 GRad are probably more realistic than the worst case assumption of a completely unshielded, completely

exposed fiber, yielding a TID of 2 Grad. This more realistic environmental TID assumption, considering that optical fibers will run along the interior of the spacecraft boom, results in only an 8.6% reduction in signal strength over 60 meters. If all traces of water can be purged from the silica prior to irradiation, this absorption band can be significantly suppressed. Another source reported that over a length of 100 meters, unirradiated high purity silica with low water content transmits over 90% of the incident signal at all wavelengths from 800 to about 1900 nanometers (0.8 to 1.9 microns), with only a small dip near 1400 nm associated with optical absorption via hydroxyl ions[1.1.1.1-3]. Attenuation increases sharply deeper in the IR region.

Solid core fibers of pure silica generally are acknowledged to tolerate radiation better than silica fibers alloyed with germania. Nevertheless, a silica + 5% germania fiber successfully withstood 87 GRad of TID from γ rays and 2×10^{19} n/cm² (E>1MeV) fast fluence with minimal effects [1.1.1.1-4]. Other material options include sapphire, and also a class of Ba/Al/Mg fluorophosphate glasses which have not to date been pulled into fibers but which have impressively withstood high neutron and gamma doses in the ATR. (The most successful fluorophosphate glass composition to date is: 25 mol% Ba(PO₃)₂ + 10 mol% Al(PO₃)₂ + 40 mol% BaF₂ + 25 mol % MgF₂. This starting composition is then "doped" with 5 w/o Yb.) Sapphire offers possibilities of transmission into the IR as well as the visible region of the electromagnetic spectrum, whereas silica based products transmit adequately only in the visible and near IR ranges. The external transmittance of sapphire is nearly constant at approximately 85% through a 1 mm thick plate from wavelengths of 0.3 microns to just beyond 4 microns [1.1.1.1-5]. (The 15% decrement in transmitted signal is virtually all a Snell loss associated with reflections off the uncoated front and rear surfaces of the test specimen.) A vendor, AFO Research claims that their fluorophosphate glasses also transmit well in the IR, but the company has not provided data to substantiate this claim. The index of refraction of sapphire is similarly quite flat in this range [1.1.1.1-5], resulting in little chromatic aberration, thus facilitating lens design. However, sapphire is birefringent with a difference of 0.08 in the refractive indices of the fast and slow rays. (This fact could mildly complicate calibration algorithms involving a time delay.) While no γ irradiation data are available for sapphire to total ionizing doses as high as 2.0 GRad (5×10^8 rads), it is noted that even a thin ~10 microns skin on any surface likely will drop the expected JIMO Mission total ionizing dose, due primarily to protons, by an order of magnitude.

The information provided in several published reports by Luna Innovations, such as that in Reference [1.1.1.1-5] indicates that a silica glass fiber alloyed with five "percent" of germania continued to transmit useable signals for a sensor located at a fuel element centerline position in an operating nuclear reactor out to a fast neutron fluence of 2×10^{19} n/cm² (E>1 MeV), and a γ dose of 87 GRad (presumably equivalent in Si). In the plot provided, reproduced below as Table 1.1.1.1-1, the degree of signal attenuation appeared minimal at 1 GRad TID.

Table 1.1.1.1-1. Irradiation Performance of Selected Waveguide Materials

Composition	Radiation Source	Observations	Supplier/Reference(s)
High purity silica	$>1.3 \times 10^{20}$ n/cm ^{2*} 200 GRad*	< 4dB (~60%) per meter signal loss	[1.1.1.1-3]
Silica + 5% germania	2×10^{19} n/cm ² (E>1MeV) 8.7×10^{10} rads γ	Sensor with fiber optic line continued to function	Luna Innovations [1.1.1.1-4]
Sapphire	10^7 rads γ	"No transmission changes above 2.5 μ m"	Marketch Intl. [1.1.1.1-5]
Sapphire	10^8 rads γ	"No visible coloration"	Marketch Intl. [1.1.1.1-5]
Sapphire	10^{12} protons/cm ²	"No transmission changes below 0.3 μ m"	Marketch Intl. [1.1.1.1-5]
Yb-doped Ba/Al/Mg fluorophosphate glass**	8.2×10^{20} n/cm ² *** γ dose unknown ***	Little or no observable darkening	AFO Research [1.1.1.1-6]

* BR-2 reactor

** to date, these materials exist in glass plate form only

*** ATR spectrum

Other properties of concern for solid core fiber materials include the maximum use temperature (a glass doesn't have a "melting temperature" *per se*, but it typically has a temperature at which it softens dramatically), and fracture resistance. The melting temperature of sapphire (crystalline alumina) is 2300°C (2573K), whereas the softening temperature for the fluorophosphate glasses is reported verbally by the vendor, AFO Research, to be approximately 1200°C (1473K)[1.1.1.1-6]. (However, there is no published documentation for the number cited by AFO.) In hypothetical JIMO mission applications, fibers would be exposed to a wide range of service temperatures between the primary shield and the stern electronics vault. Shock and vibration loads associated with vehicle launch would not likely be severe on account of the low mass of optical fibers. Fatigue and aging of silica optical fibers has been observed [1.1.1.1-7], but only in humid and/or aqueous environments. Thus launch pad conditions might have to be considered and controlled. However, the chosen fiber design will have to survive a boom unfolding operation at some as yet unspecified temperature without ill effects. Though pyrometry is a remote thermometry technique, it is nevertheless reassuring to have available fiber materials with a maximum use temperature greater than the anticipated steady-state reactor hot leg temperature, 1150K. All the materials listed in Table 1.1.1.1-1 are believed to retain sufficient material strength and integrity at that temperature. Fracture resistance is believed to be a strong function of the nature of the notch-resistant surface coatings applied to the fiber, as critical flaws tend to be introduced most often along the surface. On a spacecraft, the surface coating must also serve the function of grounding the fibers so they don't charge and develop an electrostatic potential relative to other components on the spacecraft. Metal coatings for optical fibers are commonplace, although melting temperature and thermal expansion characteristics will have to be weighed in their selection.

Based upon a review of available data, it is concluded that one or more materials are likely to exist that can serve as the basis for an optical fiber meeting all service requirements for the JIMO Mission. Such fibers could be used for any shipboard or ground based data transmission application including but by no means limited to pyrometry.

References:

- [1.1.1.1-1] B. Brichard *et al*, "Round-robin evaluation of optical fibers for plasma diagnostics," *Fusion Engineering and Design*, 56-57 (2001), pp. 917-921.
- [1.1.1.1-2] B. Brichard *et al*, "Origin of the Radiation Induced OH Vibration Band in Polymer-Coated Optical Fibers Irradiated in a Nuclear Fission Reactor," *IEEE Trans. on Nuclear Science*, Vol. 49, No. 6, December 2002.
- [1.1.1.1-3] Polymicro Technologies website:
www.polymicro.com/products/opticalfibers/products_opticalfibers_stu-stud.htm
- [1.1.1.1-4] R. S. Fielder *et al*, "High-Temperature Fiber Optic Sensors, an Enabling Technology for Nuclear Reactor Applications," Proc. ICAAP, June 13, 2004 , pp. 2295-2305.
- [1.1.1.1-5] MatWeb Materials Property Database, www.matls.com
- [1.1.1.1-6] R. J. Blasi, B-MT(EDT)F-739, dated 12/7/2004.
- [1.1.1.1-7] M. J. Mathewson, "Kinetics of degradation during fatigue and aging of silica optical fiber," SPIE Vol. 2290, February, 1994, pp. 205-210.

1.1.1.2 Hot Leg Interface Issues

Because pyrometry is a potentially remote temperature sensing method, one may have the opportunity to maintain the end of the sensor (i.e, the waveguide) at a temperature possibly hundreds of degrees lower than that of the surface whose temperature is being sensed unless a blackbody cavity is used which would be in intimate thermal contact with the piping. This fact expands the choice of construction materials and enhances prospects for long-term stability in service. However, two vacuum interfaces are thus acquired instead of the mechanical interface - at the surface of the collecting lens, and at the measurement surface. These vacuum interfaces must retain optical properties that are stable over the mission life, or at least sufficiently so as to be within the capacity of an *in situ* recalibration system to track (if such a system is implemented).

The infrared radiation emitted by the hot leg may be sourced by either the surface of the piping or a cavity attached to or otherwise imbedded in the piping. It is important that the emissivity of the source be constant in the face of extended time at high temperatures, exposure to a variety of radiation, and variable temperatures, which is an area that requires further investigation.

1.1.1.2.1 Surface Configuration

In the original evaluation of temperature sensing technologies, the assumption was made that access would be provided to at least one small area on the exterior of the hot leg piping, possibly near the Brayton inlet. With pipe-in-pipe design possibilities, this is not well-defined and all options must be considered at this time. The cavity configuration discussed below is also adaptable to the case of a well in the primary coolant envelope wall underneath insulation. However, the pyrometer probe may collect infrared radiation emitted directly from the surface of the pipe or from a special material affixed to the surface. These two configurations are depicted in Figure 1 and Figure 1.1.1.2 below.

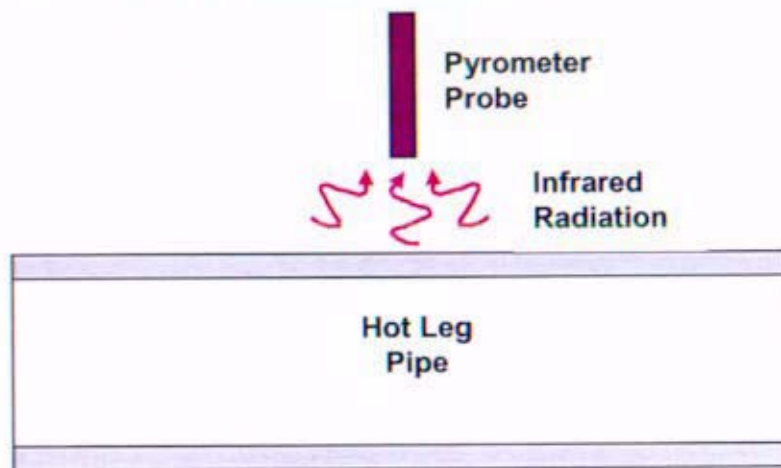


Figure 1.1.1.2.1-1: Detection using pipe surface as source

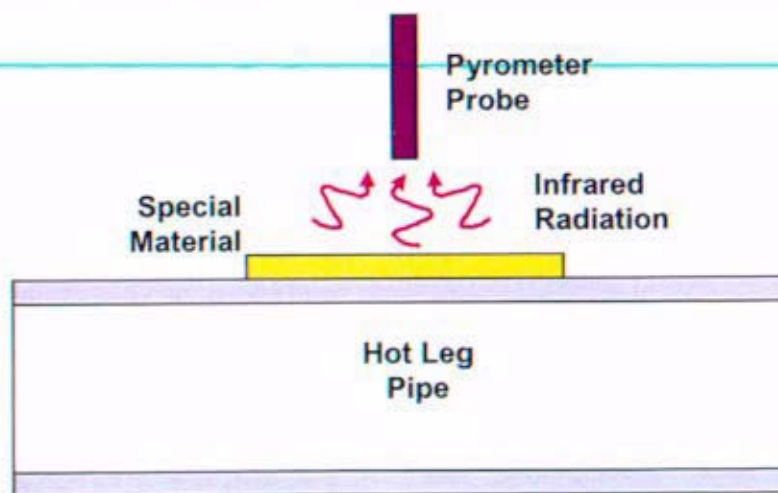


Figure 1.1.1.2.1-2: Detection using material affixed to pipe surface as source

Such configurations suffer from the following challenges:

- *Reflected infrared radiation from nearby components at similar temperatures*

This effect could result in an erroneously high temperature indication due to the probe collecting more thermal radiation than the target surface is emitting. A collecting lens (or other waveguide end configuration) with a relatively narrow acceptance angle can minimize these effects. This is the approach successfully taken in the design of portable laboratory pyrometer units. Alternatively, appropriate shielding/blinders may be engineered.

- *Surface modification or sublimation*

Time at temperature may destabilize or otherwise destroy any special coatings or texturing applied to enhance the surface emissivity. This could result in a decrease in emissivity, thus causing an erroneously low temperature indication because high emissivity surfaces emit more energy than low emissivity surfaces at the same temperature. Any change in the surface due to deposited material from other components or an oxidation layer from environmental oxygen could also alter the actual emissivity of the surface. While the hard vacuum of deep space ($\sim 10^{-15}$ torr residual pressure) is relatively propitious for pyrometry, traces of monatomic oxygen and/or sulfur found around some planets (such as Earth) could attack exposed surfaces. However, there are likely several good choices available for emitting surfaces, such as the refractory metals rhenium, tungsten and molybdenum, which have melting temperatures high above the maximum foreseeable service temperature, very low vapor pressures and evaporation rates at anticipated service temperatures, and no stable native oxides that could accumulate on the surface. This subject is discussed at greater length in subsection 1.1.1.4 .

1.1.1.2.2 Cavity Configuration

A cavity geometry may be utilized to create an effective emissivity as near to that of a blackbody as possible for the pyrometer to target. This may be desirable in order to enhance signal intensity and suppress background noise, although other considerations may favor lower emissivity values (see subsection 1.1.1.4). Cavities may be surface-mounted or imbedded in the pipe as depicted in Figures 1.1.1.2.2-1 and 1.1.1.2.2-2, respectively.

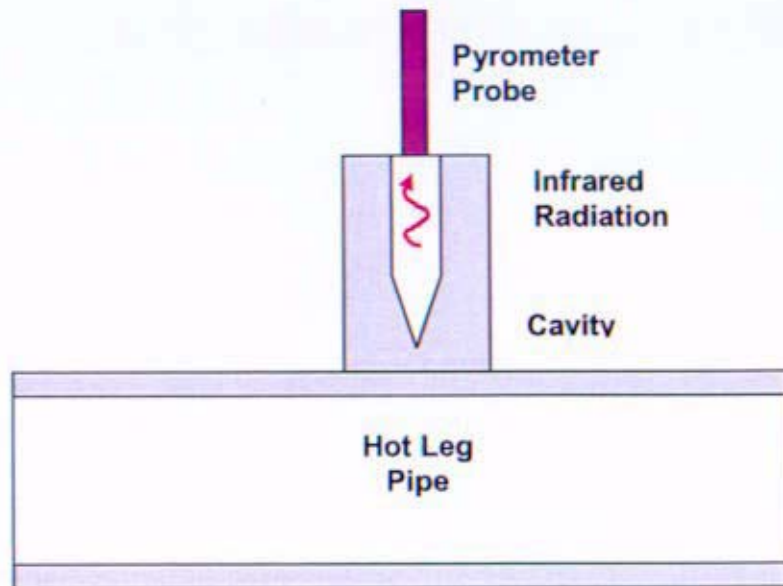


Figure 1.1.1.2.2-1: Detection using surface mounted cavity as source

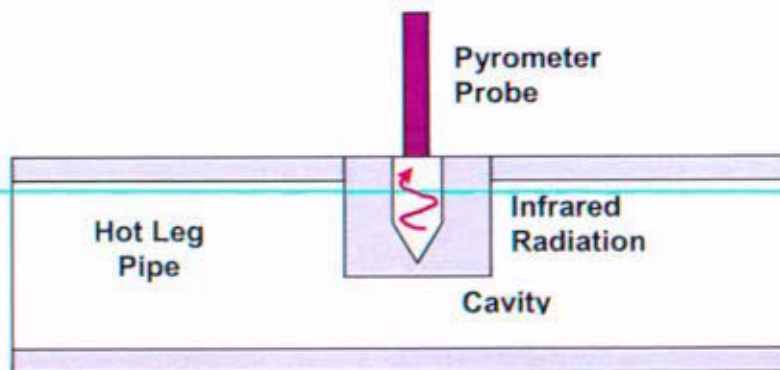


Figure 1.1.1.2.2-2: Detection using imbedded cavity as source

Near blackbody emission conditions usually are obtained with optical cavities with depth-to-width ratios greater than 5:1. However, conical cavity terminations help to better trap incident light, thus reducing reflection and raising emission (via Kirchoff's Law). Specially coated or otherwise textured surfaces can also enhance emissivity.

1.1.1.2.2.1 Surface Mounted Cavity

Mounting the cavity to the surface of the pipe has the benefit of a lack of pressure boundary penetrations. However, the projecting cavity will radiate away a portion of the heat conducted from the pipe wall and develop a temperature gradient along its length. This gradient will result in an erroneously low temperature indication unless it is accurately modeled. Extensive modeling and characterization of this effect may enable a correction factor to be generated. It is also noteworthy that an additional response time penalty will be required to allow for the pipe to conduct its heat the length of the cavity.

1.1.1.2.2.2 Imbedded Cavity

Imbedding the cavity in the flow stream has the benefit of homogenizing the temperature distribution along its length (assuming that the flow stream is isothermal in the radial direction). Even if the flow is not isothermal, the indication should at least yield an approximately average temperature. Overall response time also is quickened by the direct contact of the radiating surface to the measurand. However, as mentioned, the imbedded configuration necessitates an undesirable and otherwise unnecessary pressure boundary penetration. Furthermore, the penetration would constitute a flow obstruction and a possible source of turbulence, and thus vibration.

1.1.1.3 Sensor Electronics

The hardware interface to the optical sensor will depend on the particular technology and configuration chosen for this application. There are a variety of candidate sensor options under investigation, with varying degrees of information available as to circuit details and performance characteristics. Most commercially available optical temperature measurement devices are proprietary designs targeted to address specific applications. Although many vendor products operate in the required temperature sensing range, the need for continuous accurate operation without maintenance, and the environmental conditions that the sensor electronics must withstand will likely require custom design and qualification of any of the potential candidate sensor technologies. (Although, anecdotal evidence provided verbally by vendors suggests that pyrometry systems can operate reliably in the field for over ten years without maintenance.)

There are two basic approaches that can be taken to interface the optical sensor to the reactor instrumentation.

- a) Develop a custom bus-based board designed to fit into the instrumentation chassis. This board would connect to the optical fibers and contain all of the optical to electrical interface electronics. Digital logic and software routines implemented on this board would provide all the processing necessary to determine the monitored temperature and provide the data to the reactor control system.
- b) Utilize a separate optical-to-electrical "transducer" interfaced to an I/O chassis board. This transducer would receive the optical signal from the fiber and would output an analog or digital signal proportional to the light input. Any custom signal processing, diagnostics, or control can be done either in the transducer circuitry or in the interface board processor.

The custom board approach minimizes the space for the optical pyrometer system and allows for a complete custom design tailored for the measurement conditions. The separate transducer approach

allows for better use of existing vendor packaging and design technologies and improves the packaging options to fit the needs of the optical components.

Many optical sensor techniques are sensitive to environmental temperatures, have custom power and cooling requirements, and may utilize proprietary complex signal conditioning, specialty optics or optical filters to obtain desired performance. These constraints may make a particular design configuration difficult to implement in a single board solution. An option exists to cool certain electronic components within the vault. Thermoelectric coolers are highly reliable and effective for local area cooling applications. However, they transport heat only over very short distances. Thus it is likely that some additional heat transport system, preferably a passive one with no moving parts, would have to be linked to the thermoelectric cooler.

A summary of different available sensor types and their responses is provided in Table 1.1.1.3-1. the general trend is that silicon based devices start out better than binary and ternary III-V devices but degrade somewhat more rapidly upon irradiation. However, this trend can be mitigated through higher levels of doping.

Table 1.1.1.3-1. Radiation Response of Selected Diode Types

Detector	Response	Radiation	Comment	Reference
930 nm PIN Si	Normalized photoresponse decreased to 0.9	4×10^{11} 50 MeV protons per square centimeter	Carrier removal effects the lightly doped intrinsic region causing leakage current to increase and these changes are noticeable at levels around 1×10^{10} protons per square centimeter	<i>Radiation Damage of Electronic and Optoelectronic Devices in Space, Johnston, 4th international workshop on Radiation Effects on Semiconductor Devices for Space Application, Japan Oct. 2000</i>
650 nm PIN Si	Normalized photoresponse decreased to 0.97	4×10^{11} 50 MeV protons per square centimeter	Same as above	Same as above
930 PN Si	Normalized photoresponse decreased to 0.5	4×10^{11} 50 MeV protons per square centimeter	Leakage current changes in conventional photodiodes are much smaller because the doping levels are higher than the	Same as above

			intrinsic region level.	
650 PN Si	Normalized photoresponse decreased to 0.85	4×10^{11} 50 MeV protons per square centimeter		Same as above
Honeywell HFD 3013 – 850nm PIN silicon	Responsivity decreased 10%	Gamma irradiation 2×10^8 rad(Si)	Linearity remains the same	<i>Reliability issues for optical fibre technology in nuclear applications (Francis Berghmans)</i>
Honeywell HFD 3013 – 850nm PIN silicon	Responsivity decreased 20%. Dark current increased by a factor of 500.	Thermal neutrons 7×10^{15} neutrons per square centimeter		Same as above
Silicon PN 930nm detector	Detector current reduced 0.5 of the normalized detector current	3×10^{11} protons per square centimeter		<i>Proton Damage in Advance Laser Diodes, IEEE Trans. Nuc. Scie. Vol 48, No. 6 2001, Johnston.</i>
Lumex internal monitor diode – 650 nm	Negligible degradation	3×10^{11} protons per square centimeter	This is expected since the charge collection in direct bandgap semiconductors does not require long minority carrier lifetimes	Same as above
InGaAs FU-15PD	Normalized detector response decreased to 0.5 and increase in leakage current from 1nA to greater than 1 micro amp	1×10^{13} 63MeV protons per square centimeter		<i>Space Radiation effects of optoelectronic material and components for 1300nm fiber optic data bus: IEEE transactions on nuclear science vol 39, no. 6 dec 1992.</i>
InGaAs FU-15PD	Normalized detector	1×10^{13} 63MeV protons per		Same as above

	response decreased to 0.95 and increase in leakage current from 1nA to greater than 100nA	square centimeter		
InGaAs FU-15PD	No negligible degradation	Gamma irradiation Co-60 1Mrad(Si)		Same as above

1.1.1.3.1 Electrical Interface

The optical sensor technology used may be as simple as a photo-diode which is a quantum device that generates current in proportion to radiation intensity in its response bandwidth. Alternatively the sensor may be an array imager based on photo-diodes, charge coupled devices (CCDs), or charge injection devices (CIDs). Pyro-electric devices such as CCDs and CIDs develop an electrical charge proportional to the incident radiation. Array devices require complex analog and digital circuitry to sample and measure individual cell charges and to output the resulting measurements to an image processor application. While image processing is not required for the contemplated application, using a compact sensor array may facilitate the ability to use state-of-the-art manufactured sensors, which would be unavailable on an individual basis. Image processors have undergone rapid design advances in recent years and a common implementation would have the CCD interface circuitry integrated into the sensor package. Array devices may be combined with optical grating devices (monochromators) in some designs to implement multiwavelength detection schemes. The output of the array would be stored in memory and algorithms would be applied to condition and process the multiple array element data values for a final temperature measurement.

It is the case with all detectors that the calibration curves of detector output versus temperature are non-linear. This is because the radiant intensity emitted by objects is usually proportional to the fourth power of temperature. The radiation thermometer electronics must amplify, regulate, linearize and convert this signal to an analog or digital output proportional to temperature. Additional complexities are added by features such as environmental temperature compensation, temperature regulation, output linearization, and circuits to correct for variations in the sensor output, waveguide transmission, or emissivity of the measured surface.

If it is determined to implement a separate transducer design, packaged solutions to provide the appropriate interfaces in compact form factors are reasonably achievable. The optimum transducer will output a signal proportional to the temperature of the monitored surface with minimal post-processing requirements.

1.1.1.3.2 Radiation Tolerance

The electronics associated with the photo-detector interface will be radiation hardened up to 1 MRad TID and a damage displacement dose of 6×10^{11} (1 MeV equivalent) neutrons per square centimeter. Optical sensors of interest have not been tested or qualified to these levels, of which the DDD level is considered more critical. Displacement damage is also a concern when dealing with optical components. Areas of concern are high sensitivity analog components, digital signal processors,

memory, and sensors. High sensitivity analog components such as precision operational amplifiers are subject to gain effects and must be designed to account for gain loss. Specialty digital signal processors and associated memory and logic gates will need to be developed with a rad-hard process to meet the 1 MRad TID requirements. The risk associated with achieving an optical pyrometry interface electronics solution that meets the program objectives is believed to be moderately high. The primary area of concern is the optical sensor.

As introduced in previous sections, photon-to-electron (i.e., light-to-electrical) conversion can be accomplished via several technologies including photodiodes, which provide a current proportional to the incident light intensity, or via CCD's (charge coupled devices) or CIDs (charge injection devices), which store charge in proportion to the total amount of light energy incident upon them in some time interval. CCDs and CIDs then provide a voltage proportional to the stored charge [1.1.1.3.2-1]. In all three types of devices, carriers produced by means other than incident light within the waveband of interest interfere with the signal being measured. In photodiodes, thermally excited minority carriers lead to the presence of a so-called dark current which influences device efficiency, noise, and cooling requirements. The dark current generally obeys an exponential relationship with the ratio of the fundamental bandgap, E_g , of the diode material, divided by $k_B T$, where k_B is Boltzmann's Constant. Therefore, other things being equal larger bandgaps make for smaller dark currents, less noise, lower cooling requirements and better devices. Similarly for CCDs and CIDs, thermal excitation of minority carriers determines the required refresh rate and sets cooling requirements and operating temperature limits. An advantage of silicon technology is that it is available in extremely pure form, and it has an indirect bandgap, which contributes to long minority carrier lifetimes. Nevertheless, diodes comprised of binary III-V compounds such as GaAs tend to show smaller radiation effects because their initial defect densities are higher to begin with and because other charge carrier recombination mechanisms dominate at lower dose levels.

Reference:

[1.1.1.3.2-1]S. M. Z. Sze, "Physics of Semiconductor Devices," 2nd Edition, Wiley Publishers, 1981.

1.1.1.3.3 Ambient Temperature

The sensor electronics will reside in the vault area where it will be required to have an operating range of -50°C to 70°C . Although optical temperature sensors are sensitive to ambient temperature (the dependence of dark current of a diode with $E_g/k_B T$ has been mentioned), there are compensation methods that have been implemented by vendors to extend the operating range. Additional methods such as thermoelectric cooling have also been utilized. Many commercial infrared pyrometers have an environmental operating range of -10°C to 50°C and some are specified at -10°C to 70°C .

1.1.1.3.4 Electromagnetic Compatibility (EMC)

A major potential advantage of radiation thermometry is that the waveguides need not conduct electrical current (though it may need to be grounded in order to prevent arcing and/or Lichtenberg discharges.) As a result, a pyrometric waveguide would not suffer interference from a high frequency $>100 \text{ KW}_e$ power cable with which it might need to share a 60 meter length of cramped boom interior.

EMC considerations for the electronic components of a pyrometry system within the shielded vault involve susceptibility to and emission of conducted and radiated electromagnetic interference (EMI).

All components of a pyrometer system (sensor, cable, electronics) must meet agreed-upon requirements for electromagnetic compatibility to ensure that the sensor system functions reliably in the spacecraft EMI environment. This includes requirements that the sensor system does not interfere with the operation of other equipment. General requirements for EMI compatibility and testing are provided in MIL-STD-461. This standard is utilized by military and space agencies. MIL-STD-461 requirements will need to be tailored to the Prometheus application in a program requirements document. This process is currently underway and is being incorporated into the JPL Prometheus Project Environmental Requirements Document. Additional guidelines concerning static charging on spacecraft are provided in:

- NASA-HDBK-4002, Avoiding Problems Caused by Spacecraft On-Orbit Internal Charging Effects
- NASA-TP-2361, Design Guidelines for Assessing and Controlling Spacecraft Charging Effects

Radiated Susceptibility

The largest concern for low frequency radiated susceptibility is the long cable run between the sensor and the electronics. Sensor cables will run parallel to power line cables operating at a nominal frequency of 2250 Hz. The use of fiber optic cables eliminates this concern. Susceptibility to electric fields generally applies to high frequency signals on the order of 10 MHz and above. With proper shielding and grounding of the sensor electronics, the risks associated with radiated susceptibility are judged to be very low.

Radiated Emission

The radiated electric field emission baseline is projected to be 70 dBuV/m maximum from 10 kHz to 10 GHz. Pyrometer sensor elements and waveguides are not expected to be sources of radiated electromagnetic emissions. The associated pyrometer electronics are not expected to be significant sources of radiated emissions. These instruments will be configured and shielded as necessary to maintain radiated emissions within requirements. Radiated emission risk is judged to be low.

Conducted Susceptibility

This requirement applies to noise coupled from the power bus into the pyrometer instrumentation. The electronics will be required to operate satisfactorily within the power quality specifications of the instrumentation power bus. Conducted susceptibility risk is low.

Conducted Emission

This requirement applies to noise coupled on to power leads from the pyrometer instrumentation. The power circuits of the pyrometer instrumentation will be required to operate satisfactorily within the power quality specifications of the instrumentation power bus. Conducted emission risk is low.

Electrostatic Discharge

Equipment must be designed to prevent or tolerate electrostatic charging and discharging events. All electrical instruments will have a general requirement for single point grounding and there shall be no ungrounded conductors (non-electrical and non-electronic without a conductive bleed path to chassis) of size greater than 3 cm² on most parts of the spacecraft and no ungrounded conductor areas greater than size 0.3 cm² on or near circuit boards or cabling or other electronics. As stated earlier, the pyrometer sensor system has the advantage of high dielectric strength associated with the use of fiber optic cables. There may however be

some risk associated with displacement damage to fiber optic cables from charged particles. Analysis and testing of this potential damage mechanism will be part of the qualification of any fiber optic based system. Electrostatic discharge risk is moderate.

1.1.1.4 Temperature Measurement Techniques

1.1.1.4.1 Single Wavelength Method

Basic narrow band pyrometers operate over a narrow range of wavelengths. The spectral response is typically determined by the optical filter used. These devices are used as general purpose instruments over the temperature range of interest. For example, an optical pyrometer using a silicon cell detector will have a response that peaks at approximately $0.9\mu\text{m}$. The upper limit of usefulness is about $1.1\mu\text{m}$. Such a thermometer is typically used at temperatures above 600°C . Other detector materials can be used to obtain different temperature responses.

Compared with other pyrometry measurement schemes, the advantages of such a system include:

1. Simple, low-cost measurement
2. One has maximum flexibility to optimize the transmission characteristics of the waveguide by appropriate selection of the analytical waveband.

The corresponding disadvantages of this scheme are:

1. Narrow temperature range (accuracy falls off sharply outside this range)
2. It would likely be difficult to develop a unit satisfying all performance criteria.
3. One must assume that the emissivity of the source is known in the analytical waveband. Otherwise one cannot determine the thermodynamic temperature (contact temperature).
4. The accuracy of single wavelength techniques is maximally affected by emissivity changes.
5. This is an intensity based measurement subject to errors with changes in signal path transmission losses or amplifier gain drift.

1.1.1.4.2 Dual Wavelength Pyrometry Schemes

In this method, a ratio of the measured source radiance at two wavelengths is utilized. In contrast to an uncalibrated single window method, changes in emissivity may be factored out, as long as the spectral emissivity changes in each of the two analytical windows are in proportion. This will be true of gray-body emitters as well as many other non-gray-body emitters. Changes in target size thus have no effect on the temperature reading, and the ratio techniques may reduce or eliminate changes in indicated temperature caused by changes in surface finish. The ratio technique may also reduce the effect of energy absorbing materials such as particulates becoming interposed between the target and the thermometer, provided that the percentage of resulting absorption is the same in both bands.

The advantages of two-color pyrometry over single color are:

1. Less sensitive than single color methods to varying target size or intermittent blockage of sight path by smoke, particles, etc.
2. Less sensitive than single color methods to spectral emissivity changes, provided that the spectral emissivity changes in the same direction in both analytical windows.

Disadvantages of the two-color system are:

1. Greater complexity, potential development cost, and board space requirements
2. Two-color schemes are sensitive to changes in ratio of spectral emissivity values in different wavebands.
3. Two-color schemes are more noise sensitive. The difference in emission intensities in the two analytical wavelengths is typically small, and one must compute a ratio between two noisy signals.

1.1.1.4.3 Multi-Waveband Methods

The spectral radiance of the source is measured at three or more wavebands and the temperature of corresponding Planck curve determined. (More details are provided in subsection 1.1.2.)

The advantages of this method relative to single and double window measurements are:

1. Improved measurement of surface temperatures in the presence of background radiation from other sources.
2. Higher signal to noise, via statistical averaging and least squares fitting.
3. Improved ability to measure materials with complex optical properties such as low emissivities that vary with both temperature and wavelength.
4. Measurements should be insensitive to relatively uniform changes in signal strength caused by variations in the transmission properties of the optical fiber or efficiency changes of the optical

detector. This is because signal strength measurements at one wavelength are made relative to the signal strength measurements at the other wavelengths.

Disadvantages of the multi-waveband are:

More complex processing requirements than other methods – may involve spectral analysis methods in some implementations. Many data points need to be measured and averaged for each temperature calculation.

1.1.1.4.4 Total Broadband Method

In the total broadband method, the spectral radiance of the source is integrated across the entire wavelength spectrum. Broadband thermometers usually have been the simplest infrared radiation thermometers (IRTs), with spectral responses from 0.3 microns wavelength to an upper limit of 2.5 to 20 microns (μm), determined by the lens or window material. They have been termed “total radiation” thermometers because, in the temperature ranges of normal use, they measure a significant fraction of all the thermal radiation emitted by the object whose temperature is being measured.

Advantages of the total broadband method are:

1. Low cost due to simple opto-electronic interface and minimal signal processing required.
2. Wide temperature spans
3. Simple

The disadvantages of this method include:

1. Lower sensitivity
2. Susceptible to absorption errors due to sight path conditions. This should not affect a fiber optic implementation that is shielded from other optical radiation sources.
3. Requires complete knowledge of source spectral emissivity over a broad range of wavelengths.
4. This is an intensity based measurement subject to errors with changes in signal path transmission losses or amplifier gain drift.

1.1.2 Drift Correction Methods

The requirement for 10+ years of reliable operation without maintenance creates a necessity for effective *in situ* drift correction and/or recalibration mechanisms. Somewhat similar requirements are encountered by pyrometric systems in certain industrial applications such as steel and aluminum processing in which surfaces of molten metal change emissivity rapidly and unpredictably. The emissivity changes anticipated in a space application are smaller, but may be superimposed on larger changes in waveguide transmissivity resulting from accumulated radiation damage.

1.1.2.1 In Situ Recalibration Options

An optical pyrometry system determines the temperature of a radiating surface based on the Planck Radiation Law, Eq. 1.1.2.1-1.

$$\text{Eq. 1.1.2.1-1 } I(\lambda, T(t)) = \epsilon_{\lambda} \left(\frac{c_1}{\lambda^5} \right) \frac{1}{\exp(c_2/\lambda T(t)) - 1}$$

Above, λ is the wavelength of the radiation, c_1 and c_2 are material-independent radiation constants, and ϵ_λ is the surface spectral emissivity. The spectral intensity of the radiation emitted from the measurement surface is converted into a spectral voltage contribution, given by Eq. 1.1.2.1-2, corresponding to a particular range of emitted wavelengths. Most generally the surface temperature one needs to measure, $T(t)$, is time-dependent. Thus we may write:

$$Eq. 1.1.2.1-2 \quad V(\lambda, T(t)) = g_\lambda \epsilon_\lambda \tau_\lambda \left(\frac{c_1}{\lambda^5} \right) \frac{1}{\exp(c_2 / \lambda T(t)) - 1}$$

Above, g_λ and τ_λ are the spectral instrument response and the combined transmission coefficient of all media (such as gas, waveguides, lenses, etc.) between the radiating surface and the detector, respectively. As far as the temperature determination is concerned, the latter three factors - g_λ , ϵ_λ , and τ_λ - often are usefully combined into a single unknown, A_λ , defined as:

$$Eq. 1.1.2.1-3 \quad A_\lambda = g_\lambda \epsilon_\lambda \tau_\lambda$$

Most generally, A_λ is a function of wavelength, time, and the radiating surface temperature. However, if a reference wavelength, λ_R , exists for which A_R is constant in time and surface temperature, it can be shown that sufficient information exists in the radiant emission spectrum of the surface to uniquely determine its temperature at all times [Reference 1.1.2.1-1]. The radiating surface temperature is uniquely determined by taking ratios of the spectral voltage contributions from different wavebands. The change over time of any A_λ value can be tracked by ratioing it to that for the invariant reference waveband. Information from a minimum of two wavebands is required. If information is available from three or more wavebands, accuracy can be gained by suppressing statistical noise in the spectral voltage readings through a variational least squares fitting procedure [Reference 1.1.2.1-1]. Depending on computational speeds, the additional numerical processing associated with numerous additional wavebands can significantly slow the response time of the measurement system. Hence, a significant trade may exist between accuracy and response time.

In the general case, in which all the A_λ depend on time and surface temperature as well as wavelength, another independent measurement is needed, performed at the same time as the surface temperature is needed, or at least close enough in time that the temporal variation can be ignored. The factors tending to make A_λ vary are examined below:

Emissivity Variations: Variations in ϵ_λ may result from chemical or topological changes in the emitting surface. Surfaces exposed to prolonged high temperatures may be subject to oxidation or some other form of chemical attack. While the hard vacuum of interplanetary space is generally favorable for chemical stability of emitting surfaces, certain missions could involve exposure to monatomic oxygen (which is much more chemically aggressive than molecular oxygen) and/or sulfur. Gaseous species can change the emissivity of a surface either by forming a stable oxide thereon, or by preferentially removing surface atoms from specific areas, (such as ends of protrusions, grain boundaries, etcetera.) High emissivity surfaces sometimes are produced through surface topologies approximating a closely spaced array of blackbody cavities between narrow whiskers of material. In these instances, atoms may evaporate preferentially from the ends of salients, causing the topology to soften and the emissivity to fall over time. Preferential diffusion or evaporation of a volatile chemical constituent or gross recrystallization also can change an emissivity value.

The processes described above can be minimized but not necessarily eliminated altogether by selecting a surface made of a highly stable material with a melting temperature far in excess of maximum anticipated service temperatures. Refractory metal surfaces of rhenium, tungsten or molybdenum would all be good choices. The dielectric properties, and hence the optical properties of metals are little affected by radiation, because charge carrier densities in metals are so high that radiation induced conductivity is inconsequential and radiation induced carrier traps are saturated with little change in the mobile carrier density. If desired, the radiating surface could be roughened to increase emissivity, although emissivity values on molten metal surfaces as low as 0.02 are accommodated readily by pyrometry systems employed in industry. Conversely, polished surfaces of refractory metal, may offer even greater temporal stability over long periods than roughened refractory metal surfaces. Furthermore, lower emissivity values may be advantageous for use with recalibration schemes based on reflecting laser pulses off the measurement surface. If necessary, some kind of bubble enclosure offering minimal thermal conduction opportunities could be put in place between the collecting lens on the waveguide and the radiating surface, to minimize attack from chalcogen species or other contaminants in the space environment. All things considered, substantial emissivity variation over time in a space environment likely can be avoided through judicious choice of materials. Furthermore, practical engineering solutions can be envisioned to mitigate emissivity changes should they be more prominent than anticipated. Similarly, most materials exhibit relatively little change with temperature in *spectral* emissivity in the temperature range significantly below their melting points.

Transmissivity Variations: Between the photodetector and the radiating surface in a space pyrometric temperature measurement system would be an optical waveguide as much as 60 meters in length, entrance and exit lenses, and perhaps other beam steering equipment (such as splitters, shutters, etcetera.) At least the waveguide and the entrance lens will reside outside the aft electronics vault where it may be exposed to total ionizing doses from natural and reactor sources nominally as high as 2 GRad. This exposure level, however, is an unrealistic worst case, since it applies only to a JIMO Mission and because it further assumes that natural radiation will have completely unobstructed access to portions of the waveguide. More likely, such waveguides would run down the length of the boom interior, where reductions in dose of over an order of magnitude could be expected. (Even a 10 mil coating of aluminum would effect approximately an order of magnitude reduction in TID in a JIMO-type.) Nevertheless, as discussed in subsection 1.1.2.1, substantive transmissivity changes over the life of some contemplated missions cannot be ruled out. As long as the transmission losses within the wavelength windows selected for the analysis do not exceed 90%, it is likely that a pyrometry system could continue to operate reliably. However, a 20% transmission loss at end of life is likely a reasonable target. For space missions remaining outside the Jovian environment, transmissivity variations might become only of secondary concern.

Changes in Electronics Performance: While residing within the electronics vault, the signal processing electronics of a pyrometry system would still be vulnerable to radiation. This subject is discussed at greater length in subsection 1.1.1.4. Dark current changes in the diode can be factored out by periodically placing the diode, or a nominally identical diode, in darkness and measuring its reverse saturation current. Changes in amplifier gain can be compensated by some other recalibration method.

Recalibration Methods Currently in Use: Two *in situ* recalibration methods for the case of frequently changing emissivity values are known in industry, both of which have been developed primarily for metals processing applications. While these methods are proprietary, key aspects of them became clear from conversations with vendors.

The method developed by Pyrometry Instrument Company (PYRO) employs a pulsed laser and a second waveguide. The idea is to send identical laser pulses to a common detector via three separate paths. Path 1 sends the pulse directly from the laser source to the photodetector. Path 2 sends the pulse through the measurement waveguide to the measurement surface, reflecting off the measurement surface and back through the waveguide to the detector. Path 3 sends the pulse to the detector by way of the second calibration waveguide which is not interrupted by a gap and the measurement surface. By ratioing these three voltages, the three factors in A_λ (Eq. 1.1.2.1-3) can be determined independently for each waveband. This recalibration scheme is easiest to implement with a single waveband, but at least in principle, multiple bands could be employed with a tunable laser.

The method developed by Mikron Instruments Co. employs a calibrated, and presumably stable blackbody source incorporated into their measurement system in place of a laser. Thus Path 1 provides a direct measure of the instrument factor g_λ , and then the voltage ratio from paths 3 and 1 provides a measure of the transmissivity of the waveguide, and the voltage ratio from paths 3 and 2 gives the product of the transmissivity of the gas or vacuum gap (in our case, a constant) and the emissivity of the measurement surface. This scheme is perhaps more readily adaptable to multiple band analyses, but depends on the stability over long periods of the black body source. While relatively well shielded from radiation within the vault, the exterior of the black body source might also have to be cooled thermoelectrically to maintain the desired degree of stability. For an application in a shielded vault, where cooling and power requirements, volume and mass all are issues, a pulsed laser appears to make more sense than a blackbody source.

Reference:

1.1.2.1-1 D. Ng, "A Self Calibrating Emissivity And/Or Transmissivity Independent Multiwavelength Pyrometer," NASA Technical Memorandum 107149, issued January, 1996.

1.1.2.2 Expert System Software

Where direct human intervention is practical, the NR Program generally has favored such approaches over expert system software. However, the systems currently contemplated may need to operate at distances up to half a billion miles from the nearest human where even very slow radio links periodically become impossible (due to solar or Jovian oppositions). As expert systems go, that for an emissivity correction system has a relatively straightforward and well defined task.

In the extreme case of a hypothetical radiating surface characterized by a spectral emissivity that varies in time completely randomly (i.e., with no correlation whatsoever between values in adjacent wavelength intervals), only *in situ* recalibration can offer a valid temperature measurement. However, real surfaces do not behave in such a manner. Rather, enough is often known about the relatively regular behavior of the spectral emissivities of real surfaces that one can often pick out ranges of wavelength for which the dependence of spectral emissivity on wavelength is monotonic and smoothly varying. If optical absorption processes sharply defined in wavelength are superimposed on such smooth behaviors, human experts or expert systems can recognize such signatures and selectively ignore data. Such absorption signatures are often possessed by gaseous species present between a spectrometer and a radiating surface (as in many terrestrial applications), and/or by color centers induced by radiation damage in optical materials. Metal surfaces, the primary candidates for currently contemplated pyrometry applications, tend to have spectral emissivity functions that are monotonic and even quasilinear in nature. Hence, the expert system approach may be well suited, and possibly optimal for space applications of pyrometry.

The expert system pyrometry method presented in Reference [1.1.2.2-1] is essentially a multi-waveband technique, per subsection 1.1.1.4.3, in which the incoming spectrum is chopped into narrow analytical intervals by means of an optical grating composed of diffraction slits and a prism. The individual narrow wavelength components are focused onto individual optical diode elements of a linear array containing hundreds of diodes. By such means it is claimed that a broad wavelength spectrum can be captured, dissected and measured without recourse to moving parts. If N spectrum segments are thus produced, a total of $N(N-1)/2$ intensity ratios can be computed and compared. The expert system then attempts to find a single temperature that brings all these computed ratios into close agreement with the Planck Radiation Law (Equation 1.1.2.1-1), making some relatively simple smoothly varying assumption concerning the spectral emissivity of the radiating surface. The system then computes the goodness of fit for various trial wavebands and then seeks to improve the fit by identifying and eliminating anomalous data such as those that may have been affected by optical absorption outside the surface. (This procedure is not significantly different from discriminator circuits or other signal processing and averaging algorithms used in existing naval reactor plant instrumentation to deal with signal noise and interference) Along with the computed surface temperature, the software provides a running accuracy estimate of the temperature determination based on the variance in the optical intensity data relative to the best fit to the Planck Distribution.

It is noted that the currently contemplated application is one for a single specific surface whose initial spectral emissivity is to be well characterized, as opposed to a general purpose field instrument expected to read temperatures from any arbitrary surface placed before it. It is further expected that a judicious choice of radiating surface will keep spectral emissivity changes within relatively narrow bounds.

In regards to the processing requirements, the author of Reference [1.1.2.2-1] reports that his expert system software was successfully implemented on a 1.2 GHz Celeron computer. The author further

stated (in a telephone conversation with an NRPCT representative) that this computer possessed significantly more capacity than his software actually required. Computing resources and board space for an expert system pyrometry option would need to be examined carefully, given the restrictions that may be imposed on computer speed and memory by a harsh radiation environment.

1.1.3 Extensibility to Other Space Missions

In a lunar ground based application, one would expect a relaxation of the stringent requirements for charged particle irradiation resistance, although solar flares (given the absence of a lunar atmosphere) would continue to be a concern. A reduction in mission duration is also possible, since transit times of several years are not required to reach the moon. Depending on the exact location of the lunar base, a power station may also enjoy uninterrupted and relatively rapid 2-way communications with Earth, promoting closer monitoring and periodic support of automated procedures. These factors all have the potential to influence the details of the I&C sensor suite fairly directly. Of these factors, the biggest impact on the feasibility of pyrometric temperature measurement methods is expected to result from reduced radiation levels, both from the more benign natural environment and due to the possibility of more remotely locating the reactor relative to the electronics. If expected TID and DDD levels were to come down into the range achievable by today's radiation-hardened electronics, the development risk associated with delivering a pyrometric temperature measurement system would be significantly reduced.

1.1.4 Summary Assessment of Development Prospects

Radiation thermometry is a remote temperature measurement method that works with lightweight and flexible dielectric waveguides, rather than electrically conducting cables. The sensor waveguide would not need to experience the primary coolant temperature, although an implementation could involve a blackbody cavity in direct thermal contact with the hotleg pipe. Commercial pyrometry systems usually do not require black body cavities and some routinely are used with surfaces having emissivity values as low as 0.02. Nevertheless the potential advantages and drawbacks of a black body cavity for a Prometheus application need to be evaluated further. Electromagnetic interference (EMI) from the high frequency power cabling is also eliminated as a possible issue.

Pyrometry systems with *in situ* recalibration capability have been employed successfully in industry for applications such as metal processing where surface emissivity values change unpredictably. A vendor claims that some deployed systems have operated over ten years without maintenance. However, additional optical components and increased circuit complexity are involved with this recalibration capability. Because of electronics vulnerability, adapting such a recalibration system for space applications would engender moderate to high risk, depending on the radiation profile. Expert system pyrometry systems also have been commercially available since 1997 that search for wavelength bands in which the dependence of the spectral emissivity is linear, and contain logic that can discriminate narrow spectral features (such as those caused by radiation induced effects in fiber optics) and exclude selected data from consideration. The former approach requires more hardware components, whereas the latter is algorithmically more complex and may require greater computational resources. Both approaches pose challenges but appear promising.

Several satisfactory options likely exist for sufficiently radiation hardened waveguides to support aft-of-shield pyrometry applications for space missions with radiation profiles up to and including those as severe as JIMO.

Depending upon mission specifics, the necessary electronics components to support a space pyrometry system may require a level of radiation hardness not readily attainable with today's off-the-shelf, rad-hard components. While this statement may be generally true of JIMO mission electronics requirements, some pyrometry components such as the photon-to-electron converters and signal amplifiers may be especially vulnerable. Rational prospects exist for meeting this challenge, but the risk of failure also is significant.

A lunar surface or other space mission with a reduced charged particle radiation background would reduce the development risk of a pyrometric temperature measurement system

This page intentionally blank

Enclosure 8

Fiber Bragg Grating Temperature Sensor Technology Evaluation

Ray Blasi
Michael Corcoran
Clint Geller
Ryan Kristensen
Harvey Mikesell
Audra Rice
Dietrich Ahadi
Joe Rossman
Jake Evans

This page intentionally blank

Table of Contents

1. FIBER BRAGG GRATING SENSING TECHNOLOGY	5
2. FBGS IN INDUSTRY	5
3. FBGS AS TEMPERATURE SENSORS	6
4. RADIATION HARDNESS.....	7
4.1 FIBER BRAGG GRATING.....	7
4.2 OPTICAL FIBER.....	9
4.3 OPTICAL COUPLER	9
4.4 SOURCE	10
4.4.1 Light Emitting Diodes	10
4.4.2 Amplified Spontaneous Emission	11
4.4.3 Lasers.....	11
4.5 DETECTORS.....	12
5. CALIBRATION SCHEME FOR THE FBG SENSOR.....	13
6. FIXTURING.....	14
7. EXTENDIBILITY TO A LUNAR POWER STATION.....	14
8. SUMMARY.....	14
9. REFERENCES.....	14

This page intentionally blank

1. Fiber Bragg grating sensing technology

The sensing element for the fiber-optic sensor is based on a fiber Bragg grating (FBG). Consisting of a periodic variation etched directly into the core of an optical fiber, FBGs create a partially reflective mirror that returns selective wavelengths in the form of a narrow spectral peak determined by the grating's period. The wavelength that the fiber Bragg grating reflects is expressed as $\lambda_B = 2 n_{\text{eff}} \Lambda$, where λ_B is the Bragg wavelength, n_{eff} is the effective index of refraction of the core of the optical fiber and Λ is the grating period [1]. A change in the periodicity of any grating along the array will alter the spectral peak of the corresponding channel and signify a change in temperature, longitudinal strain, or other physical influences on the fiber at the grating's location. The Bragg wavelength varies linearly with temperature with a temperature sensitivity of about 10 pm per degree Celsius. Even though the FBG is affected by many external factors, such as, pressure, strain, and temperature, the effects of each can be decoupled through various design techniques. Furthermore, the variation in the grating period is typically the dominant factor. A fiber Bragg grating system, in its simplest form, consists of a light source to illuminate the FBGs, the FBG array written into a fiber core, a calibration scheme, a detection system, and signal processing electronics. The systems response time is typically 100 ms to 300 ms.

A typical measurement is as follows: a continuous laser is swept through a frequency range, the wavelength is calibrated with each scan, and light travels to the FBG where the Bragg wavelength is reflected. The reflected light is then measured by the photodetector. The measured wavelength is then converted to a temperature via a conversion table. The conversion table represents the sensitivity of the sensor. A typical FBG sensitivity is approximately 0.1 nm per degree Celsius. Another way to implement the FBG sensing system is: a broadband source impinges upon the FBG where the Bragg wavelength is reflected and sent to a wavelength filter and photodetector. Again, the measured wavelength is converted to temperature through a conversion table. The signal processing and optoelectronics will be located on one to two cards.

There are two important advantages of the FGB temperature sensor. First and most important is that the FBG sensor is wavelength-encoded. Shifts in the spectrum are independent of the optical intensity. Therefore, a designed amount of optical degradation within the opto-electronics and fiber can be tolerated within the FBG sensing system. Secondly, a single strand of fiber can have multiple gratings etched along its length, forming an array of arbitrarily spaced sensors to be probed. Using a tunable or broadband source each sensor can be interrogated to obtain a distributed measurement of the desired structure. Moreover, an array of FBGs can support the measurements of pressure, strain, or temperature. Because the array of sensors is written on a single fiber only one source and one detector are required. Conversely, conventional sensors require a wire lead from each sensor to the signal processing electronics.

2. FBGs in Industry

Fiber Bragg gratings have proven their usefulness in telecommunication applications, and have extended that usefulness into sensing technology. One major application within telecommunications is dispersion compensation. As a light pulse propagates down a fiber, the pulse widens because the long wavelengths lag the short wavelengths. By designing a chirped FBG, the dispersion can be negated. This principle is especially necessary for high data rates and long fibers. Another logical contribution to telecommunications by fiber Bragg gratings is in wavelength selective devices such as add/drop multiplexers [2].

Since FBGs are directly affected by factors such as temperature, pressure and strain, an extension of this telecommunication component is in sensing [2]. Any change in properties of the fiber result in a change in the modal index or grating pitch. The advantages of using such a technology in sensing industry include accuracy, sensitivity, small size, ability to be multiplexed, immunity to electromagnetic and radio frequency interference and potential low cost [2],[3]. FBGs have been employed as stress detectors in civilian structures such as buildings, bridges, and airplane bodies. They have been used for depth measurements in bodies of water, and as both temperature and pressure sensors in deep oil wells [3].

There are many civilian structures which contain multiple fiber Bragg sensors for measurement purposes. The Horsetail Falls Bridge in Oregon had 26 FBG sensors integrated for purposes of dynamic measurement as part of a strengthening overhaul of the 84 year old bridge in 1998 [4]. Another bridge, the Sylvan Bridge, in Oregon received 14 FBG sensors for purposes of strain measurement in July of 2000 [30]. In 2004, a structural health monitoring system was put in place on the East 12th Street Bridge in Des Moines, Iowa, containing 30 FBG sensors. Fiber Bragg grating sensors have been utilized to measure strain in a number of civilian structures [5].

In addition to strain, FBGs have been used as temperature and pressure sensors for deep oil wells. The advantage of using these gratings is their ability to perform in harsh environments along with their increased performance in the areas of accuracy and sensitivity. As multifunctional distributed sensors, they are used in both well and reservoir monitoring at up to 20 kpsi and 185 degrees Celsius [3]. Temperature sensors have been developed by a number of vendors, including Luna Innovations, Blue Road Research, and Micron Optics. In addition to temperature sensors, these groups utilize the fiber Bragg grating technology to implement other sensors such as strain, pressure, and relative humidity sensors [6]. The gratings have been used for a multitude of functions in a variety of applications. This functionality along with their inherent ability to operate in harsh environments makes fiber Bragg grating technology likely to find uses in other fields and as different types of sensors.

3. FBGs as Temperature sensors

Fiber Bragg gratings, written in germania doped silica, can measure temperatures up to 1100 degrees Celsius [7] and FBGs written in sapphire fiber have measured temperatures up to 1530 degrees Celsius [8]. The silica and sapphire FBG system has potential to meet the temperature sensing requirements of a space reactor. However, it is not only important that the sensor measure high temperature but also that the sensor has long lifetime, high accuracy, good resolution, and radiation tolerance.

Even though both the germania doped silica and sapphire FBGs can measure very high temperatures, their lifetimes are tens of hours [7, 9]. Typically, in an accelerated lifetime versus temperature curve a 'knee' in the curve separates two regions of different slopes. One region has a slope approaching 0 while the other region has a slope approaching 1. In the lifetime versus temperature curve the lifetime will increase drastically as the temperature is reduced below the 'knee' of the accelerated lifetime curve. Such that the lifetime of a temperature sensor written in pure fused silica, is 8.5 years at 500 degrees Celsius with an accuracy of +/- 2 degrees Celsius and 10 pm per degree Celsius resolution [9]. An accuracy of 0.7 degrees Celsius has been given by Luna Technologies; however no lifetime data was given. The fused silica technology is limited to approximately 1100 degrees Celsius since the strain point of amorphous fused silica is 1070 degrees

Celsius [10]. This is the temperature at which stresses developed during cooling which will be permanent once the material is completely cooled. Furthermore, at 1000 degrees Celsius the migration of the dopants from the fiber core becomes significant. In order to increase the lifetime of a sensor at higher temperatures a material other than silica should be considered. Sapphire, with its broad range of transmission in the near infrared and its high material strength, is a good candidate.

Sapphire fiber is single crystal, contrary to fused silica which is amorphous, and its melting point is 2030 degrees Celsius [11]. The ability of sapphire optical fiber to withstand chemically harsh and high-temperature environments, unsuitable for silica fiber, and the ability for sapphire optical fiber to transmit light over a broad wavelength range spanning from 0.15 to 5 μm makes it an attractive material for sensing temperatures up to approximately 1500 degrees Celsius. To date, two groups have fabricated FBGs on single crystal sapphire, General Electric Global Research Center (GE) in conjunction with Pennsylvania State University and the Communications Research Centre Canada. The temperature sensor fabricated by GE has survived 80 hours at 1200 degrees Celsius with an estimated lifetime of 15 years at 850 degrees Celsius [9]. Presently, additional data is being acquired to support the reliability model used for the above estimate. Similar to fused silica, the resolution of the sapphire FBG sensor is 15 pm per degree Celsius [9]. Grobncic et al. [8] with the Communications Research Centre Canada have fabricated a FBG in sapphire fiber that has successfully measured 1530 degrees Celsius. The FBGs were fabricated on a 150 micrometer diameter single crystal sapphire fiber. Multiple pulses from an 800 nm regeneratively amplified Ti: Sapphire laser were focused through a silica phase mask onto the fiber sample. The temperature was varied from 22 degrees Celsius to 1530 degrees Celsius, and there was no obvious reduction of the grating reflectivity with temperature, nor any spectral distortion of the reflected signal. Furthermore, no hysteresis of the Bragg peak wavelength was observed as the device was cycled from 1530 degrees Celsius to room temperature three times. The sensitivity of the device was approximately 25 picometers per degree Celsius up to 1200 degrees Celsius and the sensitivity tended to increase at higher temperatures [8]. Further studies need to be undergone to determine the radiation sensitivity of FBGs written in sapphire fiber. However, this technology shows great promise for sensing the temperature of a space reactor, due to the advantageous material properties of sapphire, promising accuracy and good resolution.

4. Radiation Hardness

A problem with the application of electronics and photonics in space is the presence of charged particles. Charged particles will cause ionizing radiation fields and displacement damage within the semiconductor devices, optical fiber, and fiber Bragg grating. The exposure to radiation will compromise the reliability of these components therefore the radiation tolerance of each device needs to be addressed. Gamma radiation will manifest itself as a cumulative ionized dose. The ionizing dose can create color centers in optical fiber, and it can provide a leakage path in field oxides that provide isolation between electronic devices. The neutron fluence will impart displacement damage in photonic and electronic devices. The displacement of atoms increases the minority carrier lifetime and degrades the device performance.

4.1 Fiber Bragg grating

Exposure to UV radiation between 190 nm and 330 nm causes a permanent change in the index of refraction of germanium doped silica fiber [12]. This effect can be enhanced by modifying the dopant type, the dopant levels, or by loading the core of the fiber with hydrogen. Often the grating is written by illuminating the fiber with UV light through a phase mask, which causes the beam to be diffracted and a pattern exposed on the fiber core. The resultant grating is small on the order of 1 mm to 20 mm in length. These gratings form a sensor that can be interrogated by a variety of optical means.

The radiation from the environment is 5.7×10^{15} neutrons per square centimeter and 1 GRad. If the sensor is located aft of the shield and in the birdcage the radiation levels that the FBG grating will be exposed to for a Jupiter Icy moons orbiter is 0.5 GRad(Si) and approximately 1×10^{15} neutrons per square centimeter. It has been shown that FBG sensors, much like optical fibers, are more sensitive to gamma radiation than neutron radiation. The radiation sensitivity of the FBGs strongly depends on the chemical composition of the fiber, the technique used for writing the FBGs [13], and the exposure to ionizing radiation. These factors result in a change of index of refraction along the grating, and consequently a shift in the Bragg peak wavelength. FBGs written in naturally photosensitive optical fiber have shown the best radiation tolerance with respect to minimal Bragg peak shift and stability of their spectral characteristics. FBGs written in germanium doped photosensitive fiber exhibit a saturating Bragg peak wavelength of about 20 pm toward the longer wavelengths, which corresponds to a 2 degrees Celsius shift, after 8×10^6 Rad irradiation [13]. The shift in the Bragg peak wavelength saturates at approximately 100 kRad. Not only is it important that the Bragg peak wavelength remain stable under irradiation, the reflectivity, the spectral shape, and the sensitivity of the FBG sensor must also remain stable. The Bragg peak wavelength at its full width at half maximum (FWHM), the reflectivity of the fiber grating, and the sensitivity of the sensor have been shown to remain stable under gamma radiation for germanium doped silica fibers [14]. FBGs written in high concentration Ge-doped fiber show the lowest radiation sensitivity under gamma irradiation [14]. However, a high germania-doped fiber attenuates light faster than a fiber with lower germania content [7]. The Bragg peak wavelength has been shown to depend on dose rate, but the shift due to irradiation still saturates. Furthermore, the FWHM is stable under gamma irradiation and no dose rate dependence is observed [15]. The temperature sensitivity of the Bragg peak wavelength is unaffected by gamma radiation [13], and the higher reflectivity FBGs tend to be more radiation tolerant [16].

FBGs written in germania doped silica have been shown to survive and retain a significant signal-to-noise ratio in a combined neutron and gamma environment up to exposure levels of at least 2×10^{19} equivalent neutrons per square centimeter ($E > 1$ MeV) and 8.7×10^{10} Rad (87 GRad) [7]. These levels of radiation are much higher than would be expected for an aft-of-shield application for a JIMO Mission. These encouraging data constitute a first step toward demonstrating the suitability of an FBG temperature sensing system for use in a radiation environment. For example, most data are for neutron and gamma exposure, rather than charged particle exposures, which introduce trapped charge into the fiber, potentially changing the optical properties and inducing dielectric breakdown. Dielectric breakdown temperatures in insulators and semiconductors generally decrease rapidly with increasing service temperature at constant applied field.

The effects of radiation on pure fused silica and sapphire FBGs still require investigation. The technique used to write the gratings on pure fused silica and sapphire fibers is different than the techniques discussed above for FBG written in germania doped fiber [9]. In the techniques stated above for germania doped silica fiber, the FBG is fabricated by reorganizing the dopants into a periodic modulation of the index of refraction of the fiber core. The dopants will contribute to the failure mode by diffusing at high temperatures, around 1000 degrees Celsius for silica. The influence of radiation on the shift in Bragg peak wavelength for the pure fused silica and sapphire fibers as a function still requires investigation. However, the fabrication of the FBG written in sapphire is not dependent on any dopants in the sapphire fiber [8]. The prior statement along with sapphires attractive material properties and radiation hardness provide encouragement for the radiation tolerance of the Bragg wavelength under radiation.

4.2 Optical Fiber

It is well known that the affect of ionizing radiation on optical fibers is an increase of the wavelength dependent attenuation, which is caused by development of color centers. Ionizing radiation manifests itself as material defects such that the level of radiation induced attenuation depends on the fiber composition, processing method, the total dose, dose rate and irradiation history, the temperature and wavelengths. Annealing the defects at high temperature levels can provide a reduction in induced attenuation [17]. Germanium is a common dopant used in the fiber optic industry to increase the index of refraction in the core. Dopants that are used to increase the index of refraction in the core tend to have a large influence in the radiation susceptibility [18]. Generally, pure silica fibers or fibers with low germania doping and no other dopants show the highest radiation tolerance. [7], [17]. Moreover, the radiation induced attenuation is higher for lower wavelengths [18].

The gamma exposure dose rates are typically on the order of 0.01 Rad per minute to 0.1 Rad per minute for most space flights. However, dose rates can be quite high on the order of 10 Rad per minute for short durations due to solar activity. A good summary regarding the radiation hardness in commercial optical fibers has been given in [19]. The following trends in multimode fibers are: the fiber attenuation is higher at 850 nm than at 1300 nm and 1550 nm [19], [20], the fiber attenuation decreases as temperature increases, the fiber attenuation is dose rate dependent such that the attenuation increases with increasing dose rate, and the fiber attenuation increases with total dose [19]. As stated previously, the attenuation is dependent upon many factors and there is a wide range of attenuation values reported from 1 dB per km to 1000 dB per km. A multimode fiber from OFS has an attenuation of 20 dB per km tested at: 1300 nm, 1.1 kRad per minute, up to 1MRad, and at 50 degrees Celsius [19]. This linearly scales to 0.02 dB per meter. Fortunately, the short fiber lengths typically used on a spacecraft and the fact that the FBG sensor is wavelength encoded will give some relief regarding the total attenuation in the fiber. Luna Technologies has shown germania doped silica fiber that has survived up to 2×10^{19} neutrons per square centimeter and a total gamma fluence of 8.7×10^{10} Rad [7]. Furthermore, the attenuation at 1310 nm was less than at 850 nm and at 1550 nm.

Solid core optical fibers are not the only kind of optical waveguide that has potential for use in transmitting the signal from the laser source to the sensor and from the FBG sensor to the detector. There also exist specialty fibers such as hollow tube waveguides, photonic crystal fiber bundles, and single crystal sapphire fiber. Single crystal sapphire fibers have many physical properties that make them ideal candidates for infrared transmission as high as 5.5 μm and good radiation hardness. Sapphire has an intrinsic loss (theoretical) of 0.13 dB/m at 2.94 microns, and a melting point in excess of 2000 degrees Celsius [21]. However, hollow core and photonic crystal fibers require more research and development than solid core fibers and may not be necessary for the Prometheus mission.

The radiation hardness of the source, detector, fiber optical coupler, and calibration system is now addressed. Located in the electronics vault, these components will be exposed to a more forgiving radiation environment than the fiber Bragg grating and the optical fiber. The radiation tolerance required from these optoelectronics is 1 MRad total ionized dose and 6×10^{11} 1 MeV equivalent neutrons per square centimeter. That being said, this is still a challenging environment for digital, analog, and photonic components.

4.3 Optical Coupler

Fiber optic couplers split optical signal into multiple paths or combine multiple signal into a single path. An optical coupler will be used in a FBG system. Thus the radiation hardness should be addressed. There are two types of optical couplers: broadband couplers and narrowband couplers. The FBG

system utilizes a broadband coupler since the sensor is interrogated by a range of wavelengths. The insertion loss of a 1300/1550 nm broadband coupler is increased due to radiation induced attenuation in the optical fibers associated with the coupler. Furthermore its isolation decreased to about 10 dB for both channels at 1.3×10^8 Rad, but the broadband coupler kept its functionality [17].

4.4 Source

Fiber optic sensing systems can use a variety of light sources including tunable lasers, light emitting diodes (LEDs), and amplified spontaneous emission (ASE) sources. An LED and an ASE source are broadband and incoherent in contrast to a laser that is coherent and narrow band. Contrary to optical fibers, the radiation damage in optical sources and detectors is more influenced by displacement damage caused by charged particles and neutrons than total ionizing dose. There are four main effects that damage displacement has on semiconductor devices: change in minority carrier lifetime, carrier removal, mobility degradation, and increase in optical absorption [23].

Minority carrier lifetimes in semiconductor devices are very sensitive to lattice damage. In devices, the reciprocal of minority carrier lifetime often degrades linearly with fluence, and the damage constant depends on the particle type and energy. For 50 MeV protons, the threshold for measurable changes in lifetime in III-V light emitting diodes is approximately 1×10^{10} protons per square centimeter. For heterojunction LEDs and laser diodes, the threshold for measurable damage is 1×10^{11} protons per square centimeter and 1×10^{12} protons per square centimeter, respectively [23]. Carrier removal depends upon particle type, energy, and doping level. For doping concentration of 1×10^{15} per square centimeter, the threshold proton fluence for measurable change in carrier concentration is on the order of 1×10^{12} protons per square centimeter. This implies fluences greater than 1×10^{13} protons per square centimeter are required to change the effective doping concentration of III-V devices. Displacement damage also degrades mobility; however, its contribution is typically less important than the minority carrier lifetime and carrier removal contributions [23]. Optical absorption will increase with lattice damage. This can change the optical gain in laser cavities. Typically, 1×10^{14} neutrons per square centimeter are needed to produce measurable changes in the absorption coefficient of the gain medium (III-V semiconductor material).

4.4.1 Light Emitting Diodes

LEDs are sensitive to radiation. The threshold current level for the onset of light output in LEDs changes very little after irradiation, but the light output at constant injection conditions generally decreases. Their sensitivity begins approximately at 1×10^{10} 50 MeV protons per square centimeter, for amphoterically doped devices. However there are minimal radiation effects for an HP 1300 nm LED at 1×10^{12} 50 MeV protons per square centimeter [23], [24]. The HP LED is not an amphoterically doped device. It is a heterojunction device designed for high speeds which is quite different than other LED technologies. Designed for high speed operation, the HP device will have a short minority carrier lifetime which is an advantage for radiation hardness of optical devices. The fluence for 50% reduction in light output varies by more than 3 orders of magnitude for the different types of LEDs; amphoteric LEDs and high speed heterojunction LEDs.

4.4.2 Amplified Spontaneous Emission

The ASE source typically ranges from 1525 nm to 1565 nm. It consists of an erbium doped fiber that is pumped with a high power (~100 mW) 980 nm laser. An ASE can deliver higher power in the range of 12 dBm to 16 dBm. ASE sources can be packaged with dimensions of: 90 x 70 x 12 mm, and there are many vendors available, such as NP Photonics, Lightwaves 2020, Highwave Optical Technologies, ILX Lightwave, Newport, and Fiberpro. As stated previously, one of the components of the ASE is the high power 980nm laser. Contrary to optical fibers, lasers are most sensitive to displacement damage and less sensitive to ionizing radiation. The dominant effect of radiation on laser performance is a shift in the threshold current. An InGaAs 980 nm strained quantum well laser undergoes a 14% shift in threshold current after 2×10^{12} 5.5 MeV protons per square centimeter. Note that 5.5 MeV protons will provide 20 times more damage than 200 MeV protons. Thus, there is a high likelihood that the pump laser would survive a JIMO mission, as long as the power degradation in the laser is designed into the system optical power budget. However, ionizing radiation significantly affects the optical properties in erbium-doped fiber, mainly through radiation induced absorption. An investigation of erbium doped fibers found the radiation sensitivity at the pump wavelength (960 nm) to be 5 to 6 times higher than that at the signal wavelength (1590 nm), independent of the erbium dopant concentration. Estimated losses at 0.2G Rad are 188 dB/m and 54 dB/m at 960 nm and 1590 nm, respectively. This large attenuation suggests that the ASE source will lack sufficient radiation hardness for a JIMO mission [25].

4.4.3 Lasers

The typical wavelength a FGB sensor system operates at is 1.55 μm because the optoelectronics used in FBG sensor leverages off of technology developments in the telecommunication industry. At 1.55 μm , the loss in a silica fiber is at its minimum. Furthermore, there are plenty of sources and detectors that operate at this wavelength. Fortunately, sapphire also transmits at this wavelength. The initial systems with FBG sapphire fibers have operated at 1.55 μm [8]. However, the sensor system can operate at other wavelengths if it is beneficial. Thus, sources operating from 660 nm to 1550 nm will be considered.

There are three regions of interest when investigating the influence of radiation on a laser. The first region is the laser drive current below threshold. In this region, the laser diode behaves like an LED and the output power degrades. The second region is just near threshold. In this region, near threshold, the light output increases very rapidly with the transition into lasing and the threshold current increases with increasing proton fluence. The final region of interest is in the saturation region. In this region the devices are insensitive to proton irradiation because the radiative lifetime is extremely short such that displacement damage induced non-radiative recombination cannot compete effectively with laser output [26]. With regard to radiation sensitivity, the most critical laser parameter is the laser threshold current.

The threshold of edge emitting lasers from 660 nm to 1500 nm will change 2 percent after 1×10^{12} 50 MeV protons per square centimeter fluence [23]. Typically the laser operates at a fixed current above threshold. The overall affect of radiation on the output power is to decrease the amplitude of the output power through a shift in threshold current. Thus, for space applications with large expected proton fluences, it is important to select laser diodes with a wide current range between threshold and maximum operating current. Furthermore, degraded laser diodes have been observed to recover during forward current bias [23].

Vertical cavity surface-emitting lasers (VCSEL) are another type of laser and they use a Bragg reflector formed by multiple thin layers at the back region of a vertical structure, providing compact

lasers with very low threshold current that emit light vertically. The threshold current and power are typically lower than for edge emitting lasers. The compact structure has some advantages: self-heating of the compact device reduces gain at high temperature, making the operation of the device less dependent upon temperature. VCSELs also have better output beam characteristics compared to conventional edge-emitting lasers, resulting in more efficient coupling to optical fibers. Unlike edge emitter lasers the slope efficiency changes for un-irradiated devices mainly because of thermal effects due to self heating.

VCSELs are reasonably resistant to radiation damage; at 192 MeV 1×10^{13} protons per square centimeter irradiation light output drops approximate 10% for a laser driven at a current of 15 mA [24]. In contrast to edge emitter lasers, more degradation occurs in the slope efficiency for VCSELs than in an increase in threshold after irradiation. Similar to edge emitting lasers, degradation in VCSELs can recover through forward bias annealing [27].

Edge emitting lasers and VCSELs will show degradation in power with irradiation; however this can be mitigated during the system design of the FBG sensor system. Proper design of the system can account for an overall system power loss due to degradation in source power, attenuation of the optical power in the fiber, and a reduction in responsivity in the detector. As long as the detector can detect the signal, the FBG sensor is insensitive to the amplitude change because it is wavelength dependent. An extension to the research in the affects of irradiation on a laser operating at a fixed wavelength is required since the FBG sensor requires a broadband source. Thus either an LED can be used or a tunable laser. ASE sources do not have the proper radiation tolerance; LEDs are radiation hard to approximately 10^{12} protons per square centimeter. Hence the radiation sensitivity of a tunable laser should be investigated. Typically, the laser is monitored with a photodiode located in the package of the laser. This photodiode is also radiation sensitive, and its sensitivity to irradiation is discussed next.

4.5 Detectors

There are a few popular material systems used for fabricating infrared detectors: silicon detects in the wavelength range of 400 nm to 1100 nm, InGaAs detects in the range of 1000 nm to 1700 nm, and germanium detects in the wavelength range of 800 nm to 1800 nm. Following the operation of the FGB system in the 1300 nm or 1550 nm range, it is likely an InGaAs photodetector will be used as long as the system requirements are met. However, all material systems will be discussed along with different photodetector structures such as, PN photodiodes, PIN photodiodes, and avalanche photodiodes.

In optical links exposed to radiation, photodiodes are often considered as the element which limits the system operation. They will give electrical current not only due to incident optical photons, but also due to the ionizing radiation. Since radiation introduces defects in the semiconductor crystal lattice, the optically generated minority carriers might recombine before reaching the electrodes, leading to a decrease in responsivity. The most compromising effect however is the increase of the photodiode leakage current which increases the noise and therefore also the minimum detectable signal.

PN diodes collect light at the junction and surrounding regions as long as it is within the carrier diffusion length. Thus, carriers are collected via drift and diffusion mechanisms. PIN diodes operate in a regime such that all charge is collected by drift transport mechanism. This leads to greater

radiation sensitivity of the PN diode, since the diffusion transport component is more affected by the minority carrier lifetime damage [28]. Moreover, the PN devices degrade more at longer wavelengths than shorter wavelengths because of the longer absorption depth required for longer wavelengths. Avalanche photodiodes (APD) are an attractive detector because the internal gain mechanism provides improved signal to noise ratio.

The different dominant transport mechanisms in the PIN and PN devices lead to varied radiation response. PIN photodiodes exhibit a 10% decrease in photoresponse where PN photodiodes have shown a 50% decrease in photoresponse at 4×10^{11} 50 MeV protons per square centimeter. This difference is particularly large at longer wavelengths near the maximum reponsivity of silicon, and is due to the fact that light collection in the PIN detectors does not depend on the minority carrier lifetime. However, carrier removal effects in the lightly doped intrinsic (I) region cause leakage current to increase, and these changes are noticeable at levels below 1×10^{10} 50 MeV protons per square centimeter. Leakage currents in PN photodiodes are much smaller because there is not low doped intrinsic region [28], [29].

It is important to understand the radiation induced dark current changes in avalanche photodiodes because the dark current will adversely affect the signal-to-noise ratio. The dark current can increase from over an order of magnitude for a Ge APD to over four orders of magnitude for an InGaAs APDs. This compares with pre-irradiation levels of 300 nA for Ge APD and 1.5 to 6 nA for the InGaAs APDs. The importance of dark current levels in photodetectors depends on the application and the system noise requirements [30].

Similar to optical sources, photodetectors are more sensitive to displacement damage rather than ionizing radiation [17], [31]. Moreover, the sensitivity to radiation for silicon detectors is larger than III-V detectors because the minority carrier lifetime of the silicon devices is longer [32]. The reponsivity of an InGaAs photodetector operating in the 1310 nm regime decreases 5% at 1×10^{12} 63 MeV protons per square centimeter [31]. A silicon PIN photodetector will undergo a decrease of 10 percent at 650 nm or 50 percent at 930 nm [28]. The radiation performance of PN photodiodes is inferior to PIN photodiodes for the reasons stated above.

Similarly to the source technology there will be some tolerance to system degradation of the optical power. An assessment at the system level is required to determine if the radiation performances stated above are satisfactory. Since this system is wavelength encoded detection, it is necessary to calibrate the wavelength with each scan of the sensor. The proposed calibration scheme is described in the following section.

5. Calibration scheme for the FBG sensor

The calibration scheme typically used for tunable lasers and FBG interrogation systems is a gas cell standard with a reference wavelength module. The absolute wavelength calibration is achieved with gas cell spectroscopy with every scan of the sensor. A gas cell consists of a gas, such as hydrogen cyanide, packaged in a glass cylinder approximately 75 mm long. The gas cell can be fiber pigtailed to provide a compact fiber based calibration scheme. The calibration scheme shows promise however the radiation sensitivity still requires investigation. Furthermore if a broadband source is used then a filter is required to discern the wavelength impinging on the broadband detector. Possible filters include a monochromator, a compliant micro-electro-mechanical system (CMEMS), or a grating.

6. Fixturing

FGBs have been used in the oil, avionic, and turbine industries. Investigation is required to research how the sensors were attached and to evaluate how they can be attached for Prometheus.

7. Extendibility to a Lunar Power Station

In the event that Project Prometheus becomes focused on installing the SNPP as a lunar power station, the results of this evaluation generally remain the same. Radiation hardness of the opto-electronics is probably less challenging for a lunar application.

8. Summary

The fiber Bragg grating temperature sensor is a promising technology for the space reactor. There are two important advantages of the FGB temperature sensor. First and most important is that the FBG sensor is wavelength-encoded; shifts in the spectrum are independent of the optical intensity. Therefore, a designed amount of optical degradation within the opto-electronics and fiber can be tolerated within the FBG sensing system. Secondly, a single strand of fiber can have multiple gratings written along its length, forming an array of arbitrarily spaced sensors to be probed. Using a tunable or broadband source each sensor can be interrogated to obtain a distributed measurement of the desired structure. Because the array of sensors is written on a single fiber only one source and one detector is required. Conversely, conventional sensors require a wire lead from each sensor to the signal processing electronics.

With the ability to write the FBG in a sapphire fiber, sensing temperature up to 1530 degrees Celsius has been achieved. The accuracy of a FBG in pure silica operating at 500 degrees Celsius is +/- 2 degrees Celsius over an 8.5 year lifetime. This is not in a radiation environment, and radiation induced shifts in the Bragg peak wavelength have been shown to be as little as 2 degrees Celsius. The radiation sensitivity of the FBG written on sapphire fiber still requires investigation. However, the attractive material properties and the distinct method of writing the grating on sapphire make this sensor system promising for space or lunar reactor temperature detection.

9. References

- [1] R. Ramaswami and K. Sivaraiian, *Optical Network, A practical perspective*, Second Edition, Morgan Kaufmann Publishers, 2002.
- [2] Hill, Kenneth O.; Meltz, Gerald. "Fiber Bragg Grating Technology Fundamentals and Overview." *Journal of Lightwave Technology*, Vol. 15, no. 8, pp. 1263-1276. 1997.
- [3] Li, Dong-Sheng; Li, Hong-Nan; Ren, Liang; Sun, Li; Zhou, Jing. "Experiments on an Offshore Platform Model by FBG Sensors." *Proceedings of SPIE: Smart Structures and Materials 2004; Sensors and Smart Structures Technologies for Civil, Mechanical, and Aerospace Systems*, Vol. 5391, pp. 100-106. 2004.
- [4] Schultz, W.L.; Conte, J.P.; Udd, E. "Long Gage Fiber Optic Bragg Grating Strain Sensors to Monitor Civil Structures." *Proceedings of SPIE*, Vol. 4330, pp. 56. 2001.
- [5] Doornink, J. D.; Phares, B. M.; Zhou, Zhi; Ou, Jinping; Graver, T. W.; Xu, Zhihong. "Fiber Bragg Grating Sensing for Structural Health Monitoring of Civil Structures."
<http://www.micronoptics.com/pdfs/FBGsensingSHMcivil.pdf>
- [6] Wippich, M; Dessau, K. L. "Tunable Lasers and Fiber-Bragg-Grating Sensors." *Industrial Physicist*, Vol. 9, no. 3, pp. 24-27. 2003.

- [7] Fielder, R. S.; Duncan, R. G.; Palmer, M. L. "Recent Advancements in Harsh Environment Fiber Optics Sensors: An Enabling Technology for Space Nuclear Power," *Proc. of the Space Nuclear Conference*, 2005.
- [8] Grobncic, D.; Mihailov, J.; Smelser, C; Ding, H. "Sapphire Fiber Bragg Grating Sensor Made Using Femtosecond Laser Radiation for ultrahigh temperature applications," *IEEE Photonics Technology Letters*, vol. 16 no. 11, pp. 2505-07, 2004.
- [9] GE GRC, conversations with Kung-Li Deng (2005).
- [10] Opticsland website, www.sciner.com/Opticsland/FS.htm
- [11] Matweb, The online Materials Information Resource, www.matweb.com
- [12] Gusarov, A. I.; Starodubov, D.; Berghmans, F.; Depairs, O.; Fernandez Fernandez, A.; Defosse, Y.; Decretton, M.; Megret, P.; Blondel, M. "Behavior of fibre Bragg gratings under high total dose gamma radiation," *IEEE Tran. Nuc. Sci.*, Vol 47, No. 3, 2000.
- [13] Gusarov, A. I.; Starodubov, D. S.; Berghmans, F.; Deparis, O.; Defosse, Y. "Design of a radiation-hard optical fibre Bragg grating temperature sensor," in: *Conf. on Phononics for Space and Enhanced Radiation Environments*, E. W. Taylor and F. Berghmans, eds., vol. 3872, pp. 43-50, SPIE, 1999.
- [14] Gusarov, A. I.; Starodubov, D. S.; Berghmans, F.; Depairs, Y.; Defosse, O.; Fernandez Fernandez, A.; Decretton, M.; Megret, P.; Blondel, M. "Comparative study of MGy dose level gamma-radiation effect on FGBs written in different fibers," in: *13th Int. Conf. on Optical Fibers Sensors*, B.Y. Kim and K. Hotate, eds., vol. 3746, p. 608-11, SPIE, Kyongju, Korea, 1999.
- [15] Fernandez Fernandez, A.; Brichard, B.; Bergham, F.; Decretton, M. "Dose-Rate Dependencies in Gamma-Irradiated Fiber Bragg Grating Filters," *IEEE Trans. Nucl. Sci.*, Vol. 49, pp. 2874-78, 2002.
- [16] Fielder, R. S., *LUNA Technologies, presentation at ORNL*, July 20, 2005.
- [17] Berghmans, F.; Brichard, B.; Fernandez Fernandez, A.; Van Uffelen, M. "Reliability issues for optical fibre technology in nuclear applications," *Proc. of 5th Int. Conf. on Transparent Optical Networks*, pp. 252-57, 2003.
- [18] Ott, M. "Fiber Laser Technology Readiness Overview, Report to the NASA parts and Packaging program," Electronic Part program, March 2003.
- [19] Ott, M. "Radiation Effects Data on Commercially Available Optical Fiber: Database Summary," in *Proc. Nuclear and Space Radiation Effects, Data Workshop*, Phoenix, Arizona, pp. 24-31., 2002.
- [20] Brichard, B.; Van Uffelen, M.; Fernandez Fernandez, A.; Berghmans, M.; Decretton, M.; Hodgson, E.; Shikama, T.; Kakuta, T.; Tomashuk, A.; Golant, K.; Krasilnikov, A. "Round-robin evaluation of optical fibres for plasma diagnostics," *Fusion Eng. Des.*, vol. 56-57, pp. 917-921, 2001.
- [21] Nubling, R. and Harrington, J. "Optical properties of single-crystal sapphire fibers," *Appl. Opt.*, vol. 36, no. 24, pp. 5943-40, 1997.
- [23] Johnston, A. "Radiation Effects in Light-Emitting and Laser Diodes," *IEEE Trans. Nuc. Sci.*, vol. 50, no. 3, pp. 689-703, 2003.
- [24] Johnston, A. "Proton damage in Light-emitting and Laser diodes," in *Proc. RADECS Data Workshop*, Belgium, 2000.
- [25] Brichard, B.; Fernandez Fernandez, A.; Ooms, H.; Berghmans, F. "Gamma dose rate effect in erbium-doped fibers for space gyroscopes," *Proc. Of the 16th Int. Conf. on Optical Fiber Sensors*, Nara Japan, pp. 336-39, 2003.
- [26] Barns, C., et al. "Recent Photonic Activities under the NASA Electronic Parts and Packaging (NEPP) Program," whitepaper, 2002.
- [27] Barns, C., et al. "Proton Irradiation Effects in Oxide-Confined Vertical Cavity Surface Emitting Laser (VCSEL) Diodes," in *Proc. of RADECS*, Belgium, 2000.

- [28] Johnston A., et al., "Radiation Damage of Electronic and Optoelectronic Devices in Space," 4th international workshop on Radiation Effects on Semiconductor Devices for Space Application, Japan Oct. 2000.
- [29] Johnston A., "Optoelectronic Devices with Complex Failure Modes," NSREC short course, 2000.
- [30] Becker H. and Johnston, A. "Dark Current Degradation on Near infrared avalanche photodiodes from proton irradiation," 2004.
- [31] Marshall, P.; Dale, C.; Burke, E. "Space Radiation effects of optoelectronic material and components for 1300nm fiber optic data bus," *IEEE Trans. Nuc. Sci.*, vol 39, no. 6, 1992.
- [32] Johnston A., et al. "Proton Damage in Advance Laser Diodes," *IEEE Trans. Nuc. Sci.*, Vol 48, No. 6, 2001.

CONCURRENCE RECORD SHEET

- DOCUMENT NUMBER: B-SE(SPS)IC-008
- THIS DOCUMENT CONTAINS INFORMATION WHICH SHOULD BE CONSIDERED FOR PATENT DISCLOSURES YES NO
- THIS DOCUMENT CONTAINS INFORMATION WHICH MEETS BETTIS WORK CATEGORIES [A,B,C,D or (N/A)] N/A

CONCURRENCE SIGNATURES (Activity must be included) - RESOLVE COMMENTS BEFORE SIGNING

SIGNATURE/ACTIVITY	DATE	TYPE	DETAILS OF REVIEW REQUESTED (if necessary)
<i>SIGNED BELOW</i>			
D. P. Hagerty/Bettis <i>[Signature]</i>	<i>12/20/05</i>	<i>8</i>	
C. D. Eshelman/Bettis <i>[Signature]</i>	<i>12/21/05</i>	<i>8</i>	
J. E. Hack/Bettis			Signed via e-mail
K. Loomis/KAPL			Signed via e-mail
H. Schwartzman/KAPL			Signed via e-mail
D. McCoy/KAPL			Signed via e-mail
J. M. Ashcroft/KAPL			Signed via e-mail
S. A. Simonson/KAPL			Signed via e-mail

TYPE OF REVIEWS (to be determined by author) [See table at end of instructions for definitions.]

1-Peer:Summary 2-Peer:Intermediate 3-Peer:Detail 4-Independent 5-Informal Committee 6-Formal Committee 7-Specialist 8-Interface

NAME TYPED AND SIGNATURE OF NEXT HIGHER MANAGER NOT SIGNING ON LETTER

DATE

D. P. Hagerty *[Signature]*

12/20/05

• CONTRIBUTORS AND IMPACTED PARTIES NOT REQUESTED TO CONCUR AND WHY:

CONCURRENCE RECORD SHEET

DISTRIBUTION:

NR	BETTIS	KAPL
C. H. Oosterman - 08C/8017	M. J. Zika, 01C/SE	M. J. Wollman, 111
J. P. Mosquera - 08C/8017	R. Messham, 14B/MT	J. Boyle
S. T. Bell - 08I/8024	C. Geller, 33F/RT	R. Kristensen
M. W. Henneberger - 08K/8026	R. Blasi, 14B/MT	A. Rice
S. J. Kurth - 08K/8026	J. Evans, 14B/MT	K. Loomis, 132
T. N. Rodeheaver - 08I/8024	D. Bullen, 14B/MT	H. Schwartzman, 132
	D. P. Hagerty, 38D/SE	D. McCoy, 111
	C. D. Eshelman, 36E/SE	J. M. Ashcroft, 132
	J. E. Hack, 05R/MT	S. A. Simonson, 081
PNR	C. M. Fedoris, 07D/SEA	
J. A. Andes	G. H. Eckenroad, 08F/MER	
J. Koury	D. A. Ahadi, 34L/RT	
R. J. Argenta	T. S. Blazeck, 34L/RT	
	S. S. Cable, 38D/MER	
	S. A. Hickenboth, 31B/SEA	
J. Mills, SNR	R. J. Maurizio, 38D/SE	
D. Clapper, SNR	R. M. Morgan, 07D/SEA	
	J. A. Rossman, 43T/NRF	
	E. J. Simon, 34L/RT	
	D. C. Smalley, 07D/SEA	
	I. J. Thomas, 07D/SEA	
	R. A. Vareha, 31B/SEA	
	M. J. Wierzchowski, 38D/OT	
	ADSARS	